



**ENHANCING BIOCEMENT THROUGH
INCORPORATION OF ADDITIVES**

**A THESIS SUBMITTED TO CARDIFF UNIVERSITY
FOR THE DEGREE OF DOCTOR OF PHILOSOPHY
BY**

**CHRISTINE ANN SPENCER
MAY 2021**

SCHOOL OF ENGINEERING

CARDIFF UNIVERSITY

SUMMARY

The aim of this research was to enhance properties of biocement, with a focus on development of self-healing capability, to improve the resilience of geotechnical structures. The use of additives, also referred to as carrier materials, has been explored for this purpose. This research builds upon past studies on healing of biocemented sand following mechanical damage and applies the process of microbially induced calcium carbonate precipitation (MICP). Past research had demonstrated the potential of MICP to enable healing of biocement, through the injection of nutrients and precursor chemicals (cementation medium) required for MICP into degraded biocement. These injections had enabled further MICP since the sand samples contained viable ureolytic bacteria, in vegetative form or from the assumed regeneration of spores. To enable the biocement to self-heal, the process should be an autonomous one, which would require the nutrients and precursor chemicals for the MICP process to be supplied from within the biocemented sand matrix.

The use of additives has been explored as a means of i) immobilising cementation medium within biocement to promote self-healing, and ii) improving mechanical properties of the biocemented sand and efficiency of the MICP process. Additives tested included powdered absorbent materials, as utilised in self-healing concrete such as expanded perlite and diatomaceous earth, in addition to natural fibres such as jute and hemp. Unconfined compressive strength testing was used to determine the effect of the additives on the strength of the biocemented sand columns, and to test for strength regain following deterioration. Geochemical analysis was undertaken to explore effects of the carrier materials on the MICP process during the production of biocemented sand columns, followed by mineralogical analysis. Addition of jute in particular resulted in significant improvement in respect of strength of biocemented sand, efficiency of chemical conversion during MICP and amount of calcium carbonate precipitated.

ACKNOWLEDGEMENTS

I thank Cardiff University for providing me with the opportunity to undertake this Ph.D. study and for providing the funding for my stipend.

Owing to the interdisciplinary nature of this Ph.D., the research undertaken has benefitted from engagement and collaboration with engineers, earth scientists and microbiologists. I am grateful for the support I received from Phil Renforth and Henrik Sass in the School of Earth and Environmental Sciences (Formerly Earth and Ocean Sciences) at Cardiff University, during years one and two to four of my studies respectively. I enjoyed my time teaching alongside Phil Renforth which then prepared me for delivering an MSc module in the second year of my Ph.D. studies. I am especially thankful to Leon van Paassen for facilitating the collaboration with the Centre for Bio-mediated and Bio-inspired Geotechnics (CBBG) and for their support while I was based at Arizona State University (ASU) during the third year of my Ph.D. studies. I also thank all those involved with the CBBG for their support and assistance while I was based at Arizona State University.

I am grateful also to the technicians who assisted with my use of the laboratory equipment at Cardiff University, these include Jeff Rowlands and Amanda Kitching, and the Eyring Materials Centre at ASU for supporting my use of their Scanning Electron Microscope. Jeff Rowlands operated the inductively coupled plasma optical emission spectrometer and X-ray diffractometer at Cardiff University, otherwise all other equipment used in this research at Cardiff University and at Arizona State University was operated by myself. I thank Michael Edgar, Graduate Research Assistant at ASU, for training me to use the ion chromatograph.

I also acknowledge funding from the British Geotechnical Association (BGA) and Society for Applied Microbiology (SfAM), who provided me with the funds to attend conferences during my Ph.D. studies. The Centre for Bio-mediated and Bio-inspired Geotechnics (CBBG) supported the lab costs for my research during the third year of my Ph.D. studies.

CONTENTS

SUMMARY	i
ACKNOWLEDGEMENTS	ii
CONTENTS	1
TABLES AND FIGURES	6
CHAPTER ONE	19
1 INTRODUCTION	19
1.1 Overview and Background.....	19
1.2 Aim, Objectives and Scope of Research.....	20
1.2.1 Aims	20
1.2.2 Objectives	20
1.2.3 Scope.....	21
1.3 Thesis Structure	22
CHAPTER TWO	25
2 LITERATURE REVIEW	25
2.1 Introduction.....	25
2.2 Literature Review Process	26
2.3 Self-healing Construction Materials	30
2.3.1 Mechanisms of Self-Healing.....	30
2.4 Microbially Induced Calcium Carbonate Precipitation (MICP)	33
2.4.1 Ammonia Production	35
2.4.2 Naturally Occurring MICP.....	35
2.4.3 Evaluation of MICP	37
2.5 Factors Affecting Microbially Induced Calcium Carbonate Precipitation.....	39
2.5.1 Water Availability.....	40
2.5.2 Temperature	40
2.5.3 pH.....	41
2.5.4 Oxygen Supply.....	42
2.5.5 Material Type.....	42
2.5.6 Bacterial Strain.....	43
2.5.7 Cementation Medium.....	45
2.6 Cementation Medium Delivery.....	50
2.6.1 Direct Application.....	51
2.6.2 Admixtures and Premixing	53
2.6.3 Immobilisation	53
2.6.4 Encapsulation	58

2.6.5	Groundwater	62
2.6.6	Summary and Conclusions.....	63
CHAPTER THREE		72
3	THEORETICAL FRAMEWORK	72
3.1	Self-Healing Microbially Induced Calcium Carbonate Precipitation (SH-MICP)	72
3.1.1	Embedding Self-Healing Capability	73
3.1.2	Activation of Self-Healing MICP	74
3.2	Requirements of the SH-MICP Process and Limiting Factors	75
3.2.1	Sporulation of Bacteria	75
3.2.2	Storage and Supply of Cementation Medium	76
3.2.3	Limiting Factors.....	77
3.2.4	Assumptions.....	78
3.3	Potential Applications of SH-MICP	78
3.3.1	Seepage Control Within Dam Cores.....	79
3.3.2	Foundation Repair.....	81
3.3.3	Slope Stabilisation.....	81
3.3.4	Landfill Lining Repair	82
3.3.5	Land Subsidence Remediation.....	82
3.3.6	Preservation and Restoration of Ornamental Stone	82
3.3.7	Assessing Suitability for Geotechnical Applications.....	83
3.4	Selection of Carrier Materials for Investigation.....	84
CHAPTER FOUR.....		88
4	METHODOLOGY AND MATERIALS	88
4.1	Bacteria	88
4.1.1	Selection of Suitable Bacteria	88
4.1.2	Culture of Bacteria.....	88
4.1.3	Bacterial Cell Harvesting	92
4.1.4	Bacteria Maintenance Protocol	92
4.1.5	Inducing Sporulation of Bacteria	93
4.1.6	Bacterial Cell Counting.....	94
4.1.7	Urease Activity	96
4.1.8	Specific Urease Activity	96
4.2	Sand.....	96
4.3	Immobilising Additives (Carrier Materials).....	97
4.3.1	Diatomaceous Earth	97
4.3.2	Expanded Perlite	98
4.3.3	Natural Fibres.....	100

4.4	Production of Cementation Medium.....	102
4.5	Immobilisation of Cementation Medium.....	103
4.5.1	Expanded Perlite and Diatomaceous Earth.....	103
4.5.2	Fibres - Soaking Method of CM Immobilisation.....	104
4.5.3	Fibres - Spraying Method of CM Immobilisation.....	105
4.6	Encapsulation of Cementation Medium in Alginate-Based Hydrogel.....	106
4.6.1	Synthesis using an Aqueous Medium Solution, for use with <i>S. ureae</i>	107
4.6.2	Synthesis using Powdered Medium Constituents	107
4.7	Sand Column Experiments (Bioaugmentation)	108
4.7.1	Mini-Columns (Preliminary study).....	108
4.7.2	Sand Preparation	108
4.7.3	Preparation of Columns Apparatus.....	109
4.7.4	Column Filling, Bacteria fixing and First Treatment (Stage 1)	112
4.7.5	Biocementation Treatments (Stage 2).....	114
4.8	Geochemical Analysis.....	115
4.8.1	Electrical Conductivity, pH and Dissolved Oxygen	115
4.8.2	Cation Concentration	115
4.8.3	Colorimetric Determination of Ammonium Ion Concentration (Nesslerisation)	116
4.9	Quantification of Calcium Carbonate using a Calcimeter	117
4.10	Geotechnical Parameters.....	117
4.10.1	Particle Size Distribution	117
4.10.2	Particle Density (Specific Gravity).....	118
4.10.3	Compaction	118
4.10.4	Unconfined Compressive Strength	118
4.11	Mineralogical Analysis	119
CHAPTER FIVE		121
5	MATERIALS TESTING AND SELECTION: PRELIMINARY STUDIES	121
5.1	Introduction.....	121
5.2	Bacteria	121
5.2.1	Sporulation Potential of Selected Bacteria.....	121
5.2.2	Observation of Spores.....	122
5.2.3	Chemically Induced Sporulation.....	123
5.2.4	Sporulation under Low Nutrient Conditions.....	123
5.2.5	Bacterial Growth.....	126
5.3	Testing of Additives (Carrier Materials).....	128
5.3.1	Materials and Methods.....	129
5.3.2	Results and Discussion.....	139

5.4	Testing of Geopolymer Coatings	152
5.4.1	Application of Coatings	152
5.4.2	Results and Discussion.....	153
5.5	Conclusions.....	153
CHAPTER SIX.....		155
6	COLUMN STUDY ONE: Column Tests using <i>S. ureae</i> to test the Effectiveness of Immobilising Carrier Materials for the Long-Term supply of Cementation Medium	155
6.1	Introduction.....	155
6.2	Materials and Methods.....	156
6.2.1	Sand.....	156
6.2.2	Cementation Medium.....	156
6.2.3	Bacteria Culture, Fixing and Activity	158
6.2.4	Preparation of Carrier Materials	159
6.2.5	Columns Assembly and Treatment	159
6.2.6	Geochemical Analysis.....	161
6.2.7	Unconfined Compressive Strength Testing	161
6.2.8	Mineralogical Analysis	163
6.3	Test Results and Analysis	163
6.3.1	Sand Parameters.....	163
6.3.2	Columns Test U1	165
6.3.3	Columns Test U2	171
6.3.4	Columns Test U3	181
6.3.5	Columns Test U4	186
6.3.6	Columns Test P1	189
6.4	Survival of Bacteria in Columns after 1.5 y (Long-Term Survival)	193
6.5	Conclusions.....	195
CHAPTER SEVEN		198
7	COLUMN STUDY TWO: Sand Column Studies using <i>S. pasteurii</i> , and Jute Fibres as Immobilising Materials.....	198
7.1	Introduction.....	198
7.2	Column Study Methodology Changes	199
7.3	Materials and Methods.....	200
7.3.1	Sand and Testing of Properties	200
7.3.2	Fibre Preparation.....	201
7.3.3	Bacteria Culture	202
7.3.4	Preparation of Cementation Media	203
7.3.5	Urease Activity and Batch Test	204

7.3.6	Preparation of Columns	204
7.3.7	Bacteria Fixing and Biocementation.....	205
7.3.8	Measurement of Electrical Conductivity, pH and Evaluation of Bacterial Fixing	207
7.3.9	Geochemical Analysis.....	207
7.3.10	Quantification of Calcium Carbonate Precipitate	207
7.3.11	Mineralogical Analysis	208
7.3.12	Unconfined Compressive Strength Testing	208
7.4	Results and Analysis	209
7.4.1	Urease Activity Batch Test	209
7.4.2	Material Properties.....	210
7.4.3	Columns Test P2 (6 g/L Oxoid CM0001).....	211
7.4.4	Columns Test P3 (3 g/L Oxoid CM0001).....	228
7.5	Conclusions.....	241
CHAPTER EIGHT		245
8	COLUMN STUDY THREE: Encapsulation of Cementation Medium in Alginate-Based Hydrogel Beads.....	245
8.1	Materials and Methods.....	245
8.1.1	Sand.....	245
8.1.2	Sodium Alginate and Cementation Medium Bead Production	245
8.1.3	Bacteria Culture	247
8.1.4	Cementation Medium and Treatments	247
8.1.5	Leaching test	248
8.1.6	Column Preparation	248
8.1.7	Testing procedures	249
8.2	Results and Discussion	249
8.2.1	Leaching Test.....	249
8.2.2	Columns Test P4.....	250
8.3	Conclusions.....	258
CHAPTER NINE.....		259
9	COLUMN STUDY FOUR: Cementation Medium Optimisation – Effect of Augmentation with Ammonium Chloride	259
9.1	Introduction.....	259
9.2	Materials and Methods.....	260
9.2.1	MICP Batch Test.....	260
9.2.2	Preparation of Cementation Medium	261
9.2.3	Bacteria Culture	262
9.2.4	Columns Preparation, Treatment and Testing.....	262

9.3	Results and Discussion	263
9.3.1	Batch Test Results.....	263
9.3.2	Material Properties.....	265
9.3.3	Columns Test P5.....	266
9.4	Conclusions.....	273
CHAPTER TEN.....		275
10	CONCLUSIONS AND RECOMMENDATIONS	275
10.1	Summary	275
10.2	Key Findings and Significance	277
10.3	Contributions to Knowledge	278
10.4	Suggested Improvements	279
10.5	Industrial Application	279
10.6	Challenges to Overcome	280
10.7	Future Work and Recommendations.....	281
BIBLIOGRAPHY.....		283
APPENDICES		299
A1: Product Data Sheets		299
A2: Schedule of Column Studies.....		302

TABLES AND FIGURES

Table 2-1. Web of Science summary of relevant research articles obtained from a search run on 28 th Oct. 2017.....	27
Table 2-2. Concentrations of cementation media reagents used in published sand column MICP experiments.....	49
Table 2-3. Direct application methods for cementation medium delivery for healing of porous construction materials via MICP.....	65
Table 2-4. Immobilisation methods for cementation medium storage and delivery for healing of porous construction materials via MICP.....	66
Table 2-5. Encapsulation methods for cementation medium storage and delivery for healing of porous construction materials via MICP.....	69
Table 3-1. Assessment of SH-MICP process suitability for selected geotechnical applications.	83
Table 3-2. Immobilising and encapsulating materials – evaluation for further investigation.....	86
Table 3-3. Advantages and disadvantages of selected immobilising and encapsulating materials.	87
Table 4-1. Culture, cementation, and sporulation media for use with <i>S. ureae</i>	90

Table 4-2. Culture, cementation and sporulation media for use with <i>S. pasteurii</i>	91
Table 4-3. Sterilisation procedures for chemicals used.	91
Table 4-4. Chemical composition and properties of Celite S. (Sigma Aldrich 2017).	97
Table 4-5. Typical chemical analysis of Harborlite (all grades).	99
Table 4-6. Reported chemical compositions of coir, jute and hemp fibres.	102
Table 5-1. Materials utilised for immobilisation in cementitious materials incorporating MICP.	129
Table 5-2. Properties of diatomaceous earth (Celite S) and expanded perlite (Harborlite 800) powders.	130
Table 5-3. Precursor chemicals and nutrients used in the cementation media, and sterilisation methods.	131
Table 5-4. Samples prepared for leaching tests.	145
Table 5-5. Parameters of kiln-dried silica sand, as derived from the particle size distribution curve.	149
Table 5-6. CFU from spores contained with biocement mini columns (Sample 2 with EP).	151
Table 5-7. Samples prepared for testing of coatings on CM loaded EP.	152
Table 6-1. Garside WFSS sand properties, as given by Aggregate Industries.	156
Table 6-2. Constituents of Oxoid CM0001 nutrient broth.	156
Table 6-3. Molar quantities/ masses of precursor chemicals and nutrients in cementation media used to treat sand columns inoculated with <i>S. ureae</i> (CM1u) and prepared for immobilisation within carrier materials (CM2u).	157
Table 6-4. Summary of Column Tests	160
Table 6-5. Garside Sands washed fine silica sand parameters.	164
Table 6-6. Contents of columns prepared for Columns Test U1.	165
Table 6-7. Contents of columns prepared for Columns Test U2.	172
Table 6-8. Contents of columns prepared for Columns Test U3.	181
Table 6-9. Contents of columns prepared for Column Test U4.	186
Table 6-10. Contents of columns prepared for Columns Test P1.	190
Table 7-1. F60 sand properties (U.S. Silica Company).	201
Table 7-2. Composition of cementation media for use in column studies incorporating jute fibres and using <i>S. pasteurii</i>	203
Table 7-3. Biocementation treatment schedule for Column Test P2 and Column Test P3.	206
Table 7-4. Results from urease activity batch test.	209
Table 7-5. F60 sand parameters, as derived from the particle size distribution test results.	211
Table 7-6. Contents of columns prepared for Columns Test P2.	211
Table 7-7. Optical density of effluent discharged from 5 - 10 mm depth from Test P2 columns, during biocementation treatment two, following fixing of bacteria by treatment one.	212
Table 7-8. Moisture and CaCO ₃ contents of biocemented columns from Columns Test P2 (averages from triplicates).	220

Table 7-9. Contents of sand columns prepared for Columns Test P3.....	228
Table 7-10. Optical density of effluent discharged from 5 - 10 mm depth from Test P3 columns, during biocementation treatment two, following fixing of bacteria by treatment one.	229
Table 7-11. Moisture and CaCO ₃ contents of biocemented sand columns – Columns Test P3.....	237
Table 8-1. Cementation media prepared for Columns Test P4.....	247
Table 8-2. Schedule of biocementation treatments for Columns Test P4.....	248
Table 8-3. Contents of columns prepared for Columns Test P4.....	248
Table 8-4. UCS test results for Columns Test P4, reported to 2 significant figures.	254
Table 9-1. Contents of tubes prepared for batch test to test effect of augmentation of cementation medium with ammonium chloride and sodium bicarbonate.	261
Table 9-2. Cementation medium components and sterilisation methods used for Columns Test P5.	262
Table 9-3. Column treatment schedule for Columns Test P5.	262
Table 9-4. F65 sand parameters, as derived from lab test data for particle size distribution.	266
Table 9-5. Optical density of effluent discharged from 5 - 10 mm depth from Test P5 columns, during biocementation treatment two, following fixing of bacteria by treatment one.	267
Table 9-6. UCS Test Parameters for Columns Test P5.....	272
Figure 2-1. Search terms identified through initial reading of relevant literature.....	26
Figure 2-2. Key words and identified themes in relevant literature.....	29
Figure 2-3. ACC to Calcite mechanism (Rodriguez-Blanco et al. 2011).	36
Figure 2-4. Unconfined compressive strength (UCS) and splitting tensile strength (TS) test results comparing strengths of specimens tested in saturated and dry states (Zhao et al. 2020).....	38
Figure 2-5. Quantity of calcium carbonate precipitated over time within 100 mm x 47 mm dia. sand columns inoculated with <i>S. pasteurii</i> and treated with a (1.0 M) urea- (0.5 M) calcium chloride medium (Peng and Liu 2019).....	41
Figure 2-6. Relationship between initial Ca concentration of the cementation media and the consumed Ca concentrations following MICP, adapted from Yasuhara et al. (2012).....	46
Figure 3-1. Healing MICP process - system overview.	73
Figure 3-2. Self-healing MICP process covering formation of biocement and activation of self-healing response following damage and water entry into the system.....	75
Figure 3-3. Immobilisation mechanisms of carrier materials - binding to a carrier surface (a), entrapment in a porous matrix (b) and entrapment within a hydrogel (c).	77
Figure 3-4. Optimum particle size for MICP in relation to soil classification.....	78
Figure 3-5. Cross section of an earth-fill dam, showing core cracks (A - extending from interior to downstream side of the core; B- extending across the core, adapted from Kakuturu and Reddi (2006).	80

Figure 4-1. Bacterial maintenance and culturing process.	93
Figure 4-2. Serial dilution process, adapted from OpenStax (2016).....	94
Figure 4-3. Photograph of sample of diatomaceous earth (Celite S.).	97
Figure 4-4. SEM image of diatomaceous earth at 1500x magnification.....	98
Figure 4-5. Photograph of sample of expanded perlite (Harborlite 800).....	98
Figure 4-6. SEM image of Expanded Perlite (Harborlite 800) at 1000x magnification.	99
Figure 4-7. Photograph of hemp and jute fibres used in experiments – prior to cutting and washing.	100
Figure 4-8. Photograph of coir fibres used in experiments.....	100
Figure 4-9. Internal microstructures of hemp (a)Marrot et al. (2013), coir (b), Fidelis et al. (2013), jute (c)Fidelis et al. (2013), (d), Hamad et al. (2017).	101
Figure 4-10. Photograph of expanded perlite - following immobilisation of cementation medium, drying and separation of granules using a pestle and mortar.	104
Figure 4-11. Photograph showing a triplicate set of hemp fibres, after they have been soaked in concentrated cementation medium, transferred to gauze and dried, prior to mixing with sand for use in column studies.	104
Figure 4-12. Photograph showing jute fibres, after they have been loaded with concentrated cementation medium, dried and then separated by hand.....	105
Figure 4-13. Photograph showing 1 g of jute fibres resting on gauze, after the fibres have been sprayed with concentrated cementation medium.	106
Figure 4-14. Diagram of sand column apparatus showing side of column and cross section through the column.	109
Figure 4-15. Photograph of assembled sand columns attached to the front and back of the column frame in sets of triplicates, while cementation medium is being injected into the base of the columns using a peristaltic pump.....	110
Figure 4-16. Photograph showing a perforated disk - following use within column to contain sand and to ensure even flow of cementation medium through the column, with layer of glass wool beneath which sits between the sand column and disk.	110
Figure 4-17. Photograph showing the inlet end of a column during assembly, with silicone plug inserted into the inlet hole within the bung to prevent the cementation medium draining during filling of the column.	111
Figure 4-18. Column during assembly – ready for filling via wet pluviation.....	113
Figure 4-19. Calibration curve for nesslerisation.....	116
Figure 5-1. Overview of preliminary testing	121
Figure 5-2. Photograph showing steaming of microscope slide with bacterial spores and cells fixed on the surface and malachite green spore stain applied.	122

Figure 5-3. Light microscope images of green stained spores and red stained vegetative cells of <i>S. ureae</i> (a) and <i>S. pasteurii</i> (b) following chemically induced sporulation of bacterial cells.	123
Figure 5-4. Light microscope images of green stained spores and red stained vegetative cells of <i>S. ureae</i> and <i>S. pasteurii</i> observed at 80x magnification, following incubation of liquid broth cultures at 30 °C for five days (a-b) and ten days (c-d) to observe effects of nutrient depletion on spore production. .	124
Figure 5-5. Light microscope images of green stained spores and red stained vegetative cells of <i>S. ureae</i> , following incubation of liquid broth cultures at a) 30 °C for five days, b) 40 °C for five days, c) 30 °C for five days followed by 40 °C for five days and d) 40 °C for ten days.	125
Figure 5-6. Growth curves for <i>S. ureae</i> in growth medium (GM) and cementation medium without a calcium source (CM) at 30 °C, 150 rpm. Error bars show standard errors of means of triplicates.....	127
Figure 5-7. Curves showing growth of <i>S. pasteurii</i> at 23 °C and 30 °C, 150 rpm. Error bars show standard errors of means of triplicates.....	128
Figure 5-8. Diagram showing the vacuum assisted treatment process for the mini sand columns. The 50 ml centrifuge tube containing the sand is shown placed firmly into the neck of the conical filter flask, with the conical flask connected to a vacuum which draws the cementation medium down through the column while the extracted effluent collects in the flask.	138
Figure 5-9. 50 mL polypropylene centrifuge tubes containing the mini columns of biocemented sand and biocemented sand and expanded perlite mixture in triplicates.....	138
Figure 5-10. Quantities of dried cementation medium immobilised by one-gram samples of coir (C), jute (J), expanded perlite (EP) and diatomaceous earth (DE), following repeated loadings with concentrated cementation medium.....	140
Figure 5-11. Quantities of dried cementation medium immobilised per cubic centimetre of coir (C), jute (J), expanded perlite (EP) and diatomaceous earth (DE), following repeated loadings with concentrated cementation medium.	140
Figure 5-12. Cementation medium immobilised by 1 g samples of hemp following repeated loadings.	141
Figure 5-13. Release of immobilised cementation medium into deionised water over a 24 h period from jute, expanded perlite and diatomaceous earth, using a quantity of water equal to ten times the mass of the immobilised cementation medium.	142
Figure 5-14. Percentage of immobilised cementation medium released from carrier materials into deionised water over a fifty-hour period, at 21 °C, with error bars showing standard errors of the means for the triplicates.	143
Figure 5-15. pH of solutions containing cementation medium leached from the carrier materials following soaking of the loaded carrier materials in deionised water for one-, three-, six- and twenty-four-hour periods at 21 °C, with error bars showing standard errors of the means for the triplicates.	143

Figure 5-16. Percentage of immobilised cementation medium released from hemp into deionised water over a twenty-four-hour period, at 21 °C, with error bars showing standard errors of the means for the triplicates..... 144

Figure 5-17. Percentages of immobilised cementation medium released from hemp and jute fibres into a solution containing cementation medium (CM, as used to treat columns in Chapter Six) and into deionised water (W) following an initial 24 h period of soaking (Release 1) and a subsequent 24 h period of soaking after the solutions surrounding the fibres are drained and replaced (Release 2). Error bars show standard errors of the means for the triplicates..... 145

Figure 5-18. Immobilised cementation medium released from EP and DE into solutions of cementation media of varying concentration. Error bars show standard errors of the means for the triplicates..... 146

Figure 5-19. Concentrations of sodium, ammonium and calcium ions in solutions containing cementation medium constituents leached from loaded jute fibres after 24-h and 48-h of soaking samples of CM loaded jute fibres in deionised water, with liquid drained and fresh water added after the first 24-h soaking period. Error bars show standard errors of the means for the triplicates. 147

Figure 5-20. Calcium ion concentration of solutions containing cementation medium released from carriers and compared to standard medium as the control, measured one day and three days after inoculation of these solutions with *S. ureae*..... 148

Figure 5-21. pH of solutions containing cementation medium released from carriers, compared to standard cementation medium, before (Day 0) and after inoculation of the solutions with *S. ureae*. 148

Figure 5-22. Particle size distribution curve for industrial kiln-dried silica sand. 149

Figure 5-23. Calcium ion concentrations in effluent extracted during each biocementation treatment of mini columns containing sand only and sand mixed with expanded perlite immobilising cementation medium. Error bars show standard errors of the means for the triplicates..... 150

Figure 5-24. pH of effluent extracted during biocementation treatments of mini columns, compared to the initial pH of the cementation medium. Error bars show standard errors of the means for the triplicates..... 150

Figure 5-25. Colonies of *S. ureae* grown on plates of LB agar at 30 °C (with pen markings added to petri dish lids for ease of counting), shown 48 h after inoculation of the agar plates with the 10^{+3} and 10^{+4} dilutions of *S. ureae* contained within a 1 g sample taken from biocemented mini column two prepared using sand and CM loaded EP. 151

Figure 5-26. Concentration of calcium ions within solutions containing cementation medium leached from coated and uncoated expanded perlite over a 30 min period when subjected to shaking incubation of 150 rpm at 30 °C. Following the CM immobilisation process by 1 g samples of EP in triplicates, triplicate sets of the loaded EP had been sprayed with a sodium silicate – calcined kaolin solution, mixed with this solution, or left uncoated before immersion in deionised water to test the rate of leaching of the immobilised CM. Error bars show standard errors of the means for the triplicates..... 153

Figure 6-1. Photograph of prepared columns, showing apparatus used for the column studies completed at Cardiff University.	160
Figure 6-2. Photograph of the unconfined compression test apparatus used at Cardiff University, showing a column from Columns Test U2 being subjected to loading.	162
Figure 6-3 Particle size distribution of Garside Sands washed fine silica sand, as measured in the laboratory and provided by Aggregate Industries.	163
Figure 6-4. Proctor compaction test results showing the dry density – moisture content relationship for Garside washed fine silica sand, with the zero air voids line (red line) shown for reference.	164
Figure 6-5. pH of effluent from Test U1 columns following each biocementation treatment. Error bars show standard errors of the means for the triplicates.	166
Figure 6-6. Dissolved Oxygen concentration in effluent from Test U1 columns following each biocementation treatment. Error bars show standard errors of the means for the triplicates.	167
Figure 6-7. Calcium ion concentration, as measured using ICP-OES, in Test U1 columns effluent, following biocementation treatments 1 to 4, 6, 8 and 10. Error bars show standard errors of the means for the triplicates.	168
Figure 6-8. UCS test results for Test U1 biocemented columns containing hemp (H1 – H3), jute (J1 – J3) and sand only (C1 – C3), following UCS1 (a – c) and UCS2 (d - f).	169
Figure 6-9. Results from UCS1 and UCS2 for Columns Test U1, showing peak and residual strengths from UCS1 and peak strengths from UCS2.	170
Figure 6-10. Photographs of columns from Test U1 following failure during UCS1 (a-i) and UCS2 (j-r), with annotation shown above clear failure planes observed during testing.	171
Figure 6-11. pH of effluent from Test U2 columns following each biocementation treatment. Error bars show standard errors of the means for the triplicates.	173
Figure 6-12. Calcium ion concentration, as measured using ICP-OES, in Test U2 columns effluent, following biocementation treatments 1, 3, 5, 7 and 9. Error bars show standard errors of the means for the triplicates.	174
Figure 6-13. UCS test results for Test U2 biocemented columns containing treated jute (J1 – J3), untreated jute (J4 – J6), hemp (H1 – H3), and sand only (C1 – C3), following UCS1 (a, c, e, g) and UCS2 (b, d, f, h).	175
Figure 6-14. Results from UCS1 and UCS2 for Columns Test U2, showing peak and residual strengths from UCS1 and peak strengths from UCS2.	176
Figure 6-15. Photographs of Test U2 columns during UCS1 following failure, with annotation below observed failure planes.	177
Figure 6-16. Images of Test U2 columns during UCS2 following failure, with annotation below observed failure planes.	177
Figure 6-17. SEM images of samples taken from Test U2 columns J1 (a – c) H1 (a -c) and C1 (a – c), with calcite precipitate labelled where clearly identifiable.	178

Figure 6-18. XRD analysis of sample from Test U2 column J1, of biocement produced using *S. ureae*. Green peaks show the measured spectra for SiO₂ (sand) and blue peaks show the spectra for calcium carbonate (vaterite). 179

Figure 6-19. XRD analysis of sample from Test U2 column H1, of biocement produced using *S. ureae*. Green peaks show the measured spectra for SiO₂ (sand) and blue peaks show the spectra for calcium carbonate (vaterite). 179

Figure 6-20. XRD analysis of sample from column H1, from columns test U2 with *S. ureae*. Green peaks show the spectra for SiO₂ (sand) and blue for calcium carbonate (calcite)..... 180

Figure 6-21. XRD analysis of sample from Test U2 column C1. Zoomed-in image of the spectra showing a blue peak indicating calcite near position 30. The dark green horizontal line shows the background level. 180

Figure 6-22. pH of effluent from Test U3 columns following each biocementation treatment. Error bars show standard errors of the means for the triplicates..... 182

Figure 6-23. Calcium ion concentration, as measured using ICP-OES, in Test U3 columns effluent, following biocementation treatments 1, 3, 5, 7 and 9. Error bars show standard errors of the means for the triplicates. 182

Figure 6-24. UCS test results for Test U3 biocemented columns containing treated jute (J1 – J3), hemp (H1 – H3), jute and hemp (HJ1 – HJ3) and sand only (C1 – C3), following UCS1 (a, c, e, g) and UCS2 (b, d, f, h). 184

Figure 6-25. Results from UCS1 and UCS2 for Columns Test U3, showing peak and residual strengths from UCS1 and peak strengths from UCS2..... 185

Figure 6-26. Photographs of columns from Columns Test U3 shortly after failure during UCS1, with annotations showing approximate locations of failure planes observed. 185

Figure 6-27. Photographs of columns from Columns Test U3 shortly after failure during UCS2, with annotations showing locations of failure planes observed. 186

Figure 6-28. pH of effluent from Test U4 columns following each biocementation treatment. Error bars show standard errors of the means for the triplicates..... 187

Figure 6-29. Calcium ion concentration, as measured using ICP-OES, in Test U4 columns effluent, following biocementation treatments 1, 3, 7 and 9. Error bars show standard errors of the means for the triplicates. 188

Figure 6-30. UCS test results for Test U4 biocemented columns containing expanded perlite (a) and sand only (b). 189

Figure 6-31. Photographs of biocemented columns from Test U4 taken shortly after failure during the UCS test, with annotations showing approximate locations of observed failure planes..... 189

Figure 6-32. pH of effluent from Test P1 columns following each biocementation treatment. Error bars show standard errors of the means for the triplicates..... 190

Figure 6-33. Calcium ion concentration, as measured using ICP-OES, in Test P1 columns effluent, following biocementation treatments 1, 3, 5 and 7. Error bars show standard errors of the means for the triplicates.....	191
Figure 6-34. UCS test results for Test P1 biocemented columns containing jute (J1-J3), hemp (H1-H3) and sand only (C1-C3).....	192
Figure 6-35. Photographs of biocemented Test P1 columns taken shortly after failure during the UCS test, with annotations highlighting approximate locations of observed failure planes.	192
Figure 6-36. Growth of <i>S. ureae</i> on LB agar plates inoculated with solutions prepared by taking 1 g samples from selected biocemented columns and dispersing these in a sterile saline solution and pipetting and spreading 10 μ L of the solution onto the plates, followed by 48 h of incubation at 30 $^{\circ}$ C. Prior to testing of the columns these had been stored for one and a half years following the production of columns 5P. Samples were taken from Test 2U columns J1(a), H1(b) and C1(c), Test 3U columns J1(d), H1(e), and HJ1(f), Test 5U columns J1 (g), H1 (h) and C1 (i) and Test 4U column EP1 (j). Control plate (k) was not inoculated.	194
Figure 7-1. Photograph of prepared columns, showing apparatus used for the column studies completed at Arizona State University.....	205
Figure 7-2. Calibration curve for Cole-parmer Masterflex L/S peristaltic pump, using Tygon S3 2-stop 2.79 mm ID micropore tubing and tap water as the test fluid.....	206
Figure 7-3. Effect of pH on specific urease activity in liquid broth cultures of <i>S. pasteurii</i> , with error bars showing standard errors of the means.	210
Figure 7-4. Proctor compaction curves, for F60 sand only and an F60 sand and jute fibre mixture. .	210
Figure 7-5. Particle size distribution of F60 sand, as measured in the lab and as per product data provided by US Silica.	211
Figure 7-6. Electrical conductivity and pH of effluent from Test P2 columns following biocementation treatments 1 (a,b), 2 (c,d), 3 (e,f), 4 (g,h) and 5 (i,j), with error bars showing standard errors of the means for the triplicates.	214
Figure 7-7. Cumulative reduction in concentration of calcium ions in Test P2 columns effluent following biocementation treatments one to four.	215
Figure 7-8. Chemical conversion efficiency, as determined from Ion Chromatography measurement of calcium ions within effluent from Test P2 columns following each biocementation treatment, with error bars showing standard error of means.....	216
Figure 7-9. Unconfined compressive strength test results for UCS1 of Test P2 columns following biocementation treatment five (a–c), and UCS2 following column reconstitution, flushing, saturation with water and eight days of curing to test for self-healing (d–f).	217
Figure 7-10. Photographic images of columns J1 to J3 (a–c), J4 to J6 (d–f) and C1 to C3 (g–i), following the onset of failure during UCS1 for Columns Test P2. Annotations indicate shear failure planes where observed and the vertical failure in column J5.....	218

Figure 7-11. Photographic images of columns J1 to J3 (a–c), J4 to J6 (d–f) and C1 to C3 (g–i), following the onset of failure during unconfined compressive strength test 2 for Columns Test P2. Annotations indicate direction and location of shear failure planes where observed and the vertical failure in J5.	219
Figure 7-12. Results from UCS1 and UCS2 for Columns Test P2, showing peak and residual strengths from UCS1 and peak strengths from UCS2.	220
Figure 7-13. Photograph of columns from Test P2 following UCS2 and oven drying at 105°C.	221
Figure 7-14. Average calcium carbonate content of Test P2 columns, as measured using a Calcimeter, showing relationship to UCS1.	222
Figure 7-15. Distribution of calcium carbonate precipitated at the base (B), centre (C), and top (T) of Test P2 columns, with error bars showing standard errors of the means for the triplicates.	223
Figure 7-16. Box and whisker plot showing the distribution of measurements of jute fibre diameters in samples from columns J1 and J4 of Columns Test P2, observed and measured using a scanning electron microscope.	223
Figure 7-17. SEM images of samples from Test P2 biocemented sand column J1 containing jute (a to d), column J4 containing treated jute (e, f), and sand only control column C1 (g, h).	225
Figure 7-18. Vaterite grains composed of flakes of approximately 10 to 20 μm , as observed by a) Hu et al. (2012) and b) Fricke et al. (2006).	226
Figure 7-19. X-ray powder diffraction (XRD) analysis of sample from column J1, Test P2, showing identified peaks of quartz (q), calcite (c) and vaterite (v).	227
Figure 7-20. XRD analysis of sample from column J4, Test P2, showing identified peaks of quartz (q), calcite (c) and vaterite (v). The peak at 21 [$^{\circ}2\theta$] is identified as vaterite based on results for J1 and C1, however results for J4 alone suggest this could be also be quartz.	227
Figure 7-21. XRD analysis of sample from column C1, Test P2, showing identified peaks of quartz (q), calcite (c) and vaterite (v).	228
Figure 7-22: Electrical conductivity and pH of effluent from Test P3 columns following biocementation treatments 1 (a,b), 2 (c,d), 3 (e,f), 4 (g,h) and 5 (i,j), with error bars showing standard errors of the means for the triplicates.	230
Figure 7-23. Cumulative reduction in concentration of calcium ions in Test P3 columns effluent following biocementation treatments one to four.	231
Figure 7-24. Chemical conversion efficiency, as determined from Ion Chromatography measurement of calcium ions within effluent from Test P3 columns following each biocementation treatment, with error bars showing standard errors of means for the triplicate sets of columns.	232
Figure 7-25. Combined results from Column Tests P2 (6 g/L nutrients in CM) and P3 (3 g/L nutrients in CM) showing cumulative depletion of calcium ions over time following biocementation treatments one to four. 500 mmol calcium ions are supplied with each treatment.	233

Figure 7-26. Unconfined compressive strength test results for UCS1 of Test P3 columns following biocementation treatment five (a–c), and UCS2 following column reconstitution, flushing, saturation with water and eight days of curing to test for self-healing (d–f).	234
Figure 7-27. Images of columns J1 to J3 (a–c), J4 to J6 (d–f) and C1 to C3 (g–i), following the onset of failure during unconfined compressive strength test 1, for Columns Test P3. Annotations indicate direction and location of shearing plane.	235
Figure 7-28. Images of columns J1 to J3 (a–c), J4 to J6 (d–f) and C1 to C3 (g–i), following the onset of failure during unconfined compressive strength test 2 (healing stage) of Columns Test P3.	236
Figure 7-29. Results from UCS1 and UCS2 for Columns Test P3, showing peak and residual strengths from UCS1 and peak strengths from UCS2.	237
Figure 7-30. Average calcium carbonate content of Test P3 columns, as measured using a Calcimeter, showing relationship to UCS1.	238
Figure 7-31. Distribution of calcium carbonate precipitated at the base (B), centre (C), and top (T) of Test P3 columns, with error bars showing standard errors of the means for the triplicates.	238
Figure 7-32. SEM images of samples from Test P3 biocemented sand columns containing jute (a), treated jute (b), and sand only controls (c).	239
Figure 7-33. EDX spectrum and elemental analysis of sample from Test P3 column J1.	240
Figure 7-34. EDX spectrum and elemental analysis of sample from Test P3, column J4.	240
Figure 7-35. EDX spectrum and elemental analysis of sample from Test P3 column C1.	241
Figure 8-1. Photograph showing the production of alginate-based hydrogel beads encapsulating cementation medium and the apparatus used for bead extrusion.	246
Figure 8-2. Beaker containing alginate-based beads encapsulating cementation medium.	246
Figure 8-3. Dried alginate- based hydrogel beads encapsulating cementation medium.	247
Figure 8-4. Concentrations of sodium, ammonium and calcium ions in solutions containing cementation medium constituents leached from alginate-based hydrogel beads after 24-h and 48-h periods of soaking samples of beads in deionised water, with liquid drained and fresh water added after the first 24-h soaking period. Error bars show standard errors of the means for the triplicates.	250
Figure 8-5. Electrical conductivity and pH of effluent from Test P4 columns following biocementation treatments 1 (a,b), 2 (c,d), 3 (e,f), 4 (g,h) and 5 (i,j), with error bars showing standard errors of the means for the duplicates.	251
Figure 8-6. Chemical conversion efficiency, as determined from Ion Chromatography measurement of calcium ions within effluent from Test P4 columns following each biocementation treatment, with error bars showing standard errors of means for the duplicate sets of columns.	252
Figure 8-7. Photographic images of columns B1 to B2 (a–b), B3 to B4 (c–d) and C1 to C2 (e–f), following the onset of failure during unconfined compressive strength test 1 for Columns Test P4. Annotations indicate direction and location of shearing plane.	253

Figure 8-8. Photographic images of columns B1 to B2 (a–b), B3 to B4 (c–d) and C1 to C2 (e–f), following the onset of failure during unconfined compressive strength test 2, for columns Test P4. Annotations indicate direction and location of shearing plane.	254
Figure 8-9. Unconfined compressive strength test results for UCS1 of Test P4 columns following biocementation treatment four (a, c, e), and UCS2 following column reconstitution, flushing, saturation with water and eight days of curing to test for self-healing (b, d, f).	255
Figure 8-10. Distribution of calcium carbonate precipitated at the base (B), centre (C), and top (T) of Test P4 columns, with error bars showing standard errors of the means for the duplicates.	256
Figure 8-11. Relationship between UCS1 and CaCO ₃ content of Test P4 columns.	257
Figure 8-12. Biocemented column sections showing beads at locations of failure within biocemented Test P4 columns containing alginate-based hydrogel beads.	257
Figure 9-1. Electrical conductivity following 24 h incubation at 23 °C of <i>S. pasteurii</i> inoculated tubes containing urea-calcium cementation media and urea-calcium cementation media augmented with ammonium chloride. For each media variation four sets of triplicates were prepared with varying calcium chloride dihydrate content. Error bars show standard errors of the means for the triplicates.	263
Figure 9-2. pH of effluent following 24 h incubation at 23 °C of <i>S. pasteurii</i> inoculated tubes containing urea-calcium cementation media and urea-calcium cementation media augmented with ammonium chloride. For each media variation four sets of triplicates were prepared with varying calcium chloride dihydrate content. Error bars show standard errors of the means for the triplicates.	264
Figure 9-3. CaCO ₃ precipitated after 24 h incubation at 23 °C of <i>S. pasteurii</i> inoculated tubes containing urea-calcium cementation media and urea-calcium cementation media augmented with ammonium chloride. For each media variation four sets of triplicates were prepared with varying calcium chloride dihydrate content. Error bars show standard errors of the means for the triplicates.	264
Figure 9-4. Proctor compaction test results for Ottawa F65 sand.	265
Figure 9-5. Particle size distribution of F65 sand, as measured in the lab and as per product data provided by US Silica.	266
Figure 9-6. Electrical conductivity and pH of effluent from Test P5 columns following biocementation treatments 1 (a,b), 2 (c,d), 3 (e,f) and 4 (g,h), with error bars showing standard errors of the means for the triplicates.	268
Figure 9-7. Chemical conversion efficiency over the eight-day treatment process for Columns Test P5, based on measurement of calcium ions in column effluent, with retention times of 16 h, 22 h, 24 h and 120 h for treatments one to four respectively. Error bars represent the standard errors of the means for each triplicate set of columns.	269
Figure 9-8. Efficiency of substrate conversion to form ammonium ions based on urea concentration of medium and concentration of ammonium ions in Test P5 columns effluent as determined by	

Nesslerisation, and taking into account added ammonium chloride, with error bars showing standard errors of means.....	270
Figure 9-9. Unconfined compressive strength (UCS) test results for Test P5 columns 1 to 3 (a) and 4 to 6 (b).....	271
Figure 9-10. Photographic images of Test P5 columns 1 to 6 during UCS testing, shortly after failure, with annotation showing the approximate path of the shear failure.	271
Figure 9-11. Average calcium carbonate content of Test P5 columns, as measured using a Calcimeter, showing relationship to UCS results.	272
Figure 9-12. Distribution of calcium carbonate precipitated at the base (B), centre (C), and top (T) of Test P5 columns, with error bars showing standard errors of the means for the triplicates.....	273

1 INTRODUCTION

1.1 Overview and Background

Microbially mediated self-healing, as an autonomic process, is of particular interest for use in construction for ground improvement, to enable the development of low cost, sustainable, and environmentally friendly biocements and biogroups. Soil properties often need to be enhanced to support infrastructure, to help meet the needs of a growing population (Montoya and Dejong 2013). Microbially induced calcium carbonate precipitation (MICP) can improve the mechanical properties of loose, saturated sand, by increasing its strength and stiffness and by reducing its tendency to dilate (Montoya and Dejong 2013). Like other construction materials, biocement will be subject to damage and deterioration over time. Under loading (shear, tension, compression) the calcium carbonate binding between the silica sand particles may fail. The likely failure mechanism being a fracture within the precipitated calcium carbonate or between the precipitate and the silica sand particles (DeJong et al. 2010). Successful application of self-healing microbially induced calcium carbonate precipitation could potentially reduce infrastructure maintenance and repair costs and improve the durability and sustainability of geotechnical structures.

Healing of biocement has previously been achieved by injecting the nutrients and precursor chemicals (cementation medium) required for MICP into degraded biocement (Montoya and Dejong 2013; Botusharova 2017). These studies demonstrated the ability of MICP treated sand structures to self-heal, in principle. Studies by Botusharova (2017) suggested that bacteria can survive within a biocemented sand monolith, in a dormant state, and germinate upon damage to the encapsulating precipitate, to enable the degraded biocement to automatically heal damage through calcium carbonate precipitation. To enable biocemented sand to self-heal, provided that viable spores of a suitable bacterium are present, would require a store of the cementation medium within the biocemented sand matrix. This research explores the use of additives (carrier materials) to facilitate the storage and release of cementation medium within a biocemented sand matrix, to promote self-healing.

The use of carrier materials to store and supply cementation medium is a new concept in respect of studies on self-healing of biocemented sand or soil structures. Studies on self-healing of cementitious materials have utilised a variety of porous materials to immobilise bacteria and/or cementation medium. Within cementitious materials, immobilisation has principally been used to protect bacterial cells/spores from the mechanical forces exerted during the mixing stage of concrete or mortar production

and from the highly alkaline environment within concrete and mortar. These carrier materials may also be used as internal nutrient reservoirs (Bundur et al. 2017). Reference to nutrients within this context refers to the nutrients and precursor chemicals, otherwise known as the cementation medium, required for MICP. Immobilisation has been reported to be an efficient approach for bacteria-based self-healing in cementitious materials (Zhang et al. 2017b).

This research utilises MICP to produce biocement through ureolysis. Ureolysis increases the alkalinity of fluid in soil/ sand pore spaces as a result of the degradation of urea to carbonate and ammonium, and induces calcium carbonate precipitation. To enable long term self-healing, the bacteria used for biocementation will need to be able to sporulate to ensure its survival within the biocemented soil/ sand matrix. Ureolytic *Sporosarcina ureae* and *Sporosarcina pasteurii* were selected for use in this research due to their spore forming ability.

1.2 Aim, Objectives and Scope of Research

1.2.1 Aims

Using a biomimetic approach, this project aimed to enhance sand/sandy soil structures, to improve mechanical properties while also developing a material which can adapt to its environment, develop immunity to damage and thus be more resilient, and self-heal when damaged or deteriorated. This will improve the reliability, performance and sustainability of geotechnical structures.

1.2.2 Objectives

The following objectives were achieved:

- 1) Establishing possible mechanisms for the delivery of the nutrients and precursor chemicals required for self-healing via MICP.
- 2) Ascertaining which of the identified mechanisms may be suitable for use within sand/ soil systems, to enable autonomic self-healing of geotechnical structures.
- 3) Selection of suitable bacteria to promote MICP, and furthermore self-healing via MICP. Investigation of the mechanical performance of biocemented sand columns produced via MICP using different types of ureolytic bacteria and nutrients. Establishing long-term viability of these bacteria within a biocemented sand matrix (within time constraints of this research).
- 4) Optimisation of the cementation medium to improve MICP process efficiency and facilitate a high rate of bacterial activity and thus efficient chemical conversion across multiple consecutive MICP treatments.
- 5) Determination of the effect of selected additives (carrier materials) on the strength of biocemented sand columns and on the MICP process.

- 6) Investigation of the self-healing response following physical damage to biocemented sand columns containing stores of nutrients and precursor chemicals immobilised by carrier materials.

1.2.3 Scope

The primary aim of this research project had been to further prior research on self-healing of biocemented sand, to embed self-healing capability within the biocemented material. The method of injecting cementation medium, following damage to the biocemented sand structure, had shown that this material can be healed as strength prior to damage could be regained (Montoya and Dejong 2013; Botusharova 2017). Past approaches were based on vegetative cells of bacteria being present (Montoya and Dejong 2013) or the assumption that after drying a biocemented sand for three weeks at 30 °C there would only be spores of bacteria present which could regenerate to enable self-healing (Botusharova 2017). Self-healing resulting from regeneration of spores has not however been proven.

Prior to this research, autonomous self-healing had only been a subject of research in the content of cementitious materials such as concrete and mortar. This is a novel area of research in relation to biocemented geomaterials. A review of the literature in this area concerning cementitious materials and self-healing had given some insight into the bio-based mechanisms which enabled self-healing of concrete and mortar, and this provided a starting point for this doctoral project. This project focusses on self-healing via MICP, initiated by ureolytic bacteria. The scope otherwise for exploring mechanisms to enable a biocemented geotechnical structure to self-heal autonomously were broader than could be covered within the time constraints of this doctoral project. Taking into consideration the facilities and resources available, the research undertaken concentrated on immobilisation as a mechanism for the storage and supply of cementation medium within a biocemented sand matrix to enable self-healing. In addition, alginate-based hydrogel beads have been developed and tested as a means of encapsulating cementation medium, this being the extent to which encapsulation could be investigated in this project.

Since any additives within the biocemented sand matrix would likely impact on the properties of the biocemented material, and on the MICP process, this effect has also been studied as part of this research. The effect of the additives tested was found in some cases to have a significant impact on the shear strength of biocemented sand and on the MICP process efficiency. The significance of these findings led to more focus on this aspect as the studies progressed. It is envisaged that this research may assist with furthering research into self-healing MICP applied to other geo-materials such as stone. Self-healing MICP (SH-MICP) has the potential to be used in a variety of civil and environmental engineering applications.

1.3 Thesis Structure

This thesis consists of ten chapters, the contents of chapters two through to ten are outlined below.

- Chapter 2** A review has been undertaken of the literature relating to self-healing MICP, with a focus on approaches to delivery of nutrients and precursor chemicals for self-healing of porous construction materials via MICP. The review also considers factors which affect MICP, and which would need to be taken into consideration in the experimental work undertaken.
- Chapter 3** The theoretical framework is detailed, outlining the research problem, approaches to this and the use case for self-healing microbially induced calcium carbonate precipitation (SH-MICP). Potential applications of this process have been considered. Through a critical comparison of the cementation medium supply mechanisms and evaluation of evidence obtained in research to date, carrier materials were selected for investigation.
- Chapter 4** The methodology and materials used in the studies undertaken are described. Firstly, this covers methods used to assess suitability of the selected bacteria. Detail is given of the selected immobilising and encapsulating carrier materials used in this research and of the procedures developed for immobilisation. The methodology for preparation of the sand columns and application of the MICP treatment process is detailed. This treatment procedure is updated in subsequent chapters based on findings, as explained where applicable. The geochemical and mineralogical analysis methods utilised have been summarised. The methodology applied to obtain the geotechnical parameters used to assess the material properties of the sand, carrier materials and biocemented columns is given.
- Chapter 5** This chapter covers the preliminary testing undertaken to further refine the selection of additives (carrier materials) to be used in subsequent column studies. Procedures and outcomes of selected bacterial sporulation studies, along with growth observations, are reported followed by details of the preliminary testing of the carrier materials. A series of batch tests are described and outcomes reported which cover the immobilisation and release of cementation medium from the carrier materials. This is followed by investigation of the effects of the carrier materials on MICP in aqueous solutions and a preliminary ‘mini-columns’ study incorporating expanded perlite.

Some of the content of this chapter has been published in the peer reviewed IOP Conference Series publication ‘Materials Science and Engineering’, as an open access paper on ‘Use of carrier materials to immobilise and supply cementation medium for microbially mediated self-healing of biocement’. This publication followed an oral presentation on this work at the ‘4th International Conference on Innovative Materials, Structures and Technologies’ (IMST2019) in Riga, 25-27 September 2019.

Chapter 6 This chapter focusses on column studies using *Sporosarcina ureae*, and selected carrier materials including jute, hemp and expanded perlite. At this stage *S. ureae* had been selected following on from a prior self-healing study at Cardiff University. The outcomes reported in this chapter informed changes to column study methodology, as employed in Chapter Seven and thereafter. Five column studies are reported in this chapter, the first four of which use *S. ureae*, followed by an initial study using *S. pasteurii*. Differing approaches to bacteria fixing within columns were tested, in addition to effects of incorporating the selected carrier materials within the sand columns. Self-healing responses were investigated using the unconfined compression test. At this stage columns had been dried following biocementation, to test for self-healing due to presence of bacterial spores. The leaching rate of immobilised cementation medium by the carrier materials during the MICP process over up to ten days was observed through measurement of calcium ions in column effluent.

Chapter 7 This chapter details column studies undertaken using *Sporosarcina pasteurii*, and jute fibre additions. The effect of jute fibres on the mechanical properties of biocemented sand and on the MICP process itself has been investigated. In addition to unconfined compressive strength testing to explore self-healing responses, a more in-depth geochemical analysis was implemented at this stage. This chapter reports on two studies undertaken, using differing quantities of nutrients (Oxoid CM0001) for the bacteria. At this stage of testing, the unconfined compressive strength of the columns in the saturated state was measured, and thereby testing undertaken for self-healing responses due to the presence of vegetative bacteria.

Part of this chapter, covering Column Test 6P, has been published in the MDPI ‘Materials’ journal, as an open access paper on ‘Effect of Jute Fibres on the Process of MICP and Properties of Biocemented Sand’.

- Chapter 8** Following on from testing of the immobilising carrier materials, this chapter covers the production of testing of alginate-based hydrogel beads, as a means of encapsulating the cementation medium constituents within biocemented sand columns. Geochemical analysis was undertaken, in addition to unconfined compressive strength testing to assess self-healing capability.
- Chapter 9** This chapter explores the case for augmentation of the cementation medium with ammonium chloride and sodium bicarbonate. The effects on the MICP process efficiency, for a multiple treatment MICP process, along with the effect on quantity of calcium carbonate precipitated and mechanical properties of biocemented sand have been tested and reported.
- Chapter 10** The concluding chapter brings together the key findings of the studies undertaken. Recommendations for improvements and for future research are given.

2 LITERATURE REVIEW

2.1 Introduction

Prior to this doctoral study, the literature concerning healing of biocemented sands was limited to the studies undertaken by Montoya and Dejong (2013) and Botusharova (2017). This project aimed to develop a biocemented sand-based material with built in capability to self-heal. Self-healing of cementitious construction materials has attracted significant interest in recent years, with a variety of mechanisms employed to embed self-healing capability. This review has been undertaken to inform possible approaches to the storage and supply of the cementation medium for the self-healing microbially induced calcium carbonate precipitation (SH-MICP) process in construction geo-materials, to enable long term autonomous self-healing of geotechnical structures.

To achieve this purpose, firstly, the state of the art was established in respect of self-healing and MICP in construction geo-materials, with a focus on sand and soil. This project aimed to further research previously undertaken in this area which demonstrated the concept of self-healing of biocemented sand. As this is a relatively new field of research, in respect of self-healing of geo-materials, research into nutrient and precursor chemical and bacteria delivery mechanisms for MICP has been reviewed for a range of porous construction materials, in particular cementitious materials. These mechanisms were then assessed to establish suitability for sand/soil and geotechnical applications, as detailed in Chapter Three.

To aid in fulfilling the purpose of this review as outlined above, a systematic process has been followed. This systematic literature review methodology originates from within the medical field, with the PRISMA (preferred reporting items for systematic reviews and meta-analyses) statement providing the guideline for the undertaking of systematic reviews in healthcare (Liberati et al. 2009). Systematic literature review methodology has also been developed for application in software engineering (Kitchenham 2004) and applied to Engineering and Education in general (Torres-Aravena et al. 2018). When adopting the systematic literature review process, a required component of the review is the reporting of the steps undertaken during this process (Institute of Medicine (US) Committee on Standards for Systematic Reviews of Comparative Effectiveness Research 2011), as follows.

2.2 Literature Review Process

From initial reading of papers relevant to self-healing microbially induced calcite precipitation in porous construction materials, search terms were identified. Figure 2-1 shows relationships between these search terms, with central themes among these highlighted in blue and yellow. The themes within the blue boxes are of direct relevance to this doctoral study, whilst those in yellow are outside of the scope in their context but may provide relevant insight into respect of cementation media delivery mechanisms and assessment of self-healing.

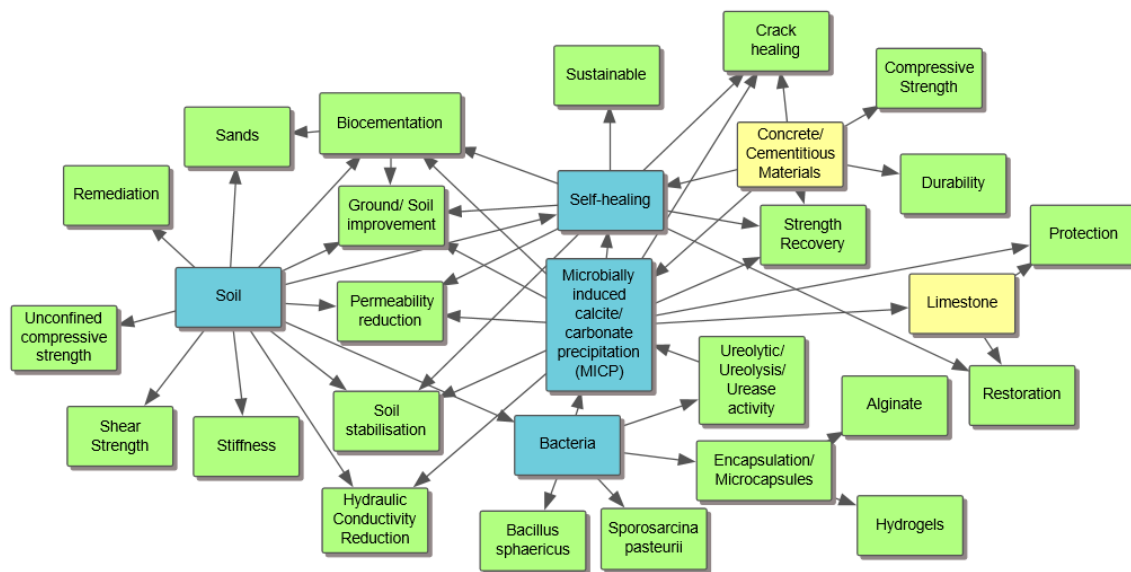


Figure 2-1. Search terms identified through initial reading of relevant literature.

Cementitious materials, although not in the scope of this project, have been included within this review to establish all possible approaches to cementation medium delivery for MICP in porous construction materials. This review encompasses a range of construction geomaterials, including stone, however experimental work was planned to focus on sand/ sandy soil (as a geomaterial) in this project. The central themes established in Figure 2-1 have been used as keywords in database searches, to obtain relevant papers for this review. Searches for literature were initially undertaken using the Web of Science (Core Collection) database on 28 October 2017. Table 2-1 summarises Web of Science search outputs. This had been compared to use of the Scopus database, in which ‘Self-healing AND Bacteria’ yielded one hundred and seventy-three results. Five additional relevant papers were obtained from the Scopus search, among which one additional cementation medium delivery mechanism was identified. Potential delivery mechanisms may have been missed if just one database was used. The Scopus database also contained a greater number of articles published in 2017 and hence a greater quantity of more recently published literature.

Table 2-1. Web of Science summary of relevant research articles obtained from a search run on 28th Oct. 2017.

Search Terms	Notes	No. Articles
Self-healing Microbially Induced Calc* Precipitation	<ul style="list-style-type: none"> • Takes into account variations in definition of MICP, where Calc* refers to calcite or calcium carbonate precipitation for example. • A separate search for ‘Self-healing Microbially Induced Carbonate Precipitation’ also produced 13 results. ‘MICP and self-healing’ produced 8 results. • Yielded limited results, too specific. 	13
Self-healing AND Bacteria	<ul style="list-style-type: none"> • This search also picked up all relevant papers found through the above search. • Results included a variety of cementation media/ bacteria delivery mechanisms. • An additional search was needed to establish the state of the art in self-healing MICP research applied to geological materials. • Sixty-six relevant papers once inclusion/ exclusion criteria applied. 	143
Self-healing AND Soil	<ul style="list-style-type: none"> • Some overlap with the above search, otherwise a few additional relevant results and other results not incorporating MICP, but could inform potential applications for self-healing in geotechnical structures. 	54
MICP AND Soil	<ul style="list-style-type: none"> • ‘MICP AND Soil’ yielded more search results than ‘Microbially Induced Calc* Precipitation AND Soil’. • One paper on healing of degraded MICP-treated sand. Twenty-six other papers possibly relevant, in particular to provide background knowledge. Demonstrated lack of research in relation to self-healing MICP in soils. 	144

The following inclusion criteria were applied when reviewing relevance of articles, with at least one criterion applying for an article to be deemed relevant.

- a) Application of MICP (to include ureolytic and non-ureolytic bacteria).
- b) Research into or applicable to self-healing.
- c) Applicable to porous construction materials.

Once relevant papers were identified, keywords from articles were again collated and relationships between these and themes identified, as shown in Figure 2-2. This had been used to inform the structure of the thematic literature review and areas this would cover and focus on. Following the initial literature search and review, email alerts were set up for both Scopus and Web of Science databases and updates added to the literature review during the course of this research up until March 2021.

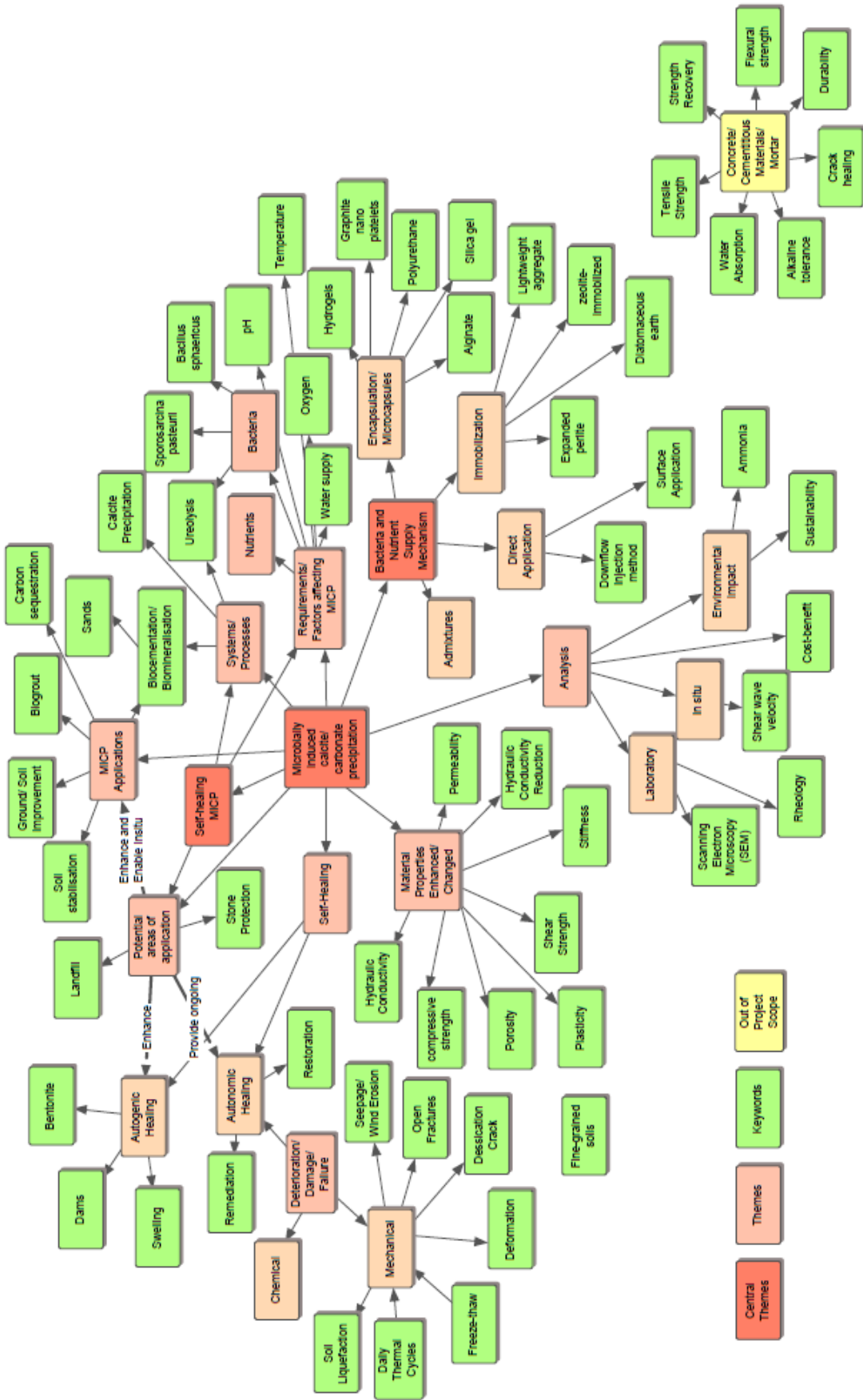


Figure 2-2. Key words and identified themes in relevant literature.

2.3 Self-healing Construction Materials

Self-healing, in the context of construction materials, can be defined as, ‘the partial or total recovery of at least one property of a material’, (Wiktor and Jonkers 2011). The development of self-healing construction materials has focused on cementitious materials to date, with little research undertaken into the development of self-healing sand or soil structures. Soil properties often need to be enhanced to support infrastructure, to help meet the needs of a growing population (Montoya and Dejong 2013). Microbially induced calcium carbonate precipitation (MICP) can improve the mechanical properties of loose, saturated sand, by increasing its strength and stiffness and by reducing its tendency to dilate (Montoya and Dejong 2013). There is a need for a natural and more sustainable solution to improve soil properties, allowing for infrastructure growth and mitigation against natural hazards. Successful application of self-healing microbially induced calcium carbonate precipitation can potentially reduce infrastructure maintenance and repair costs and improve the durability, resilience and sustainability of geotechnical structures.

The feasibility to incorporate the fundamental concepts behind self-healing into MICP installations has previously been investigated, with numerous studies demonstrating the potential of self-healing cementitious materials, but only two, by Montoya and Dejong (2013) and subsequently Botusharova (2017), which explore healing of sand which has been cemented via MICP. In these two studies, healing of biocement had been achieved by injecting the nutrients and precursor chemicals (cementation medium) required for MICP into degraded biocement. To enable a truly autonomous self-healing process, the nutrients and precursor chemicals will need to be readily available within the biocement matrix. Mechanisms developed to achieve self-healing healing within cementitious materials give some insight into possible approaches to the development of a self-healing biocement.

2.3.1 Mechanisms of Self-Healing

Self-healing mechanisms can be divided into two categories; naturally occurring ‘autogenous’ self-healing and imposed ‘autonomous’ self-healing (Al-Tabbaa and Harbottle 2015). This research focuses on bio-mediated self-healing as an autonomous process. Calcium carbonate precipitation is an example of a process which occurs naturally as a biologically controlled form of self-healing, and which can also be biologically induced/ engineered through the autonomic process of MICP.

2.3.1.1 Autogenic Healing

Autogenic self-healing may occur due to a range of physical, chemical and mechanical processes, among which calcium carbonate precipitation is reported to be the most significant factor influencing self-healing capabilities (Wiktor and Jonkers 2011). Examples of autogenic self-healing in construction materials include the swelling and hydration of cement pastes, precipitation of calcium carbonate

crystals and blockage of flow paths in concrete by deposits of impurities and cement fragments. Self-healing may also occur naturally in concrete through secondary hydration of unhydrated cement (Wang et al. 2012). Natural self-healing has been observed in geotechnical structures, such as compacted clay landfill liners (Aldaeef and Rayhani 2015) geotextile clay landfill liners (Parastar et al. 2017), earth-filled dams (Kakuturu and Reddi 2006), and streambanks (Midgley et al. 2013).

Compacted clay landfill liners may be subjected to chemical damage by leachate and also mechanical damage, both of which can have an effect on the hydraulic conductivity of natural clay soil, in which He et al. (2015) reported that the presence of cracks led to a 25-fold increase in hydraulic conductivity. He et al. (2015) found that desiccation cracks and bentonite content had the most significant effect on the hydraulic conductivity of compacted clay landfill liners, compared to chemical damage by acetic acid or calcium chloride (CaCl_2). The self-healing ability of geosynthetic clay liners (GCL) results from the swelling properties of bentonite and subsequent closure of holes in the GCL, whilst the low permeability of bentonite also helps reduce leaching (Wijaya et al. 2019).

Clayey soils can be subject to desiccation cracking as a result of wet-dry and freeze-thaw cycles. These desiccation cracks can threaten the stability of earth structures such as embankments, dams and levees (Tabassum and Bheemasetti 2020). Subsequent saturation or thawing can lead to partial closure of these cracks, which become re-bonded, resulting in natural self-healing (Aldaeef and Rayhani 2015). Eigenbrod (2003) investigated the natural self-healing capabilities of clay, by exposing clay soil to 3D freeze-thaw cycles. Resulting changes in hydraulic conductivities were attributed to natural self-healing processes. The hydraulic conductivities of fractured clays are known to decrease with increasing stress levels. Eigenbrod (2003) suggested that when the stress level nears the unconfined compressive strength, soil will be forced into open joints, this has not however been experimentally proven. Hydraulic conductivities of non-plastic soils remained unchanged after being subjected to freeze-thaw cycles. Eigenbrod (2003) notes that the self-healing of a fractured, highly plastic, fine grained soil is largely dependent on its swelling potential, as demonstrated in tests using bentonite clays. Bentonite has a strong self-healing capability (He et al. 2015), owing to its montmorillonite content (Parastar et al. 2017).

Core cracks in earth dams may be naturally self-healed through progressive erosion (Kakuturu and Reddi 2006). Cracks and concentrated leaks can develop in the otherwise impervious core of an earth dam as a result of tensile forces created by differential settlement, seismic activity or hydraulic fracturing (Kakuturu and Reddi 2006). Eroding streambanks have been observed to temporarily self-heal, through a process whereby failed bank material protects the bank toe from erosion (Midgley et al. 2013). Eroding material from a streambank can stem seepage, particularly if the soil is cohesive, restricting erosion until material protecting the base is removed by fluvial processes.

Tabassum and Bheemasetti (2020) investigated the effects of polydimethylsiloxane (PDMS) polymer and plate-like nano-montmorillonite (MMT) additions on cracking and healing behaviour of clayey soils. PDMS worked as an effective healing and sealing agent against desiccation cracks for both soils.

2.3.1.2 *Autonomic Healing*

Autonomic MICP may be introduced into a material through bioaugmentation or biostimulation, through the addition of native or non-native bacteria, or stimulation of indigenous bacteria respectively. Each approach requires the introduction of nutrients to feed the bacteria and precursor chemicals to enable calcium carbonate precipitation, which may vary dependent on the bacteria strain selected or naturally present within the soil. Bioaugmentation research has typically involved injecting cultured bacteria and cementation medium into sand (Harkes et al. 2010; van Paassen et al. 2010; Al Qabany and Soga 2013; Montoya and Dejong 2013), resulting in biocementation, which mimics the natural process of biomineralisation. Similar processes have been used for biostimulation (Burbank et al. 2011; Gat et al. 2016; Dhami et al. 2017).

The effectiveness of biostimulation will be site-specific and will be influenced by the nutrients and bacteria already present within the soil. Biostimulation can be favoured at sites with high organic carbon content (Dhami et al. 2017). Indigenous bacteria may also affect the process of bioaugmentation, should these bacteria compete with the bacteria introduced into the soil. Laboratory experiments undertaken to investigate MICP have often used sterilised sand samples, therefore little is known about the impact of indigenous bacteria on MICP. Liu et al. (2019) suggest that the presence of the indigenous bacteria decelerates the MICP process by competing with *S. pasteurii* for nutrients. Similarly, *S. pasteurii* activity has been found to be inhibited in the presence of *Cellulomonas flavigena* (Karnati et al. 2020). In comparison to naturally occurring processes, autonomic MICP stabilisation is not as constrained by microclimate since it can be achieved within several days (Chen et al. 2016).

Self-healing MICP, as an autonomous process, has largely been applied to cementitious materials to date, with limited research concerning geo-materials such as sand, soil and stone. Autonomic self-healing MICP has been achieved in cementitious materials through direct addition of bacteria and cementation medium, with limited success, and improved through encapsulating or immobilising bacteria in carrier materials within the concrete. Following crack propagation, the self-healing process is typically initiated by water entry. Incorporating self-healing via MICP within concrete has presented challenges due to the high pH within concrete, mechanical forces during mixing, and decreasing pore sizes within concrete during curing, all of which may damage or deactivate bacteria. This has led to research into immobilising and encapsulating materials.

2.4 Microbially Induced Calcium Carbonate Precipitation (MICP)

This research utilises microbially induced calcium carbonate precipitation to produce biocement through ureolysis. Growing interest in sustainable methods of soil improvement has led to increased interest and research in the application of microbially induced calcium carbonate precipitation. Microbially induced calcium carbonate precipitation, often abbreviated to MICCP or MICP, is an eco-friendly and sustainable biogeochemical process, which may be applied as a means of ground improvement, and which also has the potential to improve the properties of geotechnical structures. MICP can be used improve the mechanical properties of loose, saturated sand, by increasing its strength and stiffness and reducing its tendency to dilate (Montoya and Dejong 2013).

MICP may be used as an alternative to the traditional Portland cement-based method of soil cementation (Park Sung-Sik et al. 2014). The traditional method of cementing soil particles involves the mixing of portland cement and soil to create a soil-cement. Soil-cement obtains its stability primarily by hydration of cement and not by cohesion and internal friction (Portland Cement Association 1995). For this reason, such mixtures are susceptible to swelling, which is undesirable. In contrast, the strength of an MICP cemented soil is obtained by cohesion between the soil particles achieved via the calcium carbonate bonds.

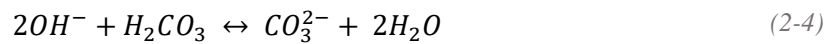
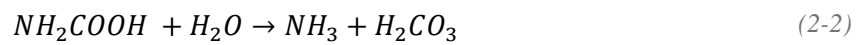
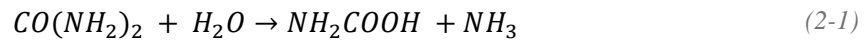
Microbially induced calcium carbonate precipitation has been utilised to produce biocement, biogROUT and surface biocoatings. Microbial based surface treatments have been developed to protect ornamental stone from deterioration (Le Metayer-Levrel et al. 1999; Dhimi et al. 2014). MICP has also been investigated for use in contaminant sequestration (Fujita et al. 2008) and post-grouting of foundation systems (Lin et al. 2016). MICP has been studied for its potential use for a variety of applications, including slope surface erosion control (Jiang et al. 2019).

MICP may occur through a variety of metabolic pathways, including photosynthesis, ureolysis, ammonification, denitrification (MIDP) and methane oxidation (Dhimi et al. 2017), in addition to sulphate reduction and iron reduction (Ersan et al. 2015). The urease enzyme may also be extracted from sources such as the beans of the Jack Bean plant and used directly for biocementation via enzyme induced carbonate precipitation (EICP), as employed by Hamdan (2015). Ureolysis or urea hydrolysis is the most efficient process among all MICP methods, as it has the potential to produce a large amount of calcite (CaCO_3) within a short period of time (Mukherjee et al. 2019). The ureolytic pathway, as selected for this doctoral research project, has been studied widely for engineering applications of MICP.

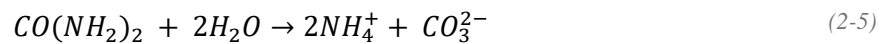
Ureolysis increases the alkalinity of fluid in soil/ sand pore spaces as a result of the degradation of urea to carbonate and ammonium, and induces calcite precipitation. The chemical process, as reported by

De Bele (2010), is outlined in Equations (2-1) to (2-6). Active ureolytic bacteria produce urease enzyme, which catalyses the hydrolysis of urea, resulting in the production of carbamate (NH_2COOH) and ammonia (NH_3), as per Equation (2-1). Carbamate hydrolyses spontaneously to produce ammonia and carbonic acid (2-2).

Simultaneously, in the presence of water, the ammonia and carbonic acid products equilibrate to produce ammonium (NH_4^+), hydroxide (OH^-) (2-3) and carbonate (CO_3^{2-}) ions (2-4). This results in a pH increase and increased alkalinity of the reaction medium. Since carbonic is a weak acid, it will only partially dissociate into ions, until equilibrium is reached.



The global reaction can be written as per Equation (2-5), summarising Equation (2-1) to Equation (2-4). In the presence of calcium, in an alkaline environment, calcium carbonate is precipitated at nucleation sites (Equation (2-6)).



The nucleation sites include sand or other soil particles, and also the bacteria themselves. Calcium carbonate (CaCO_3) can deposit at the soil particles' contact area (contact-cementing), coat soil particles (grain-coating), or create a cementation bridge between soil grains (matrix-supporting) (Lin et al. 2020). The calcium required for MICP can be provided from various sources such as calcium chloride (CaCl_2), calcareous sand (Liu et al. 2018b), fly ash (Xu et al. 2019) or calcium chloride dihydrate ($\text{CaCl}_2 \cdot 2\text{H}_2\text{O}$), with the latter often being preferred for biocementation of sand and soil. In the presence of calcium chloride (CaCl_2), crystals of calcium carbonate, often in the form of calcite, form inside the soil matrix (Cheng et al. 2016).

The calcium carbonate precipitate binds soil particles together, creating what is referred to as a biocement. Precipitation of calcium carbonate (CaCO_3) leads to pore-filling, inter-particle binding and particle roughening; resulting in improved soil strength and stiffness and also reduced permeability (Khodadadi et al. 2017). Due to the alkaline conditions produced during the process of MICP, the type of bacteria used needs to be alkaliphilic, to enable the survival of vegetative cells.

2.4.1 Ammonia Production

There is however one drawback of MICP via the ureolytic pathway, since for each carbonate ion produced two ammonium ions are simultaneously produced (Equation 2-3), which may result in excessive environmental nitrogen loading (Jonkers et al. 2008). This would need to be managed to avoid a negative effect on the environment when used for geotechnical applications. The ammonium ion (NH_4^+) is typically the nitrogen source preferred by plants, however, above a certain threshold NH_4^+ becomes toxic (Esteban et al. 2016). The highly toxic un-ionised ammonia (NH_3) species produced during the MICP process is expected to be fully converted to ammonium, as per Equation (2-3). Excess ammonia has been reported to inhibit MICP. Stewart (1965) found that free ammonia suppressed the formation of urease in growing bacterial cultures. Wang et al. (2011) found that when using silica gel or polyurethane to immobilise bacteria and nutrients this immobilising material also trapped the excess ammonia. After removing this ammonia and adding new urea, Wang et al. (2011) reported that the bacterial urease activity could completely recover.

Denitrification has been suggested as an alternative pathway for calcium carbonate precipitation, since it does not result in production of toxic by-products. In addition, this process can also occur under oxygen limited conditions (Ersan et al. 2014). However, the main drawback with this approach is the much slower rate of calcium carbonate precipitation.

2.4.2 Naturally Occurring MICP

MICP occurs as a natural process, which has been stimulated and engineered for use in industrial applications. The biodeposition of minerals is a widespread phenomenon in the biological world and is mediated by bacteria, fungi, protists, and plants. (Seifan and Berenjjan 2019). There are two pathways by which bioprecipitation of minerals by prokaryotes can be achieved; biologically controlled mineralisation (BCM) and biologically induced mineralisation (BIM) (Seifan and Berenjjan 2019). Examples of biologically controlled mineralisation include shells, bones and teeth. MICP is an example of biologically induced mineralisation.

Indigenous bacteria are known to mediate calcium carbonate precipitation autogenically, forming natural biocalcin deposits on the surface of stones, and initiating biomineralisation in soils. There is also evidence that microbes may have some influence on the production of calcium carbonate in cave environments, contributing to the production of speleothems such as stalactites (Baskar et al. 2006; Paction et al. 2013), despite these processes usually being considered entirely abiogenic. Bacterial strains *Bacillus thuringiensis* and *Bacillus pumilis* extracted from stalactite samples have been shown to precipitate calcite in vitro (Baskar et al. 2006), demonstrating the possibility that microbes could influence formation of speleothems. In instances of biologically controlled mineralisation, the organism controls the process of precipitation to a high degree (De Muynck et al. 2010). This may not be the case

for speleothems however, since there is not enough evidence to suggest bacteria have an extensive role in their development, although biomineralisation may play more of a role in the production of stromatolites. Naturally cemented sand stromatolites can be found in shallow high-salinity seawaters of Western Australia, these natural structures have inspired an engineered approach to sand cementation.

The majority of carbonate minerals in modern marine sediments are biogenic (Turchyn et al. 2021). Biogenic carbonates may be formed of skeletal remains of ocean organisms or formed by organisms as a result of enzymic induction. An example of the latter is the formation of the foraminifera shell. Calcium carbonate is one of the most abundant biological minerals formed by living organisms (Ni and Ratner 2008). There are three polymorphs of anhydrous calcium carbonate, these being vaterite, aragonite and calcite, with aragonite and calcite being the most thermodynamically stable and most common in nature (Ni and Ratner 2008). The formation of these crystalline calcium carbonate polymorphs often occurs via a nanoparticulate amorphous calcium carbonate (ACC) precursor (Weiner et al. 2005; Rodriguez-Blanco et al. 2011). Vaterite is a rare CaCO_3 polymorph, which may be found in nature as biogenic mineral (Gussone et al. 2011).

It has been proposed that these biogenic carbonates such as forams are formed as a result of a two or three stage solid state process (Jacob et al. 2017), with metastable ACC being formed initially and undergoing structural rearrangement to form calcite directly (two-stage) or calcite via a metastable vaterite phase (three-stage). Rodriguez-Blanco et al. (2011) also reported observations of a two-stage crystallisation pathway from ACC to calcite, driven by dehydration to form vaterite followed by surface controlled dissolution and reprecipitation to form calcite, as depicted in Figure 2-3.

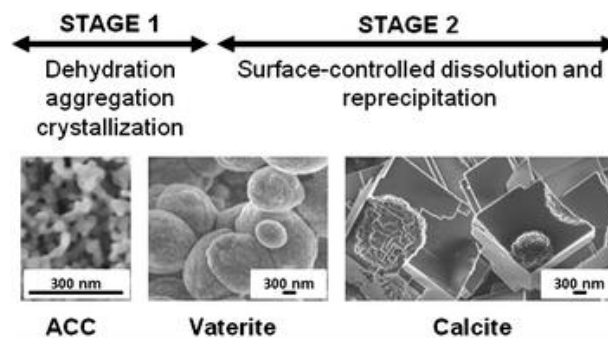


Figure 2-3. ACC to Calcite mechanism (Rodriguez-Blanco et al. 2011).

Precipitation of carbonates can be controlled by kinetic processes or by equilibrium behaviour. Carbonate minerals may also precipitate abiotically within marine environments (Turchyn et al. 2021), this being an example of equilibrium behaviour governing carbonate precipitation. Seawater typically has a calcium ion (Ca^{2+}) concentration of between 10 and 11 mM (Erez 2003). Microbial respiration is a key factor in carbonate precipitation in anoxic marine environments, since oxidation of organic carbon results in alkalinity in the form of bicarbonate (CO_3^{2-}) ions (Turchyn et al. 2021). Increasing the pH of

seawater increases the CO_3^{2-} concentration. The resulting supersaturation results in the precipitation of calcium carbonate.

Microbially mediated soil stabilisation may also occur naturally, dependent on environmental conditions. Certain microbes can form a crust to naturally protect the surface of soil from erosion and reduce airborne dust particles in dry areas. Filamentous cyanobacteria and fungal hyphae are two such examples, which have been reported to bind soil particles together (Chen et al. 2016).

2.4.3 Evaluation of MICP

Biocemented sand and soils may be subjected to a variety of analyses to assess material properties such as strength and stiffness, and to quantify and analyse the calcium carbonate precipitated.

2.4.3.1 Unconfined Compressive Strength

The unconfined compression test has been used by a number of researchers to test the unconfined compressive strength (UCS) of biocemented sand (van Paassen et al. 2010; Al Qabany and Soga 2013; Botusharova 2017; Mahawish et al. 2019b; Mujah et al. 2019; Mukherjee et al. 2019; Xiao et al. 2019; Zhao et al. 2020) and biocemented sandy silt (Mukherjee et al. 2019). Loading rates of typically 1.0 mm/min (Mujah et al. 2019) to 1.14 mm/min (Al Qabany and Soga 2013) have been applied. Botusharova (2017) utilised unconfined compression testing of cemented and healed column specimens to demonstrate the ability of the biocemented sand to self-heal. Botusharova (2017) found that cemented and healed specimens responded in a brittle manner, with peak strengths obtained for healed specimens being over and above the residual strength from the initial stress-strain curves obtained for cemented specimens.

The British Standards (BS 1377-7:1990) state that the unconfined compression test 'is suitable only for saturated, non-fissured cohesive soils' (British Standards Institution 1999). This does therefore lead to some uncertainty regarding reliability of this testing method for biocemented soils. The preparation of the test specimen prior to unconfined compressive strength (UCS) testing will have an effect on strengths obtained, with most testing reported being conducted on saturated specimens. Al Qabany and Soga (2013) and Botusharova (2017) conducted tests on oven-dried biocemented sand columns. Botusharova dried test specimens at 30 °C, Al Qabany and Soga note the UCS test was conducted on oven dried specimens but do not give the drying temperature used. If a sample is only partially dried, capillary affects due to partial drying will alter strength. When drying at low temperatures there will likely be some moisture retention due to the relative humidity within the drying apparatus. Zhao et al. (2020) reported significant strength differences for biocemented specimens (incorporating carbon fibres) when tested in dry and saturated states, as shown in Figure 2-4.

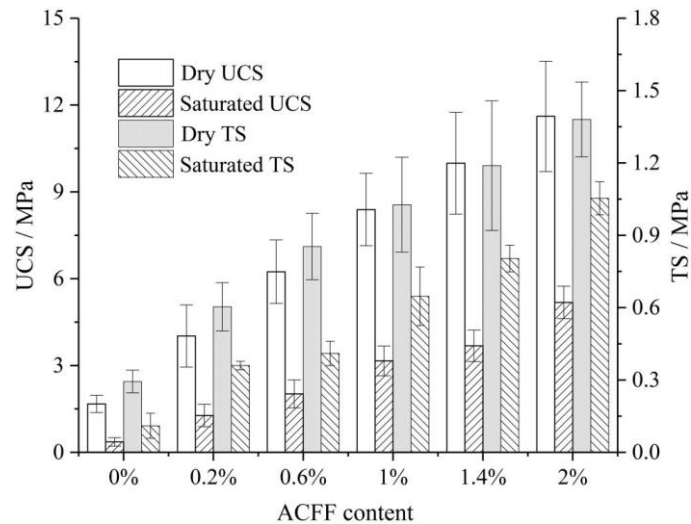


Figure 2-4. Unconfined compressive strength (UCS) and splitting tensile strength (TS) test results comparing strengths of specimens tested in saturated and dry states (Zhao et al. 2020).

2.4.3.2 Shear Strength

A less tested property of biocemented sand is shear strength. Triaxial testing has been used to measure undrained shear strength of biocemented sand (Montoya and Dejong 2013). Montoya and Dejong (2013) reported that following monotonic shearing and two injections of cementation media over 24 h, shear strength was restored to ‘essentially the same as the initial sheared behaviour’. Shear strength of biocemented sand was measured by Cheshomi et al. (2018) using the direct shear test. To use the direct shear test, the soil specimens needed to be produced in moulds measuring 6 x 6 x 3 cm to fit into the test apparatus. Specimens prepared for the direct shear test therefore needed to be treated via surface percolation, by spraying cementation solution onto the soil surface, as opposed to injection. Use of triaxial apparatus requires the samples to be prepared within the triaxial testing split mould and cementation treatments applied while the specimen is under confining stress.

Phillips et al. (2013) noted that a disadvantage of studying laboratory strains is the microbial complexity of real world environments and that injection of bacteria may result in non-homogeneous distribution of the microbes.

2.4.3.3 Stiffness

Shear wave velocity (V_s) can be used to measure stiffness of biocemented sand (Montoya and Dejong 2013) and can be applied for insitu testing (van Paassen et al. 2010). Through measurement of shear wave velocity, Montoya and Dejong (2013) were able to quantify healing responses of biocemented sand following degradation. Two pore volumes of cementation solution were injected into columns every 3 to 6 h until the shear wave velocity (V_s) of the specimen reached 650 m/s, to achieve the desired biocementation. It was found that after shearing and resulting V_s decrease to 480 m/s that this returned to 650 m/s within 24 h following two injections of the cementation medium.

2.4.3.4 Calcium Carbonate Precipitation

Various methods of indirect and direct measurement of calcium carbonate precipitation have been utilised. Calcium carbonate precipitate can be measured using acid washing (Badiiee et al. 2019; Mukherjee et al. 2019), also referred to as Pipers method. The calcimeter apparatus (Bernard/ Eijkelkamp) can be used to measure the calcium carbonate content of test specimens (Cheshomi et al. 2018; Kalantary et al. 2019). The calcimeter apparatus measures the carbon dioxide released when 4 M HCl is added to a sample, with this measurement being used to calculate the calcium carbonate percentage of the sample. Stocks-Fischer et al. (1999) used the EDTA titration method to measure calcium precipitated. Botusharova (2017) applied the mass loss on ignition method, to directly measure calcium carbonate precipitated by measuring mass loss resulting from heating of biocemented sand samples to 950 °C.

2.4.3.5 Mineralogy

Scanning electron microscopy (SEM) can be used to examine the mineralogy of biocemented materials. SEM is however inconclusive for discriminating among calcium carbonate polymorphs since the morphology of each calcium carbonate polymorph is not unique (Ni and Ratner 2008). SEM observation is therefore often combined with X-ray diffraction (XRD) to verify the presence of calcium carbonate and to identify the types of calcium carbonate polymorph present. The mechanical performance of MICP-stabilised soils largely depends on the microstructure of the precipitated CaCO₃ crystals, which are affected by various chemical, environmental, and physical parameters (Mujah et al. 2019). The factors which affect MICP are considered further in Section 2.5.

The different polymorphs of calcium carbonate have different physical properties including solubility density and hardness that could significantly affect material bio-healing properties (Seifan et al. 2016). The crystal precipitation pattern has been shown to influence the flow properties of porous media (Cheng et al. 2016). Calcite, aragonite and vaterite are the main polymorphs of calcium carbonate. Calcite is the most thermodynamically stable and least soluble polymorph of calcium carbonate (Burbank et al. 2011). Calcite has a higher bonding strength than aragonite (Wang et al. 2015).

2.5 Factors Affecting Microbially Induced Calcium Carbonate Precipitation

There are several factors which impact upon MICP, in respect of amount and rate of calcium carbonate precipitated and material properties of the biocemented material. These factors would need to be considered and controlled as appropriate in order to investigate effects of additives on biocementation and biocemented material properties. In the soil subsurface these factors include pH, temperature, hydrostatic pressure and dissolved salts (Basha et al. 2018). This section also informs potential further research required to enhance the MICP process, in addition to limitations. Further exploration would be

required to understand and exploit the conditions which could enhance long-term self-healing in MICP installations.

Calcium carbonate precipitation is reported to be largely governed by four key factors: calcium concentration, the concentration of dissolved inorganic carbon, pH and the availability of nucleation sites (De Muynck et al. 2010; Ersan et al. 2015). A review of research undertaken concerning MICP has highlighted the importance of environmental conditions such as temperature, oxygen availability and the type of soil used, in addition to bacterial species and the types and concentrations of nutrients and precursor chemicals within the cementation media used.

2.5.1 Water Availability

Water is a requirement for MICP, as shown by the equations which outline the chemical process of MICP, Equations (2-1) to (2-6). Wang et al. (2014c) advise that free water is essential to obtain a significant amount of self-healing. Hence MICP would be expected to cease when the material becomes dehydrated. Water can also be a source of oxygen for the bacteria in the form of dissolved oxygen. Microbes are found naturally where there is sufficient availability of space, nutrients and water (Basha et al. 2018). Water availability can also affect the types of calcium carbonate polymorph present. Conversion of thermodynamically unstable vaterite to stable calcite is a relatively fast process, and can happen in around 24 h, but will only occur in the presence of water (Burbank et al. 2011).

2.5.2 Temperature

The temperature of the environment is one of the key factors governing efficiency of the MICP process (Gowthaman et al. 2019a). Temperature has been reported to have an effect on urease/ ureolytic activity and also calcium carbonate crystal formation and quantity. Hence, the temperature under which the material is biocemented has an effect on the strength (Kim et al. 2018). When reporting on the effect of temperature on MICP and the optimum temperature conditions for MICP, researchers tend to focus on either bacterial growth or urease/ ureolytic activity. The optimum temperature reported by Kim et al.(2018), when using *S. pasteurii* (and also for *Staphylococcus saprophyticus*) was 30 °C, based on amount of calcium carbonate precipitated, with testing undertaken between 20 °C and 50 °C. However, Peng and Liu (2019) reported that ureolytic activity, when using *S pasteurii*, decreased more quickly at higher temperatures up to 30 °C compared to lower temperatures, with greater quantities of precipitation of calcium carbonate at the lowest temperature tested, this being 10 °C (as shown in Figure 2-5). Peng and Liu (2019) reported that at 10 °C the amount of calcium carbonate precipitation had been 37 % higher than that at 30 °C. Furthermore, Peng and Liu (2019) found the biocement produced at 10 °C had the highest strength (UCS), which was likely due to the observed increase in size of calcium carbonate crystals precipitated with decreasing temperature.

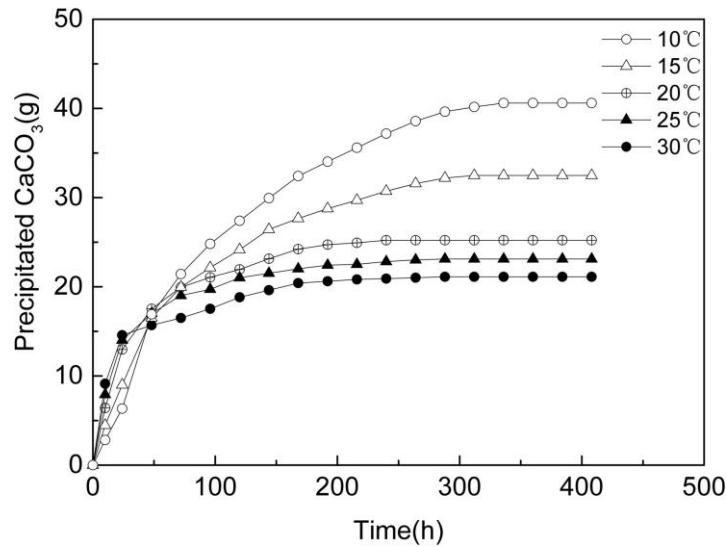


Figure 2-5. Quantity of calcium carbonate precipitated over time within 100 mm x 47 mm dia. sand columns inoculated with *S. pasteurii* and treated with a (1.0 M) urea- (0.5 M) calcium chloride medium (Peng and Liu 2019).

It has been reported that there is little difference in microbial activity and growth within the 20 °C to 30 °C range, with the rate of hydrolysis being marginally higher at 30 °C, compared to 20 °C, and temperature increases above 30 °C not leading to a further increase in the rate of urea decomposition (Ng et al. 2012).

Xiao et al. (2021) report a peak in *S. pasteurii* urease activity (mM/min) slightly above 30 °C and a significant decline at 40 °C. At this temperature however bacterial growth will continue to increase, thus showing a lack of correlation between bacterial growth and urease activity at higher temperatures. Deng and Wang (2018) report increases in optical density (OD₆₀₀) of bacterial solutions with temperature, within the 5 °C to 35 °C range of their tests. Cheng et al. (2016) found that the optimum crystal precipitation pattern was produced at a low urease concentration and temperature of 25 °C when using an isolated *Bacillus sp.*. Gowthaman et al. (2019a) found that urease activity of *Lysinibacillus xylanilyticus* peaked at 25 °C and then significantly reduced at 30 °C to roughly the level observed at 15 °C, with negligible urease activity and bacterial cell growth observed at 40 °C and above.

It would appear that the key parameter to be taken into consideration when considering temperature effects is the urease activity of the selected bacterium and also effect on crystal precipitation. Past research suggests urease activity governs the MICP process and that this decreases at higher temperatures despite increased bacterial growth and cell density.

2.5.3 pH

In addition to temperature, pH will impact upon MICP, the extent of which will be dependent upon the bacteria selected. The pH level is also an indicator of MICP, since MICP results in alkaline conditions. A high pH may cause some bacteria to become inactive, exceptions to this being alkaliphilic bacteria

which can survive in a higher pH environment. Wang et al. (2012) found that when using *Bacillus sphaericus* to promote MICP, the amount of urea decomposed decreased from 95 % in a neutral pH 7 environment to less than 5 % when the pH was 12.5, this being representative of the alkalinity in concrete. A pH of 9.1 resulted in negligible reduction in urea decomposed. The urease activity of *Sporosarcina ureae* has been reported to be stable over a pH range of 7.75 to 12.5, but has been found to rapidly lose activity at higher or lower pH values (McCoy et al. 1992). Deng and Wang (2018) found that pH had less effect on *S. pasteurii* bacterial growth than temperature. Gowthaman et al. (2019a) reported that when using *Lysinibacillus xylanilyticus* to facilitate MICP, the highest urease activity was measured within the pH 7 – 8 range.

2.5.4 Oxygen Supply

Most MICP processes are induced by aerobic bacteria, with sufficient oxygen supply being necessary for the effect of increasing bacterial biomass (Li et al. 2018). *S. pasteurii* grows more actively in the presence of oxygen (De Muynck et al. 2010), and at a higher rate (Achal et al. 2009). Oxygen uptake has been used by researchers as a measure of microbial activity and as an indication of efficiency of the MICP process. Mortensen et al. (2011) found that an anoxic environment did not appear to hinder *S. pasteurii* urease activity, suggesting that availability of oxygen does not appear to have an effect on urea hydrolysis. This finding is supported by Wang et al. (2017), who report that oxygen is essential for the growth of bacteria but not for urea decomposition. Long-term ureolytic activity in any significant amount without the application of oxygen is however questioned (Martin et al. 2012).

2.5.5 Material Type

Most research concerning MICP applied to geotechnical structures has been conducted using sand or sandy soil. In comparison, only a few studies have been undertaken which apply MICP to fine-grained soils such as clay and silt (Lee et al. 2013; Xu et al. 2016), bentonite (Guo et al. 2018; Vail et al. 2019), sand and kaolin clay (Sun et al. 2019), or larger grained soils including gravel-sand mixtures (Jiang and Soga 2017). These examples show that where fine grained soils have been studied, they have usually been mixed with larger grained soils. There is also some potential for MICP using *S. pasteurii* to help mitigate against bentonite cracking (Guo et al. 2018). Hasriana et al. (2018) found that the CBR value of clay soil could be increased via MICP using *Bacillus subtilis* and bacteria additions up to 6 %. In the studies conducted by Lee et al. (2013), the soil used was a silty residual soil extracted from a site in Kuala Lumpur with 32 % of particles in the range of 50 µm to 400 µm and the remainder varying between clay fraction and 2 mm in diameter.

The type of soil, its pore throat size, and the size of the bacteria need to be taken into consideration when selecting bacteria for MICP treatment (Ng et al. 2012). The bacteria are typically 1 µm to 3 µm, whereas pores in concrete are mostly smaller than 0.5 µm, which can lead to crushing of the bacteria

(Wang et al. 2015). Rebata-Landa (2007) reported that the optimum grain size for soils in which MICP would be viable is 50 µm to 400 µm, and that bacterial activity would not be able to take place in very fine soils such as clay. MICP may also not be viable for biocementation of very coarse soil, given the amount of precipitate that would be required to bridge gaps between very coarse soil particles. Self-healing experiments in cementitious materials have demonstrated that the MICP process can be used to heal cracks of up to 0.97 mm wide (Wang et al. 2014c).

Studies have been undertaken which support the view that MICP may be less suitable for fine grained soils. Jiang et al. (2017) reported that when using a mixture of sand and clay with a small gap ratio (fine sand and clay mixture) that insignificant soil improvement was achieved, due to an inefficiency in carbonation precipitation during MICP, compared to using coarser samples with a larger gap ratio. Volumetric contraction was reduced by MICP however, regardless of grain size. MICP was found to be effective in silt (Xu et al. 2016), however the filling of pore spaces at the edge of the sample with calcium carbonate, with little precipitate observed in the centre, suggested flow of treatment solution/ bacterial movement was restricted. Sun et al. (2019) found that Kaolin clay when added to sand inhibited urease activity of *S. pasteurii*.

2.5.6 Bacterial Strain

Under suitable conditions most bacteria are able to induce calcium carbonate precipitation (De Muynck et al. 2010). Bacteria used for MICP are required to be able to catalyse the hydrolysis of urea, and are usually urease positive bacteria, including strains of *Bacillus*, *Sporosarcina*, *Sporolactobacillus*, *Clostridium* and *Desulfotomaculum* (Ng et al. 2012). Ureolytic bacteria are commonly found in soils of varying type and mineralogy and in a variety of environments (Dhimi et al. 2017). The bacteria species and the metabolic pathway employed for MICP control the amount of dissolved organic carbon, which largely governs the type of calcium carbonate crystals formed (Dhimi et al. 2017).

Preferred bacteria for MICP via the ureolytic pathway have a high urease activity. Aerobic bacteria are preferable, since they release CO₂ from cell respiration. *S. pasteurii* has commonly been used for studies on cementation of granular soil via MICP (Stocks-Fischer et al. 1999; Whiffin et al. 2004; van Paassen 2009; Montoya and Dejong 2013; Gomez et al. 2015; Dhimi et al. 2017). As a sporulating bacterium, *S. pasteurii* has also been used in research into self-healing via MICP in cementitious materials (Harbottle et al. 2013; Bhaskar et al. 2017; Bundur et al. 2017). Urease positive *Sporosarcina pasteurii* (formerly *Bacillus pasteurii*) is a common alkaliphilic soil bacterium with high urease activity and is tolerant to a wide pH range. Stocks-fischer et al. (1999) reported urease activity of *S. pasteurii* between pH 6 and 10, with the optimum environment found to be slightly alkaline. *S. pasteurii* however failed to sporulate under test conditions during research undertaken by Botusharova (2017). For this reason, ureolytic *Sporosarcina ureae* was used by Botusharova (2017), with *S. pasteurii* referred to as a non-

sporulating control. *S. ureae* sporulated under the same test conditions, however the rate of calcium carbonate precipitation catalysed was much slower than for *S. Pasteurii*, therefore ideally an alternative sporulating bacterium needs to be identified for use in further research into self-healing within geotechnical structures. Both *S. pasteurii* and *S. ureae* will express urease, regardless of ammonia compound concentrations (Burbank et al. 2011). Bacteria are often used in spore form in self-healing MICP applications. These spores enable bacteria to remain dormant for extended periods. When exposed to suitable environmental conditions, the spores become active, returning to a vegetative state and can then resume metabolic activities (Bundur et al. 2017).

Sporosarcina ureae has seldom been used in studies on self-healing construction materials. When compared to *Sporosarcina ureae*, Bhaskar et al. (2017) found that *Sporosarcina pasteurii* use resulted in a greater healing efficiency. Another bacteria strain which has been used in a number of self-healing MICP studies is *Lysinibacillus sphaericus* (formerly *Bacillus sphaericus*) (Wang et al. 2011; Wang et al. 2012; Cheng et al. 2013; Wang et al. 2014c; Wang et al. 2014b) and other *Bacillus spp.* such as *Bacillus cereus* (Pan et al. 2019). Other strains of bacteria which have been used for MICP, to a lesser extent, include *Bacillus subtilis* (Khaliq and Ehsan 2015), *Bacillus cohnii* (Zhang et al. 2017b), and *Bacillus mucilaginous* (Chen and Qian 2016). Some studies have used native bacteria, sourced from a variety of locations including alkaline lake soil (Wiktor and Jonkers 2011) and soda lake sediment (Palin et al. 2016).

Observation of the width of cracks healed in concrete and mortar may give some indication of the calcium carbonate precipitation inducing efficiency of different strains of bacteria. In this respect promising results have been obtained with *Bacillus sphaericus*, which when contained within diatomaceous earth (Wang et al. 2012), hydrogel (Wang et al. 2014b) and melamine based capsules (Wang et al. 2014c) induced sufficient calcium carbonate precipitation to fill cracks of 0.17 mm, 0.5 mm and 0.97 mm respectively, after twenty eight days of curing. This may provide a suitable alternative to *S. pasteurii* for use on future experiments on self-healing geotechnical structures. The only apparent downside to using *B. sphaericus* is that research undertaken by Wang et al. (2012) suggests it may not be alkaliphilic, which may not however be an issue for geotechnical applications. When used in cementitious materials, bacteria must also be able to remain viable at a high pH, above 8.5, and at high calcium concentrations.

As the focus for this research project will be on long-term self-healing, the bacteria will need to be able to survive for a long period, for the service life of the structure at least. Bacteria are able to survive for a long period of time in soils, up to 200 yrs (Schlegel 1993). Research undertaken by Botusharova (2017) demonstrated that bacteria (assumed to be in spore form) can survive within a biocemented sand matrix for up to six months. At present the long-term survival of bacteria within biocemented sand or soil cannot be guaranteed and will require further investigation.

Addition of bacteria in concrete not only affects self-healing, but also has an influence on compressive strength (Khaliq and Ehsan 2015). Different types of bacteria have been shown to have differing effects on compressive strength of concrete, and also the rate of calcium carbonate precipitation and therefore the amount of calcium carbonate and self-healing observed.

The rate of precipitation of calcium carbonate is dependent mainly on the initial bacteria concentration, bacteria growth rate and metabolic activity of the bacteria used (Ersan et al. 2015). The concentration of bacteria, determined through measurement of optical density at 600 nm, should be at least 10^6 cells/ml or cfu (colony forming units), to obtain a considerable amount of calcium carbonate precipitation (Tziviloglou et al. 2016).

2.5.7 Cementation Medium

To enable SH-MICP, nutrients and precursor chemicals are required, to provide an energy source for the bacteria and to promote calcium carbonate precipitation respectively. These nutrients and precursor chemicals may also collectively be referred to as the cementation medium. An adequate supply of nutrients will help to sustain the bacteria for long enough to support calcium carbonate precipitation and achieve the desired level of soil improvement.

Precursor chemicals required for MICP (via ureolysis) include a calcium source, such as calcium lactate or calcium chloride, along with a nitrogen source (typically urea) for the bacteria. In addition, the selected bacteria will require specific nutrients for growth. Yeast extract is often used in the growth medium for bacteria, and occasionally added to the cementation medium. While nutrients are not an essential component of the cementation medium for MICP, yeast extract has been found to improve calcium carbonate precipitation, in addition to improving spore yield and viability (Zhang et al. 2017a). Wang et al. (2014c) reported that yeast extract has the effect of delaying hydration and decreasing the degree of hydration if the dosage is higher than 0.85 % of cement by mass, since organic compounds may be easily absorbed onto the surface of mineral particles.

Of particular interest for this research are the concentrations of nutrients and precursor chemicals used in the cementation medium for biocementation. The concentration of the cementation medium/solution has been found to alter the peak strength of biocemented soil but have little effect on stiffness (Lee et al. 2013). Deng and Wang (2018) found that unconfined compressive strength increased as the (equimolar urea-CaCl₂) cementation medium concentration increased from 0.5 M to 1.0 M, with a 1.5 M concentration resulting in a UCS decrease. Yasuhara et al. (2012) similarly experimented with cementation media with calcium chloride concentrations of 0.5 M to 1.5 M (while keeping the urea concentration fixed at 0.5 M), with results as shown in Figure 2-6. These results agree with the aforementioned studies by Deng and Wang (2018) in that they show that MICP becomes inhibited at a Ca concentration higher than 1.0 M.

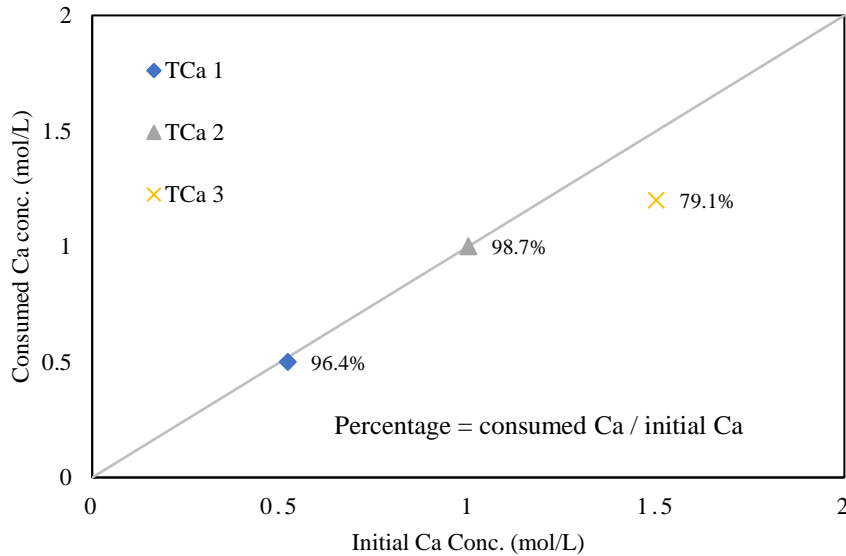


Figure 2-6. Relationship between initial Ca concentration of the cementation media and the consumed Ca concentrations following MICP, adapted from Yasuhara et al. (2012).

Similarly, Jiang et al. (2019) reported that at equimolar urea and calcium chloride concentrations above 1.0 M the calcium chloride concentration appeared to have an inhibiting effect on the MICP process. Mahawish et al. (2019a) reported obtaining the maximum unconfined compressive strength for biocemented sand when using a 1.0 M calcium chloride and urea cementation medium. Al Qabany et al. (2012) found that calcium carbonate precipitation was not adversely affected by the cementation medium concentration for input concentrations up to 1.0 M. Subsequently, when Al Qabany and Soga (2013) studied the effect of using 0.25, 0.5 and 1.0 M concentrations of urea and calcium chloride they reported that the lower concentrations resulted in a more gradual, uniform decrease in permeability and stronger samples. While a 1.0 M cementation medium appears to be preferred, concentrations of reagents used vary across published studies, a selection of which are summarised in Table 2-2. Mukherjee et al. (2019) used a 0.5 M urea-CaCl₂ cementation medium for example.

Chen et al. (2016) investigated the effects of varying both calcium ion concentration and urea concentration and found that the compressive strength of biocemented sand increased with increasing Ca²⁺ concentration up to 45 mM (with urea content fixed at 80 g/L (1.33 M)). It is noted that an excess of urea had been used for this study. At higher Ca²⁺ concentrations the strength decreased, with this result suggesting that higher calcium ion concentrations inhibited urease activity. Chen et al. (2016) found that compressive strength of biocemented sand also increased with increasing urea addition, up to a concentration of 80 g/L, with compressive strength reducing to almost zero when using a concentration of 100 g/L. It is suggested that this reduction in compressive strength occurred due to an increase in gaseous NH₃ and CO₂ products with increasing urea, which led to swelling of the sand (Chen

et al. 2016). High concentrations of urea are therefore not recommended. Chen et al. (2016) suggest 20 g/L urea may be adequate for engineering applications. Lee et al. (2013) reported that high reagent concentrations (i.e. 1.0 M) are not favourable for MICP as urea degradation activity could be retarded. Calcium ion and urea concentrations have also been suggested to affect the crystalline morphology of calcium carbonate (Xu et al. 2016).

The selected calcium source will also have an effect on MICP. Pan et al. (2019) found that when calcium chloride was compared to calcium nitrate and calcium acetate as calcium sources, use of calcium nitrate resulted in the highest shearing strengths of biocemented sand, followed by calcium chloride and calcium acetate. The calcium carbonate deposition amount was however lowest for calcium nitrate and highest for calcium acetate, with the average values varying between approximately 24 g and 27.5 g.

The standard urea-calcium cementation medium used for biocementation may also be augmented with additional reagents and nutrients. A relatively small number of biocementation studies have included nutrients within the cementation medium, and quantities of nutrients vary where used. Jiang et al. (2019) used 6 g/L of nutrient broth in their cementation media, whereas Stocks-Fischer et al. (1999) used 3 g/L (Bacto) nutrient broth. Dhimi et al. (2017) conducted MICP experiments *In vitro* using nutrient augmented cementation media (with 1 g/L or 10 g/L yeast extract). They reported that under low nutrient conditions calcium carbonate precipitation followed the extra polymeric substances (EPS) route, as has been observed in the formation of natural MICP such as stromatolites. MICP was observed to be more effective under high nutrient conditions. Nutrient concentration was also observed to have an impact on calcium carbonate crystal formation, with larger calcite crystals being produced in high nutrient conditions and smaller crystals in low nutrient conditions.

For some studies, including one of the first studies in this area by Stocks-Fischer et al. (1999), the cementation medium has been augmented with ammonium chloride (NH_4Cl), as also included in the cementation solution used by Montoya and Dejong (2013). In addition, some studies include a small amount of sodium bicarbonate (NaHCO_3) in the cementation medium, typically 2.12 g/L (Stocks-Fischer et al. 1999; Al Qabany and Soga 2013), with this reportedly being used for stabilisation of the pH of the cementation solution before injections (Al Qabany and Soga 2013). The reason for including ammonium chloride within the cementation medium has not however been clear.

The retention time between the cementation medium additions/ biocementation treatments and number of treatments also needs to be considered and will be dependent upon the concentration of the reagents used, any augmentation of the standard urea-calcium cementation medium and the selected bacterium. When using a 0.5 M urea-calcium cementation medium containing calcium chloride and 3 g/L nutrients and an isolated *Psychrobacillus* sp. bacterium, Gowthaman et al. (2019b) applied ten treatments, with 24 h intervals. Van Paassen et al. (2010) used an equimolar solution containing 1.0 M calcium chloride

and urea mixed with tap water and no added nutrients, for biocementation of sand using *S. pasteurii*, with ten treatments of this cementation medium applied over sixteen days.

The rate of application of cementation medium is also reported to have an effect on biocementation (Lee et al. 2013). Cheng and Cord-Ruwisch (2012) suggest that a slow rate of application of cementation solution enables adequate mixing of the bacteria and nutrients (cementation medium). The rate and pressure of injection of cementation medium has been reported to have an impact on the precipitation of calcium carbonate, with stiffness and peak strength reported to increase with decreasing cementation reagent flow pressure (Cheng et al. 2016). For biocementation treatments applied using the injection process into sand columns, the rate has typically equated to approximately three pore volumes per hour (Harkes et al. 2010; Montoya and Dejong 2013). Harkes et al. (2010) did however find that at this rate 21 % of bacteria introduced into columns were lost (based on optical density measurement of effluent). On this basis the rate used by Cui et al. (2017) seems quite high, since they use the same rate of 10 mL/min as Montoya and Dejong (2013), but for much smaller columns, with column dimensions and injection rates given in Table 2-2.

Table 2-2 below summarises the concentrations of precursor chemicals within the cementation media used for lab-based studies on biocementation of sand via MICP. Where multiple experiments have been carried out the concentrations stated correspond with those that led to the greatest material property enhancements. The quantity of cementation medium (CM) used will be dependent upon the compaction of the sand and the capacity of the void spaces, this is therefore difficult to compare across the variety of studies in this area and is not always clearly stated since numerous applications of CM are often applied to biocement samples to achieve desired levels of biocementation. An excess of cementation medium may also be used to ensure that any unreacted reagents from the prior treatment are fully flushed from the columns.

Table 2-2. Concentrations of cementation media reagents used in published sand column MICP experiments.

Bacterium/ Urease Source	Sand Column Size	Treatment Delivery	Cementation Media Reagent/ nutrients and Conc.	Inoculant	Pumping Rate (direction)	Quantity of Cementation Media	Reference
<i>S. pasteurii</i>	39.1 mm diameter, 80 mm height	Injection	CaCl ₂ 500 mM Urea 500 mM	40 % pore vol. bacterial solution	5 mL/min (bacteria) 10 mL/min (CM) (downwards)	One pore volume every 12 h	(Cui et al. 2017)
Naturally sourced. <i>Bacillus sp.</i>	45 mm diameter, 180 mm height	Injection	CaCl ₂ 1000 mM Urea 1000 mM	50 % pore vol. bacterial solution	Rate not given (downwards)	One pore volume every 24 h	(Cheng et al. 2016)
<i>S. pasteurii</i>	72 mm diameter, 144 mm height	Injection	Urea 333 mM NH ₄ Cl 374 mM CaCl ₂ 50 mM *NaHCO ₃ 25.2 mM *Nutrient broth 3 g/L	One pore vol bacteria suspended in CM minus calcium	10 mL/min (upwards)	Two pore volumes every 3-6 h.	(Montoya and DeJong 2013; Montoya and DeJong 2015)
Urease enzyme (020-83242, Kishida Chemical Co. Ltd.)	50 mm diameter, 100 mm height	Injection	CaCl ₂ 1000 mM Urea 1000 mM (Optimum)	Urease powder premixed with sand	5 mL/min (upwards)	100 ml at 2 h intervals, four to eight times	(Yasuhara et al. 2012)
<i>S. pasteurii</i>	66 mm diameter, 180 mm height	Injection	CaCl ₂ 1000 mM Urea 1000 mM	14 % pore vol. bacterial suspension (undiluted)	3.7 mL/min to 11 mL/min (downwards)	1.2 times pore volume (one injection to test bacterial fixation)	(Harkes et al. 2010)

* Reagent/ nutrients added in later 2015 study.

2.6 Cementation Medium Delivery

This research has in part, in the early stages, been informed by approaches to development of self-healing cementitious materials, given the novelty of this system for biocemented geomaterials such as sand and soil. Also considered are the processes which have been used to achieve biocementation, since an aim of this research had been to embed self-healing capability within the biocemented material.

Laboratory studies on the biocementation of sand via MICP have often utilised an injection process as a means of delivering the cementation media. These injection processes typically involve two stages; injection of a bacterial inoculant (bioaugmentation) or bacterial stimulating medium (biostimulation) followed by the injection of cementation medium. Cementation medium has been shown to be effective for fixing of the bacteria within a bioaugmented system (Harkes et al. 2010), this initial injection of cementation medium may also be replaced with a 0.05M solution of calcium chloride for the purposes of bacteria fixing (Harkes et al. 2010). To achieve a desired level of biocementation, precursor chemicals (and nutrients if included) have often needed to be injected into the soil multiple times over several days or weeks to enable sufficient cementation of the soil and to achieve desired material properties. Besides injection, alternative approaches to cementation medium delivery in soil have included surface percolation (Cheng and Cord-Ruwisch 2012; Cheng and Cord-Ruwisch 2014) and premixing (Yasuhara et al. 2012). Healing MICP treatments for biocemented sand have been delivered through injections (Montoya and Dejong 2013; Botusharova 2017).

Studies concerning self-healing of cementitious materials have utilised a variety of mechanisms to store and supply the cementation medium and bacteria to promote healing of cracks via MICP, including immobilisation and encapsulation. A review has been undertaken of these studies to inform possible approaches to enable self-healing via MICP within geotechnical structures. Research in the area of self-healing construction materials has focussed on concrete to date. Concrete is the most used construction material worldwide, owing to its strength, durability, and relatively low cost (Jonkers and Schlangen 2007). Concrete is susceptible to cracking, due to its relatively low tensile strength, which can reduce the service life and durability of concrete and make it susceptible to chemical attack following ingress of aggressive substances such as chloride and sulphate ions. The environment within concrete has posed challenges concerning research into bacterial-based self-healing systems in concrete. The high alkalinity within concrete is likely to deactivate incorporated bacterial spores, which may in addition get damaged or crushed entirely during the concrete mixing process. This has led to research into encapsulation and immobilisation of bacteria, and also the encapsulation and immobilisation of nutrients and precursor chemicals within cementitious materials.

A variety of what are often referred to as carrier compounds/ materials have been utilised in self-healing research applied to concrete, to increase viability of bacteria survival and self-healing efficiency (Khaliq

and Ehsan 2015). These carrier compounds can have positive and negative effects on the material properties of concrete, dependent on materials and quantities used.

2.6.1 Direct Application

Research undertaken to date on the biocementation of sand and soil via MICP has utilised a direct application approach for the delivery of nutrients and precursor chemicals. These chemicals have been applied directly to soils in solution through injection, surface percolation and premixing. These approaches however are not autonomous. MICP treatments for stone have been limited to surface application, also referred to as bio-deposition.

2.6.1.1 Injection

The provision of reagents directly by injection requires (often repeated) external intervention. Harbottle et al. (2014) reported that the medium was partially replaced several times, on a weekly basis, to provide a continued source of nutrients. Common problems encountered when injecting cementation media into soil (and also sand) include clogging of pores near the injection point and uneven distribution of bacteria and calcite (Burbank et al. 2011).

The limited research into healing of biocemented sand and soil via MICP to date has utilised a two stage injection/ treatment process to supply bacteria, followed by nutrients (where included) and precursor chemicals (Montoya and Dejong 2013; Harbottle et al. 2014; Botusharova 2017). Montoya and Dejong (2013) introduced *Sporosarcina pasteurii* bacteria into a 72 mm diameter pluviated triaxial specimen during an initial injection, with bacteria suspended in a solution containing cementation solution reagents minus calcium chloride. This initial injection excluded calcium chloride to prevent calcite precipitation during inoculation. While this omission of calcium chloride will have prevented precipitation, it may also have adversely affected bacterial fixing within the column, since solutions containing a calcium source have been shown to be particularly effective for fixing bacteria to sand (Harkes et al. 2010). The studies undertaken by Botusharova (2017) used PBS to form a bacterial suspension into which sand was wet pluviated to form the columns, with this suspension completely filling the column pore spaces. This was followed by an injection of cementation medium. Harkes et al. (2010) found that when the initial injection consisting of a suspension of bacteria entirely filled the sand column pores, only 14% of the optical density (OD) was retained upon injection of a 50 mM CaCl₂ fixation solution. This compares to 99 % bacterial retention (as determined through OD measurement) when the bacterial suspension filled just 17 % of the column pore volume and was followed by injection of one and a half pore volumes of the fixation solution (Harkes et al. 2010). Hence the approach taken by Botusharova (2017) may have resulted in significant loss of the bacterial inoculant from columns at this early stage.

Supply of cementation medium for MICP via injection has typically involved pumping this medium upwards through the base of sand columns (Montoya and Dejong 2013; Botusharova 2017) or alternatively supplying the cementation medium using the down-flow injection method (Cheng et al. 2016). The cementation medium introduced into a column following a subsequent treatment will be heavier than the solution (effluent) contained within the column pore spaces. The upwards injection process combined with the effect of gravity therefore helps ensure that all of the effluent within the columns is displaced as the column is injected and that this effluent is entirely replaced with the cementation medium.

2.6.1.2 Surface Percolation

Surface percolation is the most straightforward and economical approach for cementation medium delivery, in respect of the process used. Surface percolation has been developed for use in MICP applications for the in-situ stabilisation of sand by biocementation (Cheng and Cord-Ruwisch 2012; Cheng and Cord-Ruwisch 2014). Compared to injection, surface percolation has the advantage of not disturbing the soil when used for in-situ applications. The surface percolation process may be applied to unsaturated sand, whereas injection processes have required the sand samples to be saturated, to enable flow of bacteria and cementation media through the soil matrix. The bacterial suspension and cementation medium are transported through the soil by gravity and capillary forces.

The surface percolation process involves supplying bacteria in a solution to the surface of the material (by spraying or pouring), followed by application of cementation medium in the same manner. Cheng and Cord-Ruwisch (2012) applied this approach by first supplying bacteria to the top of columns in a solution amounting to 50 % of the water retention capacity of the sand columns, followed by the same volume of cementation solution containing urea and calcium chloride. Following 12 h incubation, 100 % of the water retention capacity of the sand of cementation medium was added to the top of the column.

For both injection and percolation there is a possibility of bacteria washout at high flow rates. The process becomes more complex with depth, since for increasing length of columns more layers of bacteria and cementation medium are needed (Cheng and Cord-Ruwisch 2012). This technique is particularly suited to porous granular soils with a high permeability (Cheng and Cord-Ruwisch 2014).

2.6.1.3 Surface Application

Surface application of biocementation treatment has been explored as a means of protecting calcareous building stone, in particular limestone (Le Metayer-Levrel et al. 1999) and to a lesser extent sandstone (Richardson et al. 2014). Microbes play a key role in mineral growth and rock weathering (Basha et al. 2018). Although this area is not a focus of this project it is an area with the potential for further research. In sedimentary stone such as sandstone and limestone the binding material is principally calcium

carbonate (Richardson et al. 2014), making MICP a particularly suitable application for protection, and potentially also repair.

Richardson et al. (2014) demonstrated the viability of cementation of sand samples, as a precursor to studies on stone, their studies were not dissimilar to the experiments involving surface percolation. Le Metayer-Levrel et al. (1999) tested the effectiveness of MICP surface treatment by spraying nutrient (cementation) medium mixed with bacteria directly onto the surface of limestone, to form a biocalcin protective crust. It is reported that, following in-situ treatment to a limestone church tower, after 3.5 yrs the external aspect remained unaltered (Le Metayer-Levrel et al. 1999).

2.6.2 Admixtures and Premixing

Early studies on self-healing via MICP in cementitious materials incorporated bacteria and cementation media into test specimens as an admixture, whereby a mixture of bacterial spores and calcium lactate were added directly to the cement mix, replacing part of the makeup water (Jonkers et al. 2008). It is noted that the bacterial spores are able to withstand high mechanical forces and may be viable for up to 200 yrs under dry conditions (Schlegel 1993). In this particular study there had been an observed loss of viability of the incorporated bacterial spores, linked with a decrease in cement matrix pore diameter sizes. It is suggested that the spores became crushed in aged specimens. Jonkers et al. (2008) suggest using encapsulation or immobilisation as way of protecting spores from being crushed. Although not noted in this paper, the highly alkaline environment within concrete may also impact upon bacterial viability and hence the MICP process, dependent upon the bacteria selected and their pH tolerance.

Similarly, the premixing process has been utilised for bio-grouting in soils, whereby calcium carbonate precipitate acts as a cementing material (Yasuhara et al. 2012). This process has been developed as a more environmentally friendly alternative to chemical grouting. Yasuhara et al. (2012) used urease enzyme as opposed to bacteria, in addition to urea and calcium chloride as reagents in the grout. It is suggested by Yasuhara et al. (2012) that the rate and magnitude of calcium carbonate precipitation would be controlled by the amounts of these reagents used. The unconfined compression strength of lab samples ranged from 400 kPa to 1.6 MPa, with a reduction in permeability achieved. Although using urease enzyme directly simplifies the process by eliminating the need for bacterial culture it also makes this particular method potentially unsuitable for use in self-healing applications unless the urease enzyme could also be stored within the biocement. The viability of urease in the long-term is however unknown.

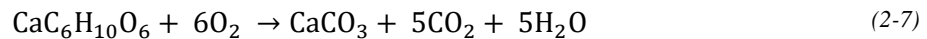
2.6.3 Immobilisation

A variety of porous materials, also referred to as carrier materials, have been used to immobilise bacteria and cementation media within cementitious materials, for the purposes of enabling self-healing via

MICP. These carrier materials may be used as internal nutrient reservoirs (Bundur et al. 2017). Immobilisation has been reported to be an efficient approach for bacteria-based self-healing in cementitious materials (Zhang et al. 2017b). Immobilised bacterial spores in this context will be activated by contact with water.

2.6.3.1 Expanded Materials: Clay, Perlite and Shale

A variety of expanded materials have been utilised as carrier materials to embed self-healing capability within concrete and mortar. Wiktor and Jonkers (2011) immobilised a mixture of calcium lactate and bacterial spores in expanded clay particles. The chemical process of calcium carbonate formation by bacterial activity, where calcium lactate ($\text{CaC}_6\text{H}_{10}\text{O}_6$) is used as the precursor, is presented in Equation (2-7) as reported by Jonkers et al. (2008), as cited in Khaliq and Ehsan (2015).



Wiktor and Jonkers (2011) obtained bacterial spores from alkaline lake soil, which were found to have a 98.7% homology to alkali resistant *Bacillus alkalinitrilicus*. Vegetative cells were deactivated by heating to 80 °C, so that only spores remained. Expanded clay, in the form of light weight aggregate of Liapor R of 1-4 mm diameter, were impregnated twice under a vacuum with calcium lactate and yeast extract followed by a bacterial spore suspension. The resulting calcium lactate content of the clay particles was six percent by weight. After fifty-six days of curing, cracks of between 0.05 and 1 mm were induced in Portland cement mortar specimens. The specimens were then immersed in tap water, allowing for free diffusion of oxygen and carbon dioxide through the water-air interface. The MICP process uses oxygen, therefore oxygen uptake was measured to quantify calcium carbonate precipitation. After a hundred days of immersion in tap water observed cracks of up to 0.46 mm were filled with calcium carbonate in bacteria-based specimens compared to 0.18 mm in control specimens without bacteria. The results of this study also showed that self-healing occurs to a small extent naturally in cementitious materials and can be significantly enhanced by MICP to heal wider cracks. Calcite and aragonite forms of calcium carbonate precipitates were identified under ESEM observation. Wiktor and Jonkers (2011) reported that after just twenty-eight days of incubation crack healing behaviour was similar for both control and bacteria-based specimens, and with increasing incubation crack healing in bacteria-based specimens increased in comparison to the control. No permeability measurements or strength tests were undertaken.

Zhang et al. (2017b) conducted experiments to compare expanded clay particles to expanded perlite, for immobilising bacteria for crack self-healing in concrete. Zhang et al. (2017b) refer to perlite immobilisation as a relatively low-cost approach compared to immobilisation using graphite nano-platelets, polyurethane or silica gel or encapsulation using melamine-based microcapsules. Perlite is found extensively in volcanic rock. *Bacillus cohnii* was used in this study. It is noted that both

vegetative cells and spores were immobilised. The perlite was impregnated with bacteria under a vacuum, and following oven drying a solution of calcium lactate and yeast extract was sprayed onto the surface of the particles. It is possible however that MICP may already be occurring at this stage since within the carrier materials since all constituents required are immobilised together.

Unlike studies undertaken by Wiktor and Jonkers (2011), Zhang et al. (2017b) did not immobilise the precursor chemical (and nutrients) under a vacuum. Instead, to prevent the sprayed-on calcium lactate and nutrients being dissolved by water in the concrete, the carrier materials were sprayed with a geopolymer coating consisting of a solution of metakaolin and sodium silicate. Following curing, cracks of 0.1 to 0.8 mm were induced in the Portland cement concrete specimens. Cracks of 0.78 mm were fully healed in concrete containing bacteria immobilised in perlite, compared to cracks of 0.45 mm in concrete with bacteria immobilised in expanded clay. These values were obtained after twenty eight days of healing, suggesting the selected bacteria, *Bacillus cohnii*, had enabled faster healing than the bacteria used by Wiktor and Jonkers (2011). Calcite crystals were observed to have been formed within cracks.

Expanded clay particles are also referred to as Ceramsite. Chen and Qian (2016) utilised Ceramsite as an immobilising carrier material for *Bacillus mucilaginous* bacteria, calcium nitrate and nutrients in concrete to enable self-healing, achieving similar results to Wiktor and Jonkers (2011) and Zhang et al. (2017b) with cracks of width 0.5 mm healed. This healing was achieved in 28 days, as opposed to after 100 days in the study by Wiktor and Jonkers (2011), with a faster rate of healing likely facilitated by the selected bacteria and also by supplying nutrients for the bacteria which the study by Wiktor and Jonkers (2011) neglects.

Expanded shale also fits into the lightweight aggregate category. Bundur et al. (2017) conducted MICP research using expanded shale aggregate with an absorption capacity of 24.2 %, with particles sizes ranging between 600 μm and 4.75 mm. Expanded shale aggregates were submerged in urea-yeast extract medium in a sealed container at 25 °C for 24 h to immobilise this medium. In this study bacteria were added in solution as part of the mixing water for the concrete. This may have rendered the study less affective compared to those whereby bacteria were also encapsulated, given the known issues concerning crushing of unprotected bacterial cells in cementitious materials during the mixing and curing stages. Mechanical forces during mixing can damage bacteria (Wang et al. 2014b). In addition to this bacteria can become squeezed when pores in concrete get continuously smaller (Wang et al. 2014b). Compressive strength of bacteria inoculated mortar at twelve days was identical to the control and less than 5 MPa higher than the control at twenty-eight days, calcium carbonate precipitation is not noted.

2.6.3.2 *Diatomaceous Earth*

Another immobilising carrier is siliceous diatomaceous earth (DE), with a particle size of typically 10 to 200 μm , which Wang et al. (2012) used to immobilise *Bacillus sphaericus*. Diatomaceous earth is highly porous and lightweight, consisting of fossilised remains of diatoms, it is resistant to heat and chemical action (Wang et al. 2012). Diatomaceous earth contains surface pores, these ranged from 0.1 to 0.5 μm and some particles were also found to have hollow inner structures.

Wang et al. (2012) reported that the optimum concentration of diatomaceous earth for immobilisation was 60 % by weight per volume of bacterial suspension. In this study the bacteria only were immobilised. Yeast, urea and ca-nitrate were added to the concrete mix, after firstly being dissolved in water. Crack widths of up to 0.17 mm were healed, which is somewhat smaller than the reported widths of cracks healed in the aforementioned studies incorporating immobilising materials. However, it was reported that after unloading, the remaining crack widths ranged from 0.15 to 0.17 mm, therefore 0.17 mm was the maximum crack width healing that could be observed. Hence, it is apparent that quantifying self-healing in terms of widths of cracks healed is not a reliable or suitable comparator across the studies reviewed since reported widths of cracks before healing varies. It was noted by Wang et al. (2012) that use of diatomaceous earth led to difficulties during casting of specimens, due to its high specific surface area and resulting high absorbency. If DE is more than 5 % by weight of the cement by mass the mortar paste becomes dry and workability decreases significantly (Wang et al. 2012).

2.6.3.3 *Zeolite*

In addition to perlite, another volcanic mineral which has been used in research incorporating immobilisation is Zeolite, a highly porous hydrated alum-silicate mineral with pore sizes between 0.1 and 0.3 μm , which is also used for ammonium removal (Guida et al. 2020). Bhaskar et al. (2017) immobilised *Sporosarcina ureae* and *Sporosarcina pasteurii* in Zeolite (Clinoptilolite), with particle sizes ranging from 0.42 mm to 1.4 mm. A 30 ml bacteria solution (10^6 cells/ml) was mixed with 12 g zeolite in falcon tubes. These tubes were shaken for one hour at 100 rpm to immobilise the bacteria in the zeolite. Since the size of most bacteria is 1 to 3 μm , the reported sizes of the pore spaces in the Zeolite would be too small for the bacteria, therefore it is likely the bacteria would have been adsorbed onto the rough surface of the zeolite. Cementation medium consisting of calcium lactate, urea and yeast extract were added to part of the concrete mixing water, as opposed to being immobilised, with concentrations of 2 %, 2 % and 0.2 % respectively of the cement mass. PVA fibres were also added to one test specimen. Both bacteria sporulated, possibly helped by the addition of manganese to the growth medium, which Bhaskar et al. (2017) reported stimulated formation of bacterial spores substantially.

When testing self-healing effects, Bhaskar et al. (2017) found that water absorption was shown to decrease with specimen age, more so for specimens containing the zeolite immobilised bacteria than

for specimens without bacteria. The specimens containing PVA fibres and immobilised *Sporosarcina pasteurii* had the highest percentage reduction (90.43 %) of primary sorptivity after eight months, this was compared to specimens without fibres which had 60.87 % reduction in primary sorptivity, showing that inclusion of PVA fibres had some effect on material enhancement. It was found most healing occurred in the first four months, with little change after. It is noted cracks of up to 0.1 mm were completely filled in specimens containing *S. Pasteurii* compared to cracks of 0.07 mm for specimens containing *S. ureae*, however it isn't clear if these were the maximum widths of cracks in the cracked specimens. These cracks are nonetheless relatively narrow and these results therefore don't provide sufficient evidence of self-healing. Since Zeolite is a pozzolan it may also influence material properties of concrete.

2.6.3.4 Lightweight Aggregate and Graphite Nanoplatelets

Khaliq and Ehsan (2015) immobilised *B. subtilis* in Lightweight aggregate (LWA) and graphite nanoplatelets (GNP). LWA were soaked in bacterial solution for 24 h prior to mixing into concrete. GNP was also soaked with bacterial solution before adding to the concrete mix, superplasticiser was required in this mix to ensure more uniform distribution of GNP. Calcium lactate was added as part of the cement mix. Self-healing efficiency was tested by conducting compressive strength tests and observing healing of cracks up to 1 mm width. It was reported by Khaliq and Ehsan (2015) that the small particle size of GNP results in it acting like a filler material and helps ensure its uniform distribution within the concrete, enabling bacteria to be readily available at crack sites. LWA was less uniformly distributed in comparison. After twenty-eight days the maximum crack healing was 0.81 mm and 0.61 mm for GNP and LWA specimens respectively, compared to 0.37 mm in specimens with bacteria incorporated directly in solution in water added to the concrete mix. GNP specimens showed maximum healing in cracked samples at seven days, compared to fourteen days after curing for LWA. It is suggested continued hydration reactions in concrete put pressure on GNP particles which are weak when subjected to multi axial loading, resulting in damage to bacteria cells, and therefore LWA provides better protection for bacteria in concrete. Compressive strength increases were 12 % and 9.8 % respectively for LWA and GNP specimens, compared to the control specimens. Self-healing is noted to be a cause of compressive strength increase. Compared to concrete aggregate, the smaller particle size of LWA and GNP makes concrete denser, resulting in a compressive strength increase. However, the influence of the properties of the carrier materials themselves is not reported, with regards to the properties of the concrete.

Sierra-Beltran et al. (2014) used lightweight aggregate (0.25 to 2 mm) to immobilise both cementation medium (calcium lactate and yeast extract) and alkali resistant *Bacillus* bacteria spores. Sierra-Beltran et al. (2014) also reported that this resulted in an increase of compressive strength when compared to

controls containing no LWA, bacteria or cementation medium. Self-healing via MICP could not however be verified in this study given lack of observed calcium carbonate precipitate.

2.6.3.5 *Fibres*

Prior to this doctoral study, research had not previously been undertaken into the use of fibres as a carrier material for the precursor chemicals, or bacteria, to enable self-healing in cementitious materials or biocemented sand and soil. Of particular interest in this research are natural fibres, as a novel and sustainable approach to the long-term storage and supply of nutrients and precursor chemicals for self-healing via MICP. Natural fibres are reported to be strongly hydrophilic (Rahman et al. 2007). This property may result in these materials being particularly suited as carriers for MICP, as the carriers are required to be highly absorbent. Low-cost natural lignocellulosic fibres such as coir, jute and hemp have been used for soil stabilisation purposes (Prasanna and Mendes 2020) and are highly absorbent. Coir, the outer fibrous covering of a matured coconut husk, was considered at this stage to be the most suitable for long-term self-healing MICP applications, since due to its high lignin content it degrades much more slowly than other natural fibres (Hejazi et al. 2012).

Natural fibres, in addition to being potential cementation medium reservoirs, will further enhance the properties of the biocemented material. While research has been undertaken into the use of natural and synthetic fibres to improve engineering properties of soil, natural fibres had not at the onset of this study been incorporated within soil biocementation systems. The inclusion of synthetic PVA fibres (0.1 mm in diameter and 12 mm length) in MICP treated sand has been reported to have the effect of reducing brittleness of the bio-cemented sand and enhancing the MICP process by bridging pores in the sand (Choi et al. 2016). Addition of polypropylene fibres has been found to increase shear strength of cemented (using portland cement) sands (Kutanaei and Choobbasti 2015). Fibres have also been used to enhance material properties of MICP-treated concrete. PVA fibres, when used in addition to immobilisation of bacteria in zeolite, resulted in a greater sorptivity reduction in concrete than use of immobilised zeolite alone (Bhaskar et al. 2017).

2.6.4 **Encapsulation**

Encapsulation techniques have been shown to be effective in cementitious materials for enabling self-healing via MICP. Capsules provide protection for the bacteria against the mechanical processes involved in concrete production which may otherwise render the bacteria ineffective through crushing. Encapsulation materials utilised within concrete and mortar have included hydrogels, glass and ceramics.

2.6.4.1 Silica Gel and Polyurethane Foam in Glass Capsules

Immobilisation and encapsulation have also been combined. Wang et al. (2011) immobilised *B. Sphaericus* bacteria in silica gel and polyurethane foam, before encapsulating these materials in glass tubes of 40 mm length and 3 mm diameter. Cementation medium consisting of urea and calcium nitrate was encapsulated separately in glass tubes attached to those containing immobilised bacteria. Silica gel is porous, biologically inert, and has good properties of mechanical, thermal and photochemical stability (Wang et al. 2011). It was found that bacterial activity decreased when immobilised in silica gel, attributed to a retarding effect of the silica gel on the diffusion of urea (Wang et al. 2011), and the possibility that ammonia may be trapped within the gel and could not escape. Likewise, the process in the immobilised PU was slower compared to using non-immobilised bacteria and nutrients, with only 30 % of urea being decomposed, compared to 50 % in silica and 70 % with free cells.

Wang et al. (2011) reported that strength regain following specimen fracture and subsequent healing was attributed mostly to polyurethane content, since calcium carbonate precipitation within the PU foam was limited. Calcium carbonate was able to precipitate more in silica gel; however, strength regain was less than 5 %. Overall, use of PU and silica gel as immobilising carrier materials appeared to have resulted in minimal positive results and combined with the complexity of this method it would be deemed an unsuitable option to consider for use in soils. Glass encapsulation of reagents would not be practical for geotechnical applications, furthermore glass would not be a desirable material to use since it is not biodegradable.

2.6.4.2 Melamine-Based Micro Capsules

Wang, Soens, et al. (2014c) used melamine-based capsules, of approximately 2-5 μm diameter to encapsulate *Bacillus sphaericus* bacteria. Cementation medium consisting of yeast, urea and Ca-nitrate was added directly to the concrete mix. The microcapsules were found to resistant to high pH and sensitive to humidity and became flexible in conditions of high humidity and brittle in low humidity environments. This ensured the capsules didn't break during the concrete mixing process but were easily broken when the concrete cracked. The bacteria were encapsulated using a poly-condensation reaction based micro-encapsulation process, with the final product being an emulsion consisting of microcapsules and water. Twenty-eight days after casting, cracks of between 0.05 mm and 1 mm were induced in the concrete specimens. The maximum crack width healed was 0.97 mm.

Wang et al. (2014c) reported that the melamine-based microcapsules led to a decrease in compressive strength of 15 % to 34 % of concrete comprising of 1 % to 5 % microcapsules respectively, after twenty eight days. Water absorption however decreased. A mercury intrusion porosimetry test indicated a slight increase in porosity in specimens containing microcapsules. The microcapsules resulted in large pores within the concrete matrix. Microcapsules ruptured under tensile force. Although the cementation

medium was not encapsulated along with bacteria, Wang et al. (2014c) report that this would be the best option since it would facilitate spore germination under suitable conditions but this had not been possible due to technical difficulties concerning encapsulating water soluble agents into microcapsules. The maximum crack width healed in this study was greater than reported for other methods of bacteria and cementation media delivery.

2.6.4.3 Alginate-based hydrogel

Recent studies by Harbottle et al. (2013), Wang et al. (2015) and Palin et al. (2016) have investigated the use of sodium alginate, as a low cost biopolymer (Palin et al. 2016), to produce calcium alginate hydrogel beads. Harbottle et al. (2013) and Palin et al. (2016) utilised sodium alginate to encapsulate cementation reagents along with *Sporosarcina pasteurii* and bacteria of the *Bacillus* genus respectively. Wang et al. (2015) encapsulated *Bacillus sphaericus* bacteria only. Sodium alginate is a water-soluble anionic polysaccharide, extracted from cell walls of brown algae, and when combined with calcium becomes insoluble in water (Wang et al. 2015).

The cementation medium encapsulated by Harbottle et al. (2013) consisted of Oxoid CM0001 nutrient broth, urea, sodium bicarbonate and ammonium chloride. A solution containing sodium alginate along with these reagents and bacterial cells was pipetted in 10 µl aliquots into a calcium chloride (CaCl₂) solution. This calcium chloride solution acted a gelling agent, with the calcium source also becoming encapsulated along with the bacteria and other cementation medium constituents as the calcium alginate beads were formed. Palin et al. (2016) mixed bacterial spores with a sodium alginate solution, along with magnesium acetate yeast extract, with beads formed by pumping this solution from a 5 cm height into a calcium acetate gelling solution. Autoclaving was not used in either study for sterilisation since this would result in depolymerisation of the alginate (Palin et al. 2016), therefore test conditions were not entirely sterile. Tests undertaken by Palin et al. (2016) showed that MICP occurred in the 8 °C test conditions, this test was a proof of concept and not applied to or within concrete. Palin et al. (2016) focus on applications in low-temperature saline marine environments. Harbottle et al. (2013) tested the effectiveness of the calcium alginate beads for enabling self-healing of cracks in mortar, in addition to establishing optimum concentrations of sodium alginate and calcium chloride. Whilst the beads were shown to form a bond in fractured mortar specimens, Harbottle et al. (2013) report that the effect on mechanical performance was relatively weak. Harbottle et al. (2013) found that the optimal combination of alginate and CaCl₂ was found to be 2.8 % and 3 % respectively. Palin et al. (2016) had used a lower 1.5 % (w/v) sodium alginate concentration and 6.4 g/L calcium acetate gelling solution.

To produce a stronger carrier, and micro-sized beads, Wang et al. (2015) modified sodium alginate, chemically and with UV polymerisation, to create covalently bonded modified alginate. The sheets of hydrogel resulting from this process, incorporating bacterial spores, were freeze dried and ground to

form fine powders, with particles sizes of 20 µm to 100 µm. Urea and yeast extract were added directly to the cement mix to provide the required precursor chemicals and bacterial nutrients for self-healing via MICP, with the calcium source contained with the modified alginate hydrogel. The addition of 0.5 % and 1 % by mass of cement of the hydrogel was reported by Wang et al. (2015) to result in a compressive strength decrease of 16.2 % and 23.4 % respectively and tensile strength decrease of 15.6 % and 30 % respectively.

Hydrogels, including alginate gels, have a high water absorption and retention capacity, water can be absorbed, retained and gradually released to support bacterial activity (Wang et al. 2015). This would make this type of carrier suitable for applications in environments which may experience prolonged dry conditions, or that may be water scarce. Moisture uptake of hydrogels was found to increase with increasing relative humidity (Wang et al. 2015).

2.6.4.4 Synthetic Hydrogel

Compared to alginate-based hydrogels that can be produced with simple lab-based procedures, synthetic hydrogels may be a costly approach given the process involved in producing the hydrogels. The hydrogels used by Wang et al. (2014b) were developed by the Polymer Chemistry and Biomaterials Group of Ghent University (PBM-UGent). These hydrogels were synthesised based on commercial Pluronic F-127, which is a tri-block copolymer of polyethylene oxide and polypropylene oxide. To form the hydrogel capsules, powdered reagents (yeast extract, urea and calcium nitrate) are added to the polymer solution, followed by a suspension containing spores, then the initiator. Immediate degassing after prevented germination of spores, since water was present the MICP process would be initiated if the solution came into contact with oxygen. Hydrogel sheets were then formed and cut into small pieces. Calcium carbonate was observed to form inside and on the surface of the hydrogel, after being placed in autoclaved distilled water. When using hydrogels in concrete, part of the crack healing appears to be due to the swelling of the hydrogel itself, since Wang et al. (2014b) report that the maximum crack width healed was 0.5 mm using hydrogels containing bacteria and 0.3 mm when using hydrogels without bacteria inside.

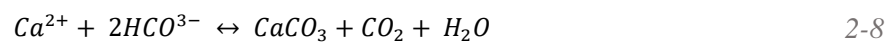
In a second paper on hydrogels, Wang et al. (2014a) reported that hydrogel microcapsules used resulted in an unacceptable decrease in compressive strength of the concrete specimen by about 50 %. In this study the hydrogel sheets were freeze dried and ground into a powder, and contained only bacteria, with the cementation medium reagents being added in solution to the concrete mix. The same amount of healing was observed however in respect of crack width healed in concrete, compared to the previous study. This demonstrated that the process was just as effective with the cementation medium immobilised. Super absorbent polymers were also utilised by Kua et al. (2019).

2.6.5 Groundwater

It is possible that in some locations groundwater may provide the calcium source required for biocementation. There have been limited studies into the use of groundwater as a source of nutrients for MICP (Cheng et al. 2016). Investigation has been undertaken into the use of MICP to remove contaminants in groundwater (Fujita et al. 2008), which provides some insight into the potential for groundwater to enable MICP. In the study by Fujita et al. (2008), food-grade molasses, as a bacterial nutrient source, and urea, were added to groundwater samples from the Eastern Snake River Plain Aquifer in Idaho to promote calcium carbonate precipitation. This resulted in a cloudy suspension of calcite being observed. This study had shown that suitable urease positive bacteria had been present within the groundwater tested, along with a sufficient calcium source.

Groundwater as a supply of nutrients and precursor chemicals may be of particular relevance and interest in respect of mitigating liquefaction damage, since seismic-induced liquefaction generally occurs in loose granular soil below the ground water table (Burbank et al. 2011). Biostimulation studies conducted by Gat et al. (2016) used cementation media based on artificial groundwater, which was representative of the composition of Israel's coastal aquifer and contained $MgCl_2$ (1 mM), $MgSO_4$ (1 mM), $NaHCO_3$ (2.56 mM), $NaCl$ (14.35 mM), $CaCl_2$ (2.43 mM) and KCl (0.32 mM). Gat et al. (2016) suspended 10 g samples of sand in 100 mL of this cementation medium with urea added. In addition to urea, samples were prepared with combinations of sources of organic carbon added including molasses, yeast extract and $NiCl_2$. It is noted that the sand in the area studied is nutrient poor, with a low carbon content of 0.5–1 % (w/w). In this study urea hydrolysis was not observed without addition of a source of organic carbon. This study, along with work by Fujita et al. (2008), demonstrates the site-specific nature with regards to potential research into groundwater as a source of cementation medium for MICP.

Biominalisation processes associated with the formation of speleothems may also provide some insight into the suitability of groundwater as a source of nutrients and precursor chemicals for MICP. Seepage of water saturated with carbonates in the right conditions, dependent on metabolic activity of indigenous bacteria, will lead to deposition of calcium carbonate, as per Equation (2-8).



Within the Sahastradhara caves, studied by (Baskar et al. 2006), water seeping into the cave saturated with carbonates had a higher partial pressure of CO_2 than the cave air, resulting in degassing of CO_2 from water to air. This decreased the solubility and saturation of calcium carbonate, leading to deposition. This example demonstrates the ability of groundwater to act as a source of precursor chemicals, provided it contains an adequate carbon (bacterial nutrient) source, which will be very much dependent on the location and chemicals already present in overlying soil.

2.6.6 Summary and Conclusions

Table 2-3, Table 2-4 and Table 2-5 summarise the different cementation medium (and bacteria) delivery options for biocementation and self-healing via MICP in porous construction materials. There is insufficient data available to fully compare the effectiveness of each immobilisation and encapsulation technique. Data reported in literature regarding delivery mechanisms for cementation media/ reagents (and also bacteria) are not fully comparable due to different approaches to test specimen preparation, use of different bacteria and reagents, and the different tests undertaken to determine changes to material properties. Among the research undertaken and reviewed concerning self-healing within cementitious materials the reagents used to promote self-healing differ and may include calcium lactate alone as a precursor chemical, or a combination of urea and calcium nitrate, with nutrients for bacteria occasionally added.

Incorporation of bacteria and reagents for self-healing into cementation materials as an admixture has been reported to be ineffective (Jonkers and Schlangen 2008) and to lead to compressive strength decrease. Direct application procedures such as injection, percolation and premixing of cementation reagents into the material to be cemented soil have been effective for achieving biocementation via MICP. Furthermore, the injection process for cementation medium delivery has been utilised to show that biocemented sands may self-heal in principle (Montoya and Dejong 2013; Botusharova 2017). This process however, along with the other direct application methods, requires external intervention.

A variety of techniques to immobilise bacteria and cementation reagents have been tested by researchers investigating self-healing systems in cementitious materials. In respect of immobilising cementation medium, these methods include vacuum assisted immobilisation (Wiktor and Jonkers 2011), spraying reagents onto the surface of carriers (Zhang et al. 2017b) and soaking the carrier materials in cementation medium for 24 h (Bundur et al. 2017). In the context of cementitious materials, and where immobilisation has been utilised, the most significant crack healing of 0.81 mm was achieved when the cementation medium reagent (calcium lactate) was added directly to the concrete mix and bacteria was immobilised by GNP (Khaliq and Ehsan 2015). A similar crack healing of 0.79 mm was achieved when bacteria was immobilised in expanded perlite sprayed with reagents and coated with geo-polymer (Zhang et al. 2017b). As previously mentioned, crack healing width is not always a reliable comparator however since the reported widths of cracks prior to healing vary.

Encapsulation has also been used as a way of containing cementation reagents and bacteria within cementitious materials for self-healing. The most significant crack healing, of 0.97 mm width, has been reported to result from using melamine microcapsules to contain bacteria and cementation reagents

added to the mortar mix (Wang et al. 2014c). Encapsulation of reagents and bacteria in hydrogel capsules has been reported to result in cracks of 0.5 mm width being healed (Wang et al. 2014b).

The use of immobilising carrier materials has not been reported to have adverse effects on material properties of the tested materials. In comparison, an often-reported disadvantage of using microcapsules to store cementation medium (and bacteria) for self-healing is the measured decrease in compressive strength of the cementitious material due to the capsules. This decrease in compressive strength has been reported with as low as 1 % of concrete consisting of melamine microcapsules (Wang et al. 2014c). Wang et al. (2015) reported that encapsulation using sodium alginate hydrogel resulted in a decrease in both compressive and tensile strengths when just 0.5 % of the hydrogel by mass of cement was used. Similarly, use of synthetic hydrogel as an encapsulating material resulted in compressive strength decrease of concrete (Wang et al. 2014a).

To enable a porous construction material to self-heal, whilst also improving material properties such as compressive strength, the immobilisation approach to cementation medium storage would appear to be the most suitable based upon the aforementioned studies of self-healing cementitious materials. Within cementitious materials, the bacteria are often immobilised or encapsulated to protect the bacterial cells or spores from the highly alkaline environment within concrete and from damage during the mixing process. It was therefore not deemed necessary at this stage to immobilise or encapsulate bacterial cells or spores within biocemented geomaterials.

Table 2-3. Direct application methods for cementation medium delivery for healing of porous construction materials via MICP.

Delivery Mechanism	Process	Application	Bacterial Strain	Strength after Healing	Permeability	Limitations/ Findings	References
Surface Application (Bio-deposition)	Surface sprayed with bacterial suspension, then sprayed daily/ every two days with nutrient (cementation) medium, to create surface calcareous coating.	Limestone	Carbonatogenic bacterial strains (Unnamed)	–	Decreased surficial permeability, while retaining permeability for gas.	Process most effective on previously cleaned stone. Regeneration is mentioned but tests relate to surface protection only, as opposed to self-healing.	(Le Metayer-Levrel et al. 1999)
Injection	Bacteria injected followed by cementation solution.	Sand	<i>Sporosarcina pasteurii</i>	Shear strength fully recovered.	–	Results indicated MICP cemented sands can be healed to original stiffness and peak shearing strength, following degradation.	(Montoya and Dejong 2013)
Surface Percolation	Cementation solution applied to the top of sand columns and allowed to percolate by gravity and capillary forces.	Sand	<i>Bacillus sphaericus</i>				(Cheng and Cord-Ruwisch 2012) (Cheng and Cord-Ruwisch 2014)
Premixing (Grouting)	Urease, urea, and calcium chloride are used as reagents contained in the grout.	Sand	Direct use of urease enzyme			Uses enzyme urease in place of bacteria. Results indicated that high CaCl ₂ -urea concentration relative to amount of urease may inhibit urease activity.	(Yasuhara et al. 2012)
Admixtures	Cement paste admixture, incorporating bacterial spores and calcium lactate.	Cement stone specimens	<i>Bacillus cohnii</i> and <i>B. pseudofirmus</i>	Calcium acetate and yeast extract additions reduced compressive strength to half that of control.	–	Substantial decrease in number of viable bacteria cells with specimen age.	(Jonkers and Schlangen 2008)

Table 2-4. Immobilisation methods for cementation medium storage and delivery for healing of porous construction materials via MICP.

Delivery Mechanism	Process and Reagents	Application	Particle size (Pore size)	Bacterial Strain	Strength after Healing	Permeability	Crack Width Healed (Curing duration)	Limitations/ Findings	References
Diatomaceous Earth (DE)	DE used to immobilise bacteria, with yeast extract, urea and calcium nitrate added to cement slurry.	Concrete	Typically, 10 to 200 μm (0.1 to 0.5 μm)	<i>Bacillus sphaericus</i>	-	-	0.17 mm (28 days)	Diatomaceous earth (DE) was found to have a protective effect for the bacteria in a high-pH cement environment. DE is highly porous and lightweight	(Wang et al. 2012)
Expanded Clay Particles	Calcium lactate and bacterial spores embedded in expanded clay particles.	Concrete	-	Bacterial spores from alkaline lake soil, with 98.7% homology to <i>Bacillus alkalinitrilicus</i>	-	-	0.46 mm (100 days)	Bacteria active several months after testing. Free water an essential component for significant amount of self-healing	(Wiktor and Jonkers 2011)
Ceramsite (Expanded Clay)	Bacteria, nutrients and calcium nitrate immobilised by ceramsite.	Concrete	(5 μm to 100 μm)	<i>Bacillus mucilaginous</i>	Increase in flexural strength	5.3×10^{-6} to 9.5×10^{-6} m/s (control) 0.8×10^{-7} m/s (immobilised)	0.5 mm (28 days)		(Chen and Qian 2016)

Expanded Shale Aggregates	Expanded shale aggregates submerged urea-yeast extract medium in a sealed container at 25 °C for 24 h, with bacteria added in mixing water for the concrete.	Concrete	600 µm to 4.75 mm	<i>Sporosarcina pasteurii</i>	–	–	–	Suggests method is particularly suited to mixes with a low water-to-cementitious ratio	(Bundur et al. 2017)
Lightweight Aggregate (LWA)	LWA impregnated with calcium lactate and yeast extract solution, followed by bacteria.	Concrete	–	<i>B. cohnii</i> , (originally isolated from alkaline soil samples)	Average compressive strength at 7, 28, and 56 days higher with LWA containing bacteria than control mix. Slight decrease in flexural strength.	–	–	Observed amounts of calcium carbonate precipitate didn't substantially differ from control specimens, it is suggested this is due to limited nutrients supplied. Test specimens were also reinforced with PVA fibres.	(Sierra-Beltran et al. 2014)
Graphite Nanoplatelets (GNP)	GNP soaked with bacterial solution before adding to concrete mix. Calcium lactate added directly to concrete mix.	Concrete	–	<i>Bacillus subtilis</i>	Increase of 9.8% in compressive strength, compared to 12% when bacteria immobilised by LWA.	–	0.81 mm (28 days)	When compared to LWA immobilisation, specimens containing GNP showed less compressive strength increase	(Khaliq and Ehsan 2015)

Zeolite	Zeolite immobilised bacteria added to mix of cement, sand, and cementation solution containing calcium lactate, urea and yeast extract.	Cement mortar	0.42 mm to 1.4 mm (0.3 to 0.1 mm)	<i>Sporosarcina ureae</i> and <i>Sporosarcina pasteurii</i>	Increase in compressive strength	–	0.1 mm (6 months)	Compressive strength increased dependent on bacteria type, greatest with <i>Sporosarcina pasteurii</i> . Water uptake decreased compared to control specimens	(Bhaskar et al. 2017)
Expanded Perlite (EP)	EP impregnated with bacterial spores under a vacuum, sprayed with calcium lactate and yeast extract and coated with geo-polymer.	Concrete	2 to 4 mm	<i>Bacillus cohnii</i>	–	–	0.79 mm (28 days)	EP contained large cavities up to 100mm in size, allowed bacterial contact with sufficient water and oxygen	(Zhang et al. 2017b)

Table 2-5. Encapsulation methods for cementation medium storage and delivery for healing of porous construction materials via MICP.

Delivery Mechanism	Process and Reagents	Application	Bacterial Strain	Capsule Size	Strength after Healing	Permeability	Crack Width Healed (Curing duration)	Limitations/ Findings	References
Glass tubes containing silica gel immobilised bacteria/ Polyurethane (PU) foam immobilised bacteria	Glass tubes containing immobilised bacteria attached to tubes containing calcium nitrate and urea and embedded into concrete. Tubes release contents when ruptured following cracking of concrete.	Concrete	<i>B. Sphaericus</i>	40 mm length, diameter 3 mm tube	50 % to 80 % regain with bacteria immobilised in PU, this was attributed mostly to the PU itself	10 ⁻⁶ m/s (control) 10 ⁻⁹ to 10 ⁻⁷ m/s (silica gel immobilised) 3x10 ⁻¹¹ to 6x10 ⁻¹¹ m/s (PU)	–	Bacterial activity decreased after being immobilised in silica gel/ PU, compared to non-immobilised bacteria. Bacteria immobilised into silica gel had higher ureolytic activity. As pH increased from 6.5 to 7 more urea was decomposed.	(Wang et al. 2011)
Sodium Alginate Hydrogel Beads	Solution containing sodium alginate, bacteria, Oxoid CM0001 nutrient broth, urea, sodium bicarbonate and ammonium pipetted into a calcium chloride solution. Added to concrete during mixing process.	Portland cement mortar (surface)	<i>Sporosarcina pasteurii</i>	–	Flexural strength regain of up to 3 % with 3 % alginate.	–	–	Requires moisture. Lack of adhesion and bacterial activity on dry surfaces. Alginate gel can support active bacteria for several weeks.	(Harbottle et al. 2013)

Modified Alginate-Based Hydrogel (AM-H)	Bacterial spores encapsulated into AM-H, freeze dried and grinded, then added to concrete as a powder. Urea and yeast extract added directly to the cement mix.	Concrete	<i>Sporosarcina pasteurii</i>	20 to 100 μm	For 0.5 to 1.0% AM-H tensile strength decrease of 15.6 to 30%, compressive strength decreased 16.2 to 23.4 %.	–	–	Addition of AM-H causes some strength reduction, it is suggested this can be reduced in concrete by adding more cement and by better particle packing and use of less water. AM-H has a good water absorption and moisture uptake capacity and protects bacteria during concrete mixing	(Wang et al. 2015)
Synthetic Hydrogel Capsules	Bacterial spores, yeast extract, urea and calcium nitrate encapsulated into hydrogels, mixed as a powder into concrete.	Concrete	<i>Bacillus sphaericus</i>	–	–	Average decrease of 68 % after crack healing.	0.5 mm (28 days)	Swollen hydrogels act as water reservoirs for continuous crack healing, allowing MICP to continue without continuous water supply. Water permeability of material significantly reduced.	(Wang et al. 2014b)
Melamine-based microcapsules	Poly-condensation reaction-based microencapsulation	Portland cement mortar	<i>Bacillus sphaericus</i>	2-5 μm	Negligible effect on tensile strength.	10^{-6} to 10^{-5} m/s (Control)	0.97 mm (28 days)	Decrease in tensile strength if >3% microcapsules.	(Wang et al. 2014c)

<p>process. Microencapsulated bacteria, with yeast, urea and Ca-nitrate added directly to the concrete mix. Breakage of capsules required to activate SH process.</p>	<p>Compressive strength decrease due to microcapsules</p>	<p>2.0×10^{-7} to 2.0×10^{-6} m/s (5 % microcapsules)</p>	<p>Decreased compressive strength with increasing microcapsule addition. Capsules have impermeable shells, are flexible at high humidity and brittle in low humidity.</p>
--	--	--	---

3 THEORETICAL FRAMEWORK

3.1 Self-Healing Microbially Induced Calcium Carbonate Precipitation (SH-MICP)

This chapter examines the use case and potential for self-healing MICP (SH-MICP) in the context of geotechnical engineering. Research into the concept of self-healing in construction materials to date has primarily focussed on cementitious materials. The development of self-healing sand or soil structures, for potential use in geotechnical applications, is in its infancy. The process is intended to be biomimetic in that it mimics self-healing responses observed naturally within soils, as detailed in Chapter Two, Section 2.4. This is an area of significant importance, considering the cost of infrastructure projects, and therefore possible savings that could be achieved through the ability of geotechnical structures to self-heal in response to damage, enhancing their durability and sustainability and minimising environmental impact.

The aim of self-healing MICP (SH-MICP) is that it should enable a material to detect and respond to damage or deterioration automatically. Self-healing, in the context of construction materials, is defined as the, ‘partial or total recovery of at least one property of a material’, (Jonkers 2011). This doctoral research has focussed on strength recovery. Self-healing MICP could improve the resilience of geotechnical structures, through embedded autonomous healing capability, and thereby enabling the restoration of geotechnical properties of the biocemented material following failure. Self-healing MICP has been demonstrated to work in principle, through lab tests undertaken by Montoya and Dejong (2013) and Botusharova (2017). These studies had only demonstrated healing as opposed to self-healing, since intervention had been required by means of injection of cementation medium to achieve the healing responses reported.

Self-healing MICP, in the context of geological materials, primarily refers to the process by which degraded MICP bonds are healed by re-initiating the biogeochemical process of MICP to restore the initial properties of the cemented material, such as stiffness, compressive strength, bearing capacity or permeability. Figure 3-1 depicts the cycle of biocement deterioration and healing via MICP, as an overview of this process. System inputs required for healing are water (external input) along with nutrients and precursor chemicals (internal input). This will result in MICP provided environmental conditions are adequate and that there are suitable bacteria present (vegetative cells or spores) in the biocemented material to catalyse the production of calcium carbonate. The healing process will be an

autonomous one (self-healing) if the nutrients and precursor chemicals required for the MICP process are already stored within the soil matrix. Healing could otherwise be achieved via external intervention to supply the cementation medium via injection or surface percolation, this would however require monitoring of the structure to know when this intervention may be needed. The process of self-healing MICP, as covered by this doctoral study, is initiated by the presence of water, this being a trigger for the process and a mechanism by which the biocemented soil matrix can be self-sensing to initiate a response to damage.

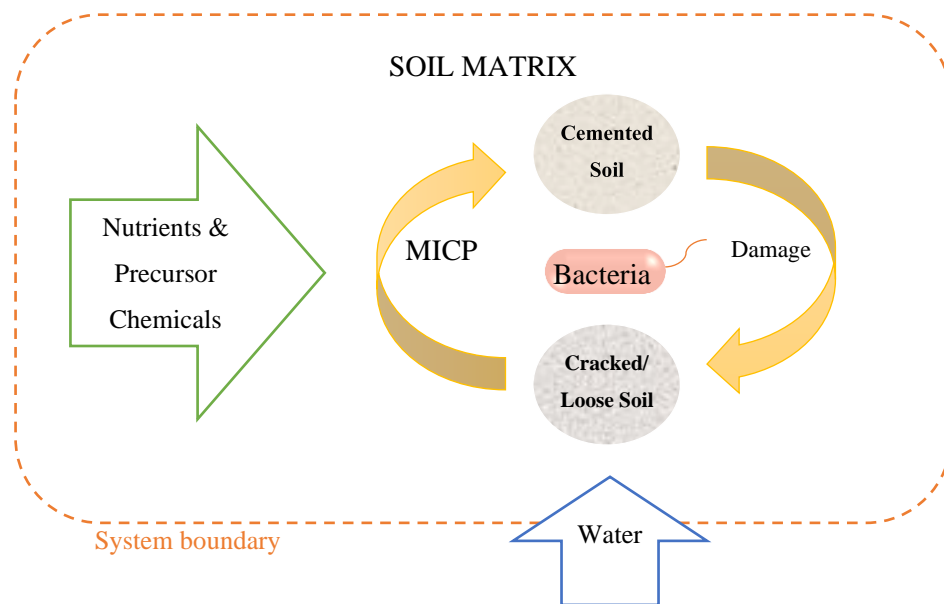


Figure 3-1. Healing MICP process - system overview.

3.1.1 Embedding Self-Healing Capability

This research focuses on the development of biocemented sand material with self-healing capability. In prior research studies, immobilisation or encapsulation have been used to embed self-healing capacity within mortar and concrete, as summarised in Chapter Two, Section 2.6. This research focusses primarily on immobilisation as a novel approach to enabling self-healing of biocemented sands, in addition to a study using an alginate hydrogel method of encapsulation.

Within a biocemented sand structure, immobilisation using suitable carrier materials, or encapsulation, would be used as a means of storing the nutrients and precursor chemicals required for self-healing via MICP. It is envisaged that the approach to incorporation of the self-healing MICP process into a sand or soil structure would most likely involve premixing and therefore it would be most suitable for new geotechnical structures. It may also be possible to introduce the self-healing MICP system into existing structures and also insitu for ground improvement via deep mixing. The SH-MICP process may also be

suitable to enable healing of geotechnical structures which have not been previously been cemented by MICP, however the focus of this research is on embedding self-healing capability within the biocemented material.

It is possible that microcapsules, due to their size, could be injected into soil. Production of microcapsules was deemed beyond the scope of this research project owing to limitations in respect of facilities and equipment.

3.1.2 Activation of Self-Healing MICP

The response to methods of encapsulated/ immobilised cementation media delivery would require investigation, since this is unknown in geomaterials. It had been assumed that the self-healing process would be initiated once requirements for MICP are met, providing the supply of bacteria, nutrients and precursor chemicals are adequate, and nucleation sites are available (cracks/fissures etc.). With the exception of glass and melamine microcapsules, the immobilising and encapsulating materials covered in Chapter Two are porous and will allow water entry following deterioration of calcium carbonate precipitate, to enable initiation of SH-MICP. The glass and melamine-based microcapsules would require movement of the biocemented material to initiate SH-MICP through capsule fracture.

Following damage/ deterioration to the biocemented sand or soil matrix, water will have a route to enter via microcracks and will fill void spaces – resulting in the release of immobilised nutrients and precursor chemicals from the carrier materials. This process is depicted in Figure 3-2, within which CM denotes the cementation medium of nutrients of precursor chemicals used for MICP. Once the immobilising carrier materials, or hydrogel beads, become saturated and surrounded by water they are expected to release the CM into the surrounding fluid. Once specific nutrients are sensed spores will germinate, followed by water uptake enabling bacterial outgrowth (Luu et al. 2015). This is the mechanism by which the biocement augmented with encapsulated/ immobilised cementation medium is proposed to be able to detect damage and self-heal. The self-healing process will therefore be reliant upon hydration. Once water re-enters via cracks the dormant bacterial spores will become metabolically active.

The approach taken in this study is a water activated self-healing MICP process (i.e., desaturated conditions to be maintained prior to activation). It is expected that the flow of water will initiate further MICP for self-healing. An alternative approach could be a pH activated process; however, it was considered this would be difficult to implement given the changes in pH during biocement production. Once soil is desaturated, the MICP process will cease, and stores of cementation medium will be retained for future self-healing.

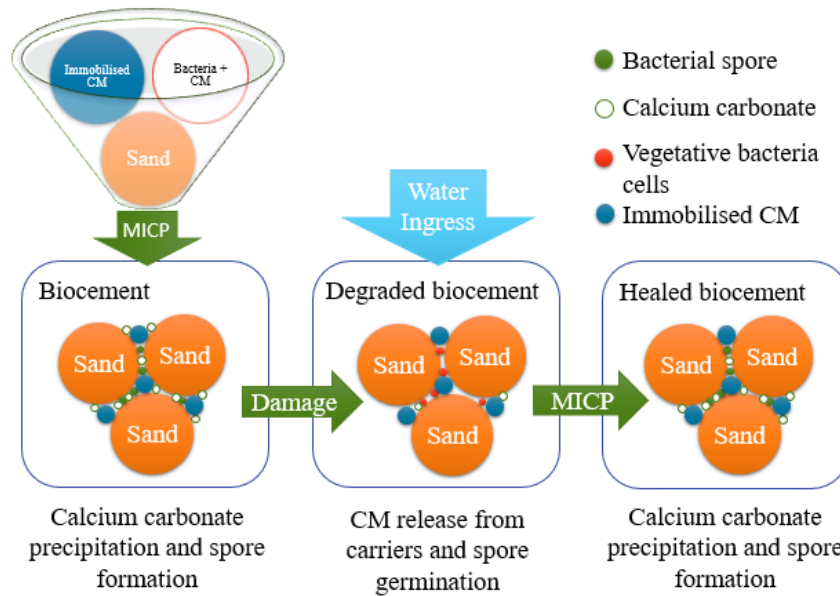


Figure 3-2. Self-healing MICP process covering formation of biocement and activation of self-healing response following damage and water entry into the system.

3.2 Requirements of the SH-MICP Process and Limiting Factors

3.2.1 Sporulation of Bacteria

Bacteria which are not only capable of catalysing production of calcium carbonate, but which can also sporulate, are essential for the SH-MICP process to be viable. To enable long-term self-healing of a biocemented material, the viability of bacteria can be ensured by inoculation of this material with bacteria in the form of spores (bioaugmentation). Alternatively, suitable native bacteria may be biostimulated. Spores have a tough outer keratin coating and are resistant to heat and chemicals. As spores, the bacteria can remain viable for extended periods of time. Bacterial spores are able to withstand deleterious conditions and can germinate and form vegetative cells when conditions for growth become favourable (Wang et al. 2014b).

Experiments conducted to explore the self-healing capability of MICP-treated sand undertaken by Botusharova (2017) subjected bacterial cells to a sporulation medium prior to injection of bacteria into the sand, to ensure the presence of spores. It is likely however that these spores would become vegetative during the production of the biocement, and it had been assumed there would be spores only after three weeks of drying at 30 °C. Similar research undertaken by Montoya and Dejong (2013) into the self-healing of biocemented sand, relied upon the initially injected bacteria cells remaining sufficiently active to induce further MICP following damage. The latter approach would not guarantee long-term self-healing without the injection of additional bacteria. It is possible that within a geotechnical structure there will always be the presence of vegetative bacterial cells/ spores.

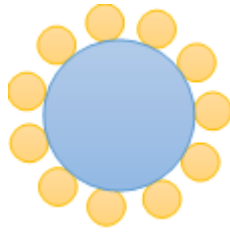
To induce sporulation, bacteria cells are subjected to unfavourable conditions such as raised temperature or the use of a sporulation inducing medium. Seifan et al. (2018) heated bacteria cells in saline solution to 80 °C for 10 min to induce sporulation. A similar process was utilised by Luo and Qian (2016) to produce spores by heating bacteria in liquid suspension in a water bath at 80 °C for 20 min. Berg and Sandine (1970) reported that a short exposure to heat of 65 °C for 10 min has been reported to rapidly activate spores. Spores may also be activated by a high or low pH (Berg and Sandine 1970). Yeast extract has been reported to stimulate spore formation, and to be an essential ingredient within cementation media for the germination of spores (Tziviloglou et al. 2016). Bacteria of the genus *Bacillus* can form spores which can remain dormant and viable for over 200 years (Schlegel 1993). Spore formation is otherwise generally induced by starvation of one or more nutrients (Setlow 2013). This latter approach was selected as the most viable approach for spore production in this research. The otherwise high temperature exposures reported to induce sporulation would not occur in the natural environment. The method of spore production via nutrient starvation was tested, in addition to use of a sporulating medium, as reported in Chapter Five, Section 4.1.

Future spore activation will be required for the self-healing MICP process to be effective following damage to the biocemented material. Transformation of the bacterial spore into a vegetative cell involves three stages – activation, germination and outgrowth, with higher temperatures being optimal for the activation stage, therefore its questionable how effective this process may be in low temperature environments.

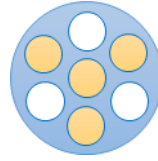
Following activation, spores will germinate due to exposure to agents which include specific nutrients, with nutrient germinants being the most likely in the natural environment. Nutrients are expected to be released from the carrier materials following water ingress. The germination process is followed by outgrowth which transforms the germinated spore to a vegetative cell (Setlow 2014). Other germination agents include high pressure. The rate and extent of germination can be greatly increased by the application of activation treatments such as sublethal heat (Setlow 2014). Bacteria spores have been observed to germinate following water ingress into cracks in concrete (Beltran and Jonkers 2015).

3.2.2 Storage and Supply of Cementation Medium

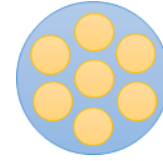
To embed self-healing capability into a biocemented sand or soil, there will need to be sufficient stores of nutrients for the bacteria and precursor chemicals to enable the MICP process. Methods of storage include immobilisation and encapsulation. This doctoral study has focussed on immobilisation and explored suitable materials, also referred to as carrier materials, for the immobilisation of nutrients and precursor chemicals, including the use of organic natural fibres and carrier materials. The possible immobilisation mechanisms are summarised in Figure 3-3. Encapsulation within hydrogel can also be considered a form of immobilisation (Figure 3-3 (c)).



Binding to a carrier surface
(Adsorption)
(a)



Entrapment in a porous matrix
(Absorption)
(b)



Entrapment within a hydrogel
(Encapsulation)
(c)

Figure 3-3. Immobilisation mechanisms of carrier materials - binding to a carrier surface (a), entrapment in a porous matrix (b) and entrapment within a hydrogel (c).

In addition to immobilisation of the cementation medium, it is also possible that the bacteria cells and the extracellular urease enzyme may be similarly immobilised by the carrier materials. Porous carrier materials are likely to immobilise via both adsorption and absorption.

3.2.3 Limiting Factors

As covered in the literature review, there are several factors which will impact on the self-healing MICP process, which needed to be taken into consideration/ controlled during the lab-based research undertaken. In addition to spores/ vegetative cells of suitable bacteria and a supply of nutrients and precursor chemicals, the environmental conditions will need to be favourable to enable the self-healing MICP process to take place following the onset of damage or deterioration. Environmental conditions which affect the MICP process are detailed in Chapter Two, Section 2.5.

3.2.3.1 Water Availability

The SH-MICP process developed as part of this doctoral study has been designed to be water activated. Sufficient water must be available to enable the regeneration of bacterial spores and to facilitate the MICP process.

3.2.3.2 Oxygen Availability

Although ureolytic activity does not depend on oxygen, microbial growth and urease production could be limited by availability of an electron acceptor. The oxygen requirement may depend upon the bacteria selected. *S. pasteurii* cannot anaerobically synthesize urease without presence of oxygen (Phillips et al. 2013). Absence of oxygen has also been reported to affect sporulation capacity (Abbas et al. 2014).

3.2.3.3 Soil Particle Size and Particle size distribution

It has been reported that bacterial activity cannot take place in very fine soils due to the sizes of the pore spaces being smaller than the bacteria. The optimum particle size of soil (or sand) to be subjected to

MICP treatment is 0.05 mm to 0.4 mm (Rebata-Landa 2007), which as shown in Figure 3-4 covers a relatively small range across the classification of soils. A fine sand or silty sand would therefore be preferable. This will also place limitations on potential applications. A greater amount of nutrients and precursor chemicals would be required to increase stiffness and strength in coarser soils, to bridge gaps between particles and fill pore spaces. In practice, the soil matrix may contain a mix of soil types and particle sizes.

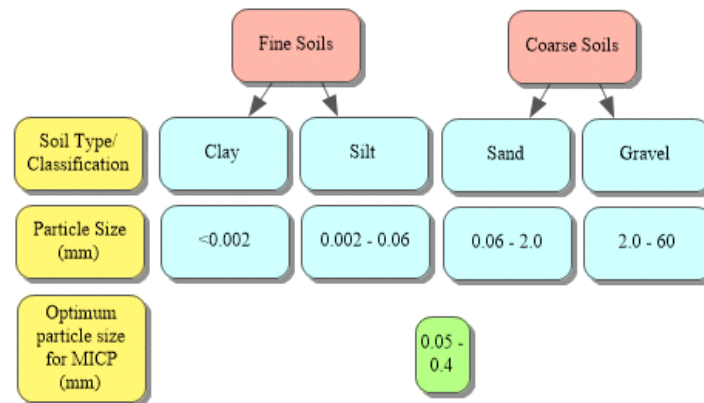


Figure 3-4. Optimum particle size for MICP in relation to soil classification.

3.2.4 Assumptions

Many studies focussing on bacteria-based self-healing in cementitious materials, in addition to the prior study on healing of biocemented sand by Botusharova (2017), have assumed that the self-healing observed or measured is due to the presence of bacterial spores. It has not been proven, without any uncertainty, that this self-healing is due to spores and not the presence of vegetative bacteria cells. This spore forming ability, and long-term viability of the selected bacteria, has been tested further within the time constraints of this research, as reported in Chapter Five, Section 5.1 and Chapter Six, Section 6.4.

3.3 Potential Applications of SH-MICP

The SH-MICP methodology is proposed principally for new structures since the incorporation of the carrier materials will need to be via premixing or deep mixing processes. The latter would be less feasible due to the high cost of this procedure.

The development of self-healing MICP has promising potential for a wide variety of applications within geotechnical engineering, for the consolidation and protection of stone and concrete surfaces, repair of defects such as micro-cracks and for the cementation and consolidation of loose particles in soils (Wang et al. 2014c). Self-healing is of particular interest where environmental conditions can lead to

continuous or repeated damage and deterioration, such as areas prone to earthquakes or vibrations from transport for example and for applications where inspection may be difficult/ costly such as dam cores and foundations.

Engineering geo-materials such as sand, soil and stone, are subject to physical, chemical and biologically mediated damage. Current maintenance techniques are limited, disruptive and costly. The current passive approach to repair of structures typically consists of monitoring, detection and repair, with repairs being undertaken after defects have been detected (Wang et al. 2012). This approach typically involves applying healing agents to the surface of a material and may also include injection of healing agents. Such an approach will still be necessary to remedy more extensive damage, such as large cracks. To ensure a timely approach to repair small or deep cracks and failures MICP could be used. An active approach would involve self-healing of the material from the inside.

MICP has the potential to enhance material properties resulting in increased strength and reduced permeability. To add to this, embedding self-healing capability into a biocement could help achieve the following:

- Reduced intervention for repairs and maintenance
- Reduced monitoring required
- Reduced risk of failure
- Increased performance of structure and longer service life
- Increased durability
- Improved resilience

Geotechnical structures have been considered where it may be possible to implement the self-healing MICP system and where this may be beneficial. Also considered are limitations with respect to this process and alternative approaches.

3.3.1 Seepage Control Within Dam Cores

Suitable applications for SH-MICP may be those requiring seepage control or flow control, such as an embankment dam core. This application has been considered as potentially the most suitable for the self-healing MICP system developed in this research. The use of MICP has already been proposed as a method to reduce permeability of the core material for earth-fill dams and for seepage control (Clarà Saracho and Haigh 2019). The self-healing MICP system may be effective within earth-fill dam cores, to help mitigate against seepage erosion, piping and subsequent dam failure. For this particular application, the self-healing capability would be embedded through premixing of immobilised nutrients and precursor chemicals into the dam core material. The dam core once constructed may then be injected with bacteria and cementation medium treatments to further reduce permeability of the core material.

Self-healing capability would then be reliant on spores forming following this process. Alternatively, immobilised bacteria in spore form, in addition to immobilised cementation medium, could be pre-mixed with the dam core material to embed self-healing. This latter approach may be effective if the dam core material already had sufficiently permeability and did not require biocementation treatment.

It is expected that the self-healing process would be initiated once micro cracks form within the dam core and permeability increases resulting in water filling these cracks. Cracking in earth dam cores cannot be completely prevented, dams are therefore designed to help ensure that cracks close up as soon as possible, to prevent leaks and erosion of the core (Kakuturu and Reddi 2006). It has been suggested some autogenic self-healing may already occur in dam cores (Reddi and Kakuturu 2004). Self-healing capability of the dam core could be further improved through the incorporation of microbially induced self-healing capability. Embedded SH-MICP capability would help to i) further mitigate against seepage and piping within the embankment dam and ii) promote self-healing upon microcracks forming or an increase in permeability leading to water seeping into the dam core. Any water entry into core material would be expected to activate the SH-MICP process.

The dam core with the embedded SH-MICP system would be combined with controlled drainage within the embankment dam structure. Current practice involves the use of a downstream filter, as depicted in Figure 3-5.

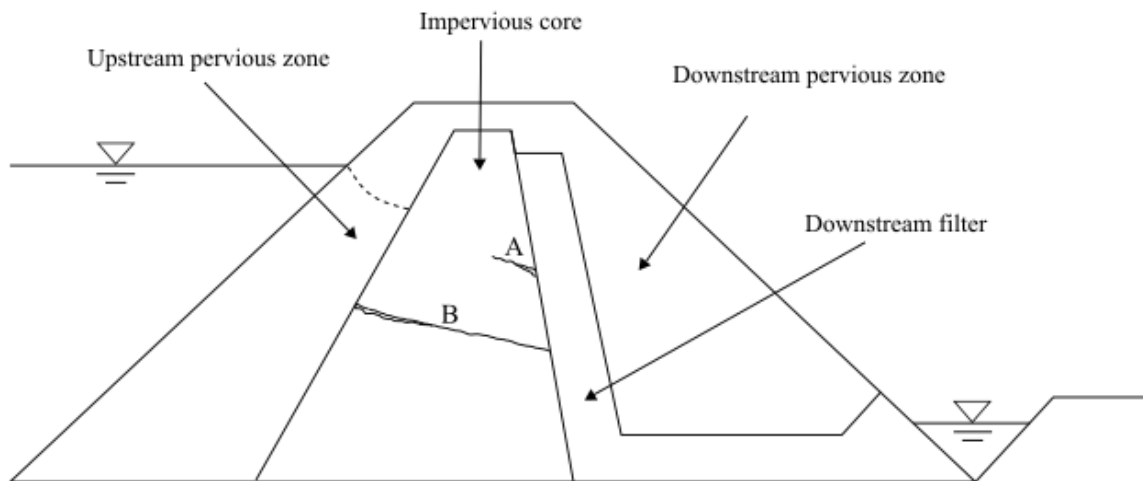


Figure 3-5. Cross section of an earth-fill dam, showing core cracks (A - extending from interior to downstream side of the core; B- extending across the core, adapted from Kakuturu and Reddi (2006).

To biocement the core of the dam, the core material would need to be suitable for treatment with MICP, such as a sand-silt or sand-clay material. MICP may be used to reduce permeability of material sourced at the site of the dam which may be otherwise deemed unsuitable. Earth dam core material may consist

of clay, sand-clay mixtures, and sand-silt mixtures and to a lesser extent gravel. MICP has been explored for its potential to control seepage-induced internal erosion in sand-clay mixtures, using sand-kaolin mixtures of different particle sizes (Jiang et al. 2017) and gravel-sand mixtures (Jiang and Soga 2017). Carbonate precipitation has been found to be effective in increasing erosion resistance by coating fine particles directly and bridging gaps between coarse particles (Jiang and Soga 2017). This improvement was greater in samples with a higher gap ratio, the gap ratio being defined as the ratio of the minimum particle size of the coarse fraction and the maximum particle size of the fine fraction on the particle distribution curve, thus demonstrating the influence of soil pore sizes (Jiang and Soga 2017). Past research by Rebata-Landa (2007) had suggested that MICP may not be suitable for fine grained soils, however these more recent studies suggest that it may be effective for biocementation of fine-grained soils where these fine-grained soils such as silt are mixed with a coarser soil such as sand. In the study by Jiang and Soga (2017) the well graded soil mixture will likely have provided sufficient pore space to mitigate against crushing of the bacteria and to facilitate the MICP process.

3.3.2 Foundation Repair

The MICP process can be used to heal degraded calcite bonds post-shearing (Montoya and Dejong 2013), restoring properties of construction materials, such as stiffness and peak strength of sand. Earthquakes are an example of a natural hazard which could cause damage to bio-cemented soil and reduce bearing capacity of foundations. This particular application would present challenges with regards to repair, which the enabling of self-healing capabilities would overcome. Montoya and Dejong (2013) simulated earthquake motions while undertaking research into the self-healing of MICP cemented sand, to demonstrate the capability of self-healing MICP to repair bio-cemented sand following earthquake damage. In this study repeated injections of cementation media were required to achieve self-healing. In practice this procedure may be difficult to apply in hard to access areas such as foundations beneath buildings and could be improved upon by ensuring an adequate nutrient and precursor chemical supply was already present in the soil to enable self-healing.

3.3.3 Slope Stabilisation

Slope stabilisation may be improved through healing of localised damage within the soil slope, such as micro-cracks, via MICP. Evidence suggests that rainfall-induced shallow landslides are preceded by a series of localised internal failures within the soil matrix, and that micro cracks within the soil contribute to these failures, with landslides tending to be triggered in the most damaged areas of a hillslope (Fan et al. 2015). Antecedent damage caused by rainfall events can destabilise slopes. Rainfall-induced landslides fail in an abrupt manner, and are difficult to predict (Fan et al. 2015).

The water initiated self-healing MICP system would in this case be unsuitable however since slope material would also need to have sufficient permeability for drainage to help prevent build-up of excess

pore water pressures that could also lead to failure. This continual/ regular flow of water would over time lead to washout of immobilised cementation medium from the soil. MICP has recently been investigated for surficial stabilisation of slope soil (Gowthaman et al. 2019b). Current approaches to slope stabilisation include Portland cement mixing (Soil-cement) and use of Geosynthetics. This application would require a different approach to embedding self-healing than has been the focus of this research. The flow of water through the slope would necessitate storage of the CM for self-healing within an impermeable capsule. An otherwise suitable bio-based approach could include use of vegetation since plant roots which may initiate soil stabilisation through regrowth following breakage.

3.3.4 Landfill Lining Repair

Compacted clay landfill liners may be subjected to chemical damage by leachate and also mechanical damage. Since MICP has been deemed unsuitable for clay soils this poses a challenge in respect of embedding an MICP based self-healing system which may not in this case be suitable. The pH of landfill leachate may impact on microbial activity in respect of MICP application in this environment. Compacted clay landfill liners have been observed to have some capacity for natural self-healing (Aldaef and Rayhani 2015).

3.3.5 Land Subsidence Remediation

Self-healing MICP could also be used to control water flow and heal soil following subsidence damage. Land subsidence can alter chemical and physical properties of the soil, particularly at depths up to 1 m (Shi et al. 2017). Subsidence, due to underground coal mining, and cracks in the ground can lead to vertical leakage of water and nutrients from soil (Shi et al. 2017). Shi et al. (2017) reported that soil in the West China Aeolian Sand area was mostly composed of medium and fine sand; however, land subsidence has resulted in a decrease in fine sand particles and increase in medium and coarse sand and leaching of nutrients into deeper layers. Water-wind erosion has also caused deterioration in this study. It is suggested that the higher porosity of the topsoil layer, up to 20 cm in this study, promoted growth and metabolism of micro-organisms.

3.3.6 Preservation and Restoration of Ornamental Stone

Bacterially induced calcium carbonate precipitation has been proposed as an environmentally friendly way to protect decayed ornamental stone (De Muynck et al. 2010), through bio-deposition. Carbonate stones such as limestone are particularly susceptible to weathering (De Belie 2010). Weathering increases the porosity of stones (De Muynck et al. 2010), leading to further damage through water and chemical ingress. The application of self-healing MICP could enable stone to heal and repair upon water ingress. Applications to stone structures were not considered further in this project as this had been deemed beyond the scope of this research.

3.3.7 Assessing Suitability for Geotechnical Applications

Assessment of selected geotechnical applications, and the suitability of self-healing MICP for these, are summarised in Table 3-1. This table compares the earth-fill embankment dam application with foundations, slopes and landfill lining. The latter example is one where bio-based self-healing is likely to be an unsuitable approach.

Table 3-1. Assessment of SH-MICP process suitability for selected geotechnical applications.

Geotechnical Structure	Earth-fill Embankment Dam	Foundation	Slope	Landfill/ Reservoir lining
Material	Core of clayey silt/ sandy clay/ sandy silt	Various soil types	Various soil types	Compacted clay
MICP Suitability	Dependent on soil type and grading	Dependent on soil type and grading	Dependent on soil type and grading	Not suited to very fine soils
In-situ CM and Bacteria Delivery Options	Not suitable	Direct application by injection/ Injection of microcapsules	Direct application by injection or surface percolation/ Injection of microcapsules	Not suitable
Pre-mixing CM and Bacteria delivery options.	Immobilised or encapsulated CM and bacteria	Immobilised or encapsulated CM and bacteria	Immobilised or encapsulated CM and bacteria	Immobilised or encapsulated CM and bacteria
Effect of MICP	Reduced permeability of core material and increased resistance to erosion	Enhanced foundation bearing capacity	Increased resistance to erosion and cementation of loose material	Reduced permeability, prevention of leaching
Possible Damage/ Deterioration	Core cracks, seepage erosion	Degraded calcite bonds	Antecedent damage, local internal failures in soil	Cracks in lining
Cause of Damage/ Deterioration	Hydraulic fracturing/ seismic activity	Seismic activity/ differential settlement/ expanding and contracting soil	Freeze-thaw/ daily thermal cycles/ excessive rainfall/ inadequate drainage/ seismic activity	Freeze-thaw/ daily thermal cycles/ desiccation/ differential settlement

SH-MICP Initiation	Water flow	Water flow, movement causing capsule fracture	Movement causing capsule fracture	Water flow
SH-MICP response to damage	Heal small cracks in core	Repair degraded calcite bonds	Heal small cracks, cement loose material	Heal small cracks in lining
Effect of SH-MICP	Prevent concentrated leaks through core/ piping leading to internal erosion	Bearing capacity regain	Help prevent progressive failures that could lead to a landslide	Prevent leaching of contaminants

3.4 Selection of Carrier Materials for Investigation

Having established several possible systems for the delivery of cementation medium, as detailed in Chapter Two, Section 2.6, a desk study was undertaken to compare these and aid in the selection of the most promising systems for further exploration, as summarised in Table 3-2. The desk study summarised in Table 3-2 considers the supply options for cementation medium, covering methods and materials used in self-healing studies on concrete and mortar, in addition to the direct application and premixing methods utilised in prior studies on biocementation of sand.

As the approach in this doctoral study concerning autonomous self-healing of biocemented sand is novel, prior approaches in other construction materials have been considered. In addition, the use of organic natural fibres as carriers has been proposed as a novel approach for immobilising cementation medium. Natural fibres had not previously been combined with sand or soil biocementation systems. The effect of these additives on mechanical properties of biocemented sand or soil and on the MICP process itself was at this stage unknown. Alongside testing of self-healing responses, the effects of the carrier materials on biocementation and material properties of biocemented sand were also explored in this research. Since immobilisation and encapsulation technologies have only been used in cementitious materials to date, their behaviour within soil systems is unknown. Little has been reported on the effects of carrier materials themselves other than the negative impact of capsules on compressive strength in concrete. For large scale implementation to be achieved, carrier materials used will need to be relatively low cost, easy to source, locally available if possible and have a high absorption capacity.

Following the analysis summarised by Table 3-2, the advantages and disadvantages of the most promising candidates for the carrier materials are outlined in Table 3-3. The selected materials covered carriers with the ability to adsorb and absorb, in addition to an encapsulating hydrogel. Following this

further analysis, the selected carrier materials for this study were organic diatomaceous earth, inorganic expanded perlite, and organic natural fibres as immobilising materials. Preliminary experiments undertaken to test the effectiveness of the selected immobilising materials are detailed in Chapter Five. Experimentation was also undertaken to develop and use an alginate-based hydrogel for encapsulation of cementation medium, as reported in Chapter Eight.

Table 3-2. Immobilising and encapsulating materials – evaluation for further investigation.

Cementation Medium and Bacteria Delivery Mechanism	Suitability in soil (1-5)	Treatment Uniformity (1-5)	Biodegradability (1-2)	Economic (1-5)	Facilitate long-term OM supply (without reapplying) (1-5)	Resistance to flow (prevent washout of nutrients) (1-5)	Ease of implementation (1-5)	Totals
Injection	5	1	2	4	1	1	5	19
Surface Percolation	5	2	2	5	1	1	5	21
Premixing (Grouting)	5	3	2	4	1	1	4	20
Diatomaceous Earth (DE)	5	3	1	3	4	3	4	23
Expanded Clay particles	3	3	1	3	4	4	4	22
Expanded Shale Aggregates	2	3	1	3	4	5	4	22
Lightweight aggregate (LWA) based healing agent	2	3	1	3	4	5	4	22
Graphite Nano Platelets (GNP)	5	3	2	1	4	3	4	22
Ceramsite Immobilised	3	3	1	3	4	4	4	22
Zeolite Immobilised	5	3	1	1	4	4	4	22
Expanded Perlite (EP)	4	3	1	3	4	4	4	23
Immobilisation in natural absorbent fibres (Coir, bamboo, jute) combine with fibre reinforcement	5	3	2	4	4	4	3	25
Glass tubes containing silica gel immobilised bacteria/ Polyurethane (PU) foam immobilised bacteria	1	3	1	1	4	5	2	17
Alginate Gels/ Beads	5	3	2	3	4	3	3	23
Hydrogel capsules (Pluronic F127 powder)	5	3	2	1	4	2	2	19
Melamine-based microcapsules	3	3	1	2	4	2	2	17

Table 3-3. Advantages and disadvantages of selected immobilising and encapsulating materials.

Carrier	Advantages	Disadvantages	Applications
Diatomaceous Earth (DE)	Moderate CaCO ₃ precipitation reported in studies on concrete. Wide ranging particle size to suit different applications, although typically 10 to 200 µm.		Any
Zeolite	Use as immobilising material found to have increased compressive strength of concrete. Widely available – natural and synthetic zeolites.	Reported to become more alkaline in water (Mumpton 1999). Could inhibit MICP. Minimal CaCO ₃ precipitation observed in concrete - 0.1 mm cracks healed.	Any
Expanded Perlite (EP)	Healing of 0.78 mm width cracks in concrete demonstrated.	Requires heat treatment, adding to cost of material.	Available in a variety of grades, therefore suitable for use with all soil types.
Fibres	Reduces brittleness of bio-cemented sand, enhances MICP process by bridging pores in the sand (Choi et al. 2016). Increases shear strength of cemented sand.		Any
Alginate Gels	Swollen hydrogels act as water reservoirs for continuous crack healing, allowing MICP to continue without continuous water supply (Wang et al. 2015).	May be less viable for large scale applications due to production process. Negative impact on compressive strength reported (Wang et al. 2015).	Since water is retained, could be most suitable for water scarce environments. May be less suited to applications such as foundations as could lead to decrease in bearing capacity, based on previous research.

4 METHODOLOGY AND MATERIALS

4.1 Bacteria

4.1.1 Selection of Suitable Bacteria

The bioaugmented approach was adopted for the MICP studies undertaken. *Sporosarcina pasteurii* and *Sporosarcina ureae* were selected for use in this research, as ureolytic, and potentially sporulating, bacteria known to induce calcium carbonate precipitation. Cultures were produced using media as specified in Table 4-1 and Table 4-2. *Sporosarcina ureae* was obtained from the National Collection of Industrial and Marine Bacteria, UK (NCIMB 9251, ACDP Group 1) as a freeze-dried culture. For work undertaken at the University of Cardiff, UK, a plated culture of *Sporosarcina Pasteurii* was provided by the University of Bath; who obtained the original stock culture, DSM 33, from the Leibniz Institute DSMZ – German collection of microorganisms and cell cultures. *S. pasteurii* originating from the American Type Culture Collection (ATCC 11859) was used for column studies conducted at Arizona State University as reported in Chapters Seven to Nine of this thesis.

4.1.2 Culture of Bacteria

Bacterial cultures were initially grown on agar plates inoculated from stock cultures, this ensured that pure cultures were used in experiments. Cultures were grown on Luria-Bertani (LB) medium, as recommended by Bianca Reeksting, 08/12/17, University of Bath. All culture media were amended with 20 g/L urea (Tobler et al. 2011). This culture medium comprised per litre of deionised water; 10 g tryptone, 5 g yeast extract, 10 g sodium chloride, 15 g agar powder and 20 g urea. The LB medium without urea was sterilised by autoclaving at 121 °C for 15 min. A urea solution was then added to this medium aseptically using a 0.2 µm syringe filter. The medium was then allowed to cool to 55 °C before pouring onto 90 mm diameter petri dishes, to minimise condensation on plates and then sealed using parafilm. The plates were inoculated using the streak plating process, to enable individual colonies to be isolated, and inverted during incubation and storage, to prevent contamination by condensation dripping onto the surface of the agar. Following incubation at 30 °C for 48 h, pure single colonies from the plates were used to inoculate a liquid broth medium. An incubation temperature of 30 °C, has been reported as the optimum for *S. pasteurii* growth (Kim et al. 2018; Xiao et al. 2021), and use of this temperature for incubation of *S. ureae* follows on from work by Botusharova (2017) and Zhang et al. (1997). Plate cultures were stored at 4 °C.

Liquid broth cultures were grown for use in experimental studies. An overnight liquid broth culture was initially produced using the bacteria grown on the agar plates, for use as an inoculant for further liquid broth cultures. Inoculation with a liquid broth culture allowed greater control in respect of the quantity of bacteria added to each flask of growth medium. Components used for the growth media for the specified bacteria are as listed in Table 4-1 and Table 4-2. The liquid growth medium used for culturing *S. ureae*, as used by Botusharova (2017), consisted of 5 g peptone, 3 g meat extract and 20 g urea per litre of tap water or deionised water as specified. Tap water provided additional nutrients for bacteria growth and facilitated faster growth compared to use of deionised water. The liquid growth medium for *S. Pasteurii*, as used by Botusharova (2017), consisted of 13 g Oxoid CM0001 nutrient broth and 20 g urea per litre of water, with deionised water used to produce cultures for columns studies as a control. The liquid growth medium without urea was autoclaved at 121 °C for 15 min, to which a urea solution was added using a 0.2 µm syringe filter. Flask openings were covered with foil prior to autoclaving, with this foil briefly removed when adding the urea and placed back on the flask after.

To produce the liquid broth inoculant, the growth medium was prepared as above, then in close proximity to a Bunsen burner, a single bacterial colony was taken from the agar plate using a sterilised inoculation loop and placed into the liquid growth medium to inoculate this. The foil covering the flask opening was removed prior to inoculation and replaced after. The liquid growth medium inoculated with *S. ureae* was then aerobically incubated (Stuart Orbital Incubator, S1600, UK) at 30 °C and 150 rpm overnight for approximately 12 h, after which time a late exponential stage of bacterial growth was achieved corresponding to an optical density at a wavelength of 600 nm (OD_{600}) of 0.9 (10^7 cells/ mL). The same procedure had been followed when using *S. pasteurii* as an inoculant at Cardiff University. For the studies undertaken at Arizona State University, the *S. pasteurii* plate cultures and liquid broth cultures were grown at a temperature of 23 °C. This lower temperature had been used in the absence of an incubator and corresponded to the constant room temperature of the laboratory in which all studies were undertaken. A spectrophotometer (Hitachi U-1900 UV-VIS, Tokyo, Japan/ Hach DR 6000, Colorado, USA) was used to measure optical density. The flasks of liquid broth inoculant were prepared in triplicate, with fresh cultures prepared for each experimental study.

Multiples of liquid broth cultures were produced as required for experiments, typically using 250 mL Erlenmeyer (conical) flasks to contain 50 mL of liquid broth culture. The liquid growth medium was prepared as described above, followed by inoculation of each 50 mL of this growth medium with 100 µL of the aforementioned liquid broth inoculant. These flasks were then incubated at 23 °C or 30 °C, dependent on the location of the study undertaken, and shaken at 150 rpm, to produce cultures with an optical density at a wavelength of 600 nm (OD_{600}) of approximately 0.9-1.2 (10^7 - 10^8 cells/mL). Use of 250 mL conical flasks, containing 50 mL solution, ensured that there would be sufficient surface area at the liquid-air interface for oxygen uptake. Aseptic technique was used throughout when working with

bacterial cultures, to mitigate against contamination. Bacteria were cultured in sterile growth media. The benchtop was cleaned with bleach or a 70 % ethanol solution before and after use. A 0.2 µm syringe filter was used when adding the urea solution to the flasks containing growth medium, since the urea could not be autoclaved. A Bunsen burner was used to sterilise the air in the vicinity of the work area, with urea and bacterial inoculant added to flasks in close proximity to the Bunsen burner. To further help prevent contaminants entering flasks of growth medium, after removal of the foil covering, the tops of the flasks were flamed using the Bunsen burner prior to addition of the urea solution and bacteria. While doing this the foil covering of the flasks was held to prevent it touching the worktop. The sterilisation processes used for the growth medium constituents and for other chemicals in this research are as given in Table 4-3, or as otherwise described in the studies undertaken. For some chemicals the sterilisation process had been dependent upon the concentrations and quantities used.

Table 4-1. Culture, cementation, and sporulation media for use with *S. ureae*.

Medium	Chemical	Quantity (g/L)
Culture Medium	Peptone (from casein)	5
	Meat extract	3
	Urea (NH ₂ (CO)NH ₂)	20
Cementation	Oxoid CM0001 nutrient broth	3
Medium (standard)	Urea (NH ₂ (CO)NH ₂)	20
	Ammonium chloride (NH ₄ Cl)	10
	Sodium bicarbonate	2.12
	Calcium chloride dihydrate (CaCl ₂ .2H ₂ O)	7.35
	Concentrated HCl	Adjust to pH 6 (prior to adding CaCl ₂ .2H ₂ O)
Sporulation	Yeast extract	2
Medium	Peptone	3
	Glucose	4
	Dipotassium hydrogen phosphate (K ₂ HPO ₄)	1
	Ammonium chloride (NH ₄ Cl)	3.238
	Calcium chloride dihydrate (CaCl ₂ .2H ₂ O)	0.13
	Magnesium Sulphate (MgSO ₄ .7H ₂ O)	0.92
	Manganese Sulphate (MnSO ₄ . 7H ₂ O)	0.112
	Iron (II) Sulphate (FeSO ₄ .7H ₂ O)	0.001
	Zinc (II) Sulphate (ZnSO ₄ .7H ₂ O)	0.018
	Copper (II) Sulphate (CuSO ₄ .5H ₂ O)	0.018
Sodium Hydroxide (NaOH)	Adjust pH to 9.0	

Table 4-2. Culture, cementation and sporulation media for use with *S. pasteurii*.

Medium	Chemical	Quantity (g/L)
Culture Medium	Oxoid CM0001 nutrient broth	13
	Urea (NH ₂ (CO)NH ₂)	20
Cementation Medium	Oxoid CM0001 nutrient broth	3 to 6
	Urea (NH ₂ (CO)NH ₂)	40
	Ammonium chloride (NH ₄ Cl)	20
	Sodium bicarbonate	2.12
	Calcium chloride dihydrate (CaCl ₂ .2H ₂ O)	73.51
	Concentrated HCl	Adjust pH to 6 (prior to adding CaCl ₂ .2H ₂ O)
Sporulation Medium	Peptone from casein	15
Medium	Peptone from soy meal (Sigma Aldrich)	5
	Sodium chloride (NaCl)	5
	Urea (NH ₂ (CO)NH ₂)	20
	Manganese sulphate (MnSO ₄ .H ₂ O)	0.01
	Sodium hydroxide (NaOH)	Adjust pH to 7.3

Table 4-3. Sterilisation procedures for chemicals used.

Chemical	Sterilisation process	Notes
Ammonium Chloride	Syringe filtered/ autoclaved	Dependent on quantity and concentration.
Calcium Chloride/ Calcium Chloride Dihydrate	Syringe filtered/ autoclaved	Calcium may precipitate out if in high concentration.
Copper (II) Sulphate	Autoclaved	
Dipotassium hydrogen phosphate	Autoclaved	
Glucose	Autoclaved	
Iron (II) Sulphate	Autoclaved	
Magnesium Sulphate	Autoclaved	
Manganese Sulphate	Autoclaved	
Meat Extract	Autoclaved	
Oxoid CM0001 Nutrient broth	Autoclaved	
Peptone (From casein and soya)	Autoclaved	
Sodium Bicarbonate	Syringe filtered	
Sodium Chloride	Autoclaved	

Urea	Syringe filtered
Zinc (II) Sulphate	Autoclaved

4.1.3 Bacterial Cell Harvesting

Liquid broth cultures were pelletised using a centrifuge at 3200 rcf for 20 min (Varifuge 3.0 Heraeus), or 5000 rpm (Bhaskar et al. 2017) for 20 min for the studies undertaken in the US. The supernatant was then drained and the bacterial cells washed with phosphate buffered saline (PBS) as needed. PBS was then added to replace the supernatant to create a bacterial suspension.

4.1.4 Bacteria Maintenance Protocol

For storage, glycerol stocks were produced at the commencement of this research and renewed every six months to ensure viability, for work undertaken at Cardiff University. A sterile 80 % glycerol solution (Koh 2013) was prepared by diluting glycerol in deionised water and then autoclaving. Working aseptically, 500 μ L of this solution was added to a sterile snap top tube, followed by 500 μ L of an overnight (12 h) liquid broth culture, which was then mixed gently using the pipette tip – by drawing the liquid in and out of the pipette tip. Mixing helps prevent crystallisation when frozen, these solutions were not vortexed as this may damage the bacterial cells. These glycerol stocks were stored at -20 °C. The glycerol stocks were used to inoculate agar plates, by inserting a sterile inoculation loop into the glycerol stock and using this to streak the agar plate. Once a snap tube of glycerol stock had been opened this was then discarded after autoclaving. This stock management protocol also ensured that there was a ‘master’ stock available to go back to should contamination or other problems occur.

At a later stage of research, for work undertaken at Arizona State University, deep solid/ stab cultures were produced and stored at 4 °C and renewed every three months. Stab cultures of *S. pasteurii* were found to remain viable for up to five months. These stab cultures were then used to inoculate agar plates, by inserting a sterile inoculation loop deep into the stab culture and using this to streak the plate. Figure 4-1 depicts the process for producing the liquid broth cultures from the glycerol or stab stock culture. The agar plates inoculated with glycerol or stab stock cultures were stored at 4 °C following a period of incubation. These plate cultures would usually be viable for up to six weeks. Single colonies from these agar plates were used to produce triplicates of liquid broth cultures in 250 mL Erlenmeyer flasks, to ensure pure cultures. These overnight liquid broth cultures would then be used to inoculate growth medium to produce the liquid broth cultures grown for use in experiments. New agar plates (working cultures) were produced using the glycerol or stab cultures every four to six weeks or as required. Repeated culturing from the liquid broth cultures was avoided since repeated culturing can result in phenotypic or genetic changes over time and also there would be a greater possibility of contamination.

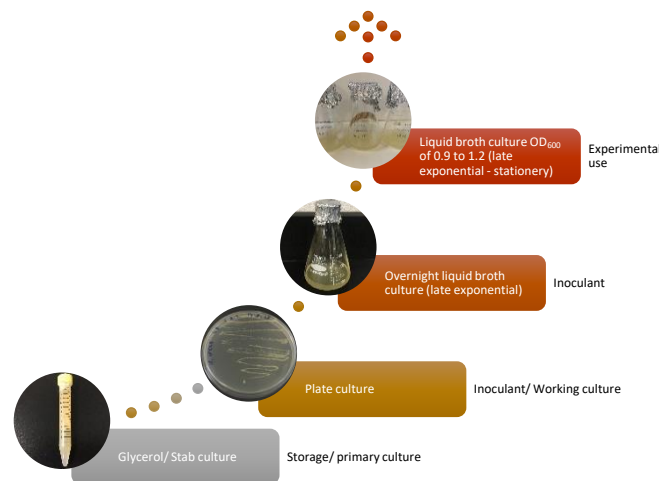


Figure 4-1. Bacterial maintenance and culturing process.

4.1.5 Inducing Sporulation of Bacteria

To induce sporulation of *S. ureae* and *S. pasteurii*, sporulation media as detailed in Table 4-1 and Table 4-2 were prepared, according to Macdonald and Macdonald (1962) and Bhaskar et al. (2017) respectively. Chemical constituents were sterilised as per Table 4-3 or as otherwise described in the experimental methods. The Macdonald and Macdonald (1962) medium is an alkali medium enhanced with manganese, similar to the Jonkers et al. (2008) medium. The addition of manganese enhances sporulation.

Overnight cultures of *S. pasteurii* and *S. ureae* were grown, in 50 mL of the respective culture media, to achieve growth within the exponential phase. Two 50 mL centrifuge tubes were half filled from each 50 mL liquid broth culture. These tubes were centrifuged for 20 min at 3200 RCF. The supernatant was discarded and replaced with phosphate buffered saline (PBS) to wash the cells and remove metabolic waste and any metabolism by-products, this solution was centrifuged again for 20 min. The PBS consisted of 8 g Sodium chloride NaCl (J.T. Baker), 1.42 g Sodium Phosphate Dibasic Na₂HPO₄ (EMD Millipore) and 0.24 g Potassium Phosphate Monobasic KH₂PO₄ (Sigma Aldrich) per litre of deionised water, adjusted to pH 7.2 with concentrated HCl and autoclaved. The bacterial cells were then added to flasks containing 50 mL of sporulation media. The bacterial cells were subjected to the respective sporulation media for 24 h, in a 30 °C shaking incubator at 150 rpm.

To determine the presence of spores, the Schaeffer and Fulton spore staining procedure was followed, based upon directions specified within the product information for the 04551 Schaeffer and Fulton spore stain kit (Sigma Aldrich 2013) and methodology as reported by Schaeffer and Fulton (1993). As a

variation to the reported methodology, the slides were gently washed in a water bath of tap water after staining, since rinsing under running tap water was found to remove cells and spores from the microscope slides. The steaming was achieved through heating approximately 100 mL of water in a 250 mL beaker over a heat plate with the microscope slide resting across the top of the beaker. Steaming is required to force stain into spores since the keratin coating of spores is stain resistant. The waste liquid was disposed of appropriately. Following staining the microscope slides were observed under a light microscope (Nikon Eclipse LV100) at 80x magnification. Spores may be observed on the end, middle or between these areas of a bacteria cell.

4.1.6 Bacterial Cell Counting

4.1.6.1 Direct

Viable bacterial cell counts can be determined directly using the standard plate counting method, as detailed by Pakpour and Horgan (2021). The standard plate counting method was used to i) verify the concentration of bacterial cells in liquid broth cultures and ii) to determine the number of viable bacterial cells in selected biocement samples, and subsequently as an indicator of the presence of spores.

To quantify cells in a liquid broth culture, 1 mL of culture is transferred to a tube containing 9 mL of a sterile buffer (either PBS or 0.9 % NaCl in deionised water). The sample and buffer are then mixed to disperse the cells/ spores, without using a vortex mixer since this may kill cells. This results in a sample with a dilution of $1/10^{\text{th}}$ of the liquid broth culture. 1 mL is then taken from this dilution and transferred to a second tube containing 9 mL of the sterile buffer to create a dilution $1/100^{\text{th}}$ of the original sample. These steps were repeated to give a series of serial dilutions as depicted in Figure 4-2.

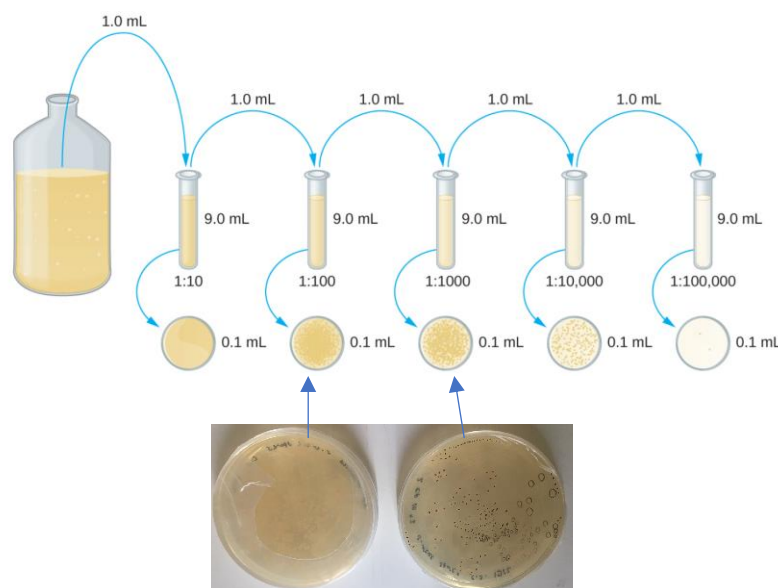


Figure 4-2. Serial dilution process, adapted from OpenStax (2016).

When testing a solid sample, 1 g of the sample is taken and the contents of the tube made up to 10 mL with the sterile buffer, the process above is then followed to make the serial dilutions.

The diluted samples were then plated. For *S. ureae* containing samples, agar plates were prepared using Luria Bertani (L-B) agar amended with 20 g/L urea, with the urea solution added using a syringe filter after autoclave sterilisation of the LB agar solution. This was poured onto sterile (usually 90 mm diameter) petri dishes, close to a Bunsen burner, once the agar mixture had cooled to 55 °C. Using a pipette and sterilised pipette tip, 100 µL of the dilution was pipetted onto the agar and spread out using a sterile plate spreader. This was repeated for at least two further consecutive dilutions. Predictions were made regarding the most suitable dilutions to plate. The plates were then sealed using parafilm and incubated for 48 h, until individual colonies of the bacteria were clearly visible. It was assumed that when testing for presence of spores in biocement samples that each colony had grown from an individual spore. Colonies were counted on plates containing thirty to three hundred colonies.

The same process had been used for *S. pasteurii* containing samples, with the plates produced using BBL Brain Heart Infusion (BHI) agar adjusted to pH 8, autoclaved and amended with 75 mM urea. BHI agar had been used following guidance from Charles Graddy, 06/04/20, University of California Davis, as they had found this agar to be most effective for achieving reliable plate counting results for *S. pasteurii*. Growth had otherwise been variable when plating dilutions containing *S. pasteurii* onto LB agar plates.

To improve the reliability of this process, the plate spreading method can be replaced by the plate pour method. Using this method, the 100 µl sample from the serial dilutions is mixed with warm agar (45 – 50 °C) and then poured onto a sterile plate. This process helps to ensure a more even mixing of the bacteria and eliminates potential contamination from the plate spreader while working under aseptic conditions. An alternative to plate counting is use of a haemocytometer.

4.1.6.2 Indirect

This method requires the use of a spectrophotometer (Hitachi U-1900 UV-VIS, Tokyo, Japan/ Hach DR 6000, Colorado, USA), to measure the turbidity of a sample of bacteria within a suspension. This is a fast and reliable method for estimation of cell counts. The optical density (OD) of bacteria suspended within a liquid broth (liquid broth culture) was measured at a wavelength of 600 nm (OD_{600}). This measurement can be correlated to the bacterial cell concentration (Y) according to the relationship obtained by Ramachandran et al. (2001), as per Equation (4-1).

$$Y = 8.59 \times 10^7 \times OD_{600}^{1.363} \quad (4-1)$$

Alternatively, the spectrophotometer measurement can be correlated to the bacterial cell count by using the plate counting method as outlined above. This is considered to give the most accurate estimate of bacterial cell concentration within a suspension, since this will be affected by the bacteria selected and constituents of the growth medium.

4.1.7 Urease Activity

Urease activity (mM urea hydrolysed/ min) is calculated as per the relationship derived by Whiffin (2004) in Equation (4-2), based on a conductivity assay.

$$Urease\ Activity = Electrical\ Conductivity \left(\frac{mS}{cm} / min \right) \times 11.11 \quad (R_2 = 0.9988) \quad (4-2)$$

To measure the electrical conductivity (EC) of a culture; 9 mL of a sterile 1.1 M urea solution was transferred to a sterile 50 mL polypropylene tube along with 1 mL of the liquid broth culture and this solution mixed before then inserting the EC probe. Electrical conductivity was measured over five minutes to obtain the average urease activity per minute, as per Harkes et al. (2010). This process was repeated three times for each sample tested and an average taken from the three results.

4.1.8 Specific Urease Activity

Specific urease activity (mM urea hydrolysed/ min/ OD₆₀₀) is defined by Whiffin (2004) as the amount of urease activity per biomass, as per Equation (4-3).

$$Specific\ Urease\ Activity = \frac{Urease\ Activity}{Biomass\ (OD_{600})} \quad (4-3)$$

4.2 Sand

Fine silica sand, sourced locally where possible, was selected for use in the biocementation experiments. For the preliminary studies undertaken at Cardiff University, an industrial kiln dried silica sand was used. For the following columns studies completed at Cardiff University, a finer Garside Sands free draining washed Fine Silica Sand (WFSS) from Aggregate Industries was selected. This sand is pale in colour and mined in Leighton Buzzard, Bedfordshire from within the Lower Greensand of the Cretaceous period and has sub angular to rounded grains.

Later studies completed at Arizona State University used F60 and F65 sand. Properties of the sands as reported by the manufacturers and tested in the laboratory are given in the respective studies.

4.3 Immobilising Additives (Carrier Materials)

4.3.1 Diatomaceous Earth

Diatomaceous earth (Figure 4-3), also known as fossil flour and by its tradename Celite (a registered trademark of Imerys Filtration Minerals Inc.) is a fine, silty, crystalline silicate material composed of fossilised sea creatures known as diatoms. The individual diatoms can be seen in Figure 4-4. Diatomaceous earth has an average bulk density of 256 kg/m³ (Flexicon Corporation 2018). The Celite S. (SiO₂) product used in this research, purchased from Sigma Aldrich, is dried and untreated diatomaceous earth and is typically used as filter aid.

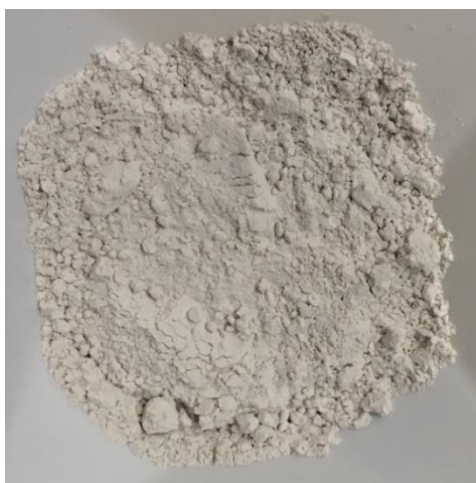


Figure 4-3. Photograph of sample of diatomaceous earth (Celite S.).

The chemical composition of Celite S. is as given in Table 4-4 (Sigma Aldrich 2017).

Table 4-4. Chemical composition and properties of Celite S. (Sigma Aldrich 2017).

Chemical	% by mass
Al ₂ O ₃	4.1
CaO	0.4
Fe ₂ O ₃	1.6
MgO	0.2
Na ₂ O + K ₂ O	1.4
P ₂ O ₅	0.3
SiO ₂	90.2
TiO ₂	0.2
Loss on ignition at 900°C	3.2-10.0
pH	~7 (25 °C, 10% in aq. suspension)

Celite (diatomaceous earth) particles are intricate, complex shapes, as shown in Figure 4-4, these particles offer a more tortuous path to the flow of the fluids. Figure 4-4 shows diatomaceous earth as observed using a scanning electron microscope and 1500x magnification.

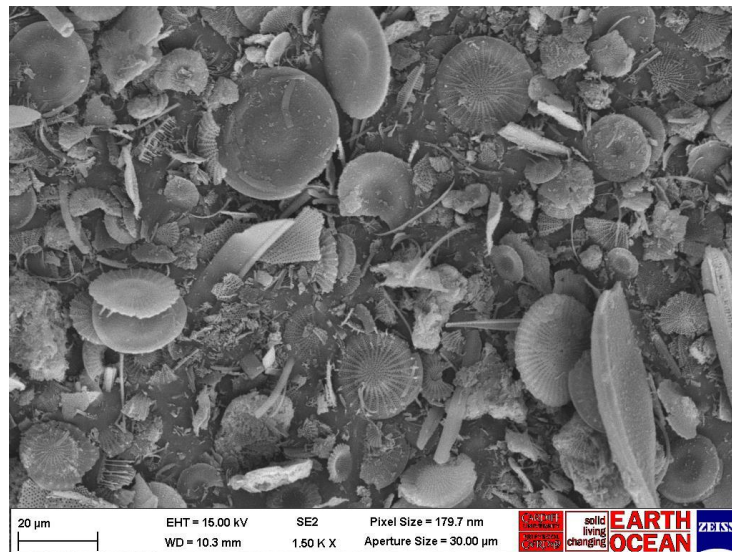


Figure 4-4. SEM image of diatomaceous earth at 1500x magnification.

4.3.2 Expanded Perlite

Perlite is volcanic mineral, formed from a magma flow of pure alumina silicate glass. Expanded Perlite is marketed as having excellent adsorption properties (Dupre Minerals 2018). Both diatomaceous earth and expanded perlite are primarily silica-based materials.

The Alfa Aesar Harborlite 800 product used in this research (Figure 4-5), purchased from Fisher Scientific, is an untreated perlite in a fine powdered form. This product is marketed as a filter aid. Perlite is an amorphous alumina silicate material, the typical chemical analysis of Harborlite is as per Table 4-5 (Harborlite Corporation 2008). Harborlite products have a low bulk density, high void volume and porosity, neutral pH, and are hydrophilic and relatively inert (Harborlite Corporation 2008).

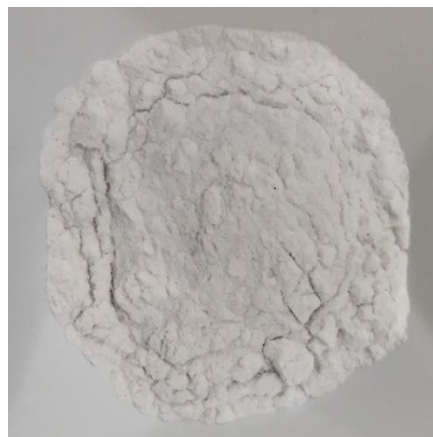


Figure 4-5. Photograph of sample of expanded perlite (Harborlite 800).

Harborlite 800 has a D'Arcy permeability of 1.7 and median particle size of 36.6 μm . Ultrafine expanded perlite with a nominal particle size of 10 to 75 μm has a bulk density when compacted of 150 to 200 kg/m^3 (Hoben International 2018). Harborlite (2008) report the wet density of Harborlite 800 as 0.16 g/cm^3 .

Table 4-5. Typical chemical analysis of Harborlite (all grades).

Chemical	% by mass
SiO₂	76.8
Al₂O₃	12.8
K₂O	5.3
Na₂O	3.7
Fe₂O₃	0.6
CaO	0.5
Loss on ignition at 900°C	<1.0
pH	7.0

The crystalline structure of Harborlite 800, as observed using a scanning electron microscope and a magnification of 1000x, is as shown in Figure 4-6.

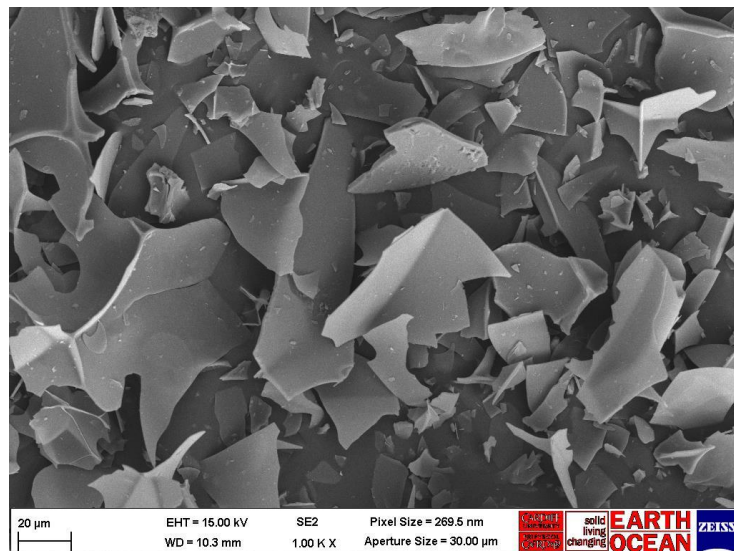


Figure 4-6. SEM image of Expanded Perlite (Harborlite 800) at 1000x magnification.

4.3.3 Natural Fibres

Of the natural fibres; hemp, jute and coir (Figure 4-7 and Figure 4-8) were selected for investigation for suitability as carrier materials.



Figure 4-7. Photograph of hemp and jute fibres used in experiments – prior to cutting and washing.



Figure 4-8. Photograph of coir fibres used in experiments.

The internal microstructures of hemp, coir and jute fibres, as observed and reported by Marrot et al. (2013), Fedelis et al. (2013) and Hamad et al. (2017) are shown in Figure 4-9.

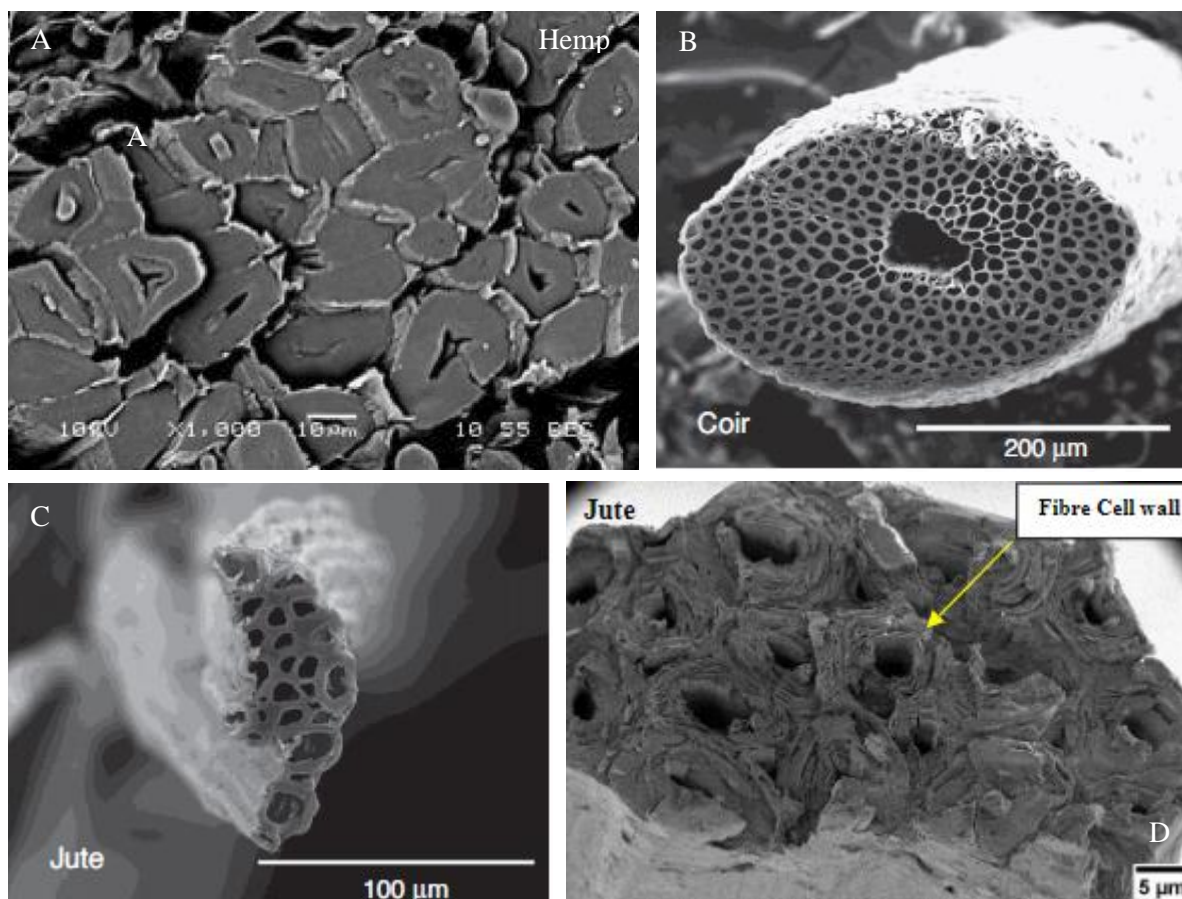


Figure 4-9. Internal microstructures of hemp (a)Marrot et al. (2013), coir (b), Fidelis et al. (2013), jute (c)Fidelis et al. (2013), (d), Hamad et al. (2017).

Prior to use, the fibres were washed thoroughly using a sieve and deionised water. All carrier materials were initially sterilised by autoclaving at 121 °C for 15 min, then dried for at least 24 h at 90 °C. Drying at 105 °C for this period was observed to result in a significant darkening of the coir fibres. This was likely due to degradation of lignin. Lignocellulosic fibres, which include coir and jute, thermally degrade through dehydration, depolymerization, and oxidation when heated (Ezekiel et al. 2011). Studies by Varma et al. (1986) Ezekiel et al. (2011) and Siakeng et al. (2018) suggest minimal effects of temperature on mechanical properties of coir fibre up to around 200 °C, with degradation occurring after due to depolymerisation. However, lignin has been reported to undergo thermal degradation at temperatures as low as 100 °C (Yang et al. 2007). A similar study by Gassan et al. (2001) on jute reported that temperatures up to 170 °C only slightly affect jute fibre properties, for studies of 2 h duration, with significant effects at a higher temperature. The time of exposure to heat is reported to effect mechanical properties, as reported by Ezekiel et al. (2011) who studied a range of durations from 10 to 30 min. For this reason, the oven temperature for drying was reduced to 90 °C for preliminary investigation and later to 50 °C, applied for all carrier materials for consistency. The primary constituents of jute, coir, and hemp fibres, as reported by Rowell and Stout (1998), Banerjee (2012) and Liu et al. (2017) respectively, are shown in Table 4-6. The range reported by Liu et al. (2017) is based on a review of seventeen papers which report the chemical composition of hemp, nine of which note

that the hemp fibres may also contain 1 – 17 % pectin. Rowell and Stout (1998) note that in addition to the three principal constituents, as given in Table 4-6, jute contains minor constituents such as fats, waxes, inorganic matter and nitrogenous matter, amounting to up to 2 % of jute.

Table 4-6. Reported chemical compositions of coir, jute and hemp fibres.

Fibre	Cellulose (%)	Hemicellulose (%)	Lignin (%)	Reference
Jute	58-63	21-24	12-14	Rowell and Stout (1998)
Coir	32-43	0.15-0.25	40-45	Banerjee (2012)
Hemp	53-91	4-18	1-21	Liu et al. (2017)

As per Table 4-6, and reported by Banerjee (2012), coir has a significant lignin content, which is likely why the darkening of fibres was observed after being subjected to temperatures exceeding 100 °C for 24 h. When the oven temperature was reduced to 90 °C, the fibre colour was only very slightly darker than the untreated fibres and no significant darkening was seen when dried at 50 °C. Prior to oven drying, any change in colour will have resulted from the autoclaving process, this was observed to have less of an effect on the coir fibre than heating at 105 °C for a long period. The extent of delignification has been reported to be dependent on the duration of heating. Ezekiel (2011) reported that the ultimate tensile strength of Jute fibres heated to 150 °C for 20 min was greater than the untreated fibre, after heating for 30 min this strength was reduced to below that of the untreated fibre. On this basis the autoclaving for 15 min is not likely to have a detrimental effect on jute fibres. Jute is reported to swell in water up to 22 %, which is indicative of its capacity to absorb the cementation media. Masoodi and Pillai (2012) report some initial swelling of Jute fibres. The low fibre percentage used in the biocemented sand column would potentially minimise the effects of any swelling on the biocemented matrix. Delignification has been reported to increase this capacity for swelling by up to almost 40 % when lignin content is reduced to 0.78 % (Rowell and Stout 1998).

Fibres for use in the column studies were hand cut to approximately 6 mm length. Samples of 20 fibres were taken to obtain an average for the length.

4.4 Production of Cementation Medium

The basic constituents of the cementation medium required for the ureolytic MICP process are urea and a calcium source. Calcium chloride dihydrate was selected as the calcium source for this research, as commonly used for MICP experiments involving biocementation of sand. The calcium chloride dihydrate concentration used varied according to the bacteria selected, typical urease activity of the bacteria, and purpose of the experiments. The cementation medium produced for biocementation of

sand using *S. ureae*, as per Table 4-1, to provide the necessary nutrients and precursor chemicals for the MICP process, was adapted from Stocks-Fischer et al. (1999). The cementation medium used to biocement sand using *S. pasteurii* is as given in Table 4-2, or as detailed in the experimental methods. Media prepared were close to pH 7.0. From samples tested across four column experiments, the pH of the augmented medium (with ammonium chloride and sodium bicarbonate) used with *S. pasteurii* was 6.95 ± 0.035 based on an average of four measurements across columns studies.

4.5 Immobilisation of Cementation Medium

4.5.1 Expanded Perlite and Diatomaceous Earth

Before use, the expended perlite (EP) and diatomaceous earth (DE) powders were autoclaved at 120 °C for 15 min and oven dried at 105 °C, for sterilisation. The EP/DE was then transferred to sterile 50 mL centrifuge tubes in the required quantities (up to 2 g in each tube) in triplicates. The tubes were weighed before filling. The EP was then submerged in concentrated cementation medium within the tubes. The tubes were vibrated for 10 s at 8 rpm using a vortex mixer, to ensure thorough dispersal of the powders in the medium, and then left to soak for 24 h. Similar methodology is applied for the immobilisation of cementation medium as used by Bundur et al. (2017) to immobilise cementation medium in expanded shale aggregates.

After 24 h, the tubes were centrifuged at 3200 rcf for 30 min and the waste medium drained. The tubes were then transferred to a 50 °C oven with lids removed and dried for at least 48 h until the mass was constant. This process was repeated as desired to apply a second loading of cementation medium. This process resulted in granules of cementation medium (CM) loaded EP and DE forming, and unlike the fibres these granules could still be easily separated after repeated loadings. The EP in particular was observed to self-aggregate following immobilisation of the cementation medium. Granules of CM loaded EP are shown in Figure 4-10. To separate out these granules, an autoclave sterilised pestle and mortar was used in close proximity to a Bunsen burner, with light pressure applied to avoid crushing the granules. The granules were then transferred back into the tubes ready for column assembly.

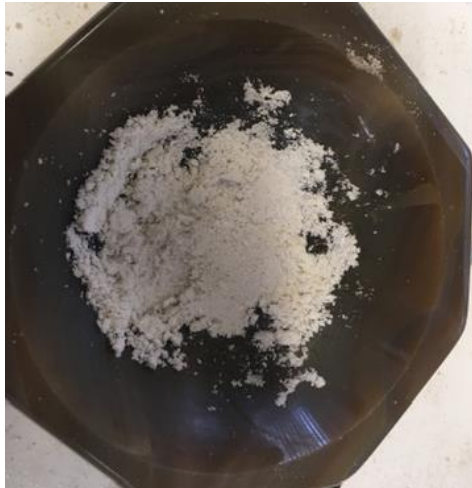


Figure 4-10. Photograph of expanded perlite - following immobilisation of cementation medium, drying and separation of granules using a pestle and mortar.

4.5.2 Fibres - Soaking Method of CM Immobilisation

Fibres were added to sterile 50 mL centrifuge tubes in 0.5 g or 1 g quantities as required, in triplicate. Concentrated cementation medium was added to each tube to fully submerge the fibres, with 25 mL cementation required to fully submerge 1 g of fibres, followed by vortexing for 10 sec to separate the fibres. Vortexing was also found to increase the immobilisation capacity. In addition, cutting the fibres to shorter lengths, of approximately 6 mm, increased the amount of cementation medium immobilised after soaking for 24 h, when comparing to preliminary testing results. The fibres were left to soak for 24 h at approximately 21 °C in a dark cupboard, since light exposure affects the strength of natural fibres. The tubes were then centrifuged at 3200 rcf for 20 to 30 min (with some change in duration dependent on the test undertaken) and the excess medium drained. Tubes were then left inverted for 2 h to help ensure all medium not immobilised was drained. Fibres for use in column studies were then transferred onto gauze to aid to aid drying and separation once dry, some clumping was observed when applying the soaking method, as can be seen in Figure 4-11. Fibres were then dried for 48 h (at 50 °C or as specified).



Figure 4-11. Photograph showing a triplicate set of hemp fibres, after they have been soaked in concentrated cementation medium, transferred to gauze and dried, prior to mixing with sand for use in column studies.

Once dried, these fibres were then separated by hand prior to mixing with sand, as shown in Figure 4-12. The fibres were mixed with the sand by hand, following addition of a small amount of cementation medium (1 to 5 % of sand and fibre mass) to aid mixing.



Figure 4-12. Photograph showing jute fibres, after they have been loaded with concentrated cementation medium, dried and then separated by hand.

4.5.3 Fibres - Spraying Method of CM Immobilisation

A spraying procedure was developed to more efficiently immobilise the concentrated cementation medium within the natural fibres. Fibres were sprayed and dried once only since repeating this procedure caused the fibres to become brittle and break while being separated prior to mixing with sand. Fibres were sprayed by hand, using a 100 mL spray dispenser. For each column, 1 g of sterile fibres were spread out onto a sterile 15 x 15 cm metal gauze laid over a weighing boat to capture waste medium, as shown in Figure 4-13. The gauze was wrapped in foil and autoclaved prior to use. Approximately one hundred spray actuations (15 mL) of the concentrated cementation medium were sprayed onto each set of 1g fibres in close proximity of a Bunsen burner. The dispensing bottle was weighed before and after each set of fibres were sprayed to monitor the amount of cementation medium used. The gauze and sprayed fibres were then transferred to a sterile airtight container and covered for 24 h to allow the fibres to soak up the cementation medium before transferring to a 50 °C oven for drying.



Figure 4-13. Photograph showing 1 g of jute fibres resting on gauze, after the fibres have been sprayed with concentrated cementation medium.

Once dried and removed from the oven, the CM loaded fibres were immediately transferred to sterile 50 mL polypropylene tubes and weighed after cooling, since the fibres are hygroscopic and start to absorb moisture once exposed to air. The weight of the empty tubes had previously been recorded to enable the masses of the immobilised cementation medium to be obtained.

Hand spraying and then leaving the fibres in a sealed container for 24 h was found to be the most effective method of immobilising the cementation medium. This method helped prevent clumping of fibres, making them easier to separate and mix with the sand and resulted in less waste of the concentrated cementation medium. Spraying also gave more consistent results in respect of the quantities of cementation medium immobilised, in comparison to soaking. The efficiency of this process could be further improved by using a vacuum, however enabling a sterile environment would have proved difficult. It would also be possible to scale up this process.

4.6 Encapsulation of Cementation Medium in Alginate-Based Hydrogel

Methods of production of alginate-based hydrogel beads were explored, as a means of immobilising cementation medium. Calcium alginate hydrogel beads can be produced following a relatively straightforward process in the laboratory. To maximise storage, cementation medium would ideally need to be incorporated into the alginate-based hydrogel bead through powder additions. This however presented challenges in respect of producing beads containing concentrated cementation medium which would also be sterile. Different methods were explored for incorporating the cementation medium into the alginate-based hydrogel beads. The methodology detailed in Chapter Four for the production of alginate gel beads immobilising cementation medium was developed for use with *S. ureae*. Similar methodology has been undertaken to produce beads for use with *S. pasteurii*, as reported in Chapter Eight.

4.6.1 Synthesis using an Aqueous Medium Solution, for use with *S. ureae*

Alginate gels were initially produced in accordance with the process and concentrations of reagents reported by Harbottle et al. (2013). This formed the basis of further exploration to produce concentrated cementation medium stores encapsulated by calcium alginate. A solution containing sodium alginate (2.8 % w/w) and cementation medium was prepared. The calcium source is derived from a calcium chloride gelling solution and hence calcium content of gel beads may vary. Calcium chloride replaces the sodium in sodium alginate with calcium ions to form a gel.

To produce the cementation medium, the Oxoid CM0001 nutrient broth solution was autoclaved, otherwise all other chemical solutions other than the sodium alginate were syringe filtered. Aseptic technique was followed during this process. The sodium alginate solution cannot be autoclaved, since this would result in depolymerisation, nor can it be syringe filtered due to its high viscosity. Glassware used was autoclaved before use, in addition to autoclaving of the de-ionised water used. During this process the only component that was not sterile was the sodium alginate powder. The cementation medium was thoroughly mixed with the sodium alginate solution, from which beads were produced by pipetting 10 μ L aliquots at a height of 5 cm into a gelling solution of autoclaved calcium chloride (3 % w/w) in deionised water. The beads were left in this solution for 30 min. This process was slow and at times air bubbles became entrapped within the beads during pipetting. The efficiency of this process was improved upon by filling a syringe with the sodium alginate solution and extruding droplets at a steady rate to form the beads. Greater control with regards to bead size could be achieved through use of a peristaltic pump. Palin et al. (2016) used a peristaltic pump to achieve a steady constant flow of the alginate gel through a 0.2 mm syringe needle, dropping this into a calcium acetate gelling solution to produce the beads.

4.6.2 Synthesis using Powdered Medium Constituents

To encapsulate a concentrated solution of nutrients, the required chemicals were added to the 2.8 % w/w sodium alginate solution in powdered form, to explore if this could be achieved. A 25 mL sodium alginate solution was prepared, to which solid nutrients were added. A mixture of solid chemicals, which would result in a x10 concentration of cementation medium in the sodium alginate compared to cementation medium used with *S. ureae*, were prepared. This mixture consisted of 0.75 g Oxoid CM0001 nutrient broth, 5 g urea, 2.5 g ammonium chloride and 0.53 g sodium bicarbonate. The powders were mixed together thoroughly, to help ensure an even distribution of these within the beads. Three additions of this mixture to the sodium alginate were made. Beads were then formed using the syringe needle extrusion process. It was possible to form beads from this solution. However, it was observed that soon after the beads were added to the gelling solution the calcium chloride gelling solution started to turn yellow, which indicated that nutrients (Oxoid CM001) were leaching out of the beads. It would not be known to what extent each chemical was leaching out of the beads into the

solution. There was the added issue that the powder additions were not sterile. To sterilise the nutrients these would need to undergo autoclaving or syringe filtering and hence would need to be in solution. A concentrated solution (x6.67) could be prepared, in which all nutrients were fully dissolved. It was found however that it was not possible to dissolve the sodium alginate in this mixture.

4.7 Sand Column Experiments (Bioaugmentation)

4.7.1 Mini-Columns (Preliminary study)

Mini-columns were produced at the preliminary stage of investigation using 50 mL polypropylene centrifuge tubes. Dry and wet pluviation methods were tested. Sand was pluviated using a funnel clamped 5 cm above the top of a centrifuge tube. The tube was vibrated, using a vortex mixer, to increase compaction and additional sand added until the tube was filled to capacity. Through the dry pluviation method the tube was filled with 95.376 g of sand. The process was repeated, after first placing 10 ml of water in the tube, additional water was added as dry sand became observed after pouring into the tube through the funnel, again the sample was vibrated. Via wet pluviation, 97.466 g of sand could be compacted into the tube, with the tube being filled to the rim. A total of 19 mL of water was needed to fill the pore spaces. The wet pluviation method was selected to fill the tubes for the mini-columns test and for subsequent experiments as this proved to be the most efficient.

4.7.2 Sand Preparation

4.7.2.1 Studies Based at Cardiff University (Kiln dried and Garside Sands)

The sand was first sieved through a 1 mm aperture sieve to remove larger particles of grit. Any carbonates present were removed from the sand prior to use by using the direct acidification method (Komada et al. 2008) and using a 3% HCl solution in deionised water. The sand was then rinsed thoroughly using a 63 µm sieve and deionised water to remove the chlorides. The sand was then dried at 105 °C. Following this process, the sand was transferred to a large glass beaker and sterilised by autoclaving at 120 °C for 15 min, with a final drying period at 105 °C until the mass was constant.

4.7.2.2 F60 and F65 Sands

For later experiments using the F60 and F65 sands, this was not acid washed since its carbonate content is known (and measured) to be negligible and such treatment would likely alter the surface of the sand particles and may adversely impact upon adhesion of calcium carbonate and resulting geotechnical properties. Sand was autoclaved prior to use in experiments.

4.7.3 Preparation of Columns Apparatus

4.7.3.1 General Assembly

The sand column apparatus was set up per the diagram shown in Figure 4-14 which shows the approximate lengths of the columns. The column apparatus fabricated for this research was based on that used in previous studies by Botusharova et al. (2017), with some enhancement including longer split moulds, to help ensure that the columns produced would exceed minimum depth to diameter ratios required for the unconfined compressive strength (UCS) testing and to ensure a secure fit of the bungs. The actual column lengths are as given in the details for the tests undertaken and were approximately twice the diameter of the columns, taking into account that the British Standards (1999) state that the length may vary from 8 % under-size to 12 % over-size without significantly affecting the results. The minimum column length would therefore be 70 cm for a 38 mm wide column.

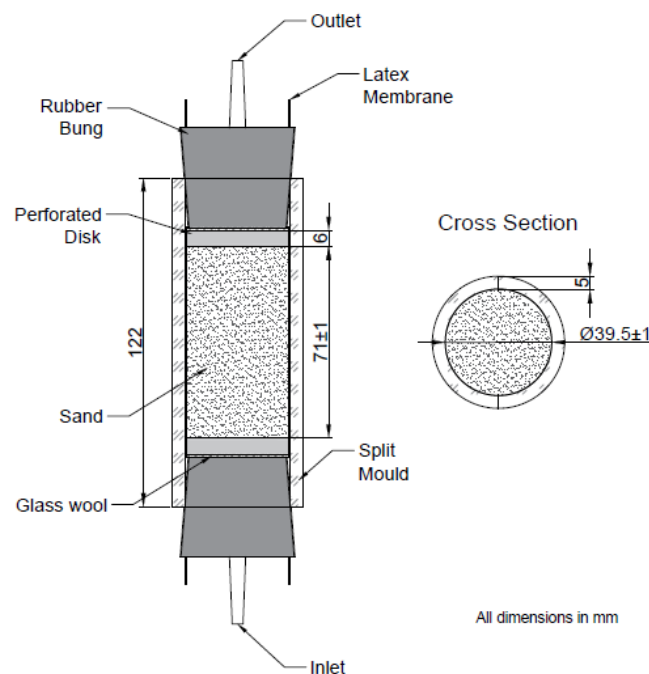


Figure 4-14. Diagram of sand column apparatus showing side of column and cross section through the column.

Sand columns were prepared in triplicates and secured to a 30 x 60 cm peg board as shown in Figure 4-15. Producing the columns in triplicates helps to improve accuracy of results, with results reported as an average from each set of triplicates unless otherwise stated. The pegboard holes allowed for insertion of inlet tubing through to the back of the board. Metal feet had been attached to the peg board to hold this upright. This apparatus allowed for columns to be attached to each side of the peg board and therefore for up to twelve columns to be prepared and treated at one time for each experiment.



Figure 4-15. Photograph of assembled sand columns attached to the front and back of the column frame in sets of triplicates, while cementation medium is being injected into the base of the columns using a peristaltic pump.

Perforated disks were placed at both ends of each sand column. These perforated disks consisted of 6 mm thickness plastic of 38 mm diameter and perforated with approximately 1 mm diameter holes. These disks were used to contain the sand and ensure an even surface at the inlet and outlet and an even distribution of cementation media throughout the sand columns. A thin layer of glass wool was wrapped around the porous disks to prevent washout of fine grains of sand during treatments and to provide a gap between the bung and disk. Figure 4-16 shows a perforated disk removed following biocementation. While within the column the glass wool layer sat between the disk and the column, as can be seen there is minimal clogging. It was found that these disks would erode slightly over time with the holes becoming slightly wider.



Figure 4-16. Photograph showing a perforated disk - following use within column to contain sand and to ensure even flow of cementation medium through the column, with layer of glass wool beneath which sits between the sand column and disk.

Each sand column was enclosed by a 180 mm long, 38 mm diameter, approximately 0.3 mm thick latex membrane (Controls Testing Equipment Ltd), encased by clear acrylic split moulds of 5 mm thickness and approximately 39 mm inner diameter. The split moulds were fabricated from a 1 m and 0.5 m length of clear acrylic tubing of outer diameter 50 mm and inner diameter 40 mm. This allowed for some reduction in the diameter due to cutting, with the desired inner diameter being approx. 39 mm. A bench saw with a cutting disk of 3 mm width was used to cut the tubes into lengths of 122 mm and to then cut these sections in half lengthways to produce the split moulds. These were then paired after to form sets of split moulds.

The tubing connecting the inlets to the peristaltic pump was cut into twelve sections of equal length. With additional sections of equal length connecting to the pump to the cementation medium supply and between the outlets and effluent collection tubes. Before use, any equipment which could not be autoclave sterilised was soaked in a solution of 1 % Virkon S. disinfectant solution for 60 min and rinsed thoroughly afterwards with autoclaved deionised water.

To prepare each sand column, the two sides of the acrylic split mould, as shown in Figure 4-14, were secured firmly together using cable ties, allowing for easy removal after biocementation. A latex membrane was inserted within this mould so that an even length of membrane protruded from each end. The membrane sections protruding from each end of the split mould were then wrapped around the outside of the split mould, ensuring the membrane was taught and straight. A perforated disk wrapped with glass wool, followed by a bung with the plastic inlet removed was then placed into one end of the mould. A sterile spatula was used to push the perforated disk against the bung. The latex membrane wrapped around the base of the tube was then pulled up and over the bung. A sterilised silicone tapered plug (4 mm < 8 mm x 20 mm, Vital Parts) was then inserted into the hole in the inlet bung (Figure 4-17), to retain the liquid into which the column contents were wet pluviated. This assembly was inverted and inserted into a glass beaker to keep this upright, ready for insertion of column contents. The column was prepared close to a Bunsen burner, aseptic conditions were maintained as far as possible.



Figure 4-17. Photograph showing the inlet end of a column during assembly, with silicone plug inserted into the inlet hole within the bung to prevent the cementation medium draining during filling of the column.

4.7.4 Column Filling, Bacteria fixing and First Treatment (Stage 1)

Columns were biocemented using a two-stage process of bacteria fixing and treatment followed by subsequent treatment cycles.

4.7.4.1 Columns Biocemented using *S. ureae*

Owing to the much slower urease enzyme activity of *S. ureae*, it was possible to fix this bacterium to the sand (and carriers) simply by wet pluviation of the sand (or sand and carrier materials) into a cementation medium and bacteria mixture. No precipitation was observed upon suspension of the *S. ureae* cells in cementation medium, prior to wet pluviation of the sand (and carriers) into this mixture. Any precipitation at this stage of columns assembly may have otherwise hindered flow of bacteria through the sand as the column is prepared and could have adversely affected bacterial adhesion to sand particles. Should precipitation occur within the bacteria and cementation medium mixture, this may also encapsulate the bacteria. The process of wet pluviating the sand into a mixture of bacterial suspension and cementation medium appeared to result in an even distribution of bacteria throughout the columns, based on pH readings of columns effluent as an indication of bacterial activity. It should also be possible to inject this solution of *S. ureae* bacteria and cementation medium to replicate this process in the field.

Bacteria were grown and pelleted following the procedure outlined in Section 4.1. A 10 mL pipette tip was used to add the cementation medium to the tubes containing the bacterial cells and to disperse the cells within the medium. The suspension containing the *S. ureae* bacterial cells and cementation medium, slightly above one pore volume of the sand, was poured into the latex lined split mould. The sand (controls), or sand and CM loaded carrier material mixture, was then wet pluviated into the cementation medium and bacteria mixture. The column assembly was vibrated three times during the filling process, using a vortex mixer, to aid compaction. After filling the column, a second perforated disk wrapped in glass wool was inserted into the column. This disk was pushed down firmly against the sand, exerting further pressure to density the sand column. The second bung was then placed into the top of the tube and the membrane pulled up and over this. This completed the column assembly, which was then secured to the peg board and labelled. This process was repeated for each individual column. The set of columns connected to the peg board were then transferred to a 30 °C (static) incubator. This methodology was also applied for the initial column study with *S. pasteurii* completed at Cardiff university as detailed in Chapter Six, prior to the studies completed at Arizona State University.

An alternative approach consisting of suspending the *S. ureae* cells in PBS (as per studies by Botusharova (2017) was also tested, see Chapter Six. Following wet pluviation of column contents into PBS, the above procedure was followed to complete column preparation. Columns were then left for

four hours before cementation medium (treatment one) was injected. Filling columns with a bacterial suspension prior to injecting cementation medium had been found to be among the least effective method of fixing bacteria according to Harkes et al. (2010). Wet pluviation of the column contents into a suspension containing cementation medium had also been the preferred approach to help to reduce leaching of the immobilised cementation medium.

To pump the cementation medium into the columns, upwards through the base of each column, a 12-channel peristaltic pump (Ismatec IPC) was used for the column tests completed at Cardiff University. This was set up to pump at a flow rate of 2 mL/min, using tubing with a 2.54 mm inner diameter. Prior to injection of the cementation medium, the inlet tubing (with column connector) was connected to the tubing running through the peristaltic pump and filled with cementation medium, to prevent air entry into columns. For each individual column, the silicon plug was removed from the inlet bung and immediately replaced with the inlet connector and tubing. When this had been done for each column the pumping of cementation medium was resumed and one to one and a half pore volumes of cementation medium were pumped into each column (as detailed for each column study). After injecting columns, the outlet tubing was drained and clamped and the inlet tubing left filled and clamped. The column assembly was then transferred to an incubator.

4.7.4.2 Columns Biocemented using *S. pasteurii* (Studies undertaken at Arizona State University)

In excess of one pore volume (35 mL) of cementation medium was poured into the column, into which column contents were wet pluviated using a funnel secured above the column, as shown in Figure 4-18.

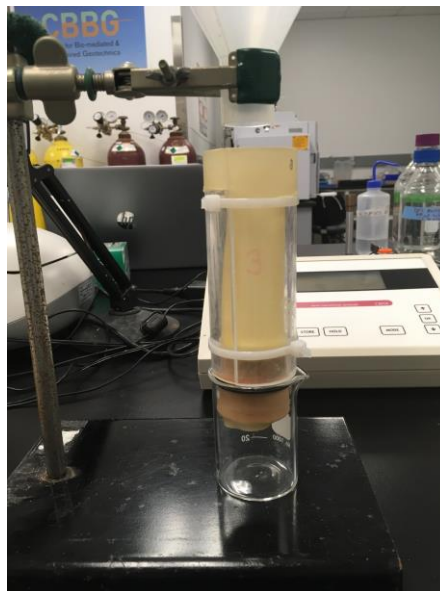


Figure 4-18. Column during assembly – ready for filling via wet pluviation.

Column contents were vibrated three times during the filling process. The outlet-end perforated disk wrapped in glass wool and bung were then firmly inserted and enclosed by the latex membrane. Rubber rings were placed around the bungs at this stage to help prevent any leaks.

An injection technique developed from Harkes et al. (2010) was used to fix the *S. pasteurii* within the sand columns (For the tests detailed in Chapter Seven onwards) and apply the first biocementation treatment. Firstly, after centrifugation and removal of supernatant, the bacterial suspension (in individual 15 mL tubes for each column) was made up to 10 mL with PBS and this solution mixed using a sterile pipette tip. For the studies undertaken at Arizona State University, two peristaltic pumps (Cole-Parmer Masterflex L/S) with eight channel pump heads attached, and 2.79 mm inner diameter tubing, were used for the injections.

The column inlet tubing (with inlet connectors attached), along with the tubing running through the peristaltic pump, was filled with the bacterial suspension from the individual 15 mL sterile polypropylene tubes and then connected to the columns. The bacterial suspension was pumped into columns at a rate of 1.5 mL/min. Having a separate supply of bacterial suspension for each column ensured all columns were injected with the same amount of bacteria. Once the bacterial suspension was depleted in the supply tubes, the pump tubing was immediately transferred to the cementation medium, which was injected at the same rate immediately following the bacterial suspension. One and a half pore volumes of cementation medium were injected into each column at this stage. The outlet tubes were then drained and clamped. Inlet tubes were clamped and disconnected from peristaltic pump tubing.

As the cementation medium is pumped into columns, the calcium is known to travel faster than the bacteria through the pore spaces, and in addition to this the cementation medium already in the columns helped to fix the bacteria. Cementation medium containing urea and calcium chloride has been found to be particularly effective for the fixing of bacteria to sand, according to studies undertaken by Harkes et al. (2010).

4.7.5 Biocementation Treatments (Stage 2)

After a period of static incubation (retention period) the columns were again injected with cementation medium, through the base of the column. This process was then repeated as described for each columns test. Retention times varied as stated for each test. Pumping the cementation medium upwards through the base of the column helps ensure the cementation medium is evenly distributed and the effluent is displaced fully from the column, since the medium injected will be heavier than the effluent. During the treatments, the effluent from each column was collected separately. For the column studies detailed in Chapter Six, the first 10 mL of effluent was retained from each column for geochemical analysis. For the later column studies with *S. pasteurii* (Chapters Seven to Nine) the columns effluent was collected

in a series of 15 mL polypropylene tubes, in 5 mL increments, from each column for geochemical analysis. The outlet tubing was emptied after each biocementation treatment, and then reconnected to the columns and clamped with pipe clips. Inlet tubing was kept filled with cementation medium and clamped. Use of pipe clips ensured the fluid was held within the columns and prevented air entry and any drying out of columns.

4.8 Geochemical Analysis

4.8.1 Electrical Conductivity, pH and Dissolved Oxygen

For the studies completed at Cardiff University, the measurement of pH and dissolved oxygen in liquid media was undertaken using a multiparameter (Mettler Toledo Severn Excellence) meter and attached probes. For measurement of electrical conductivity and pH for studies undertaken at Arizona State University (ASU), a multi-parameter (Consort C3010) analyser with electrical conductivity (EC) and pH probes was used. The EC probe had temperature compensation. Readings were taken at a constant 23 °C room temperature at ASU. Probes were washed with 2 M HCl solution as recommended by (Kennedy et al. 2005) and deionised water before and after use for all tests.

4.8.2 Cation Concentration

For studies completed at Cardiff University, calcium ion concentration in aqueous media was measured using an Inductively Coupled Plasma Optical Emission Spectrometer (ICP-OES, Perkin Elmer Optima 2100 DV). For studies undertaken at Arizona State University, the concentration of selected cations in aqueous solutions (primarily calcium ions), was measured using an Ion Chromatograph (IC, Thermo Scientific Dionex ICS 5000⁺). IC cation analysis was conducted using 20 mM methanesulfonic acid eluent starting concentration, on a Dionex CS12A column, using 112 mA suppressor output.

Prior to cation measurement, all aqueous samples were syringe filtered, using a 0.2 µm syringe filter. Solutions were diluted before testing, to ensure that the measured concentrations did not exceed 100 mg/L and were otherwise not below the range of accuracy of the testing equipment. Pipettes were calibrated before use by weighing the volume of water extruded from the tips to ensure accuracy. Testing was conducted soon after the samples were collected from the column studies, since there may be traces of urease within these samples, to ensure accuracy. The testing using the IC (Chapters Seven to Nine) was completed on the day of collection of the samples tested to ensure accuracy of readings.

The IC equipment was found not to give accurate measurement of ammonium ion concentration, results had been higher than expected and this analysis gave higher measurements when compared to results obtained using the Nessler method. It is known that the calibration curve is curved for ammonium ions

when using the suppressor method of ion chromatography (Shimadzu 2021), and this had been observed for the calibration that had been run and had led to inaccurate results when measuring ammonium ions.

4.8.3 Colorimetric Determination of Ammonium Ion Concentration (Nesslerisation)

The two major factors that influence selection of the method to determine ammonia are concentration and presence of interferences. Samples of columns effluent were diluted to be in the range of 0 to 0.5 mM prior to testing and tested within 2 h of collection.

An ammonium standard was prepared and calibration curve produced in accordance with EPA method 350.1 (US EPA 2019). Firstly, an ammonium chloride stock solution was prepared (1.0 mL = 1.0 mg NH₃-N), by dissolving 3.819 g NH₄Cl in deionised water so that the total volume was 1 L. This stock solution was used to prepare an ammonium chloride standard solution (1.0 mL = 0.01 mg NH₃-N), by diluting 10.0 mL of the stock solution in 1.0 L deionised water. The ammonium chloride standard solution was used to prepare a series of dilutions ranging from 0 to 2 mg/L concentration of ammonium chloride to produce a calibration curve, as shown in Figure 4-19.

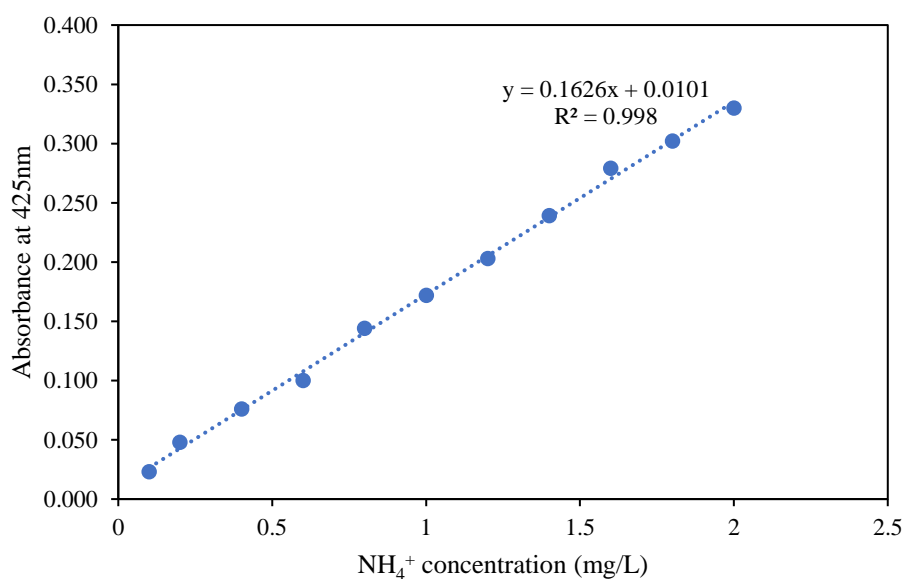


Figure 4-19. Calibration curve for nesslerisation.

The blank contained deionised water and 100 µL of Nessler's reagent NH₃-N (VWR chemicals). 2 mL of each dilution was added to a cuvette, to which 100 µL of Nessler reagent was added using a pipette and left for 1 min before measuring the absorbance at 425 nm using a spectrophotometer, in accordance with the modified Nessler method as reported by Greenburg et al. (1992). A linear correlation ($R^2 = 0.998$) was established between NH₄⁺ concentration and absorbance at 425 nm. From the calibration curve, the relationship shown in Equation (4-4) was obtained.

$$NH_4^+ \left(\frac{mg}{L} \right) = \frac{(Absorbance \text{ at } 425 \text{ nm} - 0.0101)}{0.1626} \quad (4-4)$$

Samples taken from column effluent were diluted (1:10,000) and the procedure as outlined above followed whereby 2 mL of the dilution was transferred to a cuvette using a pipette, to which 100 μ L of the Nessler reagent was added. This was left for 1 min and the absorbance measured at 425 nm. Using this reading the concentration of ammonium ions was calculated using Equation (4-4) and factoring in the dilution.

4.9 Quantification of Calcium Carbonate using a Calcimeter

The calcium carbonate content of the sand columns, for the studies undertaken at Arizona State University, was quantified using a Calcimeter and in accordance with procedures outlined by Eijkelkamp (2018). The calcimeter works in accordance with the method of Scheibler to determine calcium carbonate content based upon a volumetric method whereby carbonates in the sample are converted to CO₂ by adding HCl to the sample. The pressure of the CO₂ released causes water in a burette to rise and this difference in level from the start of the test enables calcium carbonate content by mass, $w(\text{CaCO}_3)$, to be calculated according to the Equation (4-5) obtained following calibration, whereby V_1 is the volume of carbon dioxide produced by the reaction of the test portion.

$$w(\text{CaCO}_3) = 0.0045 \times V_1 \quad (4-5)$$

The result of the above divided by the mass of the sample tested gives the percentage of the sample which contains calcium carbonate. To obtain the average calcium carbonate content of each column, as a percentage of the total dry mass, samples of between 4 g and 5 g were taken from the top, centre and base of each column for testing after oven drying at 105 °C. Tests were conducted at constant room temperature.

4.10 Geotechnical Parameters

4.10.1 Particle Size Distribution

The particle size distribution of the silica sand has been determined using the dry sieving method, using a mechanical sieve shaker, in accordance with BS 1377-2:1990 (British Standards Institution 1999). As permitted by BS1377-2, test sieves complying with BS 410 having the ISO series of aperture sizes were used. This enabled a larger range of sieve aperture sizes to be used, to cover adequately the range of particle sizes of the selected sand. The sand sample was prepared for testing as specified in 7.3 and 7.4.5 of BS 1377-1:1990 (British Standards Institution 1990). Since all sand particles were less than 2

mm in diameter, a sample mass of 150 g was used, with 100 g being the minimum sample mass specified in BS 1377-1.

The uniformity coefficient, C_u , of the sand was determined using Equation (4-6) (Craig 2004).

$$C_u = \frac{D_{60}}{D_{10}} \quad (4-6)$$

The coefficient of curvature, C_z , of the sand is defined by Equation (4-7) (Craig 2004). Parameters were otherwise read directly from the particle size distribution curve.

$$C_z = \frac{D_{30}^2}{D_{60}D_{10}} \quad (4-7)$$

4.10.2 Particle Density (Specific Gravity)

Particle density, this being numerically equal to specific gravity, of the particulate materials including the sand, EP and DE, was determined using the small pycnometer method, in accordance with BS 1377-2:1990 (British Standards Institution 1996). A 100 mL pycnometer was used for all samples. The test was repeated twice for each material (with results obtained being in the required range), and the average value of these two results recorded. The particle densities obtained for each material differed by no more than 0.005 Mg/m³, this being lower than the limit of 0.03 Mg/m³, hence no further repeats were required.

4.10.3 Compaction

The proctor compaction test was conducted in accordance with ASTM D1557-12e1 (ASTM International 2012). The results from this test enabled the target density for compaction of the columns contents to be determined.

4.10.4 Unconfined Compressive Strength

Unconfined compressive strength (UCS) testing of biocemented sand columns was carried out in accordance with 7.2 of BS 1377-7:1990 (British Standards Institution 1999). The unconfined compression test involves subjecting a cylindrical specimen (usually cohesive soil) to steadily increasing axial compression until failure. This test gives an approximate value of the compressive strength of soil. It is noted that the materials subjected to testing in this study are biocemented sand/sand and carrier mixtures. Values of compressive stress were plotted against strain to ascertain the failure criterion. The failure criterion is the point at which the maximum compressive stress is obtained, this being the unconfined compressive strength (q_u) of the test specimen. Where a maximum value of axial

stress is not readily reached, an axial strain of 20 % was otherwise used as the failure criterion, in accordance with BS 1377-7:1990. The method of UCS testing applied in this study is the definitive method using a load frame apparatus, using cylindrical specimens of a length equal to about twice the diameter.

Flat, smooth (acrylic) plastic end caps were used to ensure that axial force was transmitted equally through each end of the test specimen. The British Standards permit use of plastic end caps of not less than 20 mm thickness for soft soils. The acrylic plastic end caps used in this study had a 38 mm thickness and diameter of 38 mm. Plastic end caps ensured that very little weight was transferred to the test specimen, as opposed to using metal end caps.

The initial UCS tests on columns biocemented using *S. ureae* deviated from the standards in that the samples were dried prior to the strength testing. This methodology had been applied to determine the self-healing response as a result of spore germination and subsequent MICP.

Later testing with *S. Pasteurii* focussed on self-healing due to vegetative bacterial cells and hence standards were adhered to, and the specimen tested in its saturated state. In this state there are less likely to be any capillary effects.

Prior to unconfined compressive strength testing of the biocemented sand columns, the perforated discs were removed as otherwise the specimen may shear against these. The acrylic end caps also allowed the membranes to be reused and to remain in place for the self-healing stage of testing. The membrane was folded over the sides of the end caps and was not in contact with the base of the loading frame or load cell and this also allowed movement of the membrane over the end caps and sample so as not to restrain deformation.

A level was used prior to starting the test to ensure that the end caps and sample were in alignment and to help prevent torsional effects. The length and diameters of each column specimen were measured to 2 d.p. using a Vernier gauge prior to each UCS test. Following the final UCS test (UCS2) the moisture content was determined according to BS 1377-2:1990 (British Standards Institution 1996).

4.11 Mineralogical Analysis

Scanning electron microscopy (SEM) and X-ray diffraction (XRD) were used for the observation and characterisation of the materials contained within biocemented columns. A scanning electron microscope (Zeiss Sigma HD Field Emission Gun Analytical SEM), at an accelerating voltage of 15 kV, was used for high resolution imaging of samples from sand columns produced at Cardiff University, to observe the precipitated mineral forms. X-Ray Diffraction (XRD, Siemens Diffraktometer D5000) was used to test samples for the presence of calcium carbonate at Cardiff University.

For the US based studies, Scanning Electron Microscopy (SEM, SNE-4500M Plus) was used in high vacuum mode and scattered electrons (SE) setting at a working distance of 6 mm for the observation of precipitated crystal forms. The SEM, SNE-4500M Plus was also used for elemental identification and quantitative analysis of the chemical composition of selected samples, conducted using the energy dispersive X-ray analyser (EDX) at an accelerating voltage of 15 kV, also referred to as energy dispersive spectroscopy (EDS). X-Ray Diffraction (XRD, Malvern Panalytical, Aeris powder diffractometer, Malvern, UK) was used at Arizona State University to verify the presence of calcium carbonate, and along with the SEM observations, to identify the types of calcium carbonate polymorphs present in the samples tested.

5 MATERIALS TESTING AND SELECTION: PRELIMINARY STUDIES

5.1 Introduction

A series of preliminary tests were undertaken, to aid in, and refine, the selection of appropriate materials for the subsequent column studies. The tests undertaken in this chapter are summarised below in Figure 5-1.

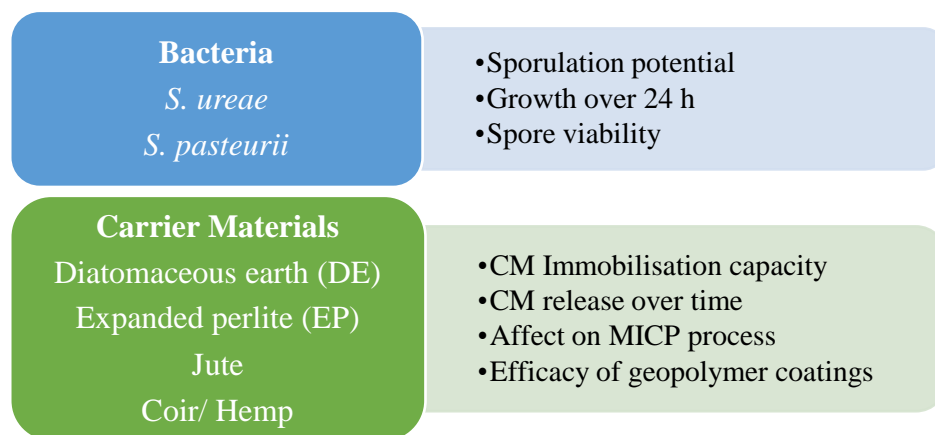


Figure 5-1. Overview of preliminary testing.

5.2 Bacteria

Following on from work by Botusharova (2017), *Sporosarcina ureae* was selected as a potentially suitable ureolytic bacteria, in addition to *Sporosarcina pasteurii* - a bacteria commonly used in studies on biocementation of sands.

5.2.1 Sporulation Potential of Selected Bacteria

To ensure longevity of the self-healing capability of the biocement, the bacteria will be required to remain viable within the biocement for the service life of the geotechnical structure. The selected bacteria will therefore need to be able to produce spores and to survive in spore form within the biocement.

Experiments were undertaken to induce the sporulation of ureolytic *Sporosarcina pasteurii* and *Sporosarcina ureae*, to ascertain if these bacteria would be able to produce spores, and to establish if this sporulation is likely to occur within the biocement. Also tested was the viability of bacteria within biocemented sand samples following 1.5 y of storage, with any bacteria present assumed to be in spore form given the absence of water.

5.2.2 Observation of Spores

To determine the presence of spores in aqueous solutions, the Schaeffer and Fulton spore staining procedure was followed, as per directions specified within the product information for the 04551 Schaeffer and Fulton spore stain kit (Sigma Aldrich 2013) and based upon methodology as reported by Schaeffer and Fulton (1993). A microscope slide was smeared with 100 μ L of liquid broth culture of bacteria following the induction of sporulation, and left to dry in a static incubator at 30 °C. The culture was then fixed using a Bunsen burner flame, by holding the slide above the flame while moving the slide back and forth for approximately 10 s, ensuring the slide was not excessively heated. The slide was then placed on top of a 250 mL beaker containing 100 mL of water that had been preheated on a heat plate to the point that steam was being produced, as shown in Figure 5-2. The slide was then flooded with Spore Stain A (malachite green). The heat plate was left on for 5 to 10 min, until the stain had dried on the slide. The slide was then placed in a container and immersed in tap water, the container was gently rocked until the stain had washed off the slide, following which this process was repeated. The slide was left to air dry and then flooded with Spore Stain B (safranin), no heat or steam was applied at this stage. The Spore Stain B was then washed off with tap water and left to air dry. The water containing the dye was collected for safe disposal. The slides were then observed under an light microscope (Nikon Eclipse 100). Following this process, spores are observed as green coloured spherules and vegetative bacterial cells appear red.

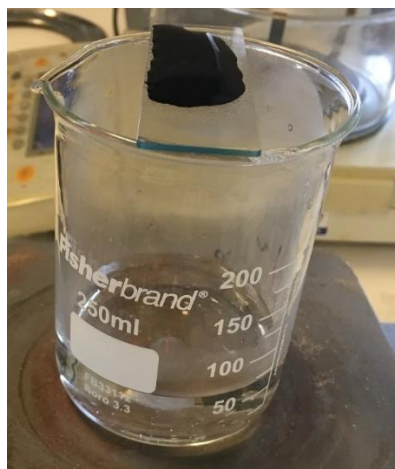


Figure 5-2. Photograph showing steaming of microscope slide with bacterial spores and cells fixed on the surface and malachite green spore stain applied.

When testing biocemented samples following 1.5 y of storage, the plate counting method was used as an indicator of spore presence within the biocement produced, and to obtain an estimate of viable cell counts following rehydration of biocemented column samples (Chapter Six, Section 6.4).

5.2.3 Chemically Induced Sporulation

Sporulation was induced using the MacDonald (1962) medium for *S. ureae* and a medium prepared according to Bhaskar (2017) for *S. pasteurii*, both being effective in inducing sporulation, however the *S. ureae* was observed to produce a greater amount of spores following 24 h of incubation. The constituents of the aforementioned sporulation media are detailed in Table 4-1 and Table 4-2.

Under a light microscope (Nikon Eclipse LV100) spores were observed as green coloured spherules, with vegetative cells stained red and appearing slightly larger. The spores are only lightly stained in comparison to the vegetative cells since the tough keratin outer coating of spores is resistant to staining and hence the requirement for steam during the spore staining process. Spores of *S. ureae* and *S. pasteurii* were observed following the staining process, as shown in Figure 5-3 (a-b), however these were observed to be far fewer in number for *S. pasteurii* when compared to *S. ureae*. Following this outcome, the *S. ureae*, as used in prior studies by Botusharova (2017), was selected for the first stage of the experimental work since this appeared to be the most viable in respect of spore production.

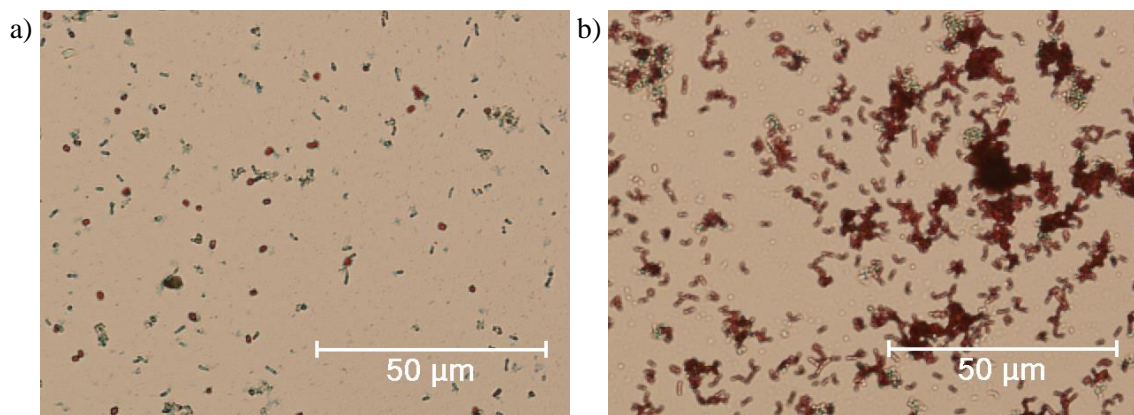


Figure 5-3. Light microscope images of green stained spores and red stained vegetative cells of *S. ureae* (a) and *S. pasteurii* (b) following chemically induced sporulation of bacterial cells.

5.2.4 Sporulation under Low Nutrient Conditions

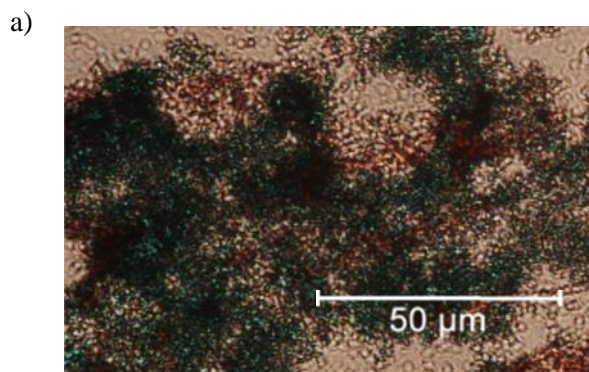
Sporulating bacteria may also form spores when nutrients become depleted (Setlow 2013). As an alternative to using a sporulation medium, the formation of spores was induced by leaving the liquid broth cultures in a static incubator at 30 °C for several days, to allow time for nutrient depletion. This would be a test of whether spore formation is likely to occur within the sand columns following depletion of the nutrients supplied within the injected cementation medium.

Liquid broth cultures were prepared in flasks using culture media as specified in Chapter Four. These cultures were grown in a shaking incubator for 11 h at 150 rpm, and 30 °C, to late exponential stage growth, and then transferred to a 30 °C static incubator (since columns would be subjected to static incubation), and then left incubated for an initial five-day period, followed by a further five days. The Schaeffer and Fulton spore staining process was then applied. The light microscope images of the stained cells are shown in Figure 5-4 (a-d).

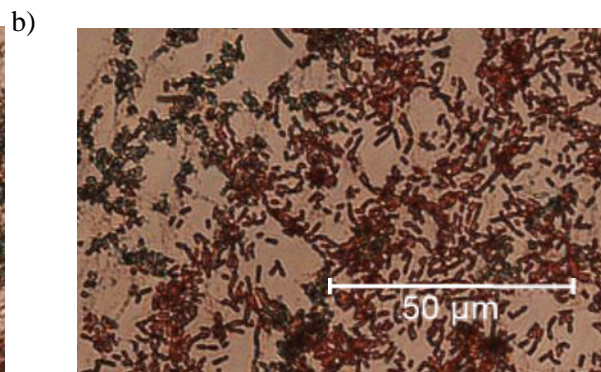
S. ureae appeared to produce spores more readily in low nutrient environments, dense areas of spores were observed on the microscope slide after five days of incubation, as can be seen in Figure 5-4 (a). Spores were also visible in the *S. pasteurii* culture after five days of incubation, in smaller clusters in comparison and around edges of vegetative cells, as shown in Figure 5-4 (b). After ten days of incubation, the increased density of bacterial cells, and also spores, made spores appear less defined, with spores observed more clearly on the edges of the culture smear, as shown in Figure 5-4 (c-d).

After five days of static incubation at 30 °C:

S. ureae

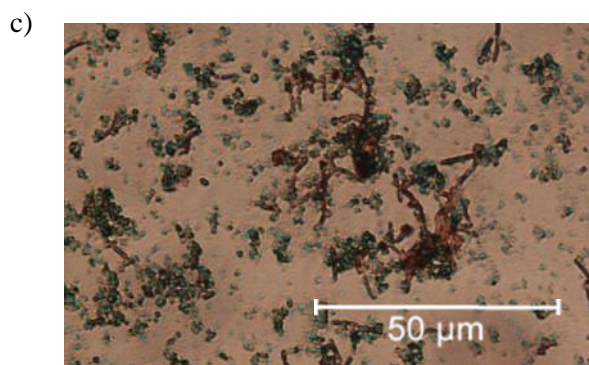


S. pasteurii



After ten days of static incubation at 30 °C:

S. ureae



S. pasteurii

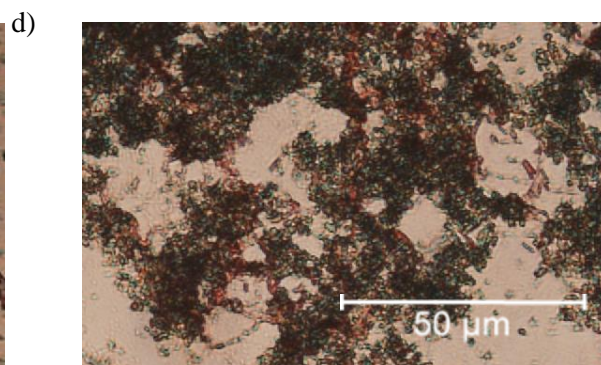


Figure 5-4. Light microscope images of green stained spores and red stained vegetative cells of *S. ureae* and *S. pasteurii* observed at 80x magnification, following incubation of liquid broth cultures at 30 °C for five days (a-b) and ten days (c-d) to observe effects of nutrient depletion on spore production.

After ten days in the same liquid broth, both *S. ureae* and *S. pasteurii* had produced significant quantities of spores. These results indicate that as nutrients are depleted within the sand columns spore production is likely to occur, and therefore a sporulation medium would likely not need to be applied.

Spore production was also found to be increased by increasing the incubation temperature, as shown in Figure 5-5 (a-d). The most effective outcome of the spore production process, as can be seen in Figure 5-5 (d), was that resulting from incubation for ten days at 40 °C. The density of the bacteria observed increased when the temperature was increased from 30 °C to 40 °C, as was expected, however much of the *S. ureae* bacteria observed after incubation at 40 °C for ten days are in spore form, with few vegetative (red stained) cells being visible. Studies by (Warth 1978) reported that for strains of various *Bacillus* species cell death occurred within 10 min for temperatures varying between 40 °C and 72 °C and spore death between 88 °C and 120 °C, in wet heat environments.

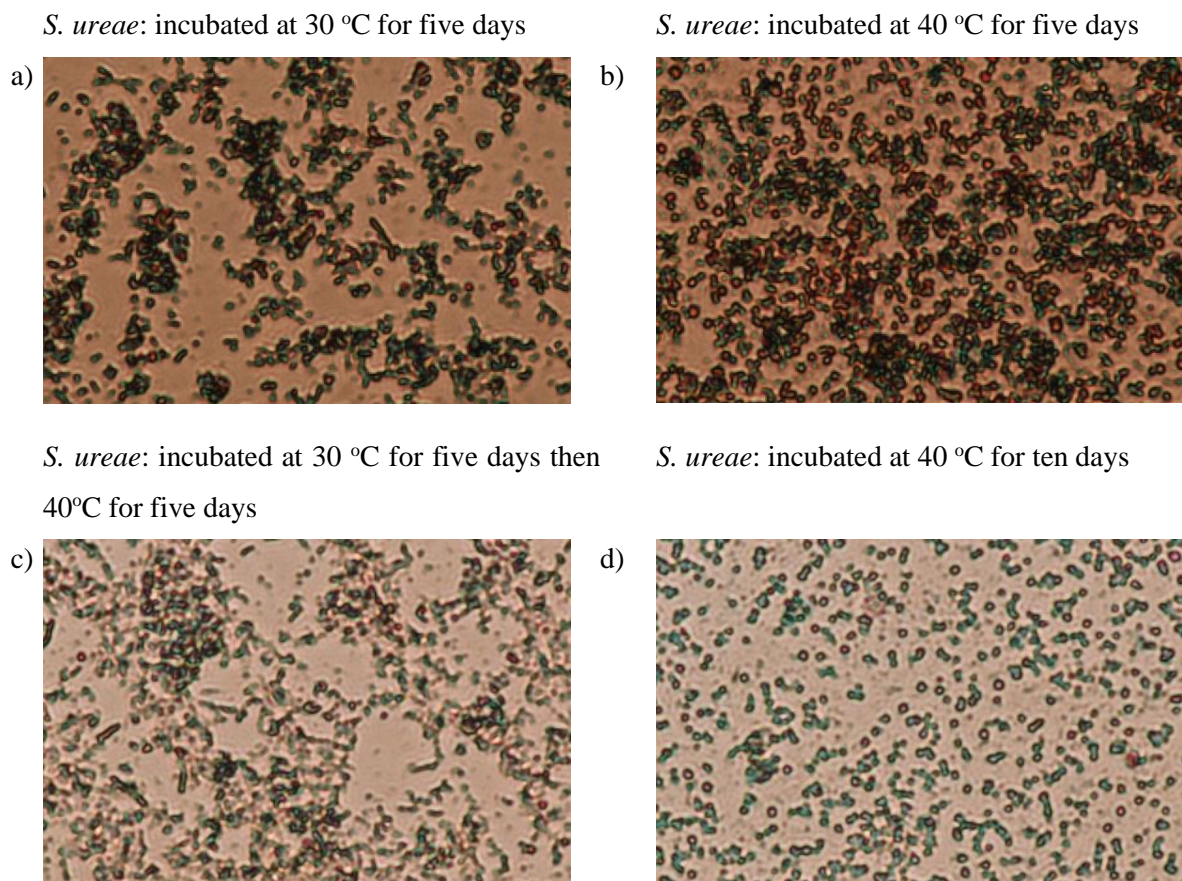


Figure 5-5. Light microscope images of green stained spores and red stained vegetative cells of *S. ureae*, following incubation of liquid broth cultures at a) 30 °C for five days, b) 40 °C for five days, c) 30 °C for five days followed by 40 °C for five days and d) 40 °C for ten days.

5.2.5 Bacterial Growth

5.2.5.1 *Sporosarcina ureae*

Overnight liquid broth cultures of *S. ureae* were produced and used to inoculate i) flasks of growth medium and ii) flasks containing cementation medium (CM) without the calcium source, in triplicates. The growth medium (GM) consisted of 5 g/L peptone and 3 g/L meat extract. In addition, single colonies of *S. ureae* grown on LB agar plates amended with 20 g/L urea, following three days of incubation at 30 °C, were used as an inoculant in growth medium for comparison with the liquid broth inoculant. The liquid broth inoculant had an optical density (OD₆₀₀) of 0.435.

The media were prepared using tap water, in 50 mL quantities within 250 mL Erlenmeyer flasks and autoclave sterilised, with either one bacterial colony or 100 µL liquid broth culture inoculant added. These flasks were transferred to a shaking incubator set to 30 °C, 150 rpm. 1.0 mL samples were taken from these flasks using a sterile pipette tip, in close proximity to a Bunsen burner, and transferred to cuvettes for measurement of optical density using a spectrophotometer. A sample was taken from each of the three flasks for optical density measurement. Figure 5-6 shows the averages from these. Samples were taken hourly up to 9 h, after which the flasks were replaced with a second set of freshly inoculated flasks of growth medium, from which samples were taken after overnight incubation from 15 h every 3 h, as growth appeared to have stabilised during this stage.

By growing the bacteria in the cementation medium (without calcium) this gives an indication of the bacterial growth within the columns. The calcium source has been excluded to prevent precipitate forming. The cementation medium containing 3 g/L Oxoid CM0001 enables a low rate of sustained growth, as shown in Figure 5-6.

The liquid broth inoculant, when compared to inoculation with single bacterial colonies, was the most effective in respect of achieving faster bacterial growth and also a higher cell concentration prior to the stationary stage being reached. The start of the exponential growth phase was shown to be just after four hours following inoculation with the liquid broth culture, with the late exponential phase reached at approximately ten hours. This end of this latter stage is estimated given the gap in readings. The desired cell concentration, corresponding to a spectrophotometer measurement of at least 0.8 (OD₆₀₀), was achieved following ten hours of incubation when using the liquid broth inoculant. The peak before the stationary stage of *S. ureae* growth suggests there may have been some clumping of the bacteria following approximately 12 h to 14 h of growth.

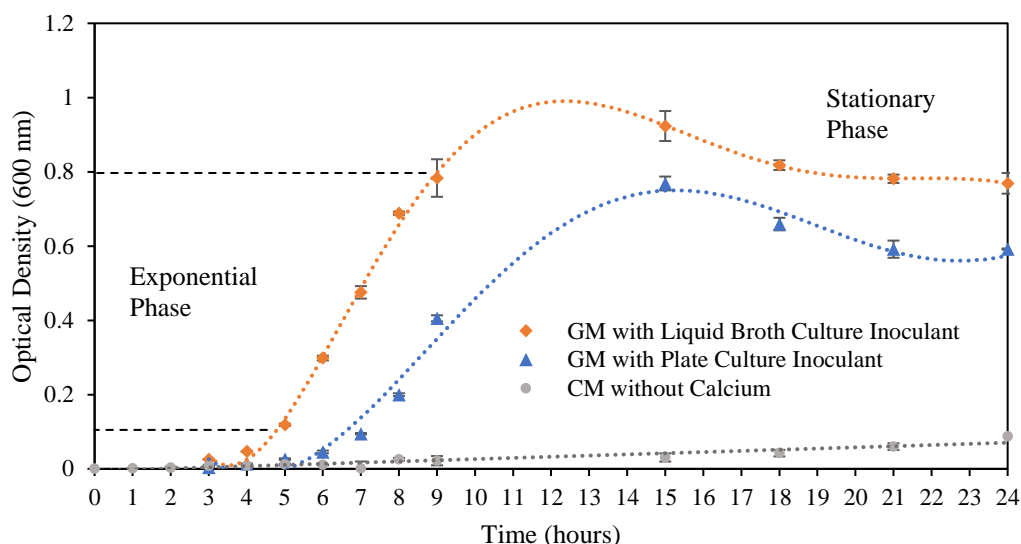


Figure 5-6. Growth curves for *S. ureae* in growth medium (GM) and cementation medium without a calcium source (CM) at 30 °C, 150 rpm. Error bars show standard errors of means of triplicates.

5.2.5.2 *Sporosarcina pasteurii*

Growth curves were produced for *S. pasteurii* using a similar procedure, as shown in Figure 5-7, with 100 μ L of overnight liquid broth culture as the inoculant. The flasks of inoculated growth medium were incubated at 30 °C, 150 rpm initially, and later at 23 °C, 150 rpm. Column studies utilising *S. pasteurii* for MICP were undertaken in 30 °C and 23 °C environments. To produce the *S. pasteurii* growth curves, readings up to 11 h were from the first set of triplicates with the readings thereafter from the second set of triplicate flasks of bacteria grown overnight before samples were taken. As the spectrophotometer readings neared 1.0 (and above) the 1.0 mL sample was diluted in 1.0 mL of tap water and the optical density of this measured and doubled to improve accuracy of readings. The exponential growth phase, as shown in Figure 5-7, was found to occur within a similar time period to that observed for *S. ureae* above. There was observed to be some variation between readings across the triplicates towards the late exponential stage of growth. Tap water was used for the growth medium, for comparison with *S. ureae* growth. Later studies with *S. pasteurii* use deionised water to prepare the growth medium since a grey film was observed on the surface of the bacteria when using tap water and this necessitated washing of the cells with PBS.

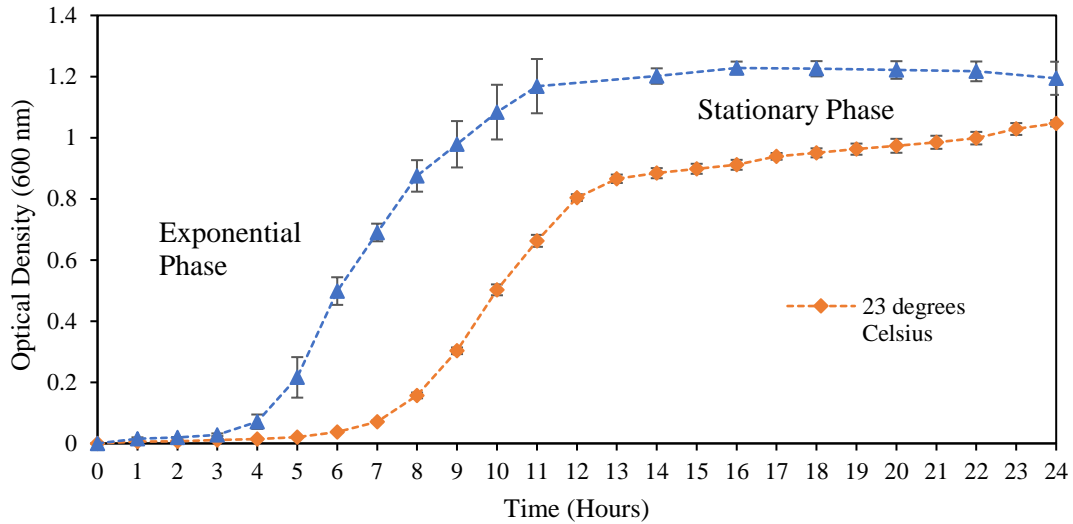


Figure 5-7. Curves showing growth of *S. pasteurii* at 23 °C and 30 °C, 150 rpm. Error bars show standard errors of means of triplicates.

5.3 Testing of Additives (Carrier Materials)

The use of carrier materials to store and supply cementation medium is a new concept in respect of studies on self-healing in biocemented materials. Studies on self-healing in cementitious materials have otherwise utilised a variety of porous materials to immobilise bacteria and/or cementation medium. Within cementitious materials, immobilisation has been used to protect bacterial cells/ spores from the mechanical forces exerted during the mixing stage of concrete or mortar production and from the highly alkaline environment within cementitious materials. These carrier materials may also be used as internal nutrient reservoirs (Bundur et al. 2017). Reference to nutrients within this context refers to the nutrients and precursor chemicals, otherwise known as the cementation medium, required for the MICP process.

Immobilisation has been reported to be an efficient approach for bacteria-based self-healing in cementitious materials (Zhang et al. 2017b). The various carrier materials utilised in cementitious materials incorporating MICP based healing systems, along with crack widths healed through MICP where reported, are summarised in Table 5-1. For many of these studies the bacteria, in the form of vegetative cells or spores, has been immobilised along with the required nutrients and precursor chemicals. However, it has been demonstrated that it is not necessary to immobilise bacteria along with the cementation medium to enable self-healing. Khaliq and Ehsan (2015) demonstrated that comparable amounts of self-healing can be achieved by immobilising the bacteria only. This particular study utilised graphite nanoplatelets to immobilise bacteria, with nutrients and precursor chemicals added directly to the concrete mix. Bundur et al. (2017) used expanded shale aggregates to immobilise nutrient medium only.

Table 5-1. Materials utilised for immobilisation in cementitious materials incorporating MICP.

Carrier material	Immobilised constituents	Crack width healed (mm) (Curing duration)	Reference
Graphite nanoplatelets	<i>Bacillus subtilis</i> bacteria	0.81 (28 days)	(Khaliq and Ehsan 2015)
Expanded Perlite	<i>Bacillus cohnii</i> bacterial spores and nutrients	0.79 (28 days)	(Zhang et al. 2017b)
Ceramsite	<i>Bacillus mucilaginous</i> bacteria and nutrients	0.50 (28 days)	(Chen and Qian 2016)
Expanded clay particles	Calcium lactate and bacterial spores from alkaline lake soil, with 98.7% homology to <i>Bacillus alkalinitrilicus</i>	0.46 (100 days)	(Wiktor and Jonkers 2011)
Diatomaceous earth	<i>Bacillus sphaericus</i> bacteria	0.17 (28 days)	(Wang et al. 2012)
Zeolite	<i>Sporosarcina ureae</i> and <i>Sporosarcina pasteurii</i> bacteria	0.10 (6 months)	(Bhaskar et al. 2017)
Lightweight aggregate	<i>Bacillus cohnii</i> bacteria and nutrients	–	(Sierra-Beltran et al. 2014)
Expanded shale aggregates	Nutrient medium	–	(Bundur et al. 2017)

Since encapsulation and immobilisation technologies have only been used in cementitious materials to date their behaviour within sand or soil systems is unknown. Laboratory studies were undertaken to test the effectiveness of selected carrier materials for the immobilisation and release of cementation medium. Subsequently, a preliminary study was undertaken whereby carriers loaded with cementation medium were incorporated into biocement.

5.3.1 Materials and Methods

5.3.1.1 Carrier Materials

Expanded perlite, diatomaceous earth, jute and coir natural fibres were initially selected for this study. Diatomaceous earth (Celite S) and expanded perlite (Harborlite 800), abbreviated to DE and EP respectively, were selected from carriers reported to have been used in cementitious materials incorporating MICP based self-healing systems. Availability, cost, and particle size of materials were

taken into consideration when selecting the carrier materials. Properties of these carrier materials are listed in Table 5-2. Specific gravity was determined using the small pycnometer method, in accordance with BS 1377-2 (British Standards Institution 1996). Loss on ignition values of the DE and EP are as per specifications provided by Sigma Aldrich (2017) for Celite S and Imerys Performance Minerals (2018) for Harborlite 800.

Table 5-2. Properties of diatomaceous earth (Celite S) and expanded perlite (Harborlite 800) powders.

Carrier	Specific Gravity	Loss on Ignition (%)
Diatomaceous Earth (DE)	2.01	3.2-10.0
Expanded Perlite (EP)	1.99	1.1

In addition to the absorbent powdered materials, natural absorbent fibres were tested for their suitability as carrier materials. The chemical constituents of coir and jute fibres, as reported by Banerjee (2012) and Rowell and Stout (1998) respectively, are given in Chapter Four, Table 4-6. Jute fibres were observed to be of a more consistent thickness compared to coir. Coir is reported to break down more slowly (Schafer 2011), this may not be an issue within a biocement however.

Prior to use, the fibres were washed thoroughly using a sieve and deionised water. All carrier materials used in this study were sterilised by autoclaving at 121 °C for 15 min, then oven dried at 90 °C. Drying at 105 °C for 24 h was observed to result in a significant darkening of the coir fibres. Lignocellulosic fibres, which include coir and jute, thermally degrade through dehydration, depolymerization, and oxidation when heated (Ezekiel et al. 2011). The extent of delignification has also been reported to be dependent on the duration of heating (Ezekiel et al. 2011). Lignin has been reported to undergo thermal degradation at temperatures as low as 100 °C (Yang et al. 2007). For this reason, the oven temperature for drying was reduced to 90 °C following a preliminary study, for all materials for consistency, and to prevent the decomposition of sodium bicarbonate which is reported to occur at temperatures above 100 °C (Otsubo and Yamaguchi 1961).

5.3.1.2 Production of Cementation Medium

The cementation medium produced for biocementation with *S. ureae*, as per Table 5-3, to provide the necessary nutrients and precursor chemicals for the MICP process, was adopted from Stocks-Fischer et al. (1999). To increase the efficiency of the immobilisation process, a concentrated cementation medium was produced using the chemical components and quantities listed in Table 5-3, in deionised water. This concentrated medium was produced in 300 mL quantities. Oxoid CM0001 Nutrient broth was dissolved in 25 mL of deionised water, adjusted to pH 6.0 using concentrated HCl, and sterilised by autoclaving at 121 °C for 15 min. The remaining chemicals, excluding calcium chloride dihydrate, were thoroughly mixed in 275 mL deionised water, using a magnetic stirrer. This solution was then adjusted

to pH 6.0 using concentrated HCl, to prevent the calcium precipitating out of the calcium chloride dihydrate. Calcium chloride dihydrate was then added as a powder. This solution was then syringe filtered into the Oxoid CM0001 Nutrient broth solution, using a 0.2 µm syringe filter.

Table 5-3. Precursor chemicals and nutrients used in the cementation media, and sterilisation methods.

Medium component	Standard cementation medium CM1u (g/L)	Concentrated cementation medium CM2u (g/L)	Sterilisation method
Urea (NH ₂ (CO)NH ₂)	20	133.33	Syringe filtered
Ammonium chloride (NH ₄ Cl)	10	66.67	Syringe filtered
Calcium chloride dihydrate (CaCl ₂ ·2H ₂ O)	7.35	49	Syringe filtered
Sodium bicarbonate (NaHCO ₃)	2.12	14.13	Syringe filtered
Oxoid CM0001 nutrient broth	3	20	Autoclaved

5.3.1.3 Microorganism, Growth Conditions and Cell Harvesting

Sporosarcina ureae was selected for this study due to its spore forming ability, as verified and reported in Section 5.1, and due to the slow rate of MICP when using this bacterium (compared to *S. pasteurii*) which enabled the leaching rate from carriers to be observed. *Sporosarcina ureae* was obtained from the National Collection of Industrial and Marine Bacteria, UK (NCIMB 9251, ACDP Group 1) as a freeze-dried culture. Cultures of *S. ureae* were grown on Luria- Bertani (LB) agar medium amended with urea. This medium comprised per litre of deionised water; 10 g tryptone, 5 g yeast extract, 10 g sodium chloride, 15 g agar powder and 20 g urea. The LB agar medium without urea was sterilised by autoclaving at 121 °C for 15 min. A urea solution was then added to this medium using a 0.2 µm syringe filter. The medium was then allowed to cool to 55 °C before pouring onto 90 mm x 15 mm petri dishes, to minimise condensation on plates. After incubation at 30 °C for 48 h, pure single colonies from the plates were used to inoculate a liquid broth medium consisting of 5 g peptone, 3 g meat extract and 20 g urea per litre of tap water. This liquid broth medium without urea was autoclaved at 121 °C for 15 min, to which a urea solution was added using a 0.2 µm syringe filter. Aseptic technique was used throughout. Multiples of 50 mL liquid broth cultures were produced as required for experiments, in 250 mL Erlenmeyer flasks incubated at 30 °C, 150 rpm for approximately 19 h to produce cultures with an optical density at a wavelength of 600 nm (OD₆₀₀) of 0.9-1.2 (10⁷-10⁸ cells/mL), as measured using a spectrophotometer (Hitachi U-1900 UV-Vis).

5.3.1.4 *Batch Test 1: Immobilisation Capacity of Carrier Materials*

To enable self-healing, the carrier material would need to be able to store a sufficient amount of cementation medium and release this slowly over time, so as to retain this during biocementation and release this when required.

A batch test was undertaken to explore the capacity of the carrier materials to immobilise the nutrients and precursor chemicals (cementation medium) required for the SH-MICP process via absorption/adsorption, and to quantify this in respect of carrier material mass. These tests provided an indication of the capacity of the carrier materials tested to immobilise the cementation medium, and enabled comparisons between these materials. These results would also assist with quantifying the mass of carrier materials required in later column experiments.

The methodology for this test had been developed following initial testing of approaches and observed responses of materials. Soaking in cementation medium and then removing excess medium helped ensure the materials were saturated and that no excess medium was left in the test tubes. During the initial testing excess medium had been observed on the surface of fibres after drying, in particular coir. Coir fibres were also observed to darken following oven drying at 105 °C, no change was observed to other materials, however. Studies by Varma et al. (1986) Ezekiel et al. (2011) and Siakeng et al. (2018) suggest minimal effects of temperature on mechanical properties of coir fibre up to around 200 °C, with degradation occurring after due to depolymerisation. Fibres were heated for a short duration in these studies however, up to one hour. A similar study by Gassan et al. (2001) on jute, reported that temperatures up to 170 °C only slightly affect jute fibre properties, for studies of two hours duration, with significant effects at a higher temperature. The time of exposure to heat is reported to effect mechanical properties, as found by Ezekiel et al. (2011) when studying a range heating of durations from 10 to 30 min. Autoclaving was not likely to have had an effect on the fibres due to the short duration of heat exposure. Coir contains more lignin compared to jute fibres and lignin can start to decompose at around 100 °C. The temperature of oven drying for carrier materials was therefore reduced to 90 °C for the subsequent batch tests.

For the immobilisation capacity batch test, 50 mL polypropylene centrifuge tubes were filled with 1 g of carrier material, in sets of six for each carrier material type, to ensure accuracy of results and determine repeatability of methodology. The centrifuge tubes along with the lids, were weighed before adding the carrier materials, since the masses of these tubes and lids were found to vary. The fibres were only lightly compacted into the tubes, to aid media flow around fibres. If fibres were compacted too much into the tubes this was found to impede immobilisation. Concentrated cementation medium was added to each tube, to fully immerse the carrier material. 10 mL of this medium was added to the powders and 25 mL to fibres, to ensure full emersion. The carrier samples were left to soak in the

cementation medium at room temperature (approximately 21°C) for 24 h, then centrifuged (3200 rcf, 30 min, Varifuge 3.0 Heraeus) to separate the solid carrier material and excess cementation medium, after which the waste medium was carefully poured from the tubes, leaving the carrier material and immobilised cementation medium remaining.

Following the initial draining of any medium not immobilised, the tubes containing the fibres were left inverted for two hours to remove excess medium, by which time the flow of this excess medium from the fibres had ceased. This waste medium was then drained, and the tube lids rinsed with deionised water to remove the medium which had collected in these. This process improved accuracy of the results by minimising the excess adsorption of the medium on the fibre surface, with little to no excess medium thereafter being observed on the inner surface of the polypropylene tubes after drying. This had a significant effect on the quantity of immobilised medium observed after drying for the coir in particular and resulted in more consistency in respect of mass of medium absorbed/ adsorbed by fibres, and repeatability was further improved.

Since there was still a small quantity of expanded perlite (EP) at the surface of the excess medium following centrifugation, the waste medium drained off was gravity filtered to determine the mass of this suspended EP, using Fisherbrand QL100 110 mm diameter filters and a funnel. Before use, the filter paper was washed with deionised water, oven dried and weighed and numbered. The dried filter paper was weighed and then soaked with deionised water, folded into quarters and placed into the funnel. The waste medium was drained through this. The retained solids were washed three times with deionised water, to remove any medium residue, by filling the filter cone and stirring as the water was drained through the filter. The filter papers were then dried and weighed, and the original mass of filters deducted to determine the mass of retained solids. It was determined through this method that the mass of suspended solids remaining in the waste medium drained from expanded perlite was between 4 mg and 9 mg and hence negligible following 30 min of centrifugation at 3200 rcf. This demonstrated the effectiveness of the centrifugation method of separation. Since perlite has a density which is less than that of water (Balam et al. 2017), some suspension is to be expected. The waste medium was observed to be clear for the other carrier materials.

The tubes containing the carriers were then oven dried at 90 °C, for up to two days, until the mass was constant. After weighing, to determine the mass of solid cementation medium immobilised, the process was repeated. For those carrier materials for which the overall mass had increased for all six samples, a third loading with cementation medium was undertaken.

These test procedures were later followed with hemp fibres, with samples tested in triplicate.

5.3.1.5 *Batch Test 2: Cementation Medium Release from Carrier Materials*

A preliminary test was first undertaken using samples from the immobilisation test, to determine the amount of water to be added to samples. Using the loaded carrier samples from Batch Test 1, the cementation release from the jute, expanded perlite and diatomaceous earth samples was investigated. At this stage it had been determined that the coir would not be an effective carrier, given its significantly lower capacity for absorption/ adsorption of the cementation medium, and as a result no further tests were undertaken with this carrier. The significant variability of the diameters of the coir fibres also likely affected repeatability of tests using this material.

5.3.1.5.1 Batch Test 2-1 (Preliminary)

Cementation medium release into deionised water was initially quantified after 1, 2, 4, 7 and 24 h. Quantities of deionised water and cementation medium (CM1u) added to the tubes of CM loaded carriers were dependent upon the mass of immobilised medium within these and were initially calculated as ten times the mass of immobilised cementation medium, to enable comparisons.

After addition of the deionised water, the tubes were left at room temperature for 1, 2, 4, 7 and 24 h. After these periods of time the tubes were centrifuged for 30 min at 3200 rcf and the excess solution drained. Remaining excess solution was lightly shaken from the jute samples, for the leaching tests these samples were not left inverted as the immobilised medium could have continued to leach out during that time. An incubator was used to maintain the temperature at 21 °C, since temperature may have an effect on the release of the cementation medium constituents. The pH of the solution drained from each sample was tested before being discarded. After draining, the samples were dried and weighed to determine the mass of immobilised cementation medium released.

5.3.1.5.2 Batch Test 2-2

Following the preliminary test, the cementation medium release test was repeated three times over a range of time periods. For this test, time periods were more evenly spread out, loaded carrier samples were soaked in deionised water for 1, 3, 6 and 24 h periods. Results from Batch Test 2-1 had shown a change in trend at the 24 h stage, this was likely due to the limiting effect on chemical release of the concentration of chemicals in the liquid surrounding the carriers. For this batch test therefore 0.5 g samples of carrier material were instead used, as opposed to 1 g samples, and carriers were loaded just once. Immobilisation of a greater quantity of cementation medium would have resulted in a greater quantity of deionised water being required for this test and additional CM loading was deemed more likely to result in adsorption as opposed to absorption.

Carrier materials were added to 50 mL polypropylene centrifuge tubes in 0.5 g quantities in sets of four for each material, loaded once with cementation medium, dried, and the mass of immobilised medium

recorded. To increase efficiency of this single cementation medium loading, the carriers were vortexed gently using a vortex mixer following the medium addition, which resulted in some increase in mass of immobilised cementation medium. Deionised water was then added to each tube. The quantity of solvent (deionised water) added was equal to 25 times the mass of dried cementation medium immobilised within each tube. The tubes were then sealed and left at room temperature (approximately 21 °C), with one tube from each set of four being drained after 1 h, the second after 3 h and the third and fourth after 6 and 24 h respectively. Tubes were then dried at 90 °C and weighed to quantify loss of cementation medium. These results gave an indication of potential release of cementation medium for self-healing MICP following water ingress into the biocement. This test was repeated three times. An additional test for a period of 50 h was later undertaken under the same conditions. This test was further repeated using hemp fibres for periods up to 24 h.

5.3.1.5.3 Batch Test 2-3

To further investigate the leaching behaviour from jute and hemp fibres, carrier samples were subjected to repeated soakings in deionised water and also cementation medium (CM1u) to test for leaching following one loading of concentrated cementation medium. Carrier samples consisting of 0.5 g of jute and hemp in two sets of six were added to 50 mL polypropylene tubes and loaded once with 15 mL of concentrated CM, following the procedure outlined above. To increase efficiency of this single loading, the tubes were vibrated with a vortex mixer for 10 sec after the cementation medium had been added to the tubes containing the fibres. Of the six sets of each loaded fibres prepared, 30 mL cementation medium (CM1u) was added to three tubes and deionised water to the remaining three tubes of each set. After 24 h at approximately 21 °C, each tube was centrifuged and drained and dried at 50 °C. Tubes had been weighed following loading and the mass loss could therefore be determined. This process was repeated after a further 24 h period. The cementation medium (CM1u) into which leaching of immobilised cementation medium was tested, was the same as that used to treat columns inoculated with *S. ureae*, and thus was expected to give an indication of potential leaching of immobilised CM during the biocementation process.

The above test was also undertaken for 0.5 g samples of EP and DE carriers loaded once with concentrated cementation medium (CM2u) and using cementation medium (CM1u) and a cementation medium prepared with twice the concentration of CM1u as the solvent solutions. Different concentrations of the cementation medium had been tested as solvents since the DE and EP had at this stage released almost all of the immobilised CM into deionised water when tested over a 50 h period.

5.3.1.5.4 Batch Test 2-4

A later test was undertaken using an ion chromatograph to test the concentrations of sodium, ammonium and calcium ions in leachate from the jute fibres over a 48 h period. This gave more insight into leaching

behaviour of immobilised reagents from the natural fibres. 1 g quantities of jute fibres were prepared in triplicate in 50 ml centrifuge tubes, to which a concentrated cementation medium was added to fully submerge the fibres, using the concentrated cementation medium as described in Chapter Seven. After 24 h of soaking at 23 °C in a cupboard the tubes were centrifuged, and excess medium drained followed by drying at 50 °C. The mass of dried CM was ascertained and 35 mL water added, this being equal to the quantity of liquid used during column assembly. After 24 h this water was drained, filtered using a 0.2 µm filter, diluted to a 1:500 dilution and tested using the ion chromatograph. Additional water was added and the testing repeated after a further 24 h.

5.3.1.6 Batch Test 3: Microbiologically Induced CaCO₃ Precipitation in Aqueous Solutions

At this stage it was unknown whether the carrier materials had absorbed/ absorbed or released the constituent chemicals of the cementation medium to the same extent. This test was undertaken to establish whether sufficient quantities of each component of the cementation medium had been immobilised by the carrier materials to enable MICP, and to make comparisons between the carrier materials.

For each carrier material, six sterile 50 mL polypropylene centrifuge tubes were filled with 1 g of carrier material and loaded once with cementation medium and dried. 20 mL of autoclave sterilised deionised water was added to each tube. The aim was for the solution drained from these tubes to have a similar concentration of nutrients and precursor chemicals as the standard cementation medium. The standard cementation medium utilised with *S. ureae* contained 4.25 % by mass of chemicals. At this stage it was known from cementation medium release tests that the fibres would release approximately 51 % of the nutrients over 24 h.

The tubes were transferred to a static incubator set to 21 °C for 24 h and then centrifuged at 3200 rcf for 30 min to separate the solid carriers and liquid. The liquid was then drained from the tubes and syringe filtered after measuring the pH, to remove any traces of carrier materials. Presence of carrier material in this liquid would affect the MICP process by providing additional nucleation surfaces. Cementation medium (CM1u) was used in the control tubes. Before these solutions were inoculated with *S. ureae*, the drained tubes containing the carrier materials were dried and weighed to determine mass of immobilised cementation medium remaining in the carriers, to enable the concentrations of cementation medium in the drained liquid from each tube to be determined. Samples were dried for 24 h at 90 °C to determine solid CM content. Based on the lowest concentration measured, a small amount of additional deionised water was then added to the tubes containing cementation medium released from jute and the standard cementation medium (CM1u), to ensure that each set of six tubes contained solutions with an average cementation medium concentration of 3.6 % to enable comparisons.

5.3.1.7 Batch Test 4: Cementation of Sand Through Microbially Induced CaCO_3 Precipitation

An industrial kiln dried fine silica sand was selected for this study. The specific gravity of this sand was measured using the small pycnometer method, in accordance with BS 1377-2:1990 (British Standards Institution 1996). A 100 mL pycnometer was used. The particle size distribution of the sand was determined using the dry sieving method, using a mechanical sieve shaker, in accordance with BS 1377-2:1990.

The sand was biocemented using *Sporosarcina ureae*. To harvest the vegetative *S. ureae* cells required for the biocement production, six 50 mL polypropylene centrifuge tubes were each filled with 19 mL of liquid broth culture, this quantity equating to the estimated pore space to be filled within the sand in each 50 mL tube. The approximate pore volume had been established via the wet pluviation technique using deionised water and a vortex mixer to vibrate and densify the saturated sand in a 50 mL centrifuge tube, which also gave an estimate of the mass of sand required. Tubes containing the liquid broth were centrifuged at 3200 rcf for 20 min. The supernatant was then drained and replaced with 19 mL PBS, followed by centrifugation at 3200 RCF for a further 20 min to wash any remaining metabolic waste and metabolism by-products from the cells. This washing was repeated twice. After draining the PBS, this was replaced with 19 mL of cementation medium.

Using a funnel secured 5 cm above the tube, tubes containing the bacteria and cementation medium were filled in triplicates, with sand only and then a premixed sand and loaded EP mixture. The EP had been mixed with the sand using a pestle and mortar. Once the tubes were half full, and again after the tubes were almost filled, these were vibrated to densify the sand. The lids were placed on the tubes which were then inverted in an incubator at 30 °C. After 24 h, a 1 mm hole was pierced in the base of the tubes using a sterilised bradawl, through which the effluent was extracted using a vacuum, as per Figure 5-8, utilising a flask within which the centrifuge tube was held firmly within the neck.

The effluent was syringe filtered for ICP-OES analysis of calcium ion content. This displaced effluent was replaced with cementation medium via surface percolation. Excess cementation medium was drawn through the sand using a vacuum, while continuing to pour cementation medium into the top of the tube, so that approximately one and a half times the pore volume was used to flush through any remaining effluent.

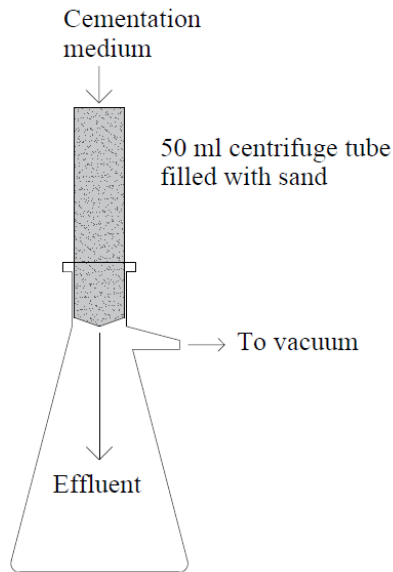


Figure 5-8. Diagram showing the vacuum assisted treatment process for the mini sand columns. The 50 ml centrifuge tube containing the sand is shown placed firmly into the neck of the conical filter flask, with the conical flask connected to a vacuum which draws the cementation medium down through the column while the extracted effluent collects in the flask.

This process was repeated for all tubes, with the holes then being covered after and tubes returned to the incubator inverted. The extraction of the effluent and addition of cementation medium was repeated on weekdays over a fourteen-day period, with the resulting biocement shown in Figure 5-9.

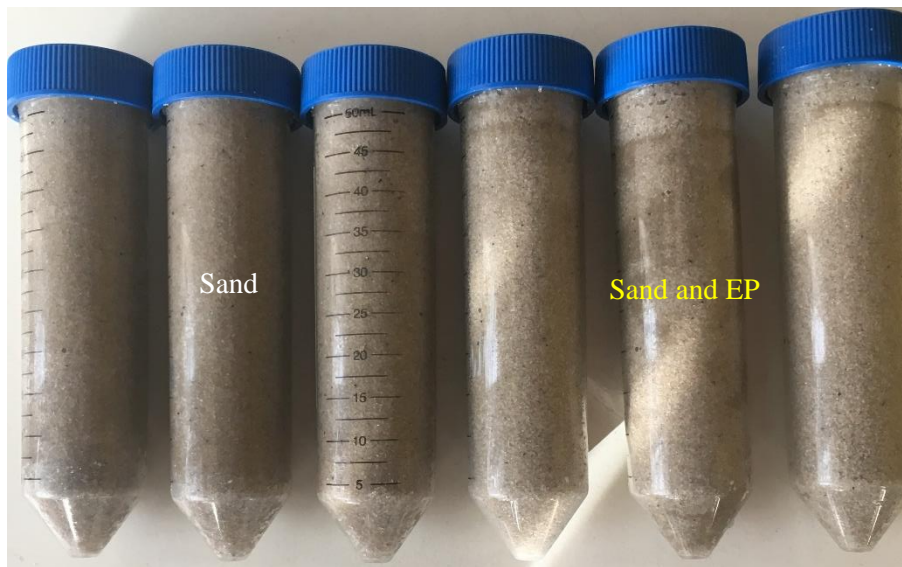


Figure 5-9. 50 mL polypropylene centrifuge tubes containing the mini columns of biocemented sand and biocemented sand and expanded perlite mixture in triplicates.

5.3.1.8 Testing of Spore Viability

The plate counting method was used to determine the number of viable bacteria in biocement samples, and as an indicator of the presence of spores. To test for the presence of spores within the biocement produced at the preliminary stage, the mini columns produced in the 50 mL centrifuge tubes were dried at 30 °C for three weeks, and then left sealed at room temperature for a further three weeks. Samples were taken from a tube that had been prepared using EP and a control tube, to initially test this technique. After this period of time, it was assumed that any remaining nutrients will have been depleted and hence it is expected that only spores would remain.

1 g samples were taken from the dried biocement, at approximately 2 cm from the top of the sample. The sample was added to a test tube and made up to 10 mL with autoclave sterilised PBS. The sample was shaken well to suspend the spores in the PBS. Four test tubes containing 9 mL of autoclaved PBS were prepared for the dilutions. Agar plates were prepared, using LB agar amended with 20 g/L urea, with the urea solution added using a syringe filter after autoclave sterilisation of the LB agar solution.

Dilutions were prepared as per the methodology outlined in Chapter Four. 100 µL samples were taken from the prepared dilutions and pipetted onto the agar plates. This sample was then spread across the plate using a plate spreader. The plates were sealed and left for a few minutes for the sample to soak into the agar before inverting the plates. These plates were incubated at 30 °C for 48 h. After this period individual colonies of *S. ureae* were clearly visible. These colonies were assumed to have grown from individual germinated spores. Colonies were counted on plates containing thirty to three hundred colonies.

5.3.2 Results and Discussion

5.3.2.1 Cementation Medium Storage: Immobilisation Capacity of Carrier Materials

The cementation medium immobilised following three loadings, for the carrier materials tested, is displayed in Figure 5-10. Coir was loaded twice only since following the second loading there had been some mass reduction in four of the six tubes, this can be attributed to the dissolution of immobilised cementation medium into the surrounding liquid cementation medium. This effect, albeit to less of an extent, was also noticed after the second loading of expanded perlite. It was evident that the immobilisation capacity had been reached after the first loading of coir fibres, and after the second loading of EP. The capacity of coir to immobilise cementation medium was relatively low and the variable fibre thicknesses (as could be seen without a microscope) likely contributed to inconsistencies in results, this carrier is therefore not used in later tests.

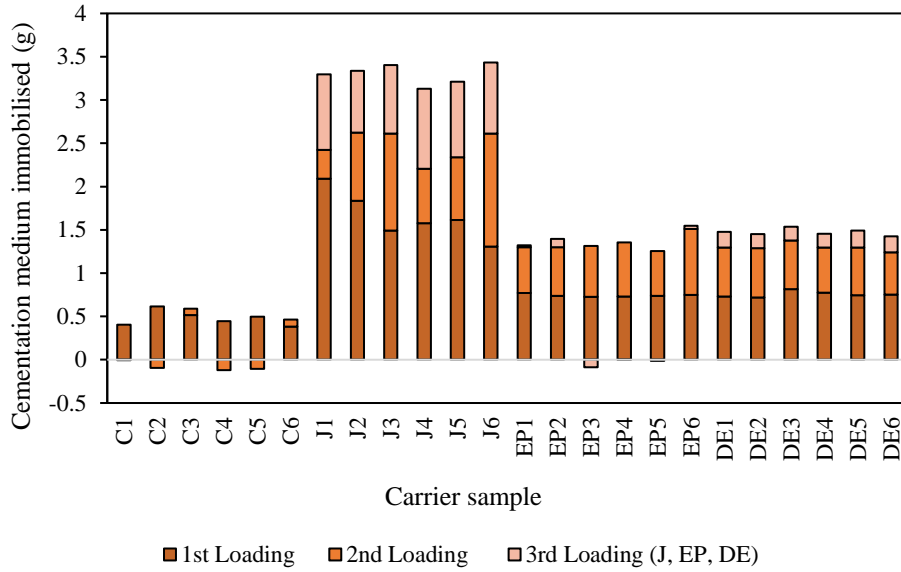


Figure 5-10. Quantities of dried cementation medium immobilised by one-gram samples of coir (C), jute (J), expanded perlite (EP) and diatomaceous earth (DE), following repeated loadings with concentrated cementation medium.

The mass of immobilised cementation medium was also compared across the carriers per cubic centimetre of carrier material, as shown in Figure 5-11.

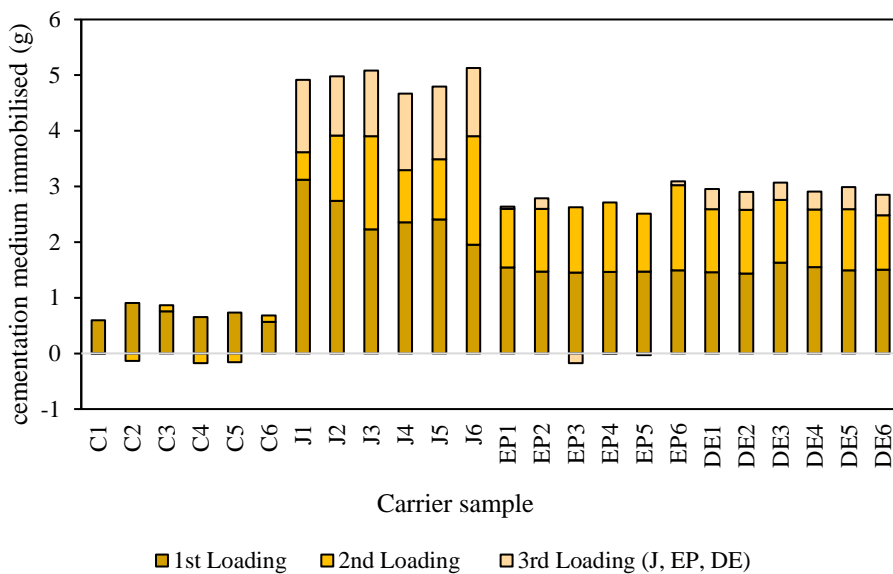


Figure 5-11. Quantities of dried cementation medium immobilised per cubic centimetre of coir (C), jute (J), expanded perlite (EP) and diatomaceous earth (DE), following repeated loadings with concentrated cementation medium.

Immobilised cementation medium release was investigated for the jute, EP and DE carriers initially. The 1 g carrier samples were representative of quantities to be used within the individual sand columns in subsequent studies.

This study was later repeated with hemp, to replace the coir fibres in this study which had been deemed unsuitable. The results for hemp, as shown in Figure 5-12, verified the potential suitability of hemp as an immobilising material.

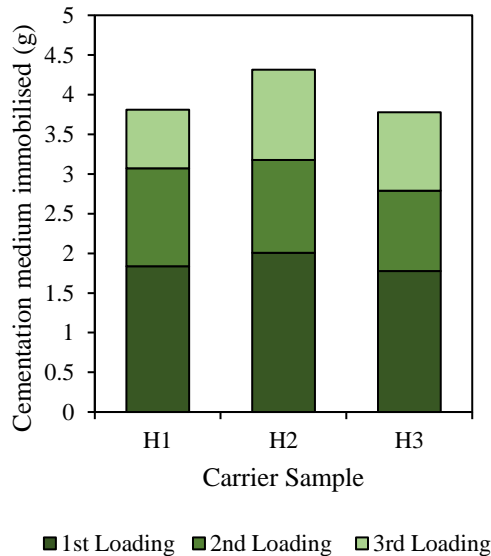


Figure 5-12. Cementation medium immobilised by 1 g samples of hemp following repeated loadings.

5.3.2.2 Cementation Medium Release: Preliminary Test

For the preliminary test, 10 mL of deionised water per gram of immobilised (dried) cementation medium was added to each tube containing the carrier and immobilised CM, to enable comparison. Results showed a constant release of cementation medium from DE over the first 7 h, as shown in Figure 5-13. The results for DE1 to DE4 follow a linear pattern, point DE5 would be expected to be higher based on this trend. These results were indicative of the quantity of solvent used being a limiting factor and inhibiting the leaching of CM. During this same period, results are more variable for Jute and EP. The immobilised CM appears to be released more readily from jute initially, with all data points being in the 47 % to 57 % immobilised CM loss range. This initial quick release may be beneficial to the self-healing process.

More testing was therefore required to better understand these results. Its possible there may be some reabsorption of CM over time or otherwise a relatively fast release of chemicals into the surrounding liquid until this reaches a certain concentration. Cementation medium release from EP over time was observed to be the slowest overall and with the exception of the EP3 sample results are close to those for DE. The higher immobilisation capacity of the DE, in addition to the consistency of CM release over time, makes this a favourable option with regards to the powdered carriers. The limiting effect of the quantity of solvent used is evident for this test and the quantity of solvent was therefore increased for the following test.

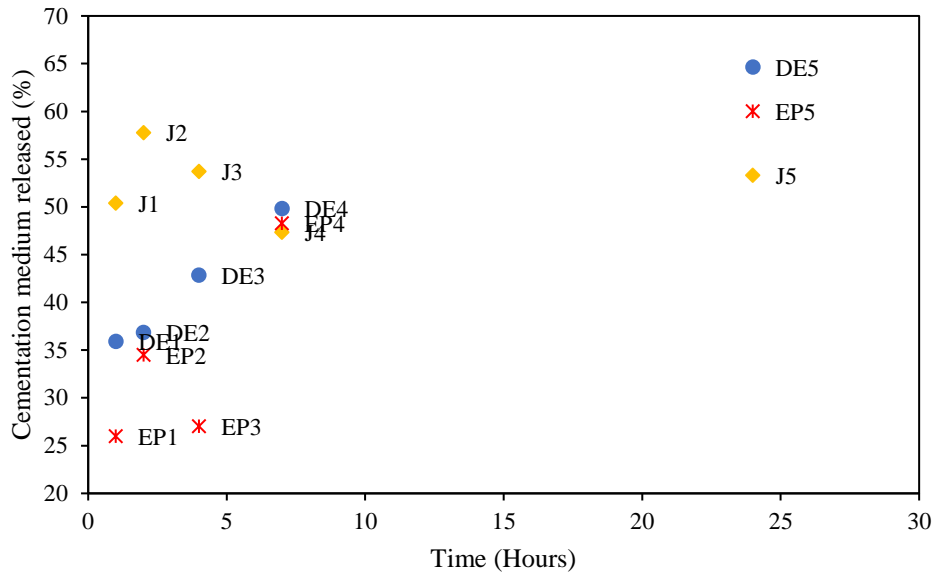


Figure 5-13. Release of immobilised cementation medium into deionised water over a 24 h period from jute, expanded perlite and diatomaceous earth, using a quantity of water equal to ten times the mass of the immobilised cementation medium.

Results obtained for cementation medium release from jute suggest cementation medium constituents are released until the surrounding solution contains up to almost 5.5 % nutrients, and that this can happen within one hour. These results also indicate that there is potentially some re-adsorption following the initial release. Since the standard medium (CM1u) contains 4.25 % (w/w) cementation medium constituents this suggested some leaching out of nutrients may occur during cementation for all carriers. At the 24 h point, the liquid surrounding the EP and DE contained 5.7 % and 6.07 % (w/w) cementation medium constituents respectively.

5.3.2.3 Cementation Medium Release: Batch Tests

Percentages of immobilised cementation medium released from the carrier materials over a period of up to 50 h are shown in Figure 5-14. The rate of release of cementation medium from jute within the first 4 h is the fastest of the carriers tested. Following this initial fast release from jute, equilibrium appears to have been reached with the surrounding solution. This quick release may be beneficial to the self-healing process, in addition to the potential to retain cementation medium for later release. For the first 9.5 h cementation medium release is the slowest from EP. Figure 5-14 shows the R^2 values of the fitted regression curves, these values being close to 1 for cementation medium release from EP and DE. Results for EP and DE show similar trends, with regression lines converging at approximately 30 h. The rate of cementation medium release from DE then slows slightly compared to EP after 34 h. The lower R^2 value of 0.65 for cementation medium release from jute may be attributed to the slight variations in length and thickness of the individual fibres within samples, and therefore variations in

surface area of fibres. More testing is required to better understand the behaviour of the jute fibres in respect of the release of immobilised chemicals.

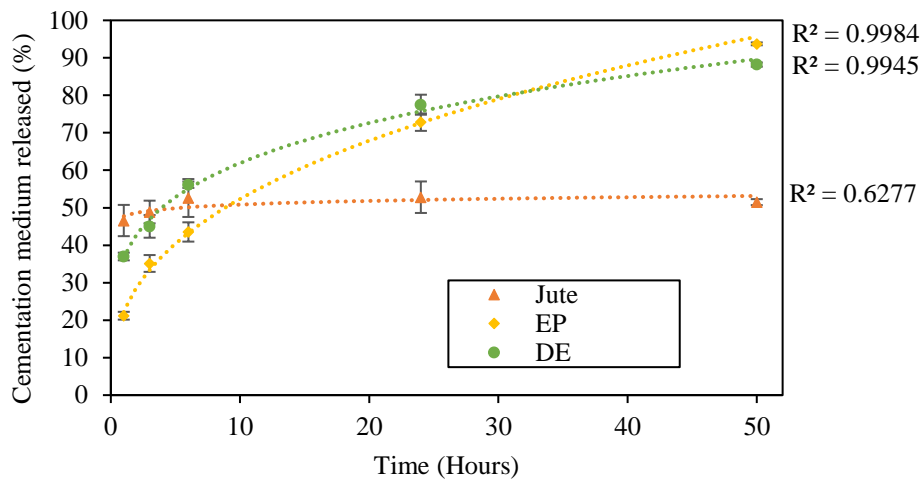


Figure 5-14. Percentage of immobilised cementation medium released from carrier materials into deionised water over a fifty-hour period, at 21 °C, with error bars showing standard errors of the means for the triplicates.

Figure 5-14 suggests that the powdered carriers, EP and DE, would have limited effect as immobilising materials in biocement since they may release their stored contents too quickly and thus stores will be depleted during the process of biocementation. This was further tested within biocement following the testing within aqueous media, with results given in Chapter Five, Section 5.2.5. The pH of the solution surrounding the fibres was measured after this had been drained, with results shown in Figure 5-15.

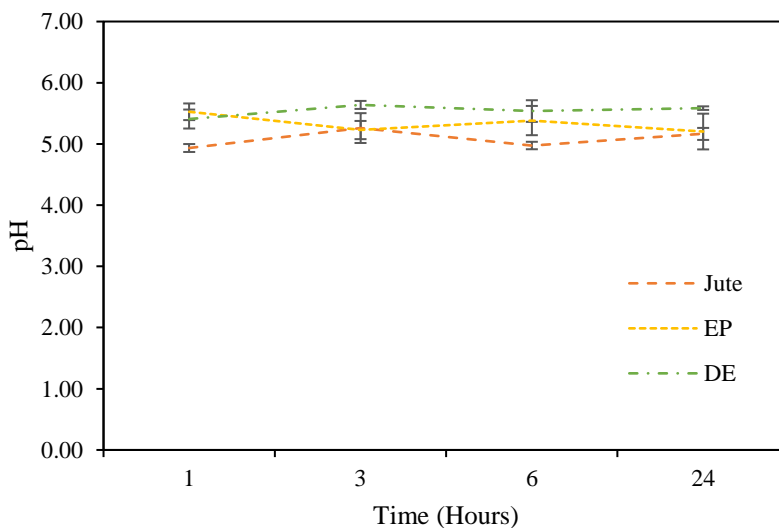


Figure 5-15. pH of solutions containing cementation medium leached from the carrier materials following soaking of the loaded carrier materials in deionised water for one-, three-, six- and twenty-four-hour periods at 21 °C, with error bars showing standard errors of the means for the triplicates.

These pH levels are fairly constant, which based on these results alone suggests there had been little variation regarding the constituent chemicals released. These solutions are more acidic than the initial pH 7.3 of the deionised water. This drop in pH is possibly due to leaching of the immobilised ammonium chloride.

The immobilised cementation medium release test was later repeated with hemp over 24 h, as shown in Figure 5-16. This period of time was of particular interest since a 24 h retention time was used in the subsequent column studies. These results suggest a more linear pattern of release from hemp.

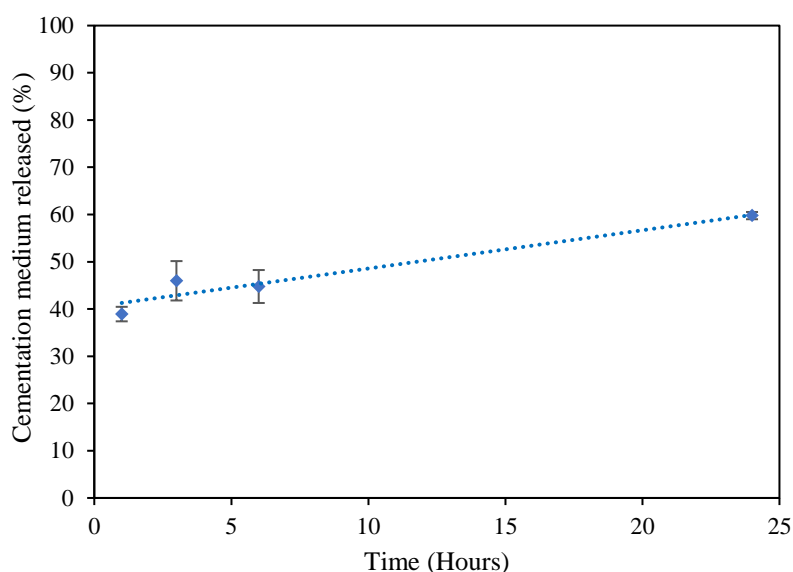


Figure 5-16. Percentage of immobilised cementation medium released from hemp into deionised water over a twenty-four-hour period, at 21 °C, with error bars showing standard errors of the means for the triplicates.

Leaching behaviour of fibres was further explored by subjecting the fibres to repeated soakings, since the fibres appeared to release just half of the cementation medium immobilised when left soaking in the same solvent for up to 50 h, compared to the powders which had released most of the immobilised cementation medium within this period of time. The samples prepared within the tubes containing 0.5 g fibres and immobilised CM were as per Table 5-4. The release of immobilised cementation medium into the standard medium (CM1) was also explored at this stage.

Table 5-4. Samples prepared for leaching tests.

Sample ID	Fibre type	CM Immobilised	Solvent added
H1	Hemp	1.833	CM
H2	Hemp	1.913	CM
H3	Hemp	2.071	CM
H4	Hemp	1.743	DI water
H5	Hemp	1.839	DI water
H6	Hemp	1.755	DI water
J1	Jute	2.633	CM
J2	Jute	2.497	CM
J3	Jute	2.557	CM
J4	Jute	2.672	DI water
J5	Jute	2.788	DI water
J6	Jute	2.813	DI water

The immobilised CM released from fibres over the two periods of soaking was as shown in Figure 5-17. These results verified that the fibres can facilitate multiple releases of immobilised cementation medium and that not all cementation medium was released from fibres in the prior test. These results also show that hemp appears to release the immobilised cementation medium more readily than jute and that jute therefore may be better able to retain the immobilised cementation medium over multiple biocementation treatments.

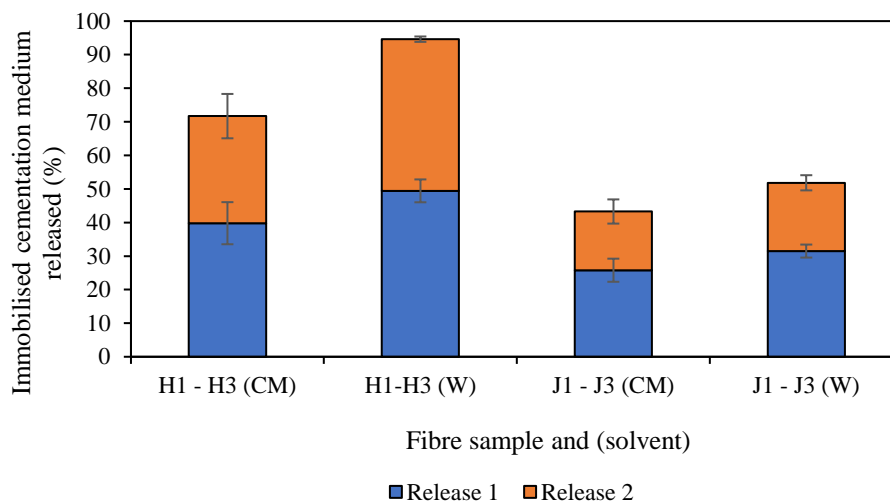


Figure 5-17. Percentages of immobilised cementation medium released from hemp and jute fibres into a solution containing cementation medium (CM, as used to treat columns in Chapter Six) and into deionised water (W) following an initial 24 h period of soaking (Release 1) and a subsequent 24 h period of soaking after the solutions surrounding the fibres are drained and replaced (Release 2). Error bars show standard errors of the means for the triplicates.

Release of immobilised cementation medium from the powdered carrier materials EP and DE was tested using the standard cementation medium (CM1u) and also a double concentrated medium based on CM1u as solvents. Doubling the concentration of the medium had little effect as can be seen in Figure 5-18, and still resulted in higher losses of immobilised reagents when compared to use of jute or hemp as immobilising carriers. Use of a more concentrated medium for cementation would not have been justified based on these results.

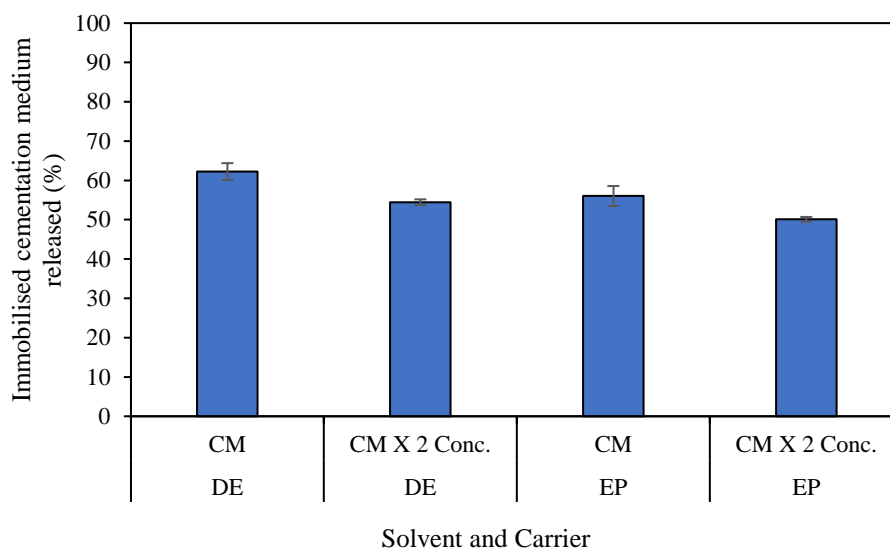


Figure 5-18. Immobilised cementation medium released from EP and DE into solutions of cementation media of varying concentration. Error bars show standard errors of the means for the triplicates.

At a later stage, following completion of column studies incorporating jute fibres, an aqueous study was undertaken over 48 h to test concentrations of reagents leached from jute fibres that had been treated with a concentrated cementation medium (as used in Chapter Seven), with results as shown in Figure 5-19. It is noted that the concentrations of ammonium ions measured by the ion chromatograph were not accurate and were higher than the actual concentration, the pattern of leaching is however as shown. These results suggest that calcium leaches out faster than ammonium from the fibres.

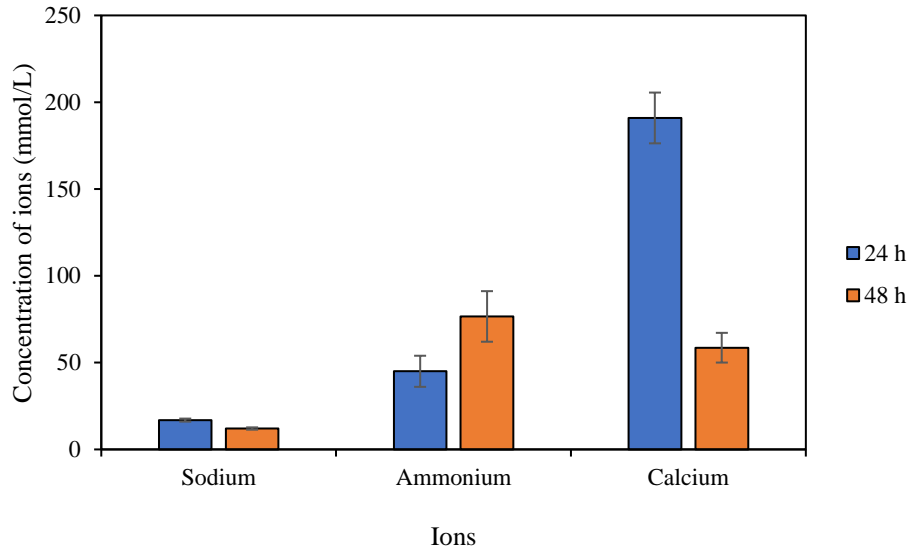


Figure 5-19. Concentrations of sodium, ammonium and calcium ions in solutions containing cementation medium constituents leached from loaded jute fibres after 24-h and 48-h of soaking samples of CM loaded jute fibres in deionised water, with liquid drained and fresh water added after the first 24-h soaking period. Error bars show standard errors of the means for the triplicates.

5.3.2.4 MICP in Aqueous Solutions

Following the addition of deionised water to the loaded carriers, and subsequent leaching of immobilised cementation medium, the solutions surrounding (and drained from) the expanded perlite and diatomaceous earth carriers were found to have an average reagent content of 0.36 %. Since the amount of immobilisation, and therefore leaching, had been higher for fibre samples, the solution drained from these samples, in addition to the control (CM1u) medium, needed to be diluted to a small extent for this test.

The *S. ureae* cultured for this particular experiment had a cell density corresponding to a spectrophotometer reading of 1.058 (OD₆₀₀). To ensure this reading was accurate, since it is over 1.0, the sample of liquid broth culture was diluted by adding 1 mL of culture to 1 mL of deionised water and the resulting spectrophotometer reading multiplied by two. The blank used was deionised water.

On the basis of calcium ion depletion in solutions, as shown in Figure 5-20, it can be deduced that all carriers tested immobilise and release the cementation medium constituents to the extent that MICP can be enabled. This is further supported by results shown in Figure 5-21, which show a pH increase following inoculation of solutions with *S. ureae*. This pH rise is indicative of MICP and is consistent across all samples. The solutions containing cementation medium constituents which had been immobilised by and released from jute have a noticeably lower pH prior to inoculation with *S. ureae*. The lower reduction in calcium ion concentration for these samples suggests that the jute fibres may not be immobilising or releasing the cementation medium constituents as effectively as EP or DE.

However, a slower release over time could help ensure that more nutrients and precursor chemicals are retained by the carrier material during biocementation. These results again suggest that more testing is required on jute prior to use within biocement. The calcium ion reduction in the solutions containing cementation medium which had been immobilised by DE is greater than that of the control solution. This result indicates that the use of DE as a carrier for cementation medium may have a beneficial effect on the MICP process.

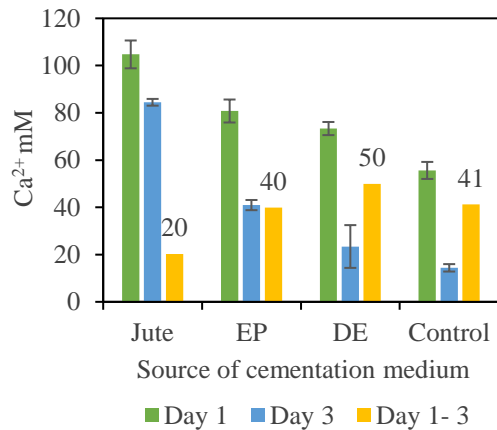


Figure 5-20. Calcium ion concentration of solutions containing cementation medium released from carriers and compared to standard medium as the control, measured one day and three days after inoculation of these solutions with *S. ureae*.

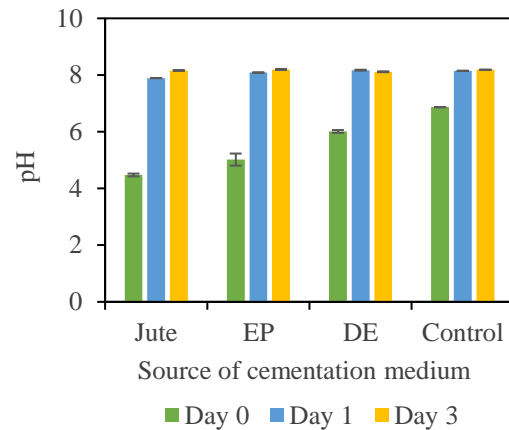


Figure 5-21. pH of solutions containing cementation medium released from carriers, compared to standard cementation medium, before (Day 0) and after inoculation of the solutions with *S. ureae*.

5.3.2.5 Effect on MICP and Leaching of Immobilised CM During Biocementation

5.3.2.5.1 Geotechnical Testing: Characterisation of Sand

The particle size distribution of the kiln-dried silica sand is shown in Figure 5-22. The region bounded by the orange vertical lines shows the percentage of particles which lie within the optimum particle size range for MICP as defined by Rebata-Landa (2007).

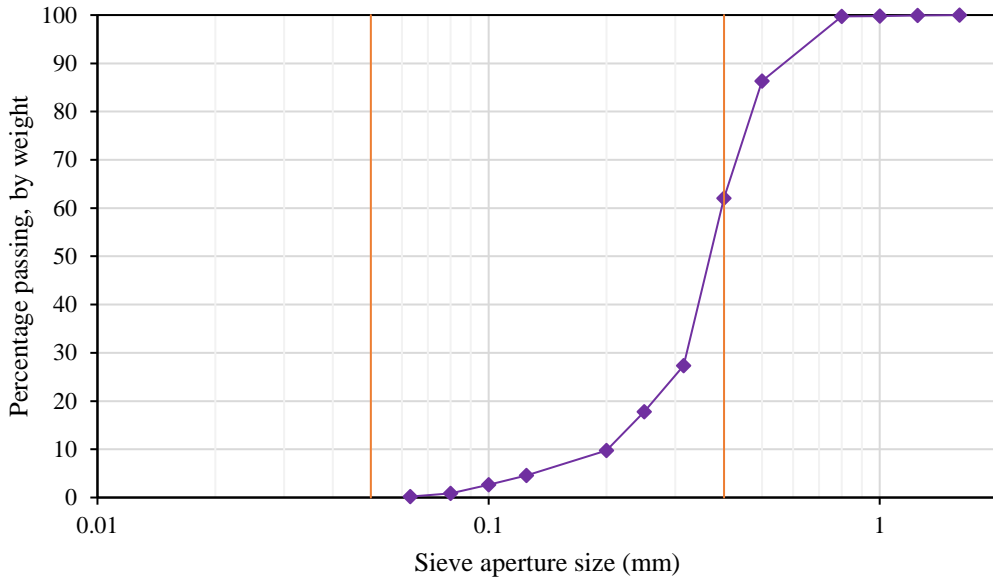


Figure 5-22. Particle size distribution curve for industrial kiln-dried silica sand.

In accordance with values read from the particle size distribution curve and calculated in Table 5-5, the sand is considered poorly graded since it has a uniformity coefficient (C_u) below six, despite the coefficient of gradation/ curvature (C_z) being between one and three. For this research, particle sizes in the range 50 μm to 400 μm were desirable. Based on the particle size distribution determined from a 200 g sample of sand, and mechanical sieving, approximately 62 % of the mass of this sand is within this desired range. Sand with a smaller D_{50} value was sourced for later studies. The sand was sieved prior to use to remove particles larger than 1 mm diameter and smaller than 63 μm . The pycnometer test defined the particle density (specific gravity) as 2.67 Mg/m^3 .

Table 5-5. Parameters of kiln-dried silica sand, as derived from the particle size distribution curve.

D_{10}	D_{30}	D_{50}	D_{60}	C_u	C_z
0.200	0.320	0.365	0.400	1.975	1.296

5.3.2.5.2 Geochemical Analysis

A powdered carrier was selected for this stage of testing, to further test suitability of these carriers. Based on results in Section 5.2.2.3, it was expected that these powdered carriers (EP and DE) may release all stored cementation medium constituents during the biocementation process, which would be undesirable since a store of cementation medium is required for later self-healing. EP was found to be easily separated into granules after loading and drying and was selected for this preliminary biocementation test in which biocement was produced using 50 ml polypropylene centrifuge tubes. Given the mass loss on ignition of DE this would complicate analysis later should mass loss on ignition be used to measure calcium carbonate content of biocemented sand (at Cardiff University).

Results from the preliminary biocementation tests are shown in Figure 5-23 and Figure 5-24. Elevated calcium ion levels in the effluent extracted from the tubes containing cementation medium loaded EP, in comparison to the controls, up to day five, can be attributed to leaching of cementation medium constituents from carriers. This appears to have accelerated the biocementation process. At day fourteen, after ten cementation medium treatments, the calcium ion content of the effluent drained from tubes containing loaded EP drops below that of the controls, at this point the test had been ended since the flow in tubes containing the loaded EP had stopped as a result of pores in the sand being plugged with calcium carbonate. Similarly, Stocks-Fischer et al. (1999) reported that the flow in biocement columns stopped after ten days of medium treatment, after supplying the medium continuously via gravity flow. For those tubes containing the sand only, further treatments would have been required before flow ceased. Plate counts from samples taken from the dried biocement showed variable results and were deemed unreliable, the growth of cultures on plates did however indicate the presence of viable spores within the biocement.

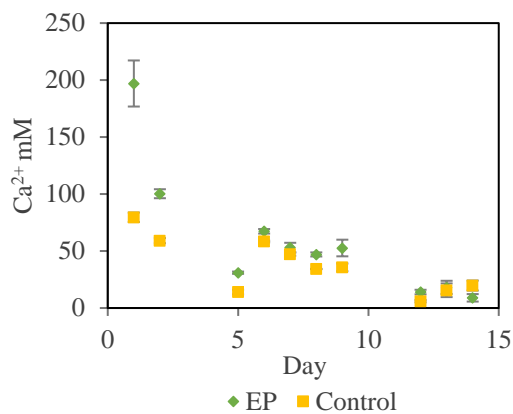


Figure 5-23. Calcium ion concentrations in effluent extracted during each biocementation treatment of mini columns containing sand only and sand mixed with expanded perlite immobilising cementation medium. Error bars show standard errors of the means for the triplicates.

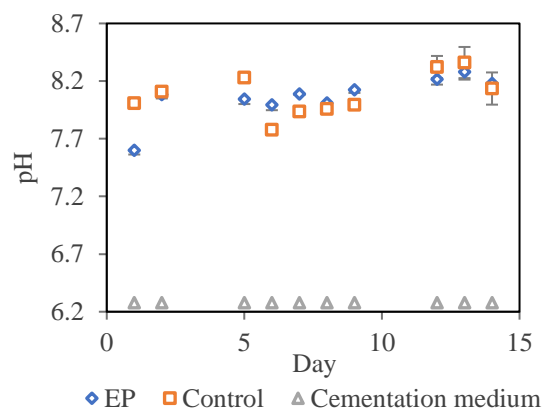


Figure 5-24. pH of effluent extracted during biocementation treatments of mini columns, compared to the initial pH of the cementation medium. Error bars show standard errors of the means for the triplicates.

Figure 5-23 shows a significant reduction in calcium ion concentration in the effluent extracted on days five and twelve, when compared the calcium ion concentration in effluent extracted on days two and nine respectively. This decrease follows weekend periods during which there are no cementation medium treatments and hence calcium ions are further depleted, which has impacted further on depletion of immobilised stores of substrates. This data suggests daily treatments will be preferable to mitigate against depletion of immobilised CM. The increase in process efficiency as the test progresses towards day fifteen supports the need for daily treatments. This increase in process efficiency may have occurred due to the presence of nutrients in the CM and subsequent bacterial growth over time. The pH

increase shown in Figure 5-24, when comparing the pH of the effluent to that of the cementation medium treatments, is a further indicator of MICP. As the calcium ion concentration in columns effluent drops below that of the controls towards the end of the treatment period, this suggest that EP may have a beneficial effect on the MICP process. At this point effects of leaching have ceased.

The results in Figure 5-23 suggest that the immobilised cementation medium in carriers may be fully depleted by treatment eight, corresponding to day twelve of this biocementation process. Fibres as carriers were explored further following this test.

5.3.2.5.3 Spore Viability

Plates showing growth of colonies from the selected serial dilutions are shown in Figure 5-25.



Figure 5-25. Colonies of *S. ureae* grown on plates of LB agar at 30 °C (with pen markings added to petri dish lids for ease of counting), shown 48 h after inoculation of the agar plates with the 10³ and 10⁴ dilutions of *S. ureae* contained within a 1 g sample taken from biocemented mini column two prepared using sand and CM loaded EP.

Plate counts from the mini columns are given in Table 5-6, for a sample from biocement mini-column 2 containing expanded perlite. It was assumed that the colonies observed had resulted from germinated spores.

Table 5-6. CFU from spores contained with biocement mini columns (Sample 2 with EP).

Plate	Colonies	CFU/ ml
10 ²	Too many to determine	NA
10 ³	206	206,000
10 ⁴	None visible	NA

It was observed that some of the sample had collected at the edges of the plate, making it difficult to obtain a precise count of the colonies since some had merged. A second set of plates, using a sample taken from a control tube which contained biocement without expanded perlite, showed negligible growth, for this sample twenty-six colonies were counted on the 10¹ plate, with no growth observed on the plates inoculated with dilutions 10² onwards. Based on the results in Table 5-6, sufficient bacteria have survived (assumed to be from germinated spores) to enable MICP. Tziviloglou (2016) reported that the bacteria concentration should be at least 10⁶ cells/ ml (cfu) to obtain a considerable amount of calcium carbonate precipitation.

5.4 Testing of Geopolymer Coatings

5.4.1 Application of Coatings

The effect of applying coatings to powdered carriers was studied as a means of improving the retention of immobilised CM. Expanded perlite was selected for this study, due to this carrier more effectively forming granules during the immobilisation process, which could be easily separated when dried. A coating solution was prepared based on Zhang et al. (2017b) and Alghamri et al. (2016) which contained 15 % sodium silicate activator and calcined kaolin (Metakaolin), in a 1:1 ratio by weight. The 15 % (by weight) sodium silicate was prepared from a 40 % sodium silicate stock solution. Two methods of applying the coatings were tested, spraying and mixing. Triplicates of CM loaded EP were prepared, with each sample containing 0.5 g EP and on average 0.51 g immobilised nutrients and precursor chemicals.

The recommended quantity of calcined kaolin to be used is 60 g per 100 g coated particles. Therefore, for each sample, a coating solution was prepared using 0.3 g calcined kaolin and 0.3 g sodium silicate. The CM loaded EP samples were spread out onto glass evaporating dishes, with the coatings applied by spraying or by pouring the coating onto the CM loaded EP granules and mixing. After applying the coatings, the resulting granules were dried at 50 °C then transferred to 50 mL centrifuge tubes. A quantity of deionised water was added to each tube equal to twenty times the mass of immobilised CM. CM loaded EP without coatings were tested as a control. The samples prepared for this test were as given in Table 5-7. To test the effectiveness of the coatings, the tubes containing the prepared samples suspended in deionised water were placed in a shaking incubator at 100 rpm and 20 °C. A 100 µL sample of the solution in each tube was taken every 10 min, up to 30 min, to test the concentration of the calcium ions leached into the deionised water surrounding the coated granules.

Table 5-7. Samples prepared for testing of coatings on CM loaded EP.

Coating method	Sample ID	Nutrients Immobilised (g)	Mass of coatings (g)	Deionised water added (mL)
Mixing	B1	0.527	0.316	10.54
Mixing	B2	0.528	0.363	10.56
Mixing	B3	0.506	0.360	10.12
Spraying	B4	0.448	0.280	8.960
Spraying	B5	0.530	0.341	10.60
Spraying	B6	0.561	0.300	11.22
None	B7	0.532	-	10.64
None	B8	0.487	-	9.740
None	B9	0.439	-	8.780

5.4.2 Results and Discussion

The results, as seen in Figure 5-26, showed that the coatings had some effect, in particular when sprayed onto the granules. At the 10 min stage the coatings appeared to have reduced the loss of immobilised cementation medium by 25 %. However, in a short period of time the coatings had ceased to be effective. Coatings were therefore not used in the subsequent studies and were deemed unsuitable for the fibres.

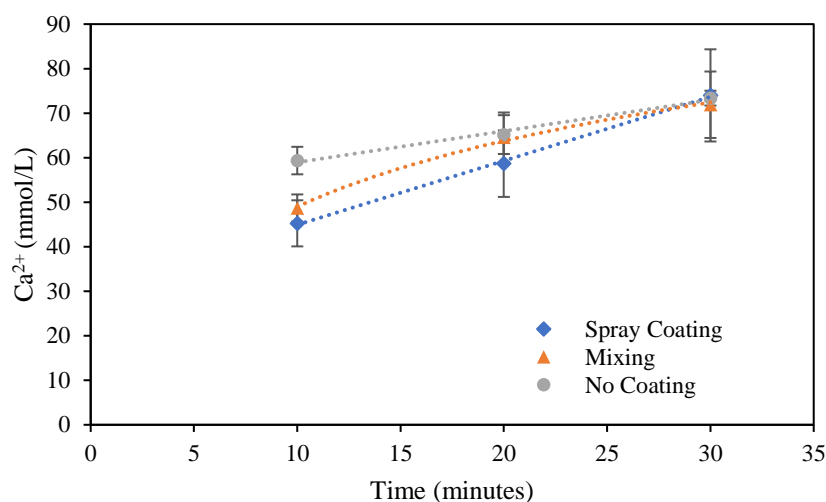


Figure 5-26. Concentration of calcium ions within solutions containing cementation medium leached from coated and uncoated expanded perlite over a 30 min period when subjected to shaking incubation of 150 rpm at 30 °C. Following the CM immobilisation process by 1 g samples of EP in triplicates, triplicate sets of the loaded EP had been sprayed with a sodium silicate – calcined kaolin solution, mixed with this solution, or left uncoated before immersion in deionised water to test the rate of leaching of the immobilised CM. Error bars show standard errors of the means for the triplicates.

5.5 Conclusions

Chapter Five covers the preliminary testing undertaken to aid in the selection of suitable bacteria and carrier materials, to enable the development of a biocemented sand material with self-healing capability. Results from these tests informed subsequent column studies. Following on from Chapter Three, the selected carrier materials tested were jute, hemp and coir natural fibres, in addition to expanded perlite and diatomaceous earth powdered additives. Coir had been substituted with hemp when coir was found to be a relatively poor immobilising material.

Based on results obtained, either *S. ureae* or *S. pasteurii* may be suitable for use to promote SH-MICP, as sporulating ureolytic bacteria. Both bacteria demonstrated spore forming ability, particularly in low nutrient environments. Tests with *S. ureae* in growth medium subjected to differing temperatures

showed that increasing the incubation temperature to 40 °C may also help to produce more spores. This does also demonstrate that in past studies by Botushorava (2017), the use of *S. pasteurii* as a non-sporulating control may not have been suitable, since studies undertaken have shown that once nutrients are depleted *S. pasteurii* is likely to sporulate under incubation at 30 °C. It is possible however that the strain used may affect sporulation ability.

A series of tests were designed and undertaken to test the effectiveness of selected carrier materials for cementation medium immobilisation, subsequent release/ retention of immobilised CM, and to gain insight into effects these carriers may have on MICP. Of the carriers tested, jute was found to be the best immobilising material, coir in comparison was a poor immobiliser and was substituted with hemp. Expanded perlite and diatomaceous earth were also found to be effective immobilising materials, however results from tests undertaken at this stage suggested that they may not be as effective at retaining cementation during the treatment biocementation process as the jute and hemp fibres may be. Fibres had been shown to facilitate multiple releases of cementation medium. Tests repeated with hemp showed results close to jute when immobilisation was considered. Cementation release patterns over time showed some variation when comparing jute and hemp. Within a cementation medium solution jute appeared to retain more immobilised cementation medium than hemp, column studies were needed to get a better insight into this release of immobilised CM behaviour.

The MICP testing in aqueous solutions containing cementation medium constituents leached from CM loaded carriers indicated that diatomaceous earth may potentially have a beneficial effect on the MICP process. It was evident at this stage that the carriers were not releasing constituents of the cementation medium to the same extent. MICP was nonetheless facilitated by leached CM from all carriers.

The mini-columns test gave insight into leaching of immobilised cementation medium from EP when multiple treatments of cementation medium were supplied over several days, with the immobilised CM being retained for longer than had been expected based on prior batch test results. These results suggested that immobilised cementation medium may be retained to some extent for up to at least seven treatments, when using CM1u for the biocementation treatments. The surface percolation method of cementation medium supply was applied for this test. This methodology was not as efficient as the injection method used in subsequent studies. Spore viability was also evidenced from testing of material from these columns after an extended period of drying and appeared to be enhanced by use of the carrier material.

Geopolymer coatings were tested as an approach to improving the retention of immobilised cementation medium by the powdered carrier materials. This was not however found to be sufficiently effective for this methodology to be adopted in the subsequent column studies.

6 COLUMN STUDY ONE: Column Tests using *S. ureae* to test the Effectiveness of Immobilising Carrier Materials for the Long-Term supply of Cementation Medium

6.1 Introduction

A series of column studies were conducted using the apparatus as described in Chapter Four. Columns were injected with cementation medium (treatments) every 24 h for a period of ten consecutive days (or as otherwise stated) using the upward flow mechanism to achieve biocementation of the sand within the columns. The study detailed in Chapter Six commenced with the use of *Sporosarcina ureae* as the selected ureolytic bacterium to promote MICP, following on from similar column studies using this bacteria that had been completed in a prior doctoral study by Botusharova (2017).

This set of column studies explored the use of a variety of carrier materials for the immobilisation of cementation medium within biocemented sand columns. Carrier materials tested included jute and hemp natural fibres, in addition to an expanded perlite powdered carrier material. The methodology for the column experiments was developed further as these studies progressed. Differing approaches to bacterial fixation within columns were tested, in addition to changes to column drying/ curing durations following the treatments. A preliminary study using *S. pasteurii* has also been included (Test 5) as a precursor to Chapter Seven. Samples from these columns produced using *S. ureae* and *S. pasteurii* were later tested after being stored for approximately 1.5 y, to give an insight into bacterial spore production in the columns and the long-term viability of these spores.

Strength regain following mechanical (shearing) damage was used as a test for self-healing capability of the columns. The columns were first subjected to unconfined compressive strength (UCS) testing after the cementation medium treatments had been completed and the columns had been dried. Following this first test (UCS1), the columns were then reconstituted and hydrated with water and left for a week, following which columns were dried and the unconfined compression test was then repeated (UCS2) to assess strength regain. During this period of rehydration, it was expected that the remaining immobilised cementation medium would leach from the carrier materials and spores of bacteria would germinate, which would result in MICP. A sufficiently slow release of the immobilised cementation medium would be needed for sufficient retention of cementation medium following the initial

biocementation process. The studies detailed in Chapter Six gave further insight into the effectiveness of the selected carrier materials for retaining and releasing the immobilised cementation medium.

6.2 Materials and Methods

6.2.1 Sand

For the studies detailed in Chapter Six, a Garside Sands (Aggregate Industries) washed fine silica sand (WFSS) was used. The properties of this sand, as provided by Aggregate Industries (2013), are given in Table 6-1. Further parameters were obtained for this sand by conducting proctor compaction and particle size distribution tests in accordance with ASTM D1557-12e1 (ASTM International 2012) and BS 1377-7:1990 (British Standards Institution 1999) respectively.

Table 6-1. Garside WFSS sand properties, as given by Aggregate Industries.

Sand Origin	G_s	ρ (mg/m³)	Mineralogy	Shape
Leighton Buzzard	2.65	1.4	Quartz	Sub angular to rounded

6.2.2 Cementation Medium

The cementation medium (CM1u) prepared for use in this study, adapted from Stocks-Fischer et al. (1999) and as used in studies by Botusharova (2017), comprised per litre of distilled water; 3 g Oxoid CM0001 nutrient broth, 10 g ammonium chloride, 2.12 g sodium bicarbonate, 7.35 g calcium chloride dihydrate and 20 g urea. The formula of Oxoid CM0001 is as per Table 6-2, as given by Thermo Fisher Scientific (2018).

Table 6-2. Constituents of Oxoid CM0001 nutrient broth.

Typical Formula	g/litre
`Lab-Lemco' powdered beef extract	1.0
Yeast extract C ₁₉ H ₁₄ O ₂	2.0
Peptone	5.0
Sodium chloride NaCl	5.0
pH 7.4 ± 0.2 @ 25 °C	

Molar concentrations of the cementation media are shown in Table 6-3. A more concentrated version of this cementation medium (CM2u) was used to pre-treat fibres prior to mixing with sand, (As outlined in Table 6-3 below).

Table 6-3. Molar quantities/ masses of precursor chemicals and nutrients in cementation media used to treat sand columns inoculated with *S. ureae* (CM1u) and prepared for immobilisation within carrier materials (CM2u).

Cementation medium component	CM1u/ Botusharova (2017)	CM2u (x 6.67 Conc.)
Urea (CH ₄ N ₂ O)	333 mM	2220 mM
Ammonium chloride (NH ₄ Cl)	187 mM	1246 mM
Calcium chloride dihydrate (CaCl ₂ .2H ₂ O)	50 mM	333 mM
Sodium bicarbonate (NaHCO ₃)	25 mM	168 mM
Oxoid CM0001	3 g/L	20 g/L

6.2.2.1 Production of Concentrated CM for Immobilisation

To produce the concentrated cementation medium (CM2u) for immobilisation within carriers, firstly the minimum quantities of deionised water to enable complete dissolution of constituent chemicals (reagents and nutrients) needed to be ascertained. The quantities of chemicals required to make two litres of the cementation medium were weighed out separately. To each of these, apart from the calcium chloride dihydrate, deionised water was added in 25 mL increments until the powdered reagents had fully dissolved. The resulting Oxoid CM0001, urea, ammonium chloride and sodium carbonate solutions were then mixed. The pH of this solution was adjusted to 6.0 using concentrated HCl, before then adding the powdered calcium chloride dihydrate. This pH adjustment prevented the calcium precipitating out of the calcium chloride dihydrate. Calcium chloride dihydrate was observed to form a precipitate when added to deionised water (pH of 7.30 at Cardiff University). Stocks-Fisher et al. (1999) reported that the pH of the cementation media they prepared was adjusted to 6.0 before autoclaving, with the final pH of their media, after calcium chloride (CaCl₂) addition, being 8.0. It was found that no additional deionised water needed to be added at this stage to fully dissolve chemicals. A total of 300 mL water was required to make the concentrated cementation medium. The prepared concentrated cementation medium had a pH of 6.92.

Following on from the above, to make 300 mL of sterile concentrated cementation medium for use in experiments, Oxoid CM0001 nutrient broth was first dissolved in 25 mL of deionised water in a 500 mL glass jar, adjusted to pH 6.0 using concentrated HCl, and sterilised by autoclaving at 121 °C for 15 min. The remaining chemicals, excluding calcium chloride dihydrate, were thoroughly mixed in 275 mL deionised water, using a magnetic stirrer. This solution was then adjusted to pH 6.0 using concentrated HCl, calcium chloride dihydrate was then added as a powder. This solution was then syringe filtered into the Oxoid CM0001 nutrient broth solution, using a 0.2 µm syringe filter. The pH

of the resulting medium was measured to be 6.8 (as an average of four readings across experiments), this being close to the optimum pH of 7.0 for *S. ureae* growth.

Of the medium constituents, only the Oxoid CM0001 Nutrient broth could be autoclaved without there being any effect on the concentrated medium or chemicals used. Urea and ammonium salts should not be autoclaved, in addition the calcium in calcium chloride dihydrate can precipitate out when autoclaved, particularly if the concentration is high. When subjected to temperatures above 70 °C the sodium bicarbonate will decompose into sodium carbonate, water and carbon dioxide. It has been reported that solid NaHCO₃ begins to lose carbon dioxide and water around 100 °C (Senese 2010), originally from (Otsubo and Yamaguchi 1961). However, other sources suggest this may occur at temperatures exceeding 50 °C, hence following the preliminary stage of investigation all loaded samples were dried at 50 °C. The concentrated cementation medium prepared for immobilisation was 6.67 times more concentrated than the cementation medium injected into the columns, with molar masses of chemicals shown in Table 6-3 for comparison. This concentrated medium consisted, per litre of deionised water; Oxoid CM0001 nutrient broth 20 g, urea 133.33 g, ammonium chloride 66.67 g, sodium bicarbonate 14.13 g and calcium chloride dihydrate 49 g.

6.2.3 Bacteria Culture, Fixing and Activity

Liquid broth cultures of *S. ureae* (Column Tests 1 – 4) and *S. pasteurii* (Column Test 5) were grown to inoculate the columns. These liquid broth cultures were prepared as detailed in Chapter 4, Section 4.1. The liquid broth cultures for the column tests were prepared using multiples of 250 mL Erlenmeyer flasks and using tap water. Owing to the low urease activity of *S. ureae*, when compared to bacteria such as *S. pasteurii*, the bacterial suspension could be mixed with the cementation medium (CM1u) prior to addition to the column assembly since precipitation did not immediately occur. Thus, the calcium contained within this cementation medium will have fixed the bacteria to the sand as the sand (and carrier materials) were wet pluviated into this bacteria and cementation medium mixture to form the columns within the latex membranes. Harkes et al. (2010) had found solutions containing calcium chloride to be effective for fixing bacteria within sand columns. At this stage of testing, when using *S. pasteurii* (Columns Test 5), this bacterium had also been mixed with the cementation medium into which the sand (and carrier) mixture was wet pluviated, with a little precipitate observed at this stage.

6.2.3.1 Urease Activity

Using the process as reported by Harkes et al. (2010), it was found to not be possible to measure urease activity of *S. ureae*, given that *S. ureae* promotes a much slower MICP process when compared to *S. pasteurii*.

6.2.4 Preparation of Carrier Materials

6.2.4.1 Fibres

Fibres were either soaked or sprayed using the concentrated cementation medium (CM2u), as detailed for each test. Fibres treated using the spraying method were sprayed with 100 actuations of the concentrated cementation medium while placed over 60-mesh gauze with an aperture of 0.263 mm and 39 % open area. Prior to use of the 60-mesh gauze, a 200-mesh gauze was tested, with 0.075 mm aperture and 34 % open area, however this didn't allow for draining well and the grids curled up after one use.

6.2.4.2 Expanded perlite

Before use, the expanded perlite (EP) was autoclaved at 120 °C for 15 min and oven dried at 105 °C to sterilise the EP powder. The EP was then transferred to sterile 50 mL centrifuge tubes in 2 g quantities in triplicates. The tubes had been weighed before filling. The EP was then submerged in concentrated CM2u (10 mL) within the tubes. The tubes were vibrated for 10 sec using a vortex mixer, to ensure thorough dispersal of the EP in the medium, and then left to soak for 24 h. After 24 h, the tubes were centrifuged and the waste CM2 drained. The tubes were then transferred to a 50 °C oven with lids removed and dried for at least 48 h until the mass was constant. This process was repeated to apply a second loading of CM2u to the EP.

This process resulted in granules of EP and CM forming, unlike the fibres these granules could still be easily separated after repeated loadings. To separate out these granules, an autoclave sterilised pestle and mortar was used in close proximity to a Bunsen, with light pressure applied to avoid crushing the granules. The granules were then transferred back into the tubes ready for column assembly.

6.2.5 Columns Assembly and Treatment

Columns were assembled as detailed in Chapter Four. The multichannel (Ismatec IPC) peristaltic pump was set up to pump at a flow rate of 2 mL/min, using tubing with a 2.54 mm inner diameter. The cementation medium and bacteria mix into which the sand or sand and carrier mixtures were wet pluviated constituted biocementation treatment one. Following treatment one, the cementation medium (CM1u) treatments were supplied via injection using the peristaltic pump. The columns once prepared, as shown in Figure 6-1, were incubated in a static incubator at 30 °C, this being considered the optimum temperature for MICP, as reported by (Kim and Youn 2016). Columns were removed from the incubator for a short period for the daily cementation medium injections. Up to twelve columns could be treated at once, with up to six columns attached to each side of the column frame shown in Figure 6-1. For each injection, the required amount of cementation medium was transferred to a sterile container in close

proximity to a Bunsen, to ensure the medium remained sterile. Preparing the cementation medium in larger quantities helped ensure consistency of treatments.

Inlet tubing was left filled and clamped at the ends between treatments to help prevent air entry into columns. Outlet tubing was drained following each treatment.



Figure 6-1. Photograph of prepared columns, showing apparatus used for the column studies completed at Cardiff University.

The five column tests detailed in Chapter Six are summarised in Table 6-4.

Table 6-4. Summary of Column Tests

Column Test	Bacteria Fixation/ Treatment 1	Treatments (volume)	Carrier materials tested	Carrier material treatment	Drying time (days)	Rehydration process following UCS1
U1	Wet pluviation of column contents into <i>S. ureae</i> and CM1u mixture.	11 (one pore volume)	Jute and Hemp	Soaked in CM2u	14	Surface percolation
U2	Wet pluviation of column contents in <i>S. ureae</i> and PBS mixture, left for four hours, followed by CM1u injection.	10 (1.25 pore volumes)	Jute and Hemp	Sprayed with CM2u	14	Injection

U3	Wet pluviation of column contents into <i>S. ureae</i> and CM1u mixture.	10 (1.25 pore volumes)	Jute and Hemp	Sprayed with CM2u	28	Injection
U4	Wet pluviation of column contents into <i>S. ureae</i> and CM1u mixture.	10 (1.25 pore volumes)	Expanded Perlite	Sprayed with CM2u	28	-
P1	Wet pluviation of column contents into <i>S. pasteurii</i> and CM1u mixture.	8 (1.25 pore volumes), 3 conc. final injection	Jute and Hemp	Sprayed with CM2u	28	-

6.2.6 Geochemical Analysis

6.2.6.1 Column Test U1

Following daily treatments with cementation medium, the pH and dissolved oxygen levels of effluent from columns were measured. The first 10 mL of effluent was tested since this would not contain any of the freshly injected medium. Dissolved oxygen levels were measured to ascertain oxygen availability during the MICP process. Probes were washed with 2 M HCl solution as recommended by (Kennedy et al. 2005) and deionised water before and after use for all tests. Measurement of calcium ions in effluent was obtained using ICP-OES following treatments one to four, then on alternate days following treatments six, eight and ten.

6.2.6.2 Columns Tests U2 to P1

For Column Tests U2 through to P1, measurement of pH and calcium ions only was undertaken. The pH of effluent from each column was measured daily following each cementation medium injection. The calcium ion concentration in the effluent from each column (using the first 10 mL displaced) was measured following treatments one, three, five, seven and nine.

6.2.7 Unconfined Compressive Strength Testing

The unconfined compressive strength of the column specimens was determined in accordance with 7.2 of BS 1377-7: 1990 using a load frame (Wykenham Farrance). The apparatus used is as shown in Figure 6-2, with the column placed above a load cell and displacements measured using an LVDT. A platen displacement rate of 1.4 mm/min was applied for Columns Test S1 and reduced to 1.14 mm/min

thereafter. The same apparatus was used for all tests detailed in Chapter Six. The unconfined compressive strength was recorded as the strength coinciding with the first peak on the stress-strain curve, or where a clear peak was not observed the final reading. The residual strength is recorded as the value where the curve plateaus after failure and remains at this level, or the value at 20 % strain when the readings rise again following failure or where there is no clear peak. This is similar to analysis applied by Liu et al. (2018a) for unconfined compression testing of fibre reinforced sands. Lui et al. (2018a) reported that the first peak values and the end values of stress–strain curves of all specimens were considered as the unconfined compressive strengths and residual strengths, respectively. The length and diameters of the columns were measured before each of the unconfined compression tests.



Figure 6-2. Photograph of the unconfined compression test apparatus used at Cardiff University, showing a column from Columns Test U2 being subjected to loading.

To test for self-healing responses, firstly an unconfined compressive strength test (UCS1) was undertaken following initial biocementation and drying. A second UCS test (UCS2) was undertaken following reconstitution, hydration and drying of columns. Where the peak strength following UCS2 is higher than the residual strength for UCS1 this strength recovery has been attributed to self-healing. For this type of self-healing response strength recovery was calculated as per Equation (6-1).

$$\text{Strength recovery above residual} = \frac{\text{Shear Strength 2} - \text{Residual Strength 1}}{\text{Shear Strength 1} - \text{Residual Strength 1}} \quad (6-1)$$

Columns were dried prior to UCS testing, it is noted however that this is a deviation from the British Standards for UCS testing. This was done however to enable testing for self-healing and to help ensure self-healing responses were due to spores of bacteria as opposed to live bacteria. It had been assumed that following prolonged periods of drying that spores only would be present, this had been tested by varying drying times.

6.2.8 Mineralogical Analysis

Scanning electron microscopy (Zeiss Sigma HD Field Emission Gun Analytical SEM) was used to observe the precipitated calcium carbonate for selected columns from Column Test U2. Samples for SEM observation and analysis were prepared using a sputter coater and gold-lead (Au-Pb) coating. X-ray diffraction (XRD; Siemens Diffraktometer D5000) was used to characterise the mineral crystals observed and confirm the presence of CaCO₃.

6.3 Test Results and Analysis

6.3.1 Sand Parameters

The laboratory measured particle size distribution results in Figure 6-3 give a more detailed breakdown of the particle sizes within the sand used, compared to those provided by the supplier. Of interest are the distribution of particles within the desired 50 µm to 400 µm range as indicated by the vertical orange lines on the chart. Results show that approximately 93% of the sand particles lie within this range according to the laboratory test.

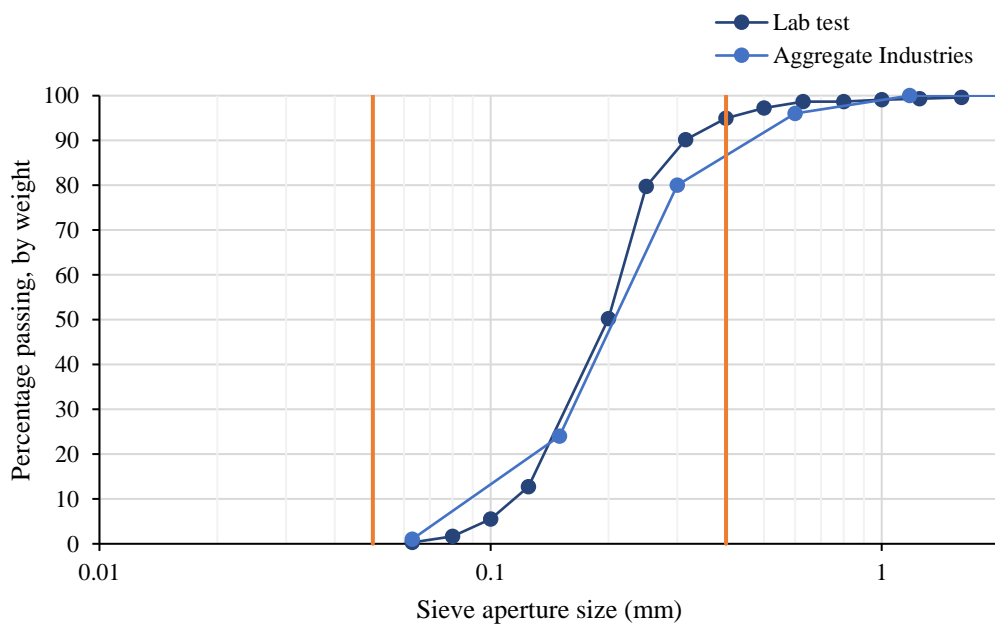


Figure 6-3 Particle size distribution of Garside Sands washed fine silica sand, as measured in the laboratory and provided by Aggregate Industries.

From the laboratory test particle size distribution curve, sand parameters had been obtained as given in Table 6-5. The sand is poorly graded given the low coefficient of uniformity (C_u) value.

Table 6-5. Garside Sands washed fine silica sand parameters.

D_{10}	D_{30}	D_{50}	D_{60}	C_u	C_z
0.115	0.155	0.200	0.215	1.870	0.972

The dry-density water content relationship of the Garside WFSS is shown by the proctor compaction test results in Figure 6-4. From the proctor compaction curve, the target density (maximum dry density) derived for compaction of the sand in the columns is 1.67 g/cm^3 . The proctor compaction test on sand of 16 % moisture content resulted in water coming out around the base of the proctor mould and hence values of dry density at this point will be less accurate.

Across the column tests, the sand was compacted to an average of 95 % of this target density for the sand-only control columns. For columns containing fibres, when considering the total mass of sand and fibres, the compaction varied from 91 % to 92 % of the target density across the tests, and remained consistent and therefore demonstrated repeatability of the column preparation methodology. The proctor compaction test in this study only considers the sand however and not the sand and fibre mixtures, the target density for sand and fibre mixtures is expected to be lower. Compaction of sand and fibre mixtures is analysed further in Chapter Seven.

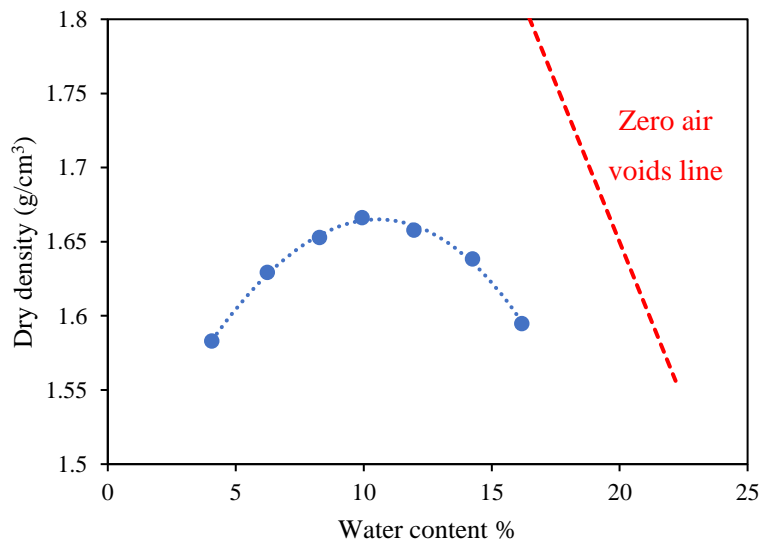


Figure 6-4. Proctor compaction test results showing the dry density – moisture content relationship for Garside washed fine silica sand, with the zero air voids line (red line) shown for reference.

6.3.2 Columns Test U1

Columns Test U1 utilised *S. ureae*, with eleven treatments of cementation medium CM1u (ten injections). The daily treatments constituted one pore volume, with pore volumes for each injection estimated from scale up of the preliminary study undertaken to produce the biocemented sand mini-columns (Chapter Five). The liquid broth inoculant of *S. ureae* had an optical density (OD₆₀₀) of 0.817. Fibres had been soaked in the concentrated cementation medium and dried prior to premixing with the sand.

To test for self-healing, the columns were rehydrated with autoclave sterilised tap water water via surface percolation. The sand columns were placed upright in a sterile plastic container, with water poured slowly into the ends of the columns, in close proximity to a Bunsen burner flame. Once fully saturated, the columns were placed horizontally and transferred to a 30 °C static incubator for fourteen days. Prior to the initial unconfined compression testing, the overhanging ends of the membranes had been trimmed and hence injection of water could not be facilitated at this stage.

Once the treatment stage was completed, the columns were left in the 30 °C incubator with porous discs removed for fourteen days, which was found to be sufficient for drying until constant mass was achieved. It is therefore possible that some vegetative bacterial cells remained in these biocement columns. The ends of membranes had been trimmed to facilitate unconfined compression testing. As a result of which, the columns needed to be hydrated via surface percolation for the self-healing stage of testing.

For this first column study the columns were prepared with an approximately equal initial mass close to 134 g for each column, with column contents as per Table 6-6, this however resulted in columns containing fibres being longer than the controls. Masses of sand used were adjusted for subsequent studies, with reduced sand content in the columns containing fibres, to achieve more uniform column lengths across all of the columns tested.

Table 6-6. Contents of columns prepared for Columns Test U1.

Column ID	Carrier type	Carrier mass (g)	Sand mass (g)	CM2u Immobilised (g)
J1	Jute	1	132.6	0.438
J2	Jute	1	132.5	0.481
J3	Jute	1	132.5	0.524
H1	Hemp	1	132.6	0.414
H2	Hemp	1	132.6	0.415

H3	Hemp	1	132.5	0.483
C1	-	-	134	-
C2	-	-	134	-
C3	-	-	134	-

To prepare the fibres for this test, the hemp and jute had been soaked in concentrated CM (CM2u) for 24 h and then separated out onto paper towels. A paper towel was lightly pressed on top of these fibres to absorb excess medium, this however had the effect of removing a significant quantity of the medium so that an average of 0.46 ± 0.04 g of nutrients was immobilised per gram of fibres. The soaking method resulted in greater variation of masses immobilised CM2u for specific fibre types, although more consistency was obtained across different fibre types.

6.3.2.1 Geochemical Analysis

The pH readings shown in Figure 6-5 indicate a consistent rate of bacterial activity following each of the cementation medium injections after treatment one. The pH of around 8.5 is typical of that observed during the MICP process, as reported by van Paassen (2009). The pH of the cementation medium, as measured prior to use, had been 6.45, the rise to 8.5 is indicative of MICP. The low pH following treatment one is unexplained and may be attributed to a faulty pH probe, a different probe was used for later readings. The probe had been calibrated prior to each test. *Sporosarcina ureae* urease was reported by McCoy et al. (1992) to be stable over a pH range of 7.75 to 12.5, with activity rapidly lost at lower or higher pH levels.

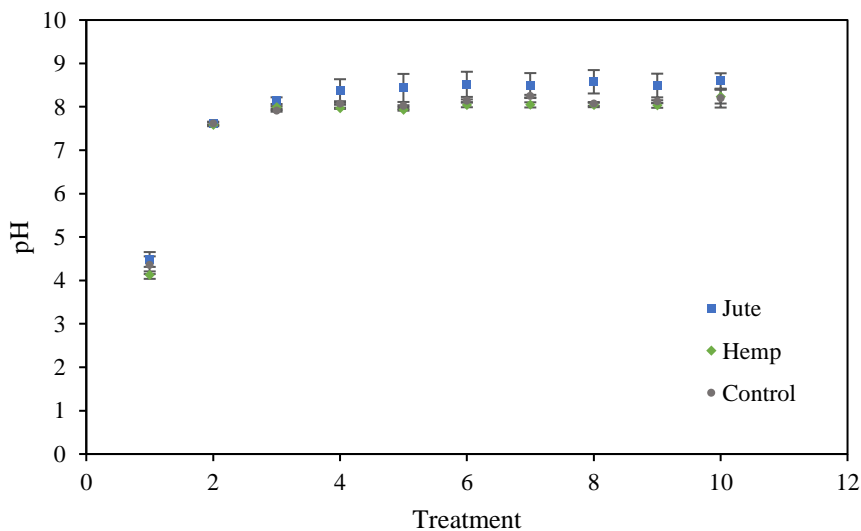


Figure 6-5. pH of effluent from Test U1 columns following each biocementation treatment. Error bars show standard errors of the means for the triplicates.

The dissolved oxygen measurements of the column effluent, as shown in Figure 6-6, show that oxygen is present in the cementation medium. The dissolved oxygen measurement of the cementation medium had been 10.2 mg/L. As there is still oxygen remaining in the effluent following each treatment oxygen availability has therefore not been a limiting factor affecting MICP for this study. Where a drop in the dissolved oxygen level had been observed following treatment six this showed that the pore volumes had not been accurately predicted based on the preliminary test since it would appear that insufficient medium had been used to flush through old medium. Therefore, for subsequent studies, an excess of cementation medium was used (approximately one and a half pore volumes). Following this test, the pore volume of columns could be more accurately estimated. These dissolved oxygen levels are in the expected range, Gomez et al. (2018) reported a treatment solution dissolved oxygen concentration of 7.8 mg/ L.

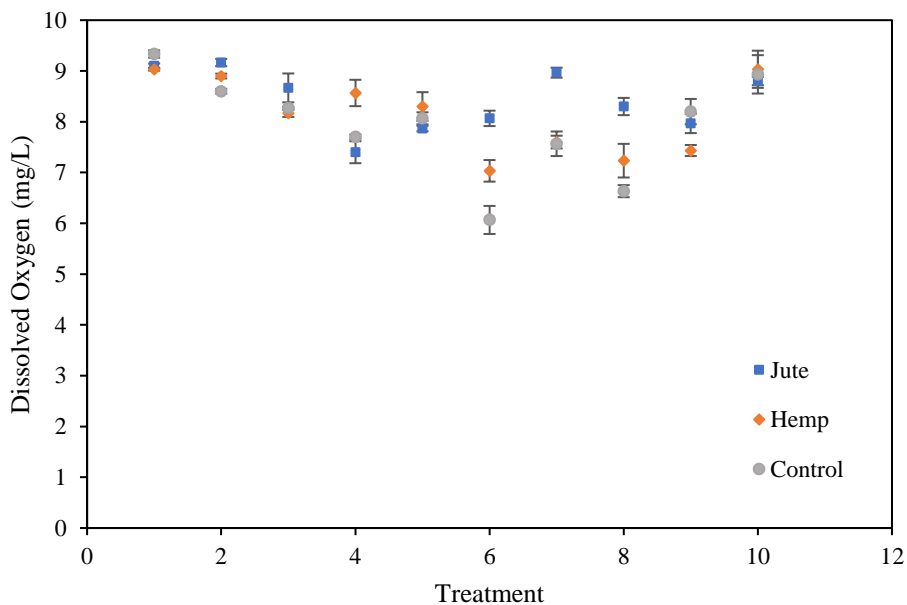


Figure 6-6. Dissolved Oxygen concentration in effluent from Test U1 columns following each biocementation treatment. Error bars show standard errors of the means for the triplicates.

Calcium ion concentrations in the columns effluent were measured using ICP-OES, with results shown in Figure 6-7. Where the readings for the columns containing fibres are above those of the controls the increased calcium ion concentration is deemed to be a result of leaching of the immobilised concentrated cementation medium from the fibres. This shows that this leaching affect is not immediate and occurs over a number of days following successive CM1u injections. For the studies undertaken at this stage, an excess of calcium chloride dihydrate (calcium source) was supplied in the cementation medium (CM1u) injections, this enabled the effects of leaching from fibres to be observed. Where the calcium ion measurement of the effluent from columns containing fibres is observed to drop below the controls

this suggests that the fibres have increased the efficiency of the MICP process, this effect was explored further in subsequent studies using *S. pasteurii*, as detailed in Chapter Seven.

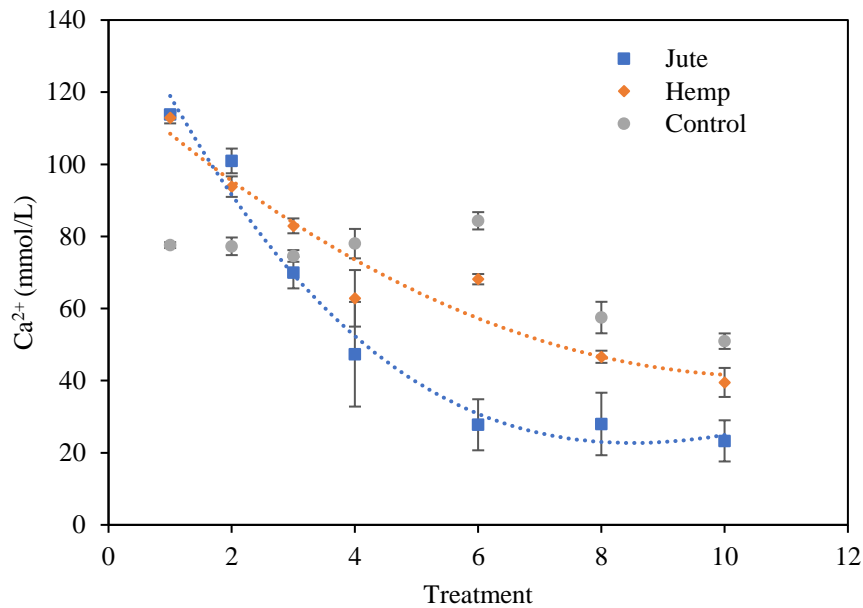


Figure 6-7. Calcium ion concentration, as measured using ICP-OES, in Test U1 columns effluent, following biocementation treatments 1 to 4, 6, 8 and 10. Error bars show standard errors of the means for the triplicates.

6.3.2.2 Unconfined Compressive Strength

The unconfined compression test results are shown in Figure 6-8 and Figure 6-9. The first peak value was recorded as the unconfined compressive strength, unless there was no clear peak and the strength continued to rise, in which case the value at 20% strain was recorded as the unconfined compressive strength. The final value recorded was considered the residual strength, as per studies by Liu et al. (2018a). The testing was ended when a clear residual strength was reached or otherwise at 20 % strain.

Where there was no peak observed the columns experienced a barrelling type failure as opposed to showing a clear shear failure. The results for column J3 are not consistent with those for J1 and J2. The effluent had appeared darker from J3 suggesting a possibility of contamination.

The initial UCS1 results in Figure 6-8 (a-c) show clear peaks for all columns containing jute, in addition to H1 and H2, followed by some strain softening. The columns containing jute were on average 6.5 times stronger than the sand only control columns following the initial biocementation.

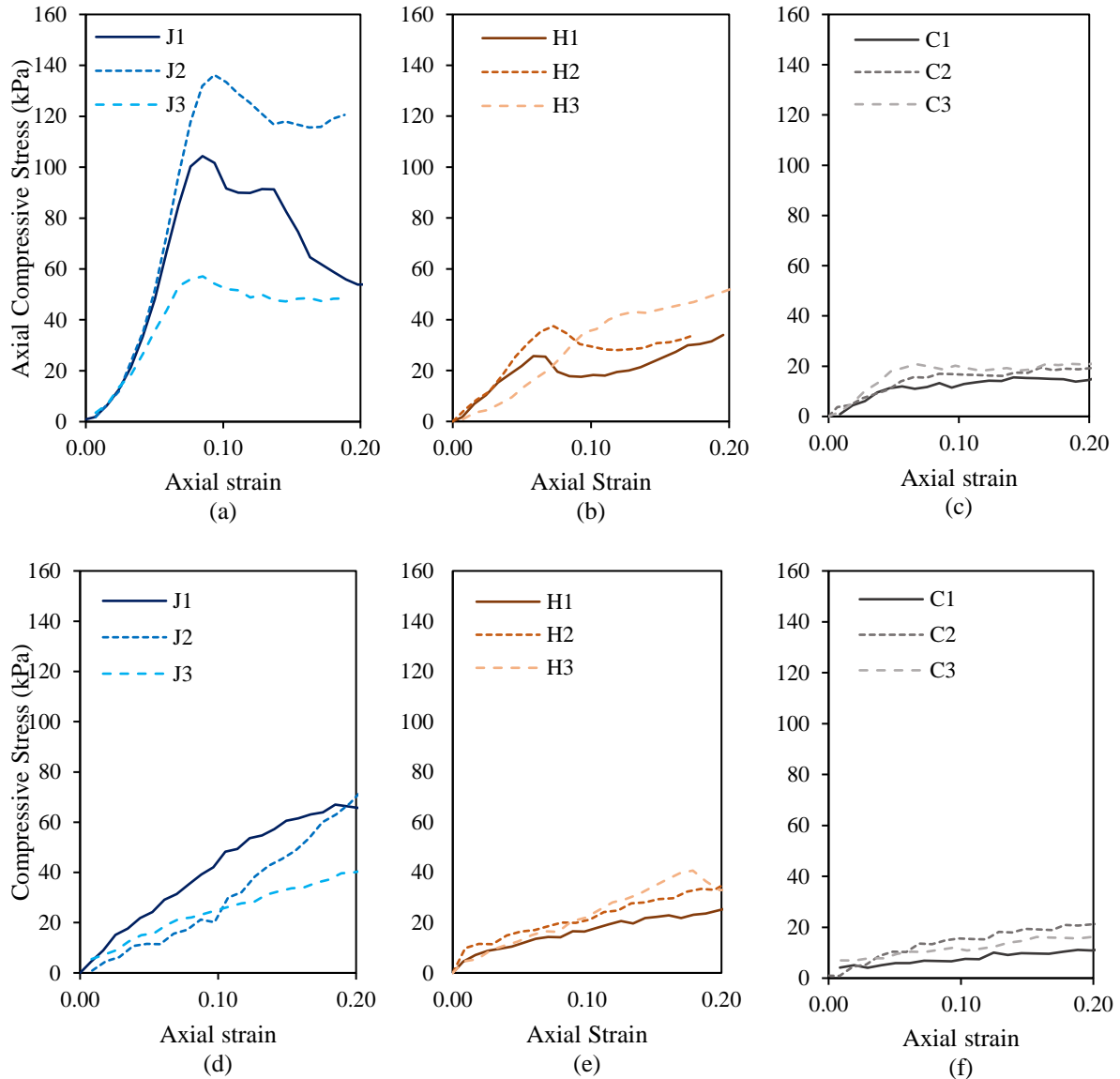


Figure 6-8. UCS test results for Test U1 biocemented columns containing hemp (H1 – H3), jute (J1 – J3) and sand only (C1 – C3), following UCS1 (a – c) and UCS2 (d – f).

Figure 6-9 compares the results for the two UCS tests, with peak strengths for UCS1 and UCS2 and the residual strength for UCS1 plotted. This enables potential self-healing behaviour to be assessed. Where the residual for UCS1 is higher than the peak for UCS1 this complicates the analysis. If self-healing is considered as strength recovery above the residual, then columns J1 and H2 may display some self-healing capability based on results in Figure 6-9. Applying Equation (6.1), the strength recovery above the residual is calculated as 26 % and 64 % respectively for J1 and H2. This analysis however isn't deemed suitable where the residual strength obtained from UCS1 is higher than the peak strength for UCS1. If peak strength values alone are considered, results for column H1 may also indicate some self-healing capability.

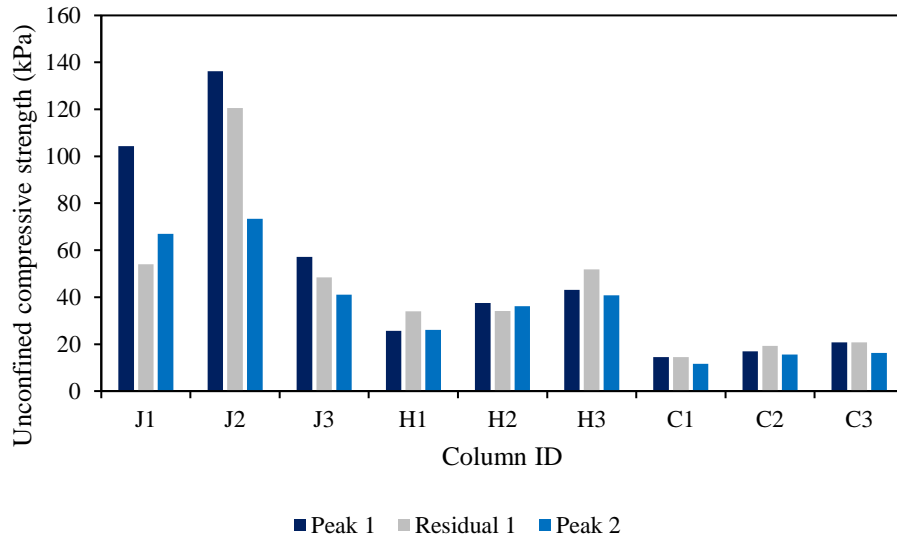
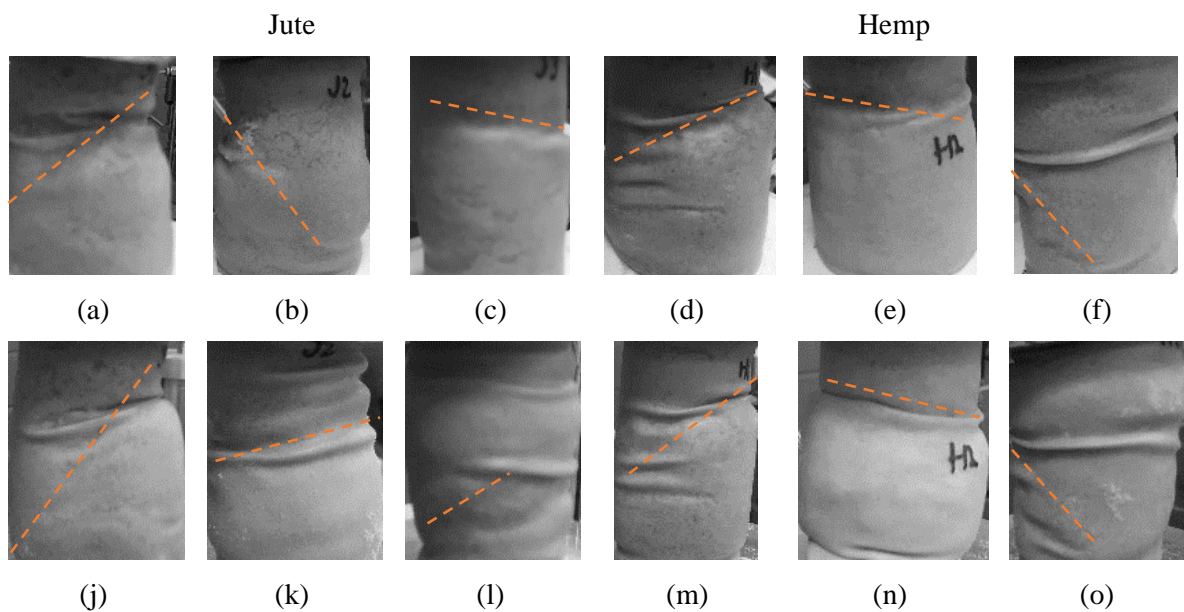


Figure 6-9. Results from UCS1 and UCS2 for Columns Test U1, showing peak and residual strengths from UCS1 and peak strengths from UCS2.

Figure 6-10 shows images taken of the columns during the unconfined compressive strength (UCS) tests shortly after failure, for UCS1 (Figure 6-10(a-i)) and UCS2 (Figure 6-10(j-r)). The failure mechanisms observed during UCS1 were, in most cases, reflected in the images taken during UCS2. At this stage of testing there were observed to be some air voids and possible clumping of fibres in the columns. At this stage the sand and fibres were dry mixed. Mixing and compaction was improved for subsequent tests by adding a small amount of liquid (CM1) prior to mixing of the fibres with sand. Although the stress- strain curves show no clear peak for controls a shear failure plane can be observed in Figure 6-10 (g to i) and for the same columns during UCS2 as shown in Figure 6-10 (p to r).



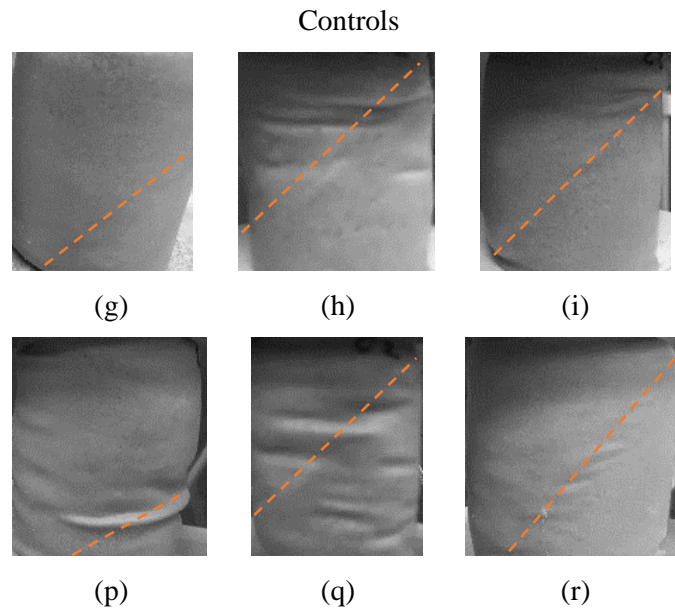


Figure 6-10. Photographs of columns from Test U1 following failure during UCS1 (a-i) and UCS2 (j-r), with annotation shown above clear failure planes observed during testing.

Results from Columns Test U1 showed that it may be possible to recover some strength lost by using natural fibres as the immobilising material for a concentrated cementation medium. This effect would need to be explored further. By maintaining open conditions during the self-healing stage, with the columns exposed to the air, this may have further promoted self-healing through increased oxygen supply. A strong odour of ammonia (NH_3) was detected in all the specimens during the self-healing stage. For the following tests, the air restricted conditions are maintained during both treatment and healing stages since the latex membranes were kept intact and the columns returned to the apparatus after the first UCS test to inject water for the healing stage.

6.3.3 Columns Test U2

The bacterial inoculant used had a measured optical density (OD_{600}) of 0.819. Following Columns Test U1, the drying temperature following column treatments prior to UCS testing was increased after the first five days of drying. A slow rate of drying allows time for further MICP and sporulation to occur as nutrients become depleted. Drying at a higher temperature over an extended period was expected to help ensure only spores remained in columns and not viable vegetative cells. It is also possible that an elevated temperature may help stimulate spore production, based on findings detailed in Chapter Five, Section 5.1.4. The temperature however was not increased above 40°C to ensure membrane strength would be unaffected. Any remaining MICP activity will likely have ceased within the initial 5-day period of drying based on results by Botusharova (2017). As per Columns Test U1, fourteen days were allowed for the drying period in total. The membranes were not trimmed as these columns were

remoulded and placed back into the column apparatus following the first UCS, to facilitate injection of water to test for self-healing.

For this test, the effect of treating and not treating fibres was also explored. A total of twelve columns were produced, including six containing jute, three of which were not pre-treated with the concentrated cementation medium CM2u. The fibres were treated with CM2u using the spraying method. The contents of the columns assembled for this test are given in Table 6-7.

Table 6-7. Contents of columns prepared for Columns Test U2.

Column ID	Carrier type	Carrier (g)	Sand (g)	CM Immobilised(g)
J1	Jute	1	125	1.450
J2	Jute	1	125	1.461
J3	Jute	1	125	1.799
J4	Jute	1	125	-
J5	Jute	1	125	-
J6	Jute	1	125	-
H1	Hemp	1	125	1.462
H2	Hemp	1	125	1.544
H3	Hemp	1	125	1.247
C1	-	-	131	-
C2	-	-	131	-
C3	-	-	131	-

From Columns Test U2 onwards, the columns had been remoulded to some extent to fit into the split moulds for the self-healing testing stage. The samples would experience some dilation once removed from the compression testing apparatus but were otherwise not further disturbed during the hydration process. It is therefore likely that the remoulding in later tests changed the alignment of the carriers and resulted in greater rearrangement of the sand particles, however the results from both sets of results from UCS1 and UCS2 suggests this effect was minimal.

The strengths of these columns had been affected by wet pluviation of the sand mixtures into a mixture of PBS and bacteria as opposed to cementation medium and bacteria as per test U1 and subsequent tests. It was found that wet pluviation of column contents into CM1u mixed with the bacteria helped to fix the bacteria to the sand and prevent flush out of bacteria. The leaching from treated fibres in columns J1 to J3 had likely helped fix the bacteria. This fixing effect is explored further in later studies with *S pasteurii*. PBS had also used for wet pluviation for test U2 to observe the effect this may have on leaching of immobilised CM2u, and following on from methodology used in prior studies by Botusharova (2017).

6.3.3.1 Geochemical Analyses

The pH and calcium ion measurements of the effluent from columns are shown in Figure 6-11. The pH of column effluent is observed to have reduced slightly compared to Columns Test U1, the only change at this stage had been the wet pluviation of the sand mixtures into PBS instead of the cementation medium. This demonstrates the beneficial effect that wet pluviation into the cementation medium had on bacterial fixation and this methodology is therefore using going forwards. For this test there appears to have been less retention of bacteria within columns.

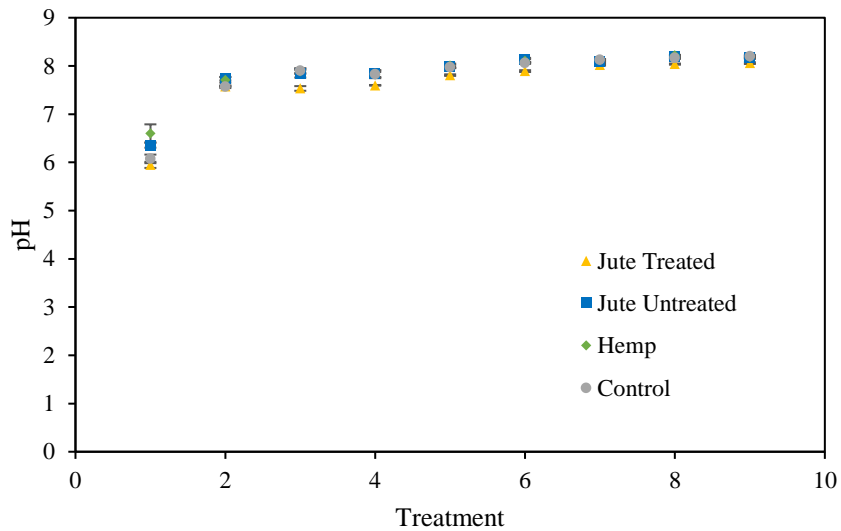


Figure 6-11. pH of effluent from Test U2 columns following each biocementation treatment. Error bars show standard errors of the means for the triplicates.

The calcium ion concentration remains at a much higher level when compared to results from Columns Test 3 which uses the same quantities for each injection. This is indicative of the reduction in bacteria fixing effectiveness for this test.

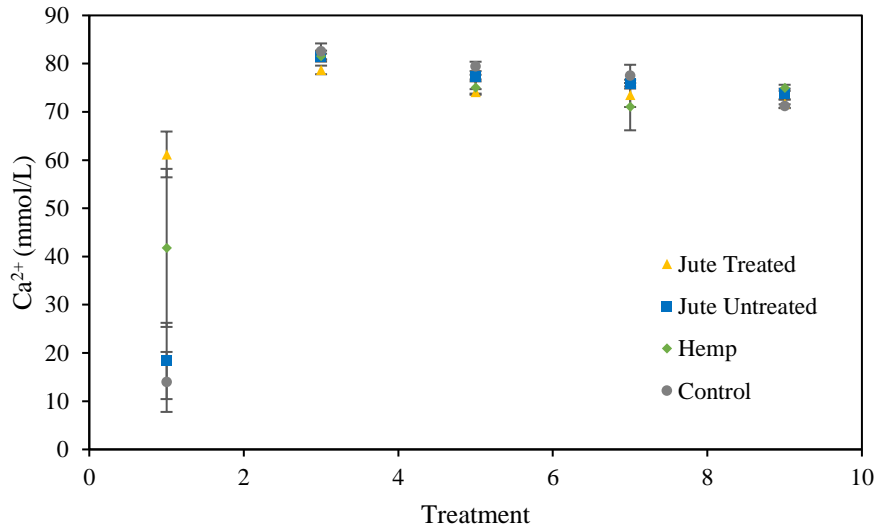


Figure 6-12. Calcium ion concentration, as measured using ICP-OES, in Test U2 columns effluent, following biocementation treatments 1, 3, 5, 7 and 9. Error bars show standard errors of the means for the triplicates.

The results for Columns Test U2 are indicative of an earlier leaching of immobilised CM, due to wet pluviation of the column contents into PBS, which also shows it is beneficial to wet pluviate in to CM as opposed to PBS to aid retention of immobilised CM by reducing the concentration gradient between immobilised chemicals and the surrounding liquid.

6.3.3.2 Unconfined Compressive Strength

UCS testing results are shown in Figure 6-13 and Figure 6-14. For this test there is some indication of self-healing capability for columns containing jute, less so for those containing hemp when comparing to Columns Test U1. Graphical outputs from Columns Test U2 are shown in Figure 6-13.

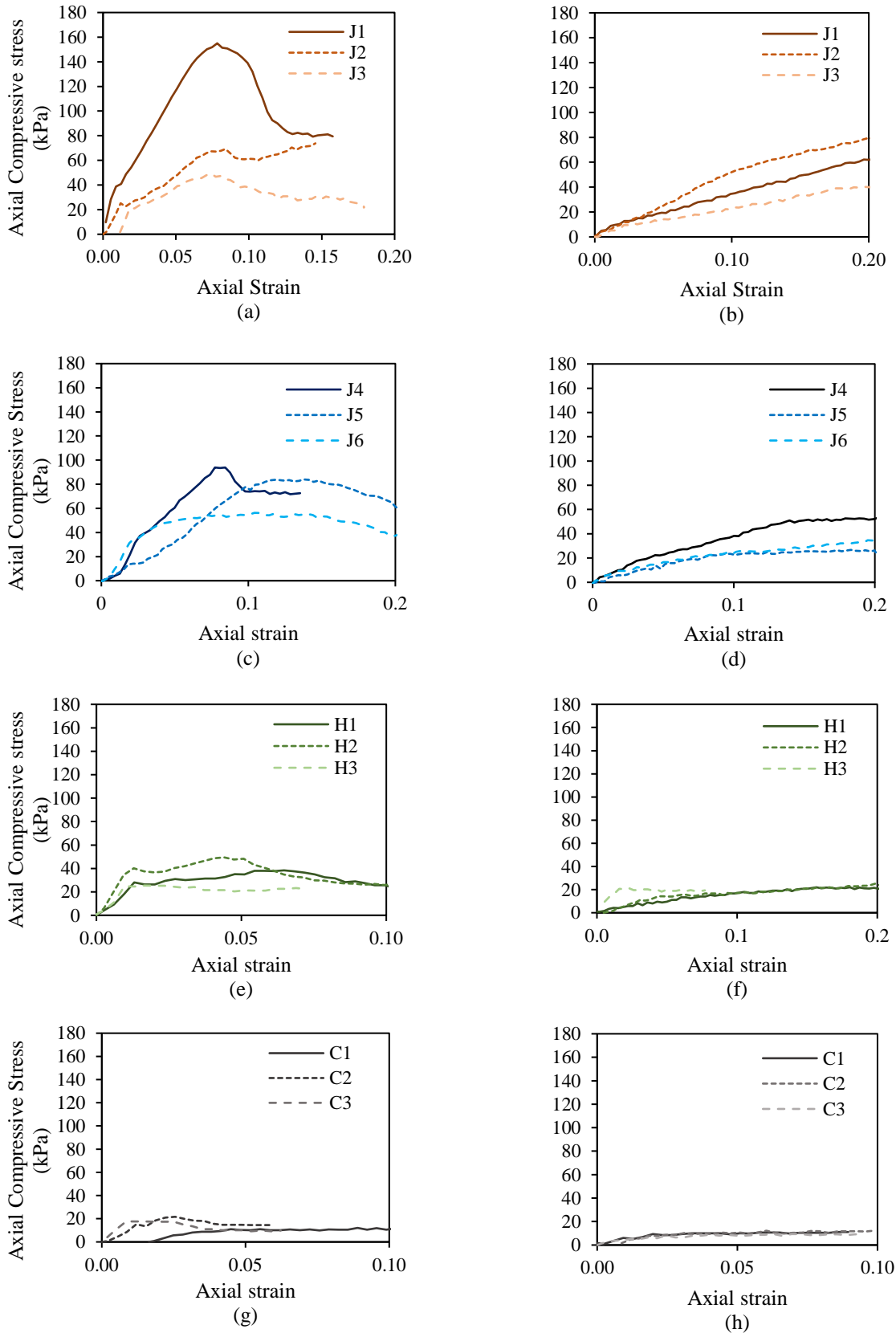


Figure 6-13. UCS test results for Test U2 biocemented columns containing treated jute (J1 – J3), untreated jute (J4 – J6), hemp (H1 – H3), and sand only (C1 – C3), following UCS1 (a, c, e, g) and UCS2 (b, d, f, h).

When comparing results for UCS1 and UCS2, as shown in Figure 6-14, columns J2 and J3 show strength recovery above the residual of UCS1, this being 66 % for J3. For column J2 the peak for UCS2 is higher than that for UCS1. No strength recovery is demonstrated for columns J3 to J6 which contained the untreated fibres. There is also no evident strength recovery for columns containing hemp fibres for this test.

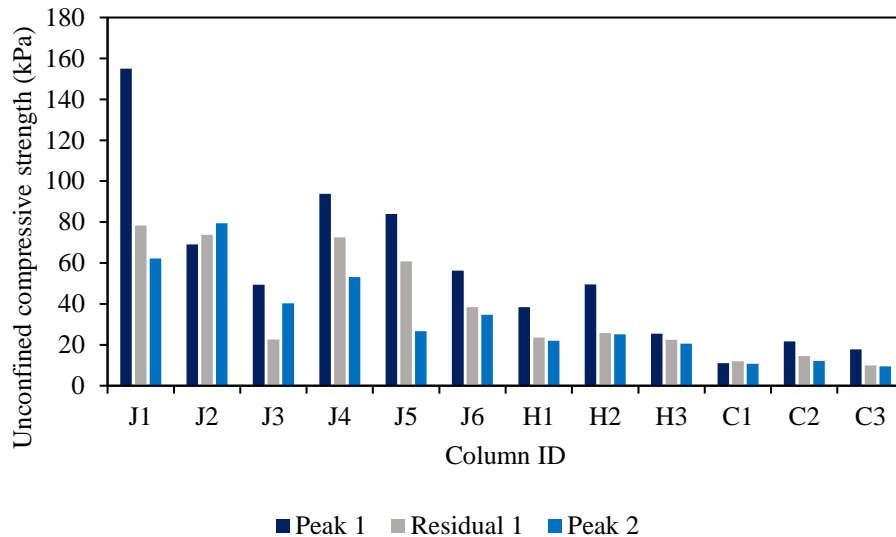


Figure 6-14. Results from UCS1 and UCS2 for Columns Test U2, showing peak and residual strengths from UCS1 and peak strengths from UCS2.

This test demonstrated the positive effect of pre-treating the fibres, as can clearly be seen for jute. Interestingly the self-healing due to the inclusion of CM loaded hemp fibres was not seen in this test. It was noticed that during the drying stage there was no smell of ammonia, unlike during the drying stage for test U1. The lower levels of bacteria likely affected this test and the increased heat during drying seems to have had a positive impact in respect of jute and negative in respect of hemp. The fibre spraying process may also have been more suitable for jute than hemp for immobilising the concentrated CM effectively.

Images taken of the columns during the UCS1 and UCS2 are shown in Figure 6-15 and Figure 6-16 respectively. When compared to Columns Test U1, voids are not observed and shear failure lines can be seen, as highlighted with annotations. Indications of shear failure are less evident in the control column specimens at the UCS2 stage.

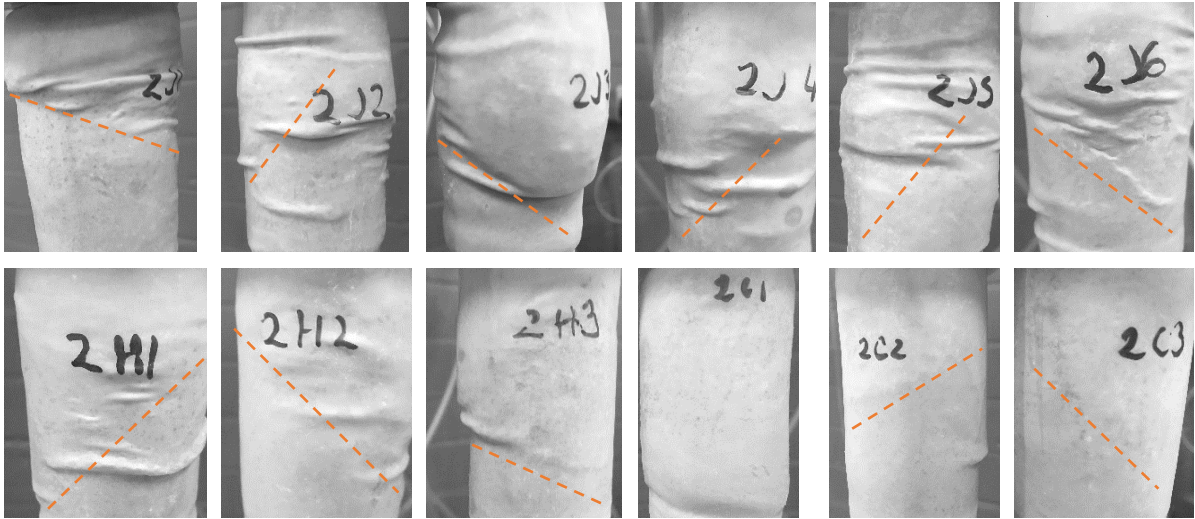


Figure 6-15. Photographs of Test U2 columns during UCS1 following failure, with annotation below observed failure planes.

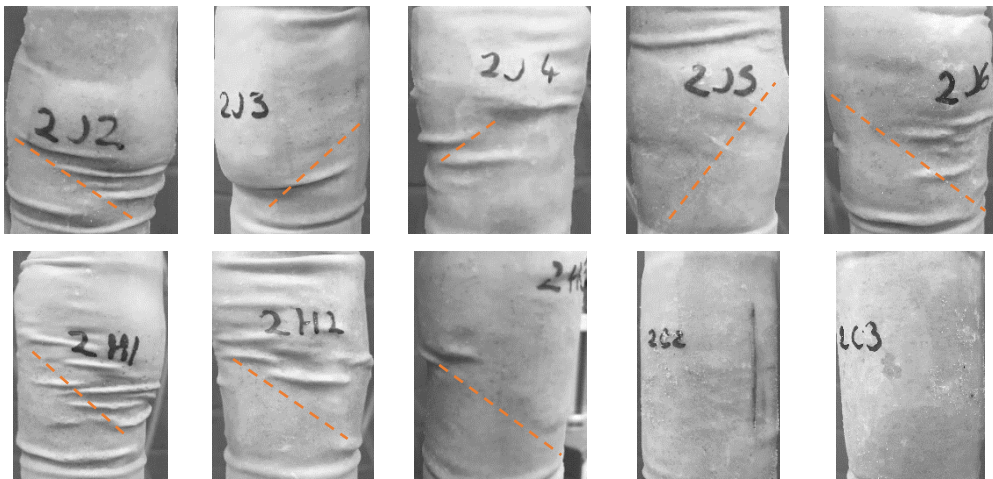


Figure 6-16. Images of Test U2 columns during UCS2 following failure, with annotation below observed failure planes.

6.3.3.3 Mineralogical Analysis

Samples from Test U2 columns were analysed using SEM in April 2021. The clearest examples of precipitate can be seen on the surface of the hemp fibres in Figure 6-17(d-f). The rhomboidal appearance of this precipitate suggests that it is likely calcite. Based on observations in Figure 6-17(e) in particular, the forms on the surface of sand in Figure 6-17(c) are likely also to be calcite. While other images appear to show some precipitate on surfaces of fibres and sand particles it is less clear whether this may be calcium carbonate.

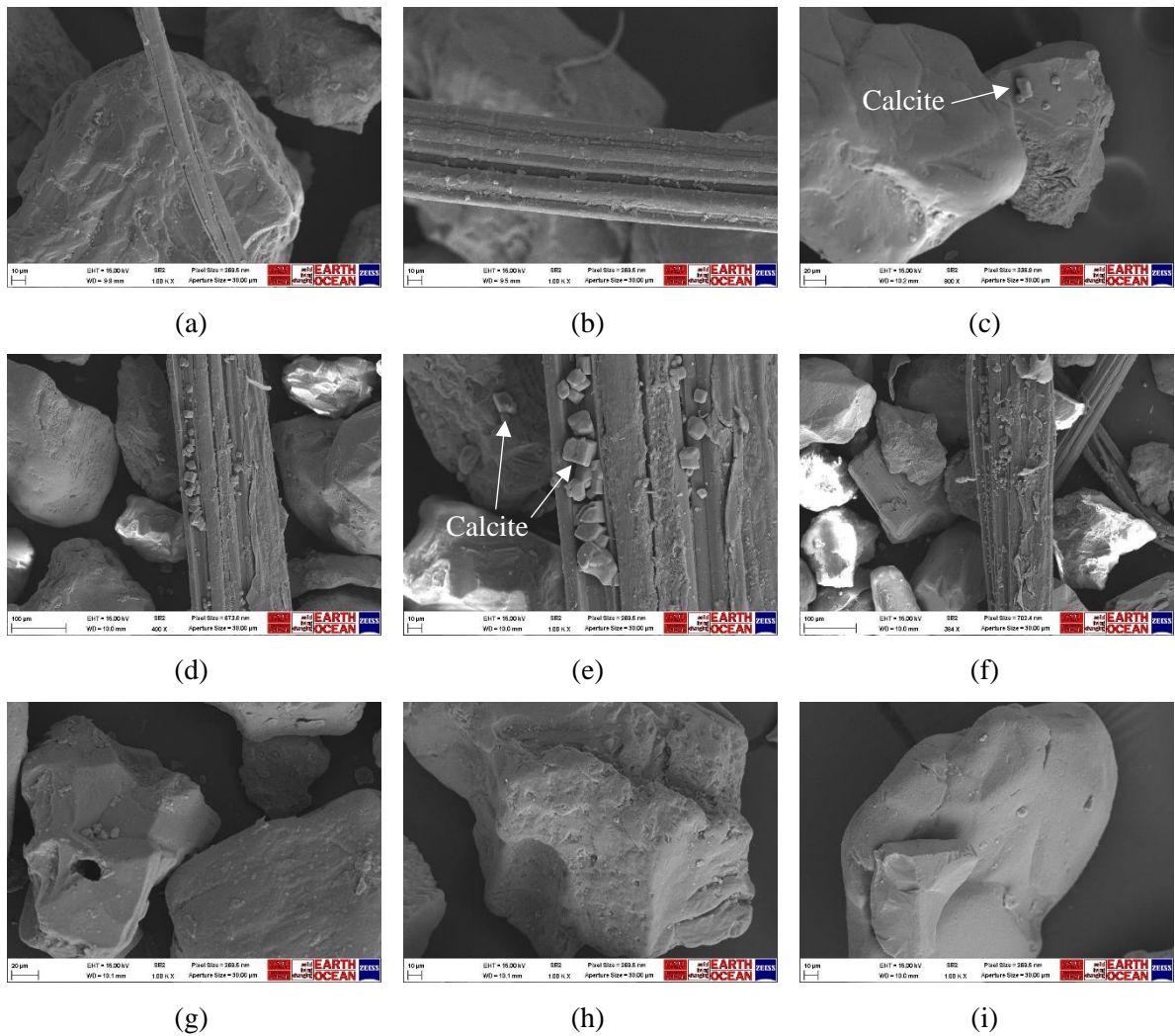


Figure 6-17. SEM images of samples taken from Test U2 columns J1 (a – c) H1 (a -c) and C1 (a – c), with calcite precipitate labelled where clearly identifiable.

The presence of calcium carbonate was confirmed using X-ray Diffraction. XRD testing had been limited due to restricted access to facilities at this time and only a selection of three samples was from Columns Test U2 was tested. The calcium carbonate peaks are shown in blue, with peaks for the silica sand shown in green. The calcium carbonate was identified using Highscore as vaterite, calcite had not been detected for the samples containing hemp or jute. Based on results shown in Figure 6-18, the peak at position 50 is possibly vaterite. Quantities of calcium carbonate had not been significant enough to get clear XRD results when using *S. ureae* for biocementation. These tests were undertaken on samples from columns which had been stored since UCS2 was completed in June 2019.

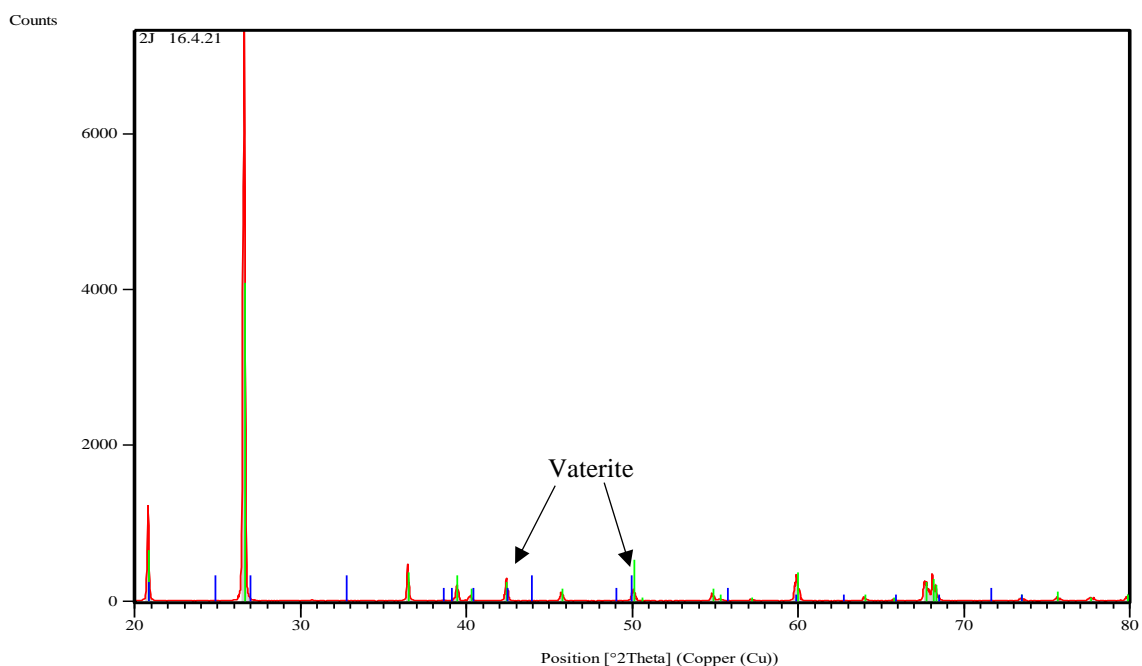


Figure 6-18. XRD analysis of sample from Test U2 column J1, of biocement produced using *S. ureae*. Green peaks show the measured spectra for SiO₂ (sand) and blue peaks show the spectra for calcium carbonate (vaterite).

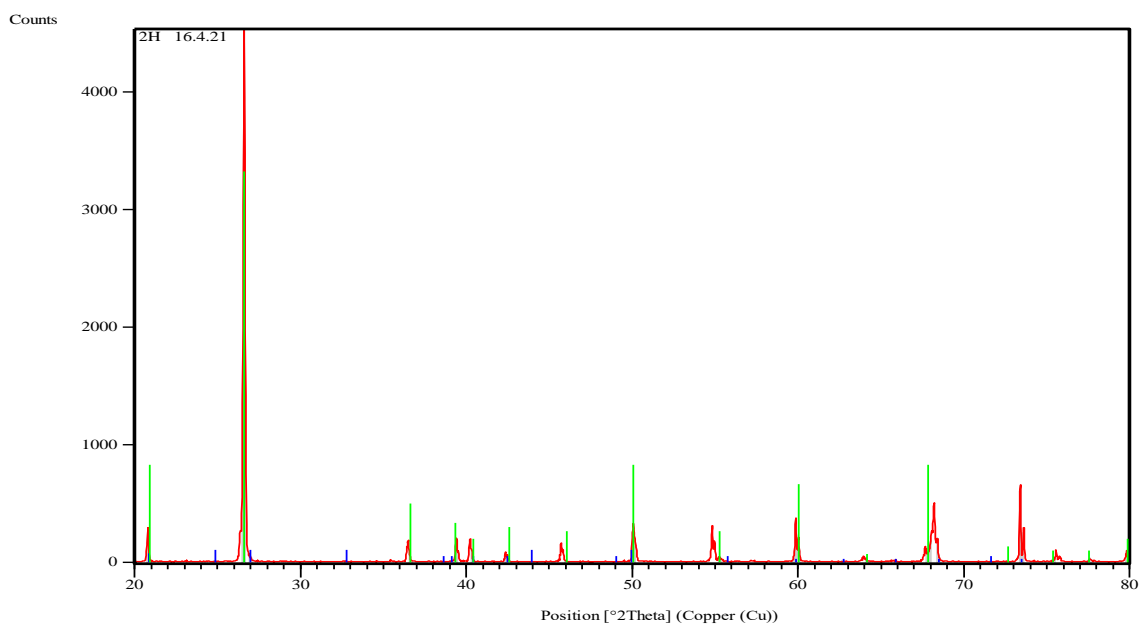


Figure 6-19. XRD analysis of sample from Test U2 column H1, of biocement produced using *S. ureae*. Green peaks show the measured spectra for SiO₂ (sand) and blue peaks show the spectra for calcium carbonate (vaterite).

The XRD results for Columns Test U2, control column one are shown in Figure 6-19. The blue calcium carbonate (calcite) peaks are not visible on this spectrum. Only by zooming in at a peak where there is

no indication of sand, and a good correlation with calcite, is it possible to verify presence of calcium carbonate, as seen in Figure 6-21.

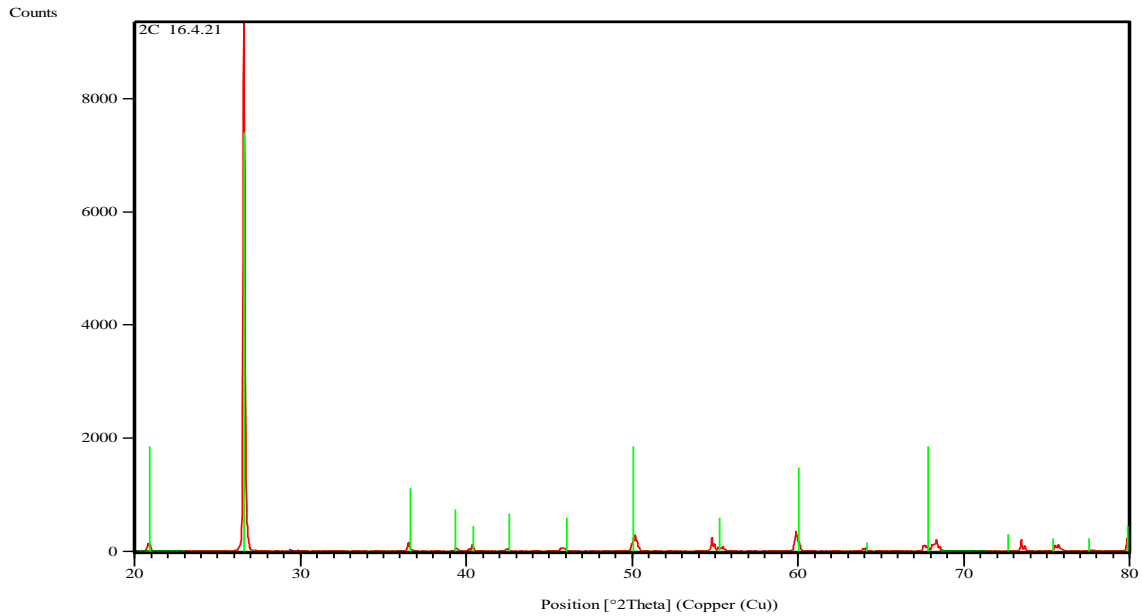


Figure 6-20. XRD analysis of sample from column H1, from columns test U2 with *S. ureae*. Green peaks show the spectra for SiO₂ (sand) and blue for calcium carbonate (calcite).

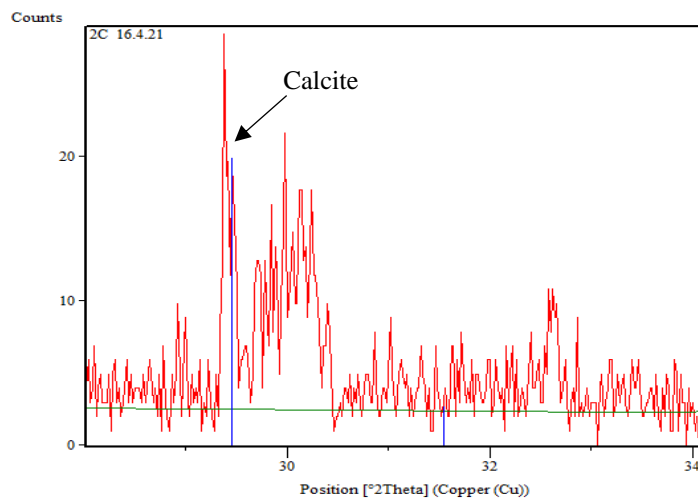


Figure 6-21. XRD analysis of sample from Test U2 column C1. Zoomed-in image of the spectra showing a blue peak indicating calcite near position 30. The dark green horizontal line shows the background level.

6.3.4 Columns Test U3

The methodology for this test was based on and developed following the findings of the prior two column tests. The bacteria for Columns Test U3 were grown to an optical density of 0.890, pelletised and washed, and mixed with cementation medium and the sand pluviated into this mixture to form the columns. The drying temperature prior to UCS testing was maintained at 30°C. This test demonstrated clearly the leaching pattern of the immobilised CM2u from the fibres, through calcium ion measurements, with sufficient medium used to flush columns after each treatment. To help ensure only spores remained in columns for the self-healing stage, the drying time was extended to 28 days.

Table 6-8. Contents of columns prepared for Columns Test U3.

Column ID	Carrier type	Carrier (g)	Immobilised CM (g)	Sand (g)
J1	Jute	1	3.234	123
J2	Jute	1	3.714	123
J3	Jute	1	3.315	123
H1	Hemp	1	1.795	127
H2	Hemp	1	1.638	127
H3	Hemp	1	1.818	127
HJ1	Hemp & Jute	1	2.569	125
HJ2	Hemp & Jute	1	2.290	125
HJ3	Hemp & Jute	1	2.439	125
C1	-	-	-	131
C2	-	-	-	131
C3	-	-	-	131

6.3.4.1 Geochemical Analysis

The pH results are again reduced for this test in comparison to Columns Test U1, albeit consistent across all columns. It is unknown why the bacterial activity appeared to have reduced. The pH rise is however still indicative of MICP, but perhaps reflects that the old medium had not been flushed adequately from columns during each new injection.

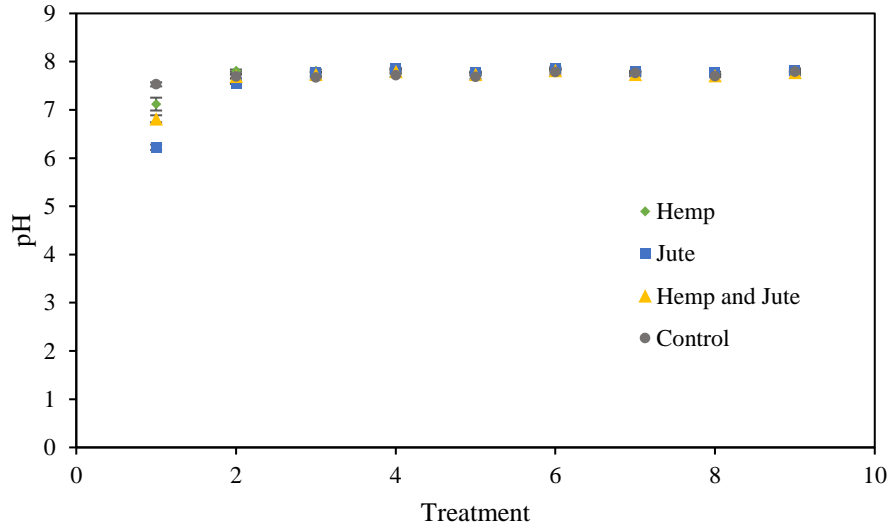


Figure 6-22. pH of effluent from Test U3 columns following each biocementation treatment. Error bars show standard errors of the means for the triplicates.

The results in Figure 6-23 show that the immobilised cementation medium had leached out by treatment five, although there remains a slightly elevated level of calcium ions in effluent from columns containing jute fibres throughout the treatment period.

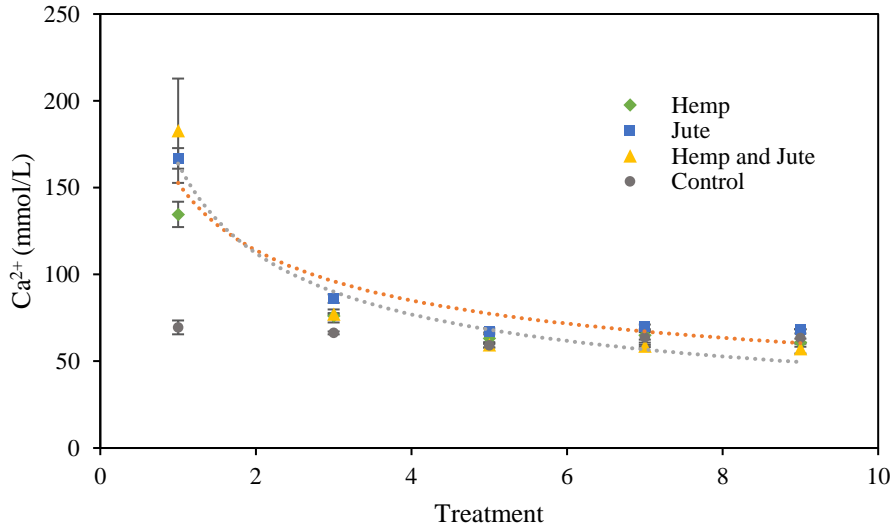


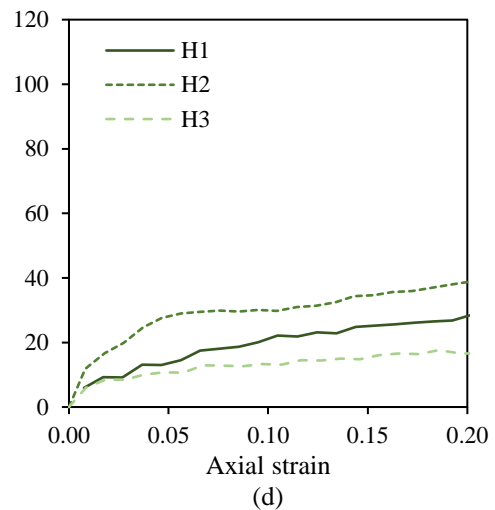
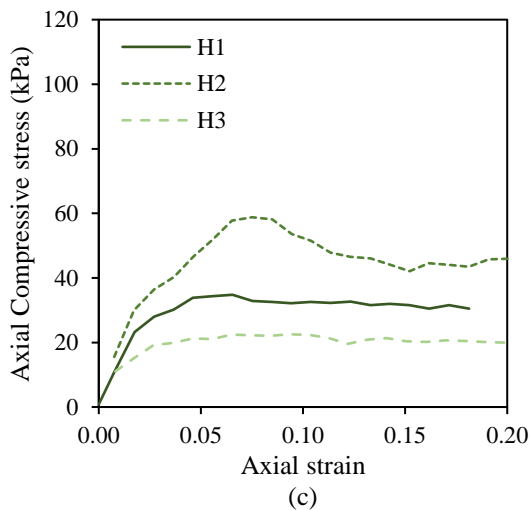
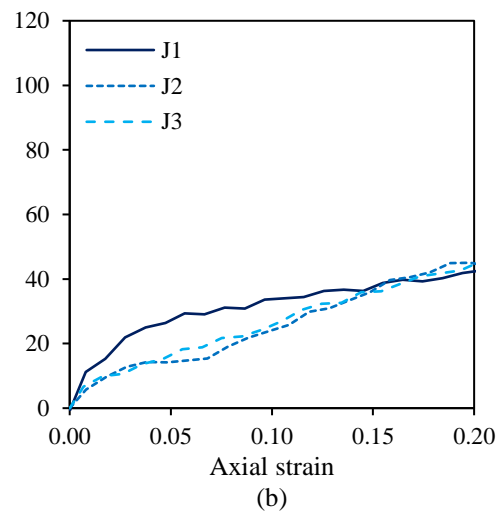
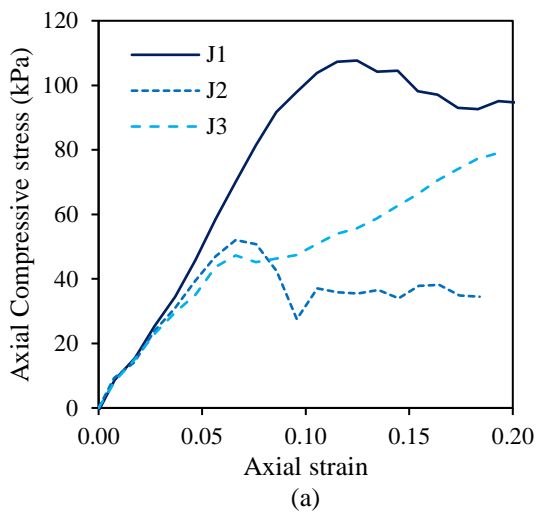
Figure 6-23. Calcium ion concentration, as measured using ICP-OES, in Test U3 columns effluent, following biocementation treatments 1, 3, 5, 7 and 9. Error bars show standard errors of the means for the triplicates.

The results for leaching show an initial faster release of immobilised CM2u in the first 48 h and slower release thereafter. It is also possible for some re-adsorption to have occurred at later stages.

By Columns test U3, it had been observed that the growth of the liquid broth of bacteria used for experiments appeared to be hindered since it would not reach much above an optical density (OD_{600}) of 0.89. The *S. ureae* growth curves verified that growth wasn't as expected. It was therefore necessary to go back to a frozen stock culture. There may also have been a problem with the culture medium.

6.3.4.2 Unconfined Compressive Strength

For this particular test the residual strengths were very high compared to the peak and seemed to have resulted from the extended drying time used, this being twenty-eight days. It is possible therefore that the previous results were due to the presence of vegetative cells and not spores. The leaching from the fibres would not have been altered. This required further exploration. The results for this study do show that the treated fibre additions do appear to embed self-healing capability within the biocement.



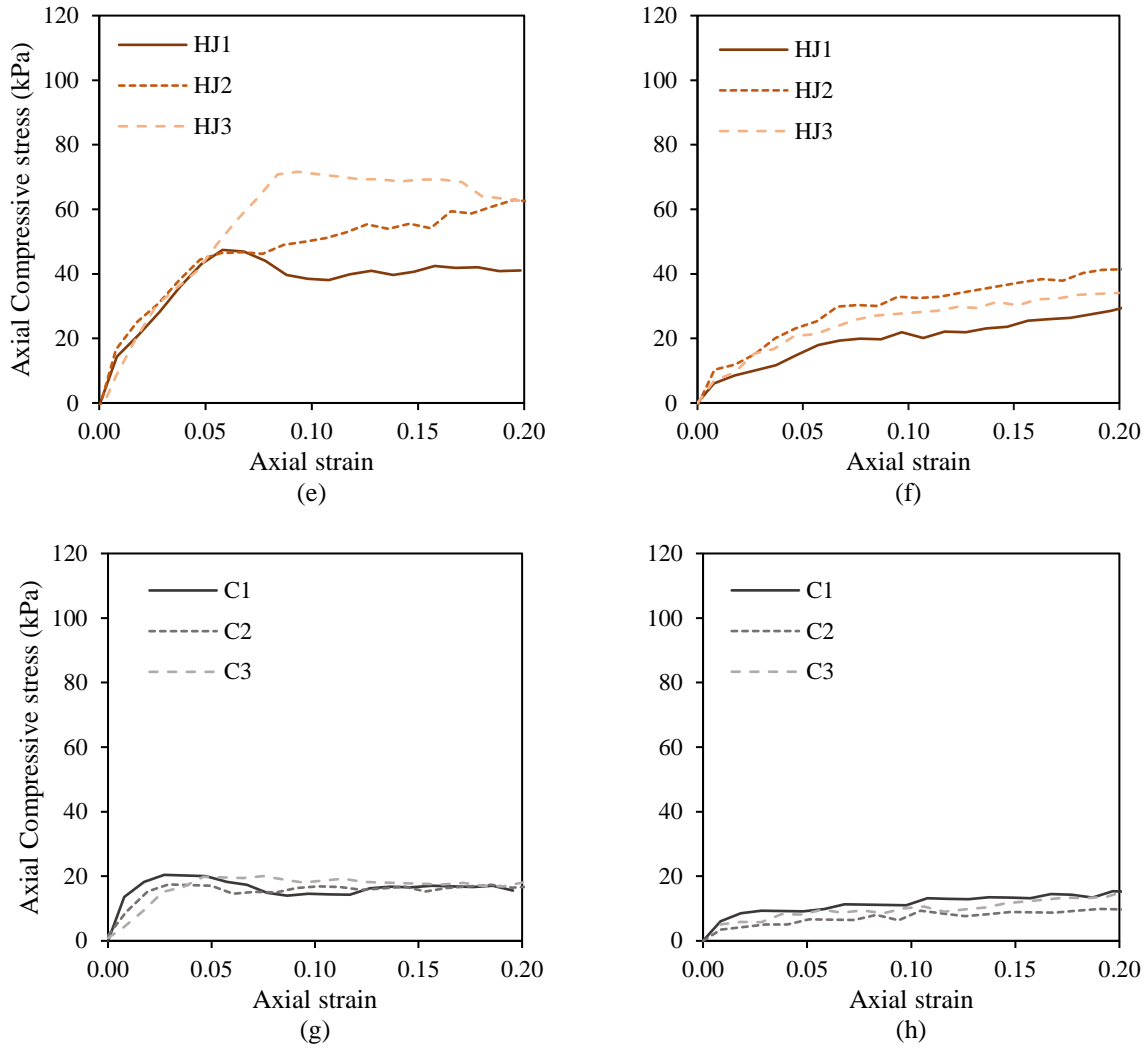


Figure 6-24. UCS test results for Test U3 biocemented columns containing treated jute (J1 – J3), hemp (H1 – H3), jute and hemp (HJ1 – HJ3) and sand only (C1 – C3), following UCS1 (a, c, e, g) and UCS2 (b, d, f, h).

Self-healing responses are indicated in results for columns J1 and HJ1 in Figure 6-25, where it can be observed that the peak for UCS2 is higher than the residuals for UCS1.

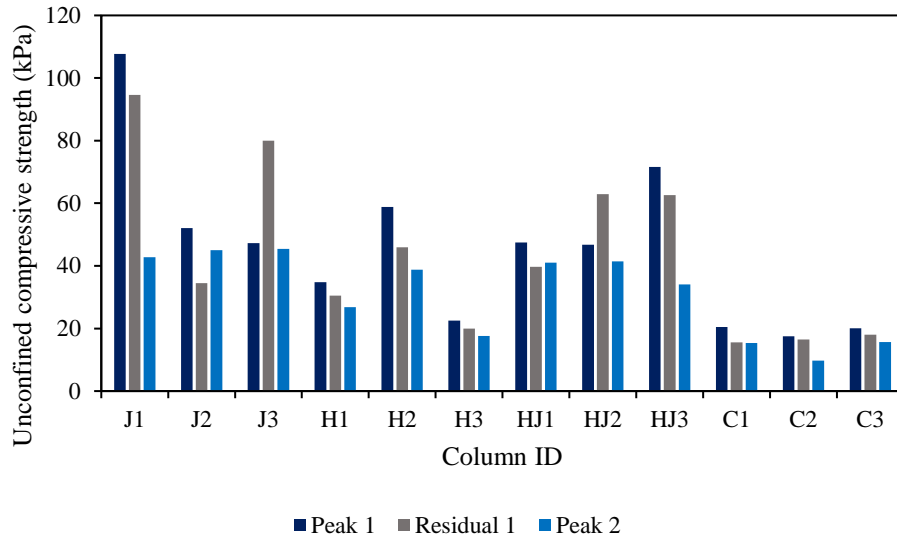


Figure 6-25. Results from UCS1 and UCS2 for Columns Test U3, showing peak and residual strengths from UCS1 and peak strengths from UCS2.

The distribution of fibres will also impact upon strength results, up to this point just 1 % moisture was added to fibres when mixing. This was increased to 5 % for later tests to achieve better fibre distribution. Images of columns following failures for UCS1 and UCS2 are shown in Figure 6-26 and Figure 6-27.

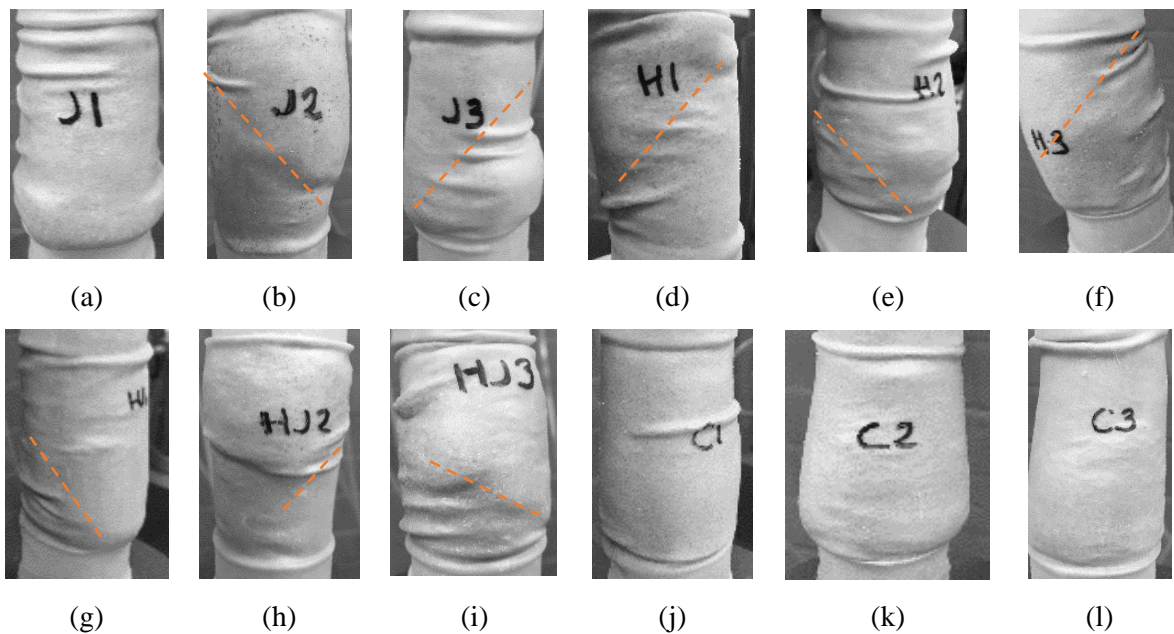


Figure 6-26. Photographs of columns from Columns Test U3 shortly after failure during UCS1, with annotations showing approximate locations of failure planes observed.

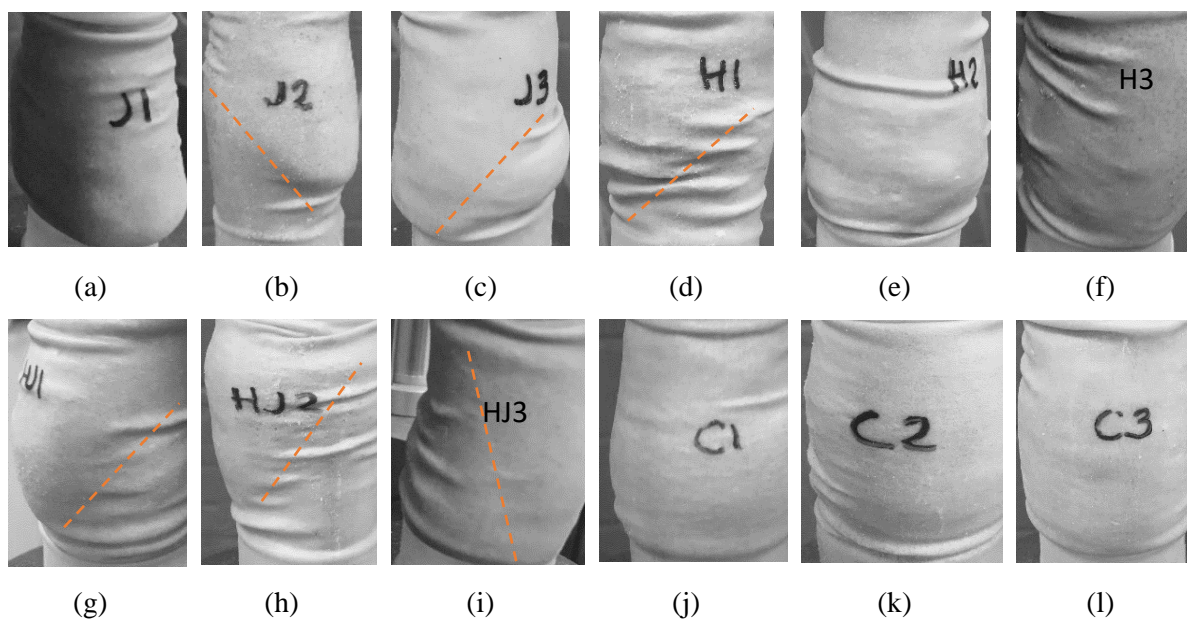


Figure 6-27. Photographs of columns from Columns Test U3 shortly after failure during UCS2, with annotations showing locations of failure planes observed.

6.3.5 Columns Test U4

This column study utilised expanded perlite as the carrier material, with column contents as per Table 6-9. The liquid broth culture for this study was prepared using 13 g/L Oxoid CM0001, to test if this resulted in improved growth and bacterial/ urease activity of *S. ureae*. The culture was grown for the same period of time as for the prior studies, with a resulting optical density (OD₆₀₀) of 1.41. The columns containing EP were compacted to approximately 94 % of the target density, compared to 95 % for controls.

Table 6-9. Contents of columns prepared for Column Test U4.

Column ID	EP (g)	Immobilised CM (g)	Sand (g)	Total Mass (g)
EP1	2.000	3.462	126	131.462
EP2	2.000	3.402	126	131.402
EP3	2.000	3.612	126	131.612
C1	NA	NA	133	132.000
C2	NA	NA	133	132.000
C3	NA	NA	133	132.000

6.3.5.1 Geochemical Analysis

The pH of the columns effluent was found to be higher from the tubes containing EP, after the first treatment, as shown in Figure 6-28. The calcium ion concentration gives insight into the rate of leaching of immobilised CM from the expanded perlite. This appears to happen fairly quickly, results indicate that most of the immobilised CM has leached by treatment three when comparing to the results for controls. There is some variation in results for controls across the treatments, with results having been more consistent for the prior studies detailed in this section.

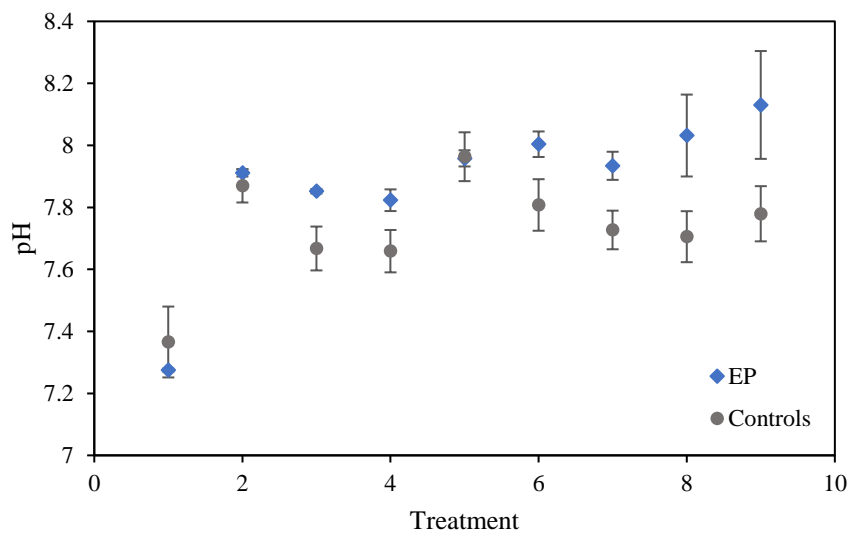


Figure 6-28. pH of effluent from Test U4 columns following each biocementation treatment. Error bars show standard errors of the means for the triplicates.

Results for calcium ions concentration following treatments five are omitted having been deemed anomalous. These results had been lower than the results obtained following treatments seven and nine. It is likely this occurred as there had been a delay in testing the diluted effluent. ICP-OES tests had otherwise been conducted shortly after collection of effluent since any traces of urease in the effluent sample would cause the calcium ions to be depleted further. With the results obtained it had been possible to fit a trendline, with an R squared value of 0.9999.

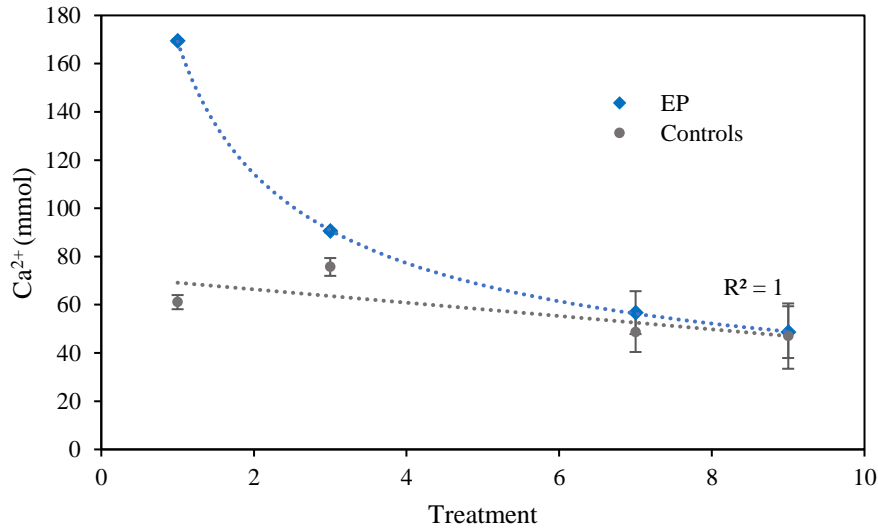


Figure 6-29. Calcium ion concentration, as measured using ICP-OES, in Test U4 columns effluent, following biocementation treatments 1, 3, 7 and 9. Error bars show standard errors of the means for the triplicates.

6.3.5.2 Unconfined Compressive Strength

The strengths of columns, see Figure 6-30 (a-b), produced in this test had been relatively weak following the biocementation treatments, when comparing strengths of controls to the prior studies. The likely cause of this is the use of Oxoid CM0001 for the growth medium, and shows that a high bacterial cell concentration in the inoculant does not correlate with higher urease activity. Oxoid CM0001 is therefore not deemed as suitable for growth of *S. ureae* when using this bacterium to promote MICP. On average there is a slight strength increase for columns containing EP compared to controls, the average unconfined compressive strengths were 16.14 kPa for columns containing EP and 11.85 kPa for the control set of columns. Results therefore show some strength enhancement as a result of EP, however this is a relatively small improvement. Due to the low strengths measured at this stage of testing the test was concluded at this point without the self-healing stage of testing, and no further testing undertaken with the powdered carrier materials.

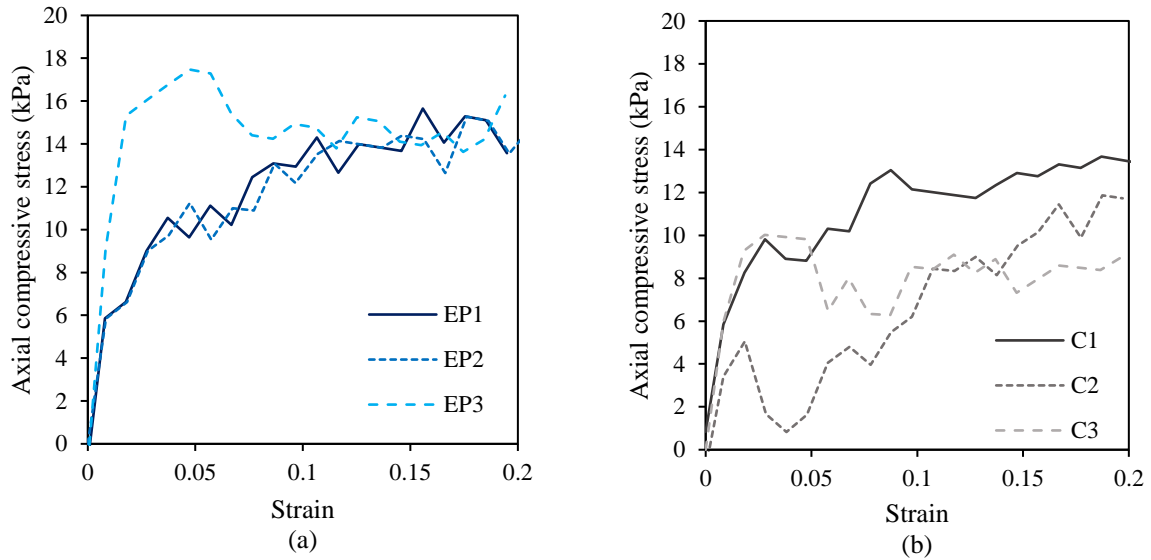


Figure 6-30. UCS test results for Test U4 biocemented columns containing expanded perlite (a) and sand only (b).

The images of the columns shortly after failure, Figure 6-31, when subjected to the UCS testing are indicative of low strengths with mostly barrelling observed at failure in control columns and otherwise some indication of shear as shown.

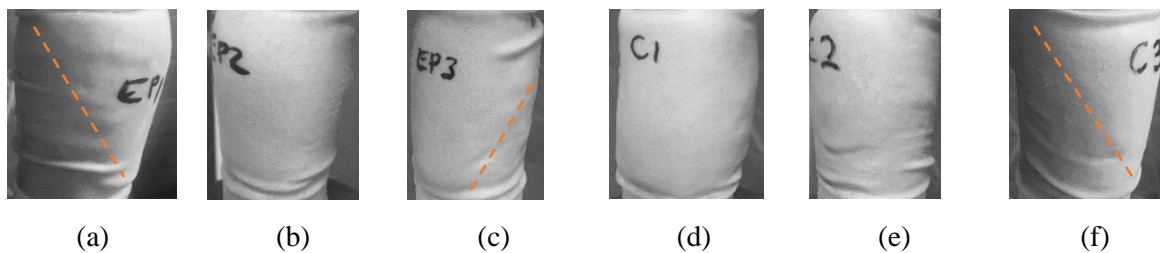


Figure 6-31. Photographs of biocemented columns from Test U4 taken shortly after failure during the UCS test, with annotations showing approximate locations of observed failure planes.

6.3.6 Columns Test P1

An initial columns study was undertaken at this stage using *S. pasteurii*, as a preliminary study prior to the study in the subsequent Chapter Seven. Columns were prepared with contents as per Table 6-10. For comparison with *S. ureae*, the same cementation medium (CM2u) is used for this test. Eight treatments have been supplied as opposed to ten, as at this stage activity was noticed to drop across all columns and due to time constraints. The final cementation medium treatment was a more concentrated one (x3), with the intention of testing if there was reabsorption by fibres.

Table 6-10. Contents of columns prepared for Columns Test P1.

Column ID	Carrier Type	Carrier (g)	Immobilised CM (g)	Sand (g)
J1P	Jute	1	2.929	123
J2P	Jute	1	2.632	123
J3P	Jute	1	2.759	123
H1P	Hemp	1	1.609	127
H2P	Hemp	1	1.631	127
H3P	Hemp	1	1.622	127
C1P	-	-	-	133
C2P	-	-	-	133
C3P	-	-	-	133

6.3.6.1 Geochemical Analysis

The *S. pasteurii* was grown to a cell density of 1.052 (OD₆₀₀). The pH measurements, as displayed in Figure 6-32, show some decline towards later treatments but are still at a level indicative of MICP activity and a common trend is shown across all columns. The calcium ion measurements shown in Figure 6-33, show an indication of increased efficiency in the columns containing the fibres, this was explored in more depth in the subsequent studies detailed in Chapter Seven. When comparing the pH results obtained when using *S. ureae* and *S. pasteurii*, these suggest that from treatment five onwards the *S. pasteurii* bacteria start to decline in number, as evidenced by the pH drop at this point, in contrast this pH level remains constant across the *S. ureae* treatments.

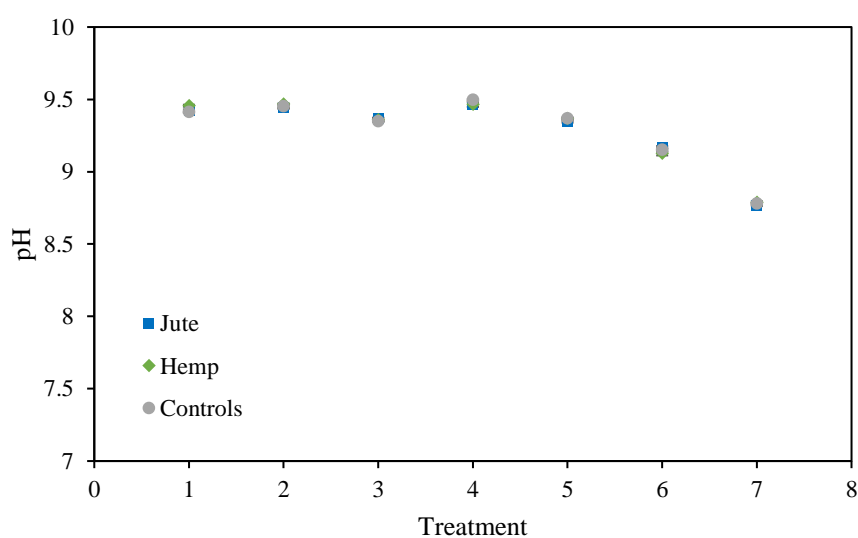


Figure 6-32. pH of effluent from Test P1 columns following each biocementation treatment. Error bars show standard errors of the means for the triplicates.

Calcium ions have been close to 100 % depleted following each treatment, as shown in Figure 6-33. Again, the lower values for columns containing fibres suggests the fibre additions have increased MICP efficiency, this being slightly higher for columns containing hemp compared to those containing jute.

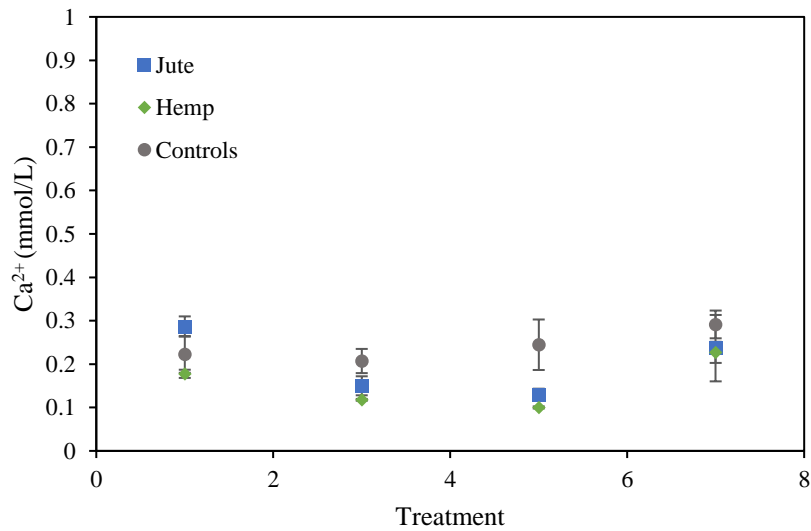


Figure 6-33. Calcium ion concentration, as measured using ICP-OES, in Test P1 columns effluent, following biocementation treatments 1, 3, 5 and 7. Error bars show standard errors of the means for the triplicates.

6.3.6.2 Unconfined Compressive Strength

The unconfined compression test results are shown in Figure 6-34 for all columns. At this stage only UCS1 results were obtained as use of *S. pasteurii* would be explored in detail in subsequent studies, as reported in Chapter Seven. Again, the same trends are observed whereby there are significant strength increases as a result of the fibre additions, in particular jute. The failures occur at between 5 % and 8 % strain. In comparison to results using *S. ureae*, clear peaks are shown for all columns and there is only one instance across the nine columns (column J3) where the residual strength is higher than the peak.

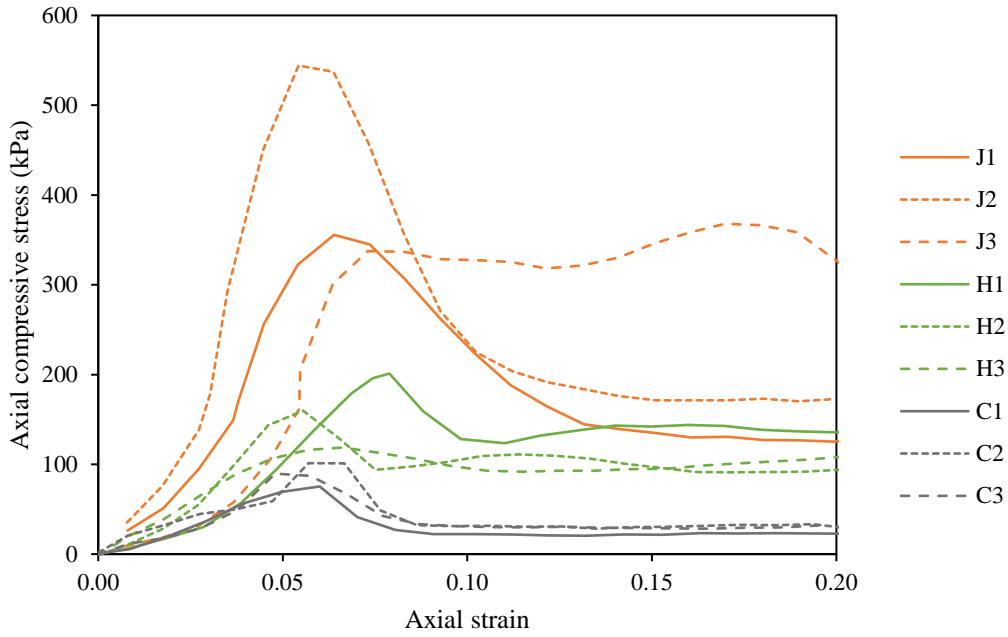


Figure 6-34. UCS test results for Test P1 biocemented columns containing jute (J1-J3), hemp (H1-H3) and sand only (C1-C3).

The images of columns following failure, as shown in Figure 6-35, suggest a more brittle failure has occurred than in the prior column tests, with failure planes also more visible in control columns.

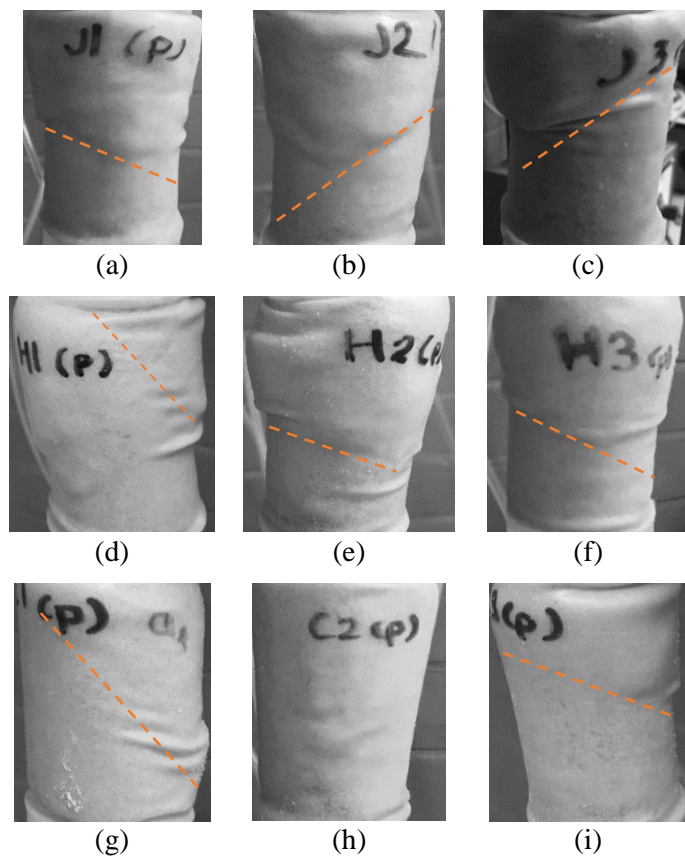


Figure 6-35. Photographs of biocemented Test P1 columns taken shortly after failure during the UCS test, with annotations highlighting approximate locations of observed failure planes.

6.4 Survival of Bacteria in Columns after 1.5 y (Long-Term Survival)

This experiment tested the ability and effectiveness of sporulation of the bacteria, by testing for evidence of bacterial sporulation in biocement samples after drying and a period of storage. Botusharova (2017) noted that in the long-term, survival of bacterial cells cannot be guaranteed, their tests showed that the spores were able to survive for at least six months. Biocemented material from columns produced at Cardiff University in 2019 was retained and later tested for the presence of viable bacteria. Samples were taken from columns produced using *S. ureae* and *S. pasteurii* and containing jute, hemp and EP. The columns had been stored in individual sample bags within a sealed container at room temperature for eighteen months (1.5 yrs). The columns had been transferred to the sample bags immediately after UCS testing.

1 g samples of biocemented sand were taken from approximately the centre of each selected column, from Columns Test U2, U3, U4 and P1, and transferred to autoclave sterilised 50 ml polypropylene centrifuge tubes, to which 10 ml of autoclave sterilised 9 % sodium chloride saline solution was added. These tubes were gently shaken to detach the bacterial spores from the sand to suspend these in the saline solution. It is assumed after this period of storage following nutrient depletion and drying that the bacteria retained within these samples would be in spore form.

A set of agar plates were prepared using the Luria Bertani agar mixture, without urea. The agar was autoclave sterilised and plates prepared in close proximity to a Bunsen burner, to prevent contamination. Initially 55 mm diameter plates were used, onto which 0.5 µl of solution from the tubes containing the biocemented sand and saline solution was transferred using sterile pipette tips. This solution was spread across plates using sterile disposable plate spreaders (Fisherbrand L-shaped sterile cell spreader). This test was then repeated using 90 mm diameter plates. The plates were inverted and incubated for 48 h at 30 °C.

This repeat test verified the results initially obtained. The only difference observed was that for the biocemented sand sample containing jute fibres prepared using *S. pasteurii*. On the first set of plates there was no growth observed on the agar for this column, whereas in Figure 6-36(g) there is a small amount of growth observed, this being much less than that observed on the other plates where growth had been observed. Only a small amount of growth is shown on plate J1 for the test using *S. pasteurii*, evidencing that there had been little to no viable bacteria in this column. It is possible some condensation had got into the plate, the control is clear however which evidences the environment in which the plates were prepared close to the Bunsen had been free of contamination.

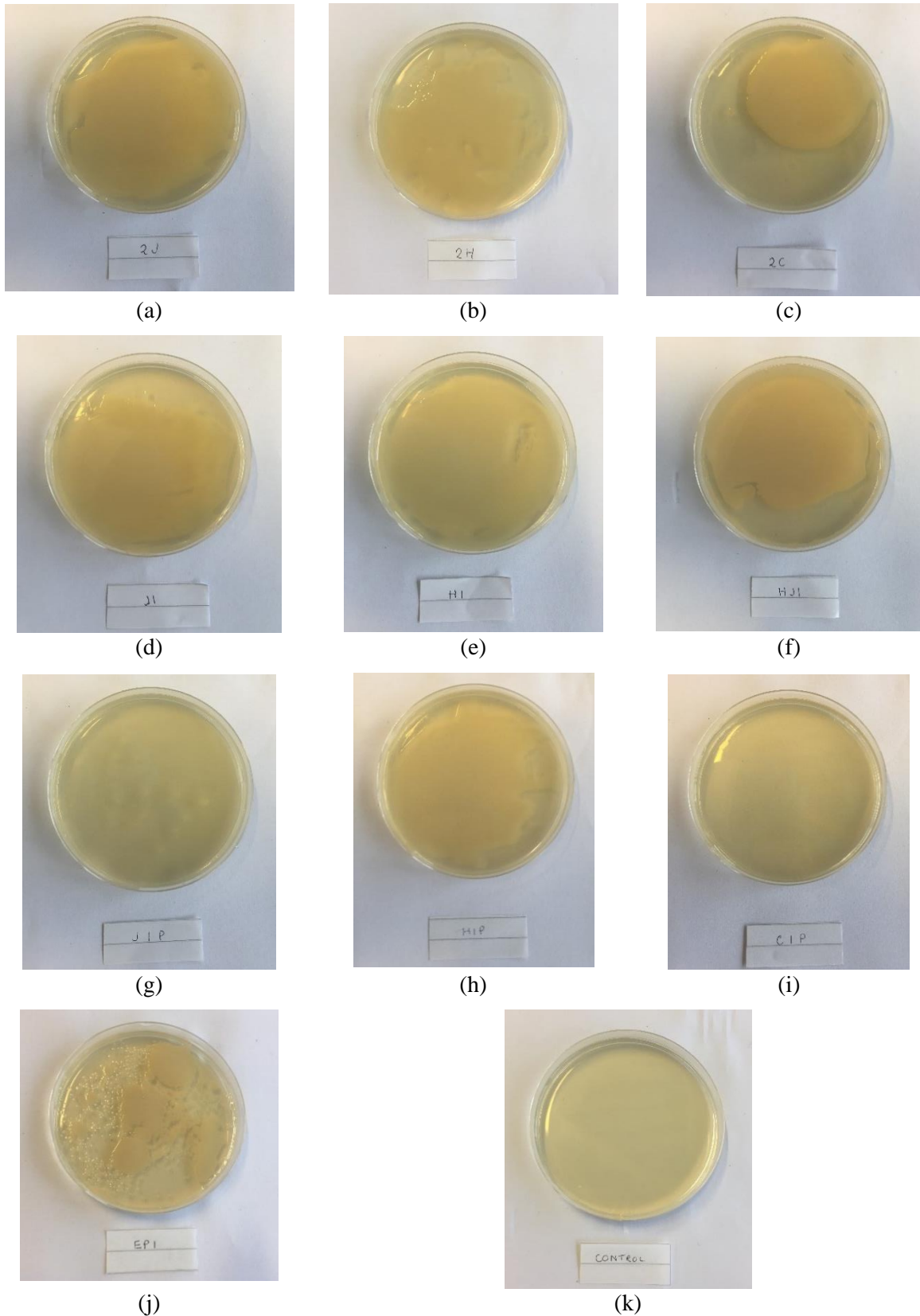


Figure 6-36. Growth of *S. ureae* on LB agar plates inoculated with solutions prepared by taking 1 g samples from selected biocemented columns and dispersing these in a sterile saline solution and pipetting and spreading 10 μ L of the solution onto the plates, followed by 48 h of incubation at 30 $^{\circ}$ C. Prior to testing of the columns these had been stored for one and a half years following the production of columns 5P. Samples were taken from Test 2U columns J1(a), H1(b) and C1(c), Test 3U columns J1(d), H1(e), and HJ1(f), Test 5U columns J1 (g), H1 (h) and C1 (i) and Test 4U column EPI (j). Control plate (k) was not inoculated.

This study provides evidence of the ability and effectiveness of sporulation of both the *S. ureae* and *S. pasteurii* bacteria, since after drying of columns and storage over a long period it is unlikely that there would have been any vegetative cells present given the lack of water, oxygen and nutrients. The results show that the fibre additions have enhanced the long-term viability of the bacteria, particularly when using *S. pasteurii*, which is evident for hemp fibre additions in particular. Where *S. ureae* has been used there is growth observed on all plates. The addition of EP appears to have slightly hindered long-term bacteria viability when compared to jute additions.

6.5 Conclusions

There had been possible indications of self-healing activity where this effect had been tested in Column Tests U1 to U3, more so for Column Tests U1 and U2. For these tests the drying time had been fourteen days, which had been increased to twenty-eight days from Test U3 onwards. It is possible that some vegetative bacteria had remained in the columns for the earlier tests at the self-healing testing stage. Columns had been dried at 30 °C to 40 °C (Test U2) prior to UCS testing. This may not have resulted in all bacteria present in columns only being in spore form, if at all there were spores present. Although a constant mass was achieved when dried for at least fourteen days, the columns will not have been entirely dry due to the relative humidity within the incubator. It is likely that when left at this temperature for longer periods the number of live bacteria will be further depleted owing to the lack of nutrients.

The activity of the *S. ureae* bacteria appeared to decrease as the column tests progressed. The fibre treatment had involved soaking the fibres for use in Columns Test U1. This methodology was developed and fibres were then sprayed from Columns Test U2 onwards, this improved efficiency of the immobilisation process. This appears to have been beneficial when using jute in particular. However, it is possible the hemp fibres did not respond as well to spraying given the lack of self-healing response for hemp containing columns following Columns Test U1. When comparing Figure 6-7 and Figure 6-23, the pattern of leaching shows that the concentrated CM2u appears to leach out of the hemp slower when the fibres have been treated using the soaking process as opposed to being sprayed with the CM2u. This is likely to have had more of an effect than the change to drying duration.

Mixing of the bacteria with cementation medium and wet pluviation of sand columns contents into this mixture appears to have been effective for fixing bacteria to the sand (and carriers). In the prior studies by Botusharova (2017) the bacteria had been suspended in PBS following the pelletisation and washing process. The sand had then been wet pluviated into this mixture. Column Test U2 applied this methodology, before then leaving the column contents for 4 h prior to injecting the cementation medium. It was found that this methodology was not as effective for bacterial fixing, there was some reduction in bacterial activity in columns, as indicated by reduced pH measurements. Calcium ion

measurements also remained higher, when comparing results from Tests U2 and U3. Another issue with this approach is that the immobilised CM1u had leached out early on in the process, thus showing that wet pluviation into CM1u helped reduce leaching quite significantly. Findings show that following wet pluviation of column columns into a bacteria and cementation medium mixture, the immobilised cementation medium is retained to some extent for up to six treatments (based on Columns Test U1). Results suggested the soaking method of immobilising CM2u within/on fibres may help with retention, however this also made fibres difficult to separate and hence strength was less due to clumping. The hemp fibres appeared smoother when observed under an SEM, and therefore may not have retained as much cementation medium on the surface during spraying.

The (assumed) low urease activity associated with *S. ureae* resulted in a weak cementation of the sand. According to Badiie et al. (2019) specimens with UCS values of 50–100, 100–500, and > 500 kPa are defined as lightly, moderately, or heavily cemented, respectively. The results with *S. ureae* fall into the lightly cemented range and below. Botusharova (2017) had achieved similarly low strengths, when comparing columns containing sand only and *S. ureae*, despite the longer retention times used by Botusharova (2017). *Sporosarcina pasteurii* is used for subsequent column studies, since this bacterium has been found to exhibit high urease activity (Whiffin et al. 2004). Fibre additions and the resulting strength increase may improve viability of using *S. ureae* to promote self-healing MICP. Fibre additions appear to have increased the MICP efficiency in addition to significantly increasing strength. This effect is explored further in Chapter Seven. Given the low cementation level when using *S. ureae*, strength increases measured in these tests when compared to controls are likely to be largely due to the fibres alone.

For the column studies reported in Chapter Six, the sand had been acid washed before use. The purpose of this acid washing was to remove any carbonates that may be contained within the sand, before use in the experiments. Acid washing reduces the surface charge of silica sand particles (Peruzzo et al. 2018), which is likely to have the effect of reduced bacterial adhesion and hence the sand becoming toxic to the bacteria. The cell surface charges of *S. pasteurii* are reported to be highly negative (Keykha et al. 2018; Ma et al. 2020), with *S. ureae* cells also known to be negatively charged (Michael Whitaker et al. 2018). Hence, should any chlorides remain on the sand after acid washing this may also result in a reduction in bacterial adhesion. The acid washing of the sand at this stage of the study may have therefore had an adverse effect on bacterial adhesion to sand particles and subsequently a reduction in calcium carbonate precipitation on the sand particle surfaces.

The results from testing selected biocemented sand columns for the presence of bacteria approximately one and a half years after biocement production, demonstrated the spore forming ability of both *S. ureae* and *S. pasteurii*, without a need for this to be induced using a sporulation medium. Viable bacteria was found to be in all columns tested that had been biocemented using *S. ureae*, including the sand only

controls. Use of hemp fibre additions appeared to have had a beneficial effect on spore formation and survival of *S. pasteurii*, since otherwise little to no bacteria was detected in the columns cemented using this bacterium.

7 COLUMN STUDY TWO: Sand Column Studies using *S. pasteurii*, and Jute Fibres as Immobilising Materials

7.1 Introduction

For this phase of experimentation, and for all studies reported from Chapter Seven onwards, the sand columns were inoculated with *Sporosarcina pasteurii*, to overcome limitations of using *S. ureae*. Jute fibres had been selected as the immobilising carrier material for this study, since there were found to be minimal beneficial effects, according to parameters measured, of using the powdered materials in the prior column studies.

This incorporation of sustainable natural fibres such as jute, is an innovative approach to enhance the properties of biocemented sand and soil. The use of fibres to reinforce soil is an established technique, first proposed by Vidal (1969). Jute fibres are widely used in building materials, textiles and packaging. Jute is the most common natural fibre cultivated in the world, it is biodegradable and has good tensile strength (Vigneswaran and Jayapriya 2010). Natural fibres, such as jute, are affordable and recyclable. For structural applications, fibres may be premixed with soil during construction or incorporated in situ using deep mixing techniques. Fibres can be mixed with soil to construct embankment dams and other water-retaining structures to improve resistance to piping erosion, with fibre content determined by suitable piping tests (Shukla 2017).

The study of fibres in combination with MICP, to enhance engineering properties of biocemented geomaterials, is a recent development in this area and to date has focused on synthetic fibres and improvement of the mechanical properties of biocemented sand. Fibres utilised by other researchers to improve strength characteristics of biocemented sand have included PVA (Choi et al. 2016), polypropylene - Fibermesh 150 (Li et al. 2016), basalt fibre (Xiao et al. 2019) and carbon fibres (Zhao et al. 2020). Gao et al. (2019) used polypropylene fibres in an MICP based surficial treatment of sand for seepage control.

This chapter presents the results of a study on the effect of natural jute plant fibres when incorporated into the soil biocementation system. Laboratory sand column experiments had been undertaken to (i) determine the effect of jute fibres on the process of MICP, (ii) quantify effect of jute fibres on strength properties when incorporated into a biocemented sand material, (iii) investigate the effect of varying nutrient (Oxoid CM0001) concentration and (iv) to further investigate potential for use of jute fibres in

self-healing geotechnical systems. The first laboratory test presented in this chapter is a columns study in which a cementation medium containing 6 g/L Oxoid CM0001 nutrient broth is supplied to all columns, followed by a second set of columns injected with a cementation medium containing 3 g/L Oxoid CM0001. The cementation medium constituents and laboratory conditions are otherwise the same for each of the two columns studies. The effects on the process of MICP of the jute additions have been measured through monitoring of pH and electrical conductivity, measurement of chemical conversion, and quantification of calcium carbonate precipitated within columns. The resulting material properties and self-healing in respect of strength regain following mechanical damage were determined using the unconfined compression test.

7.2 Column Study Methodology Changes

Following outcomes of prior studies as detailed in Chapter Six, the methodology has been further developed. At this stage of testing the columns were not dried prior to UCS testing. This methodology incorporating drying of columns had followed on from studies by Botusharova (2017) to help ensure only spores remained in biocement and not vegetative cells. Ordinarily, and in accordance with BS 1377-7:1990 (British Standards Institution 1999) samples are not dried prior to the UCS test. When dried at low temperatures samples will contain some moisture due to the relative humidity of the apparatus in which they are dried, which could introduce capillary affects and thus introduce some unreliability with regards to the unconfined compressive strengths measured. Recrystallisation of any unused substrates due to drying will also have some effect on strength of the biocemented columns. Columns that are biocemented to a greater extent, as can be achieved using *S. pasteurii*, will be more difficult to remould prior to the self-healing stage of testing if dried prior to UCS testing. Drying also appears to result in significant increases in residual strength when compared to peak strength.

The cementation medium constituents (precursor chemicals and nutrients) remain the same, however the quantities of these have changed as stated in the studies detailed in this chapter. The higher urease activity of the *S. pasteurii* facilitates a more rapid chemical conversion and therefore a higher molarity of substrates was used. The effect of variation of quantities of nutrients (Oxoid CM0001) has been studied in this chapter. The studies in Chapter Seven utilise an optimised cementation medium, with outcomes of experimentation detailed in Chapter Nine providing more insight into effects of augmentation of the medium with ammonium chloride. A slightly higher molarity of urea is used compared to calcium chloride dihydrate to enable complete hydrolysis.

At this stage of testing sand columns were injected with five cementation treatments. This follows insight gained from prior studies where the rate of leaching of immobilised cementation medium from the carrier materials was observed, as detailed in Chapter Six.

The *S. pasteurii* bacterial suspension was injected into the base of the assembled columns for studies detailed in Chapters Seven to Nine, as opposed to being mixed with the cementation medium during column assembly. This injection of bacterial suspension was immediately followed by the injection of cementation medium for treatment one, using a pumping rate of 1.5 mL/min (approximately three pore volumes per hour). This injection had the effect of fixing the bacteria as this was pushed through the sand column. This is also methodology which can be applied in the field.

The sand used in studies reported from Chapter Seven onwards was not acid washed since it was recognised at this stage that this may alter the surface roughness of the sand and therefore its effectiveness to fix bacteria. The F60 sand used, and also F65, was also found to have negligible carbonate content prior to use in the experiments.

Prior to the tests reported in Chapter Seven, a set of test columns had been prepared through which cementation medium was injected at differing pumping rates ranging from 1.25 mL/min to 2.0 mL/min. The distribution of bacteria in columns was assessed based on electrical conductivity measurements of effluent. When using pumping rates of 1.75 mL/min and above some cloudiness was observed in the effluent, as a result of bacteria leaching from columns and the *S. pasteurii* inducing MICP and therefore calcium carbonate precipitation in the effluent. A rate of 1.25 mL/min resulted in uneven distribution of electrical conductivity. A pumping rate of 1.5 mL/min was therefore selected based upon measured conductivities across these test control columns. The electrical conductivity measurements provided an indication of the distribution of bacterial activity and therefore calcium carbonate precipitate in the columns, which would be later verified through Calcimeter tests. It was expected that there may be differences in respect of bacterial distribution in columns when comparing columns containing sand only and those containing sand and fibres, given potential immobilisation by fibres of the bacteria/urease.

7.3 Materials and Methods

7.3.1 Sand and Testing of Properties

A fine F60 foundry sand (U.S. Silica, Ottawa, IL, USA) was selected for this study since the optimum grain size for MICP is 0.05 mm to 0.4 mm (Rebata-Landa 2007). Particle size distribution tests were conducted in accordance with ASTM D6913/D6913M-17 (ASTM International 2017), to verify the provided product data as given in the appendix, in addition to Proctor compaction tests, in accordance with ASTM D1557-12e1 (ASTM International 2012), to establish target density for the sand columns when using F60. Properties as otherwise reported by U.S. Silica Company (Ottawa, IL, USA) are as per Table 7-1.

Table 7-1. F60 sand properties (U.S. Silica Company).

Sand Origin	G _s	ρ (g/cm ³)	Mineralogy	Shape
Ottawa	2.65	1.522	Quartz	Round

Prior to use, the sand was autoclaved at 120 °C for 20 min and oven dried at 105 °C for sterilisation purposes. The F60 sand was found to have negligible calcium carbonate content when tested using a calcimeter, and therefore no further treatment of the sand was required.

7.3.2 Fibre Preparation

Natural jute fibres (Sunrise Agriculture, Ajmer, Rajasthan, India) were used for this study. The fibres were initially of variable length prior to processing. Clumps of fibres were gently brushed and then hand cut to approximately 6 mm. The length of fibres ($n = 20$) averaged $5.88 \text{ mm} \pm 1.60$. A scanning electron microscope (SEM; SNE-4500M Plus Tabletop, SEC, Korea) was used in this study to measure the diameter of the fibres following the production of the biocemented sand columns. Prior to use, the jute fibres were washed thoroughly using a sieve and deionised water, followed by autoclaving at 121 °C for 20 min. The fibres were then oven dried at 50 °C. Autoclaving was not considered to have an adverse effect on the fibres given its short duration. Lignocellulosic fibres have been observed to thermally degrade through dehydration, depolymerisation and oxidation when heated (Vigneswaran and Jayapriya 2010), dependent upon temperature and duration of heat exposure. Van de Velde and Baetens (2001) reported that after exposing flax fibres to 120 °C for up to 2 h no significant decrease in tensile strength was observed.

7.3.2.1 Pre-Treatment of Jute Fibres

A concentrated cementation medium, CM4p, was prepared as per Table 7-2, to treat fibres to be contained within three of the nine columns prepared for each of the two studies presented in this chapter. The treated fibres for each study had been prepared at the same time and the spraying method earlier developed applied. This concentrated medium contained the basic chemicals required for the MICP process, urea and calcium chloride in the form of calcium chloride dihydrate, along with Oxoid CM0001 to provide a nutrient source for the bacteria. Oxoid CM0001 (Oxoid Ltd, Basingstoke, UK) is a dehydrated culture medium. The typical 13 g/L solution of Oxoid CM0001 used for the production of liquid broth cultures contains 1 g/L 'Lab-Lemco' beef extract, 2 g/L yeast extract, 5.0 g/L peptone and 5.0 g/L sodium chloride.

After following the fibre preparation procedure outlined above, 1 g quantities of jute fibres were placed onto individual 15 cm × 15 cm squares of 60-mesh stainless steel gauze with an aperture of 0.263 mm and 39 % open area, with draining trays beneath and sprayed with equal amounts of CM4p

(approximately 15 mL) until fully covered with this liquid. The fibres were then placed in a sealed plastic container for 24 h to allow for absorption of the CM, before oven drying at 50 °C for 48 h. Fibres were removed from the mesh and immediately transferred to sealed sterile containers after drying. Due to the hydrophilic nature of the jute, these fibres will readily absorb moisture once exposed to air. The containers were weighed before and after filling (once fibres had cooled to room temperature) to quantify the amount of solid immobilised CM on each set of fibres. From this set of six fibres, the treated fibres were divided into two sets with closely matching quantities of dried immobilised CM.

7.3.3 Bacteria Culture

Non-pathogenic (ACDP Group 1) *Sporosarcina pasteurii*, commonly found in soil, was obtained from the American Type Culture Collection, Manassas, VA, USA, (ATCC 11859) as a freeze-dried culture and used to produce a stab culture for storage at 4 °C. Bacteria were transferred from the stab culture using a sterile inoculation loop onto plates of Luria–Bertani (LB) agar amended with 20 g/L syringe filtered urea. Growth medium for plates contained 5 g/L yeast extract, 10 g/L tryptone, 10 g/L sodium chloride, 15 g/L agar and 20 g/L urea in deionised water. The inoculated plates, sealed with gas-permeable film, were incubated at 23 °C room temperature for 48 h. Single colonies from the plates were used to inoculate liquid growth medium. Triplicates of 50 mL liquid broth cultures were produced in 250 mL Erlenmeyer flasks, for use as an inoculant for further liquid broth cultures to be used in experiments. The liquid growth medium consisted of 13 g/L autoclave sterilised Oxoid CM0001 and 20 g/L syringe filtered urea in deionised water. Flasks were shaken at 23 °C, 150 rpm until the late-exponential phase of growth was reached after approximately 12 h and then stored at 4 °C. Liquid broth cultures were produced in 50 mL quantities using 250 mL Erlenmeyer flasks for batch tests, followed by multiples of 150 mL in 500 mL flasks for the column studies for which greater volumes were required.

Bacterial cultures for use in experiments were inoculated using 100 µL liquid broth culture per 50 mL growth medium and aerobically grown at 23 °C, 150 rpm until an optical density at a wavelength of 600 nm (OD_{600}) of 0.9–1.2 was obtained, which equates to approximately 7.5×10^7 – 1.1×10^8 cells/mL, according to the relationship reported by Ramachandran et al. (2001). For the column studies, freshly grown liquid broth cultures were transferred to 50 mL sterile polypropylene tubes, each containing 35 mL culture, and centrifuged at 5000 rpm for 20 min. The supernatant was then removed, and a sample taken from this to measure the optical density, to take into account any loss of bacteria in the supernatant. The bacteria were then resuspended in a small quantity of phosphate buffered saline (PBS), dispersed using a pipette and transferred to 15 mL centrifuge tubes from which bacteria would be injected in the columns. These bacterial suspensions were made up to 10 mL with additional PBS. Use of PBS ensured the bacteria would not undergo osmotic shock which would otherwise occur in water. Aseptic technique was followed throughout, and involves using lab practices which prevent

contamination, to help ensure that the only bacteria present within the culturing flasks and columns was *Sporosarcina pasteurii*.

7.3.4 Preparation of Cementation Media

Four variations of the cementation medium (CM) were produced for column treatments, as per Table 7-2. The basic constituents of the CM as required for the process of MICP are urea and a calcium source. Calcium chloride dihydrate was selected for the calcium source. A slightly higher molarity of urea was used in comparison to calcium chloride dihydrate, since this helps ensure all calcium can be utilised. In addition, a source of nutrients, Oxoid CM0001, was added to the cementation medium to promote ongoing bacterial growth and therefore urease activity during treatment. CM1p consisted of 0.67 M urea and 0.50 M calcium chloride dihydrate, in addition to 3 g/L Oxoid CM0001 and was used as a fixation medium to fix the bacteria to the sand within the columns in addition to initiating MICP. Cementation media CM2p and CM3p are augmented with ammonium chloride, sodium bicarbonate and nutrients for the bacteria, as per cementation media used by Montoya and Dejong (2015), Stocks-Fischer et al. (1999) and Al Qabany and Soga (2013), and contain 6 g/L and 3 g/L Oxoid CM0001 respectively, 0.187 M ammonium chloride and 0.025 M sodium bicarbonate. Sodium bicarbonate is added to stabilise the pH of the cementation medium before injections (Al Qabany and Soga 2013), and addition of ammonium chloride was found to help stimulate the MICP process beyond the initial injection (Treatment 1) with CM1p.

Table 7-2. Composition of cementation media for use in column studies incorporating jute fibres and using *S. pasteurii*.

Precursor Chemicals and Nutrients	CM1p	CM2p	CM3p	CM4p	Sterilisation
	(g/L)	(g/L)	(g/L)	(g/L)	Method
Calcium chloride dihydrate (CaCl ₂ ·2H ₂ O)	73.51	73.51	73.51	147.02	Autoclaved
Urea (NH ₂ (CO)NH ₂)	40	40	40	80	Syringe filtered
Ammonium chloride (NH ₄ Cl)	0	20	20	-	Autoclaved
Sodium bicarbonate (NaHCO ₃)	0	2.12	2.12	-	Syringe filtered
Oxoid CM0001 Nutrient broth	3	6	3	12	Autoclaved

The cementation media were prepared using tap water. Results from a batch test conducted as part of this study provided evidence of the beneficial effect of using tap water for the media compared to deionised water. CM1p was produced by first autoclaving a solution containing calcium chloride dihydrate and Oxoid CM0001, into which a solution containing urea was syringe filtered. To prepare 2.0 L of CM2p and subsequently CM3p, firstly the ammonium chloride and Oxoid CM0001 were

dissolved in 1.6 L tap water. This solution was adjusted to pH 6.0 using 2.0 M HCl prior to then adding the powdered calcium chloride dihydrate. The pH adjustment prevented the calcium precipitating out into the solution. This solution was autoclaved then made up to 2.0 L by adding a solution containing the urea and sodium bicarbonate using a 0.2 μm syringe filter.

7.3.5 Urease Activity and Batch Test

Urease activity (mM urea hydrolysed/ min) was determined as per the relationship derived by Whiffin (2004) Equation (4-2), based on a conductivity assay. Electrical conductivity was measured over five minutes to obtain the average activity per minute, as per Harkes et al. (2010). This process was repeated three times for each sample tested and an average taken from the three results. Specific urease activity (mM urea hydrolysed/ min/ OD_{600}) as further defined by Whiffin (2004) as the amount of urease activity per biomass, was calculated as per Equation (4-3).

A batch test was conducted to determine effects on urease activity of (i) bacterial growth in tap water and deionised water, (ii) inoculation of medium with plate cultures or liquid broth culture, (iii) initial pH of growth medium. 50 mL liquid broth cultures were prepared using tap water or deionised water as described above and grown at 23 °C for 19 h, to achieve a stationary stage of growth. The nutrient medium was inoculated with either 100 μL of a liquid broth culture grown to 1.0 OD_{600} or with one colony from a plate culture. To test the effect of pH of the nutrient medium on urease activity the pH of the solution of Oxoid CM0001 nutrient broth in water was adjusted prior to autoclaving and adding urea, after which a 1 mL sample was taken to test the pH prior to inoculation.

7.3.6 Preparation of Columns

Columns were assembled as described in Chapter Four, and as shown in Figure 4-14 and Figure 7-1, with lengths of 71 ± 1 mm and diameters of 39.5 ± 1 mm. Masses of sand and fibres used within columns were as given in sections 7.4.3 and 7.4.4 and were consistent across the two column tests. The jute fibre content of columns was 0.75 % by weight of sand. Columns were prepared in triplicates, with three columns containing sand and jute fibres, three columns containing sand and jute fibres pre-treated with CM4p and three sand only controls. Column contents were wet pluviated into 35 mL of sterile CM1.



Figure 7-1. Photograph of prepared columns, showing apparatus used for the column studies completed at Arizona State University.

Prior to addition to the columns, the untreated and treated jute fibres were mixed with the sand for each column. After weighing the sand and adding fibres a small quantity of CM1p was added, equating to 5% of the total mass of the sand and fibre mixture, to aid mixing. Hydration prior to mixing also helps prevent fibre sand segregation (Ibraim et al. 2012). This was then mixed by hand for approximately five minutes, until an even distribution of fibres was observed. The quantity of liquid added to the sand aided mixing while ensuring that it was still possible to pluviated the sand into the columns. Columns were kept at an ambient constant room temperature of 23 °C throughout.

7.3.7 Bacteria Fixing and Biocementation

To achieve biocementation, a two-stage process was applied involving (i) the injection of a bacterial suspension, followed by (ii) injections of cementation medium (treatments), as per the schedule outlined in Table 7-3. The first treatment, using CM1p, is injected immediately after the bacterial suspension and has the effect of fixing the bacteria within the columns in addition to initiating MICP. Harkes et al. (2010) found that when a cementation solution consisting of 1 M equimolar urea and calcium chloride was injected into columns immediately after a bacterial suspension this resulted in 100% retention of bacteria, as determined by optical density measurement of effluent samples. Divalent cationic ions such as Ca^{2+} may enhance the attachment of bacteria to surfaces by reducing electrostatic repulsion (Renner and Weibel 2011). The bacterial suspension was injected upwards into the base of all columns simultaneously using a Cole-Parmer Masterflex L/S peristaltic pump and multi-channel pump head. The peristaltic pump was calibrated beforehand using the Tygon S3 2-stop 2.79 mm ID microbore tubing and was set to a constant 1.5 mL/min pumping rate. At this rate flow through columns is expected

to be laminar. The pump was calibrated before use, to obtain the relationship between the pump speed (RPM) and volume of liquid dispensed (mL/min) as shown by the calibration curve in Figure 7-2.

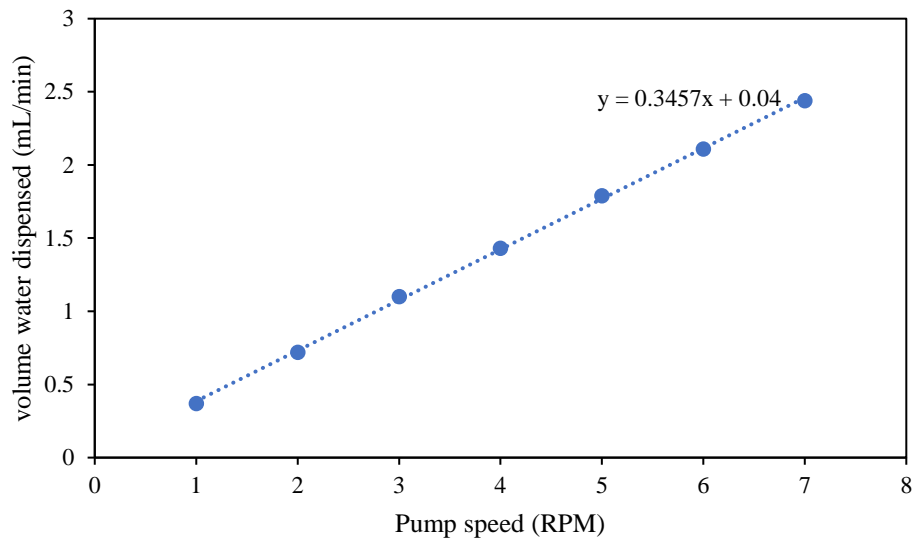


Figure 7-2. Calibration curve for Cole-parmer Masterflex L/S peristaltic pump, using Tygon S3 2-stop 2.79 mm ID micropore tubing and tap water as the test fluid.

This inoculation injection was followed immediately by one and a half pore volumes of CM1p being pumped upwards into the columns. To ensure that no air entered the columns, the inlet tubing was transferred to the container containing CM1p while the tubing was filled with the bacterial suspension. The outlet tubing from columns was then drained and reconnected after each treatment and ends secured to prevent air flow. The inlet tubing was also closed off with clamps and disconnected from the pump tubing following each treatment. On each of the following four days, one and a half pore volumes of CM2p (Column Test P2) or CM3p (Column Test P3) were pumped through the columns, as per the schedule detailed in Table 7-3. Retention periods had been estimated based upon a preliminary column test in which columns had been injected every 24 h.

Table 7-3. Biocementation treatment schedule for Column Test P2 and Column Test P3.

Day	Time Since Prior Injection (h)	Test 1 Column Injection (1.5 × Pore Volume)	Test 2 Column Injection (1.5 × Pore Volume)	Treatment
0	0	CM1p	CM1p	1
1	16	CM2p	CM3p	2
2	22	CM2p	CM3p	3
3	24	CM2p	CM3p	4
4	24	CM2p	CM3p	5
12	192	Tap Water	Tap Water	None

The timing between treatments had been determined by preliminary studies undertaken as part of this research, and based upon the time taken to deplete the calcium source in columns containing jute, in which this occurred fastest. While injecting CM2p the effluent was collected in a series of 5 mL quantities in 15 mL polypropylene tubes.

7.3.8 Measurement of Electrical Conductivity, pH and Evaluation of Bacterial Fixing

The measurement of pH and electrical conductivity can provide an indication of the extent of substrate conversion, and thus bacterial or urease activity within columns. The effluent displaced from columns during the injection of new CM was collected in a series of centrifuge tubes in 5 mL quantities. For each 5 mL column effluent collected, the conductivity and pH of the effluent was measured using a Consort multi parameter analyser C3010, pH probe and conductivity probe with temperature compensation. Following the first CM treatment, 1 mL of effluent from the 5–10 mL sample of effluent from each tube was taken to measure optical density, as an indication of biomass concentration, to determine effectiveness of bacteria fixing. Optical density was measured using a spectrophotometer (Hach DR 6000, Colorado, USA) at a wavelength of 600 nm. The first 5 mL was not used since this may include some CM that had been retained in the column outlet after treatment.

7.3.9 Geochemical Analysis

The calcium ion concentration of column effluent was measured using an Ion chromatograph (IC). Dionex ICS 5000+ Cation analysis was conducted using 20 mM methanesulfonic acid eluent starting concentration, on a Dionex CS12A column, using 112 mA suppressor output. The first 5 mL effluent from each column was discarded at this stage, since this may contain some unreacted substrates that had been held within the column outlet, outlet tubing had otherwise been drained after each treatment. Beyond this point, up to 20 mL the effluent was mixed for each column to obtain a representative average concentration of calcium ions for each column. The effluent beyond this point was not tested, since this may contain the new CM being injected at later stages in the treatment process as pore volume decreases. Effluent samples were tested daily within two hours of collection to ensure accuracy of results.

7.3.10 Quantification of Calcium Carbonate Precipitate

The amount of calcium carbonate precipitated in the sand columns as a result of MICP was quantified using a calcimeter, as per Section 4.7 and applying Equation (4-5). To obtain an estimate of the average calcium carbonate content of each column, as a percentage of the total dry mass, samples of between 4 g and 5 g were taken from the top, centre and base of each column for testing after oven drying columns at 105 °C. Tests were conducted at constant room temperature of 23 °C.

7.3.11 Mineralogical Analysis

A combination of scanning electron microscopy (SEM) and X-ray diffraction (XRD) was used to confirm the presence of calcium carbonate and analyse the characteristics of the mineral precipitate in samples taken from biocemented columns. SEM was used to observe the morphology of the mineral crystals and fibres, and to measure the diameter of the jute fibres in the samples. In addition, Energy Dispersive X-Ray analysis (EDX) has been used for elemental analysis of samples from Columns Test P2. Samples for SEM observation and analysis were prepared using a sputter coater (MCM-100 Ion Sputter Coater, SEC, Korea) and gold coating. X-ray diffraction (XRD; Malvern Panalytical, Aeris powder diffractometer, Malvern, UK) was used to characterise the mineral crystals observed and confirm the presence of CaCO₃.

7.3.12 Unconfined Compressive Strength Testing

The unconfined compression test was carried out in accordance with 7.2 of BS 1377-7:1990 (British Standards Institution 1999), to determine the unconfined compressive strength (UCS) of biocemented columns using the load frame method. A loading rate of 1.27 mm/min (0.05 in/ min) was applied. Stiff and brittle soils fail at small strains (British Standards Institution 1999), therefore the readings of deformation were recorded at more frequent intervals for the column studies using *S. pasteurii*, to ensure accuracy of test results.

This test was performed twice, firstly after the biocementation treatment process had been completed (UCS1), and a second time to test for self-healing (UCS2).

Following the injection of treatment five the cementation medium was left in columns for eight days before UCS1, with the inlet and outlet tubing clamped. The retention time had been increased at this stage due to the significant reduction in calcium ion depletion rate in control columns and also those containing treated fibres. Tested columns were in a saturated condition, with evaporation prevented during testing by the test specimens being encased by the latex membranes and end caps. Membranes were kept in place for this test, perforated discs were removed, and perspex end caps were used to provide a level testing surface between the column and UCS testing apparatus. Following the initial UCS1 test, the columns were reconstituted and returned the column assembly, with one and a half pore volumes of autoclaved tap water injected into columns. Samples were left hydrated a further eight days before the UCS test was conducted again. At this stage, the theory that some CM may have been retained, and later leached out of fibres to enable healing was also being tested.

7.4 Results and Analysis

7.4.1 Urease Activity Batch Test

Urease activity test results, as per Table 7-4, show that bacterial growth was faster in a medium prepared using tap water as opposed to deionised water, based on measurements of optical density. Consequently, the cementation medium for the column treatments was prepared using tap water. Liquid broth culture (LBC) inoculant resulted in a higher urease activity than inoculation of the growth medium with a single colony plate culture (PC). It is, however, noted that this may be due to inoculum size, and that this can be better controlled by using liquid broth culture as an inoculant. The liquid broth cultures for the columns were prepared using deionised water (DI). Three measurements of urease activity were taken and averaged for each of the samples prepared.

Table 7-4. Results from urease activity batch test.

ID	Water type	Inoculant	pH	Culture Time	OD₍₆₀₀₎	Electrical Conductivity (mS/cm/min)	Urea Hydrolysed (mM/min)	Specific Urease Activity (mM/min/OD)
1	Tap	PC	8.37	19	0.940	0.56	6.22	6.62
2	DI	PC	7.97	19	0.937	0.41	4.59	4.90
3	Tap	LBC	8.37	19	1.308	0.75	8.30	6.34
4	Tap	LBC	8.37	16	1.222	0.69	7.63	6.24
5	Tap	LBC	8.37	14	1.068	0.57	6.30	5.89
6	DI	LBC	6.46	19	1.005	0.63	6.96	6.93
7	DI	LBC	7.15	19	0.822	0.57	6.37	7.75
8	DI	LBC	7.97	19	1.038	0.55	6.15	5.92
9	DI	LBC	8.53	19	1.134	0.50	5.56	4.90
10	DI	LBC	8.86	19	1.196	0.44	4.89	4.09
11	DI	LBC	9.17	19	1.156	0.41	4.59	3.97

The specific urease activity of the liquid broth culture grown using deionised water peaks at a pH of approximately 7, as shown in Figure 7-3. This is close to the pH of sample 7 above, this being the sample with unadjusted pH, and, hence, the pH of the growth medium was not adjusted for the following column studies.

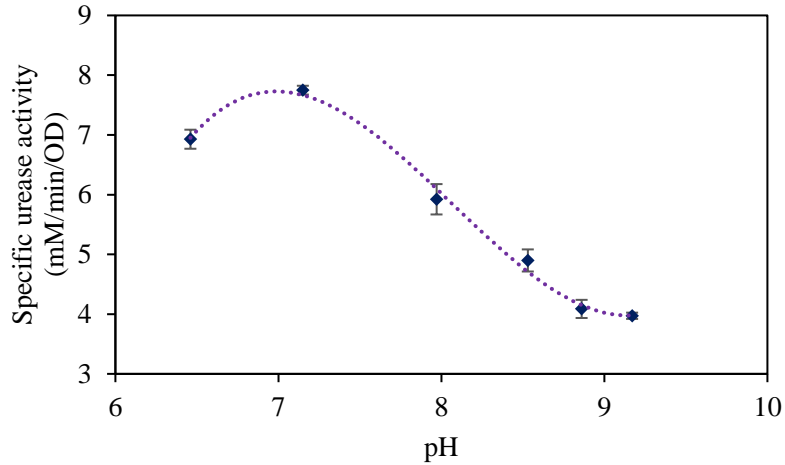


Figure 7-3. Effect of pH on specific urease activity in liquid broth cultures of *S. pasteurii*, with error bars showing standard errors of the means.

7.4.2 Material Properties

Figure 7-4 gives the optimum dry density (target density) of sand, and the sand and jute mixture, for compaction into the columns, this being 1.726 g/cm^3 and 1.700 g/cm^3 respectively. An additional measurement was taken for the test with the sand and jute mixture, as it had been evident during testing that the optimum water content was higher when compared with the sand only test. This had been expected due to absorption of water by the jute fibres. Based on column measurements taken using vernier callipers prior to the first UCS test, columns containing sand only and sand and jute were compacted to 95.7 % and 91.4 % respectively of their target densities. These results, as an average of the triplicate columns, show that the inclusion of fibres hindered compaction of column contents to some extent.

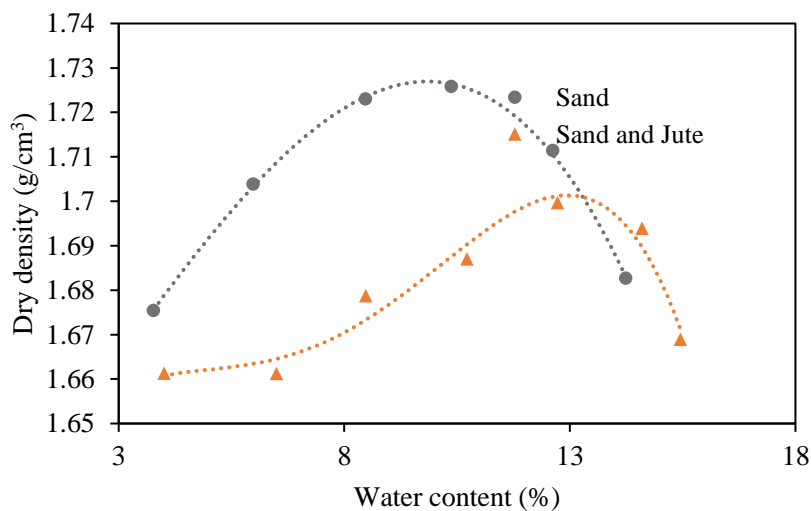


Figure 7-4. Proctor compaction curves, for F60 sand only and an F60 sand and jute fibre mixture.

Results obtained for particle size distribution, as shown in Figure 7-5, are in close alignment with those reported by U.S. Silica. The general slope and shape of this distribution curve are described by means of the coefficient of uniformity (C_u) and coefficient of curvature (C_z), with a C_z value of between 1 and 3 indicative of a well-graded soil (Craig 2004), provided the value of C_u exceeds 4.

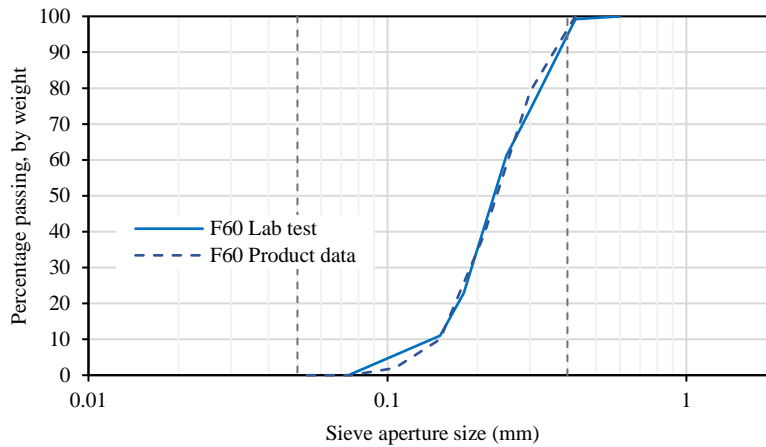


Figure 7-5. Particle size distribution of F60 sand, as measured in the lab and as per product data provided by US Silica.

The parameters determined from the gradation curve for the F60 sand are given in Table 7-5. The C_z value of 1.064, along with the low C_u value of 1.786, is indicative of poor grading and a narrow range of particle sizes.

Table 7-5. F60 sand parameters, as derived from the particle size distribution test results.

D_{10}	D_{50}	D_{60}	D_{30}	C_u	C_z
0.140	0.226	0.250	0.193	1.786	1.064

7.4.3 Columns Test P2 (6 g/L Oxoid CM0001)

The content of the columns prepared for this test is given in Table 7-6.

Table 7-6. Contents of columns prepared for Columns Test P2.

Column ID	Sand (g)	Jute (g)	Immobilised CM4 (g)
J1	133	1	0
J2	133	1	0
J3	133	1	0
J4	133	1	1.687
J5	133	1	1.681
J6	133	1	1.686

C1	143	0	0
C2	143	0	0
C3	143	0	0

7.4.3.1 Bacteria Fixation and Initial Activity

The optical density (OD₆₀₀) of the *S. pasteurii* liquid broth culture grown for the column studies was measured as 0.992 using a spectrophotometer. Following centrifugation, the supernatant optical density was 0.154. Taking into account this loss of bacteria in the supernatant the resulting optical density was 0.840. When using the larger 500 mL Erlenmeyer flasks to produce 150 mL volumes of bacterial cultures, grown for 24 h at 150 rpm and 23 °C, the measured urease activity had been lower than when using the 250 mL flasks to produce the 50 mL cultures. Urease activity of the culture used to inoculate the columns was measured as 4.37 mM/min. The reduced surface area to volume ratio demonstrated the effect of limited oxygen transfer on the urease activity of the culture. The concentration gradient between the oxygen at the surface and within the medium promotes oxygen transfer into the medium (Doran 2013).

The bacteria appeared to have been successfully fixed by CM1p as shown by the low optical densities of effluent in Table 7-7, as measured following the injection of CM2p. Some bacterial losses were occasionally observed in effluent just after one pore volume of CM had been pumped into the column, when some cloudiness was observed in the effluent. It is noted that should any mineral precipitate be contained within the effluent that this would affect the optical density measurements. However, given the very low optical densities measured, as given in Table 7-7, this has been deemed to have a negligible effect if any at this stage.

Table 7-7. Optical density of effluent discharged from 5 - 10 mm depth from Test P2 columns, during biocementation treatment two, following fixing of bacteria by treatment one.

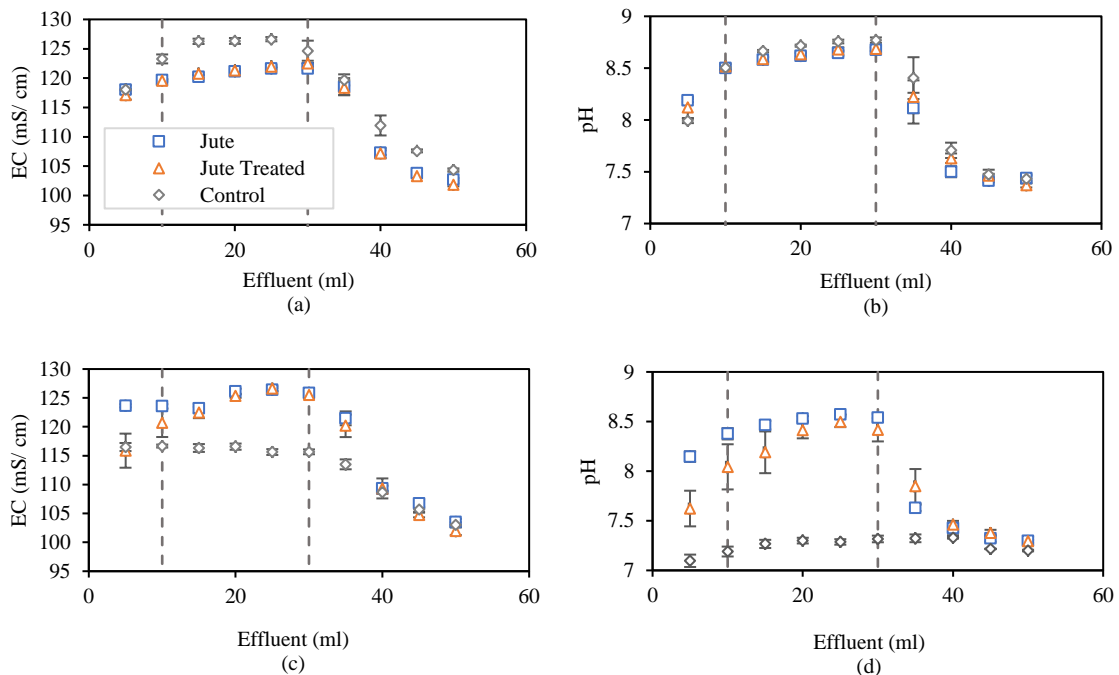
Column	J1	J2	J3	J4	J5	J6	C1	C2	C3
Effluent OD₆₀₀ (5–10 mL)	0.018	0.01	0.015	0.011	0.008	0.011	0.055	0.02	0.044

7.4.3.2 Distribution of Bacterial Activity

Figure 7.6 (a–j) shows the breakthrough curves for measured electrical conductivity and pH of effluent displaced during each treatment flush, which are used to analyse the distribution of the reaction products within the columns. These results indicate that the distribution is fairly even for control columns, with more variation in the columns containing jute, as was expected given the jute may absorb some of the bacteria. The results also indicate a slightly lower bacterial activity towards the top of columns (outlet) containing jute following treatment one. This trend was observed to reverse after three CM treatments.

The dashed vertical lines in Figure 7.6 (a-j) represent the interpreted location of column boundaries at the outlet (approx. 5 mL) and inlet (approx. 30 mL) locations.

Electrical conductivity measurements of the effluent from columns show that there is some initial inhibition of MICP activity in columns containing jute fibres (both treated and untreated) during treatment one, as shown in Figure 7.6 (a), when compared to the control columns containing sand only, as was similarly observed in aqueous studies reported in Chapter Five. However, results from testing of the effluent flushed following subsequent treatments show that for columns containing untreated jute fibres the EC and pH values corresponded to full conversion. The results from effluent tested after treatment three and four show a decline in measured pH and EC from columns containing treated jute compared to the untreated jute. Due to the excess of urea, full conversion of urea would deplete almost all calcium and the remaining solution would be expected to contain about 1.25 mol/L ammonium, 1 mol/L chloride and 0.25 mol/L carbonate/bicarbonate, which according to Van Paassen (2009), has an EC of about 125 mS/cm and an expected pH of 8.5 to 9. Incomplete conversion would render lower EC and pH values. The pH and conductivity results in Figure 7-6 show a similar trend for columns containing treated and untreated fibres, however, the longer error bars for those with treated fibres indicative a greater variability of bacterial activity within these columns.



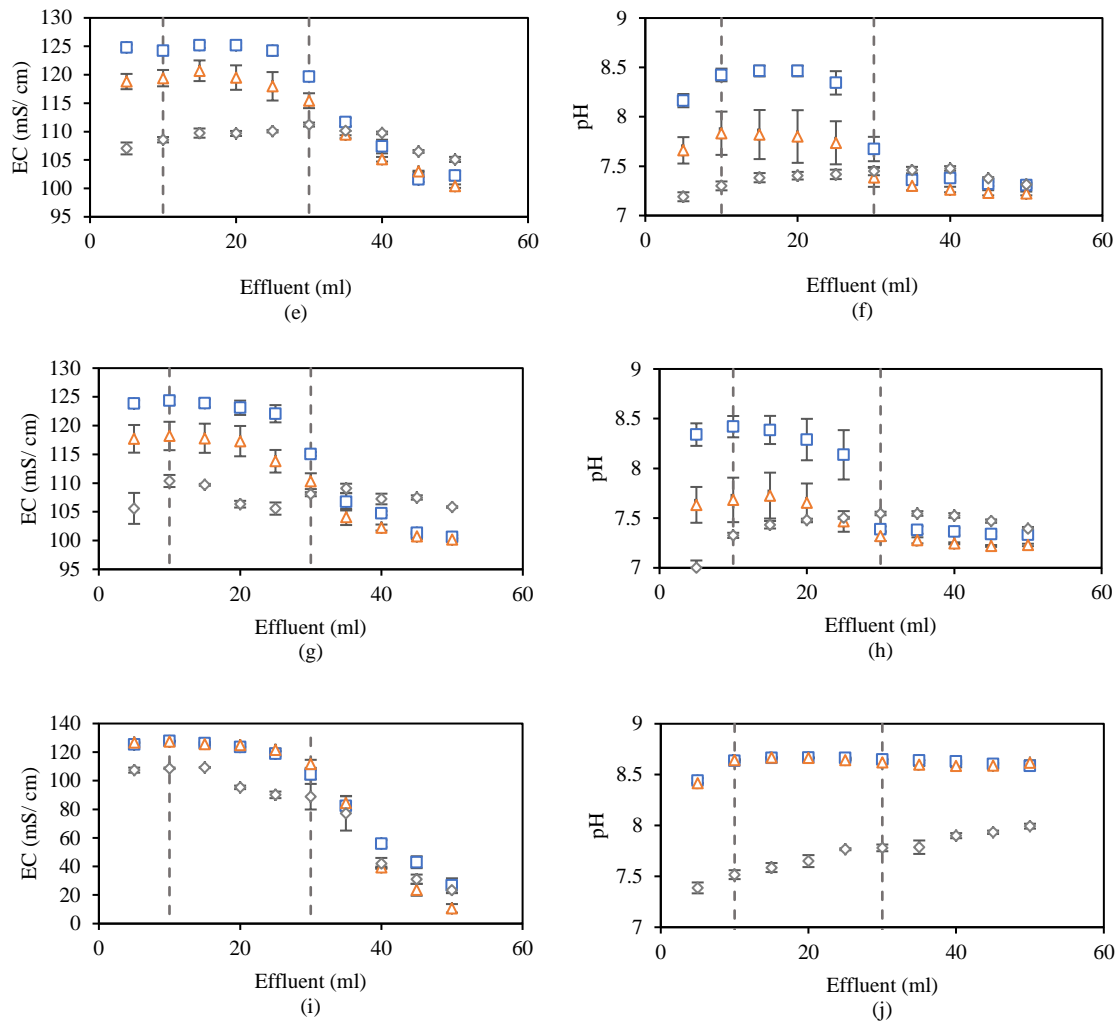


Figure 7-6. Electrical conductivity and pH of effluent from Test P2 columns following biocementation treatments 1 (a,b), 2 (c,d), 3 (e,f), 4 (g,h) and 5 (i,j), with error bars showing standard errors of the means for the triplicates.

7.4.3.3 Efficiency of Chemical Conversion

The concentration of calcium ions in the effluent has been used as a measure of the efficiency of substrate conversion following CM treatments one to four. The initial calcium ion concentration in the injected CM was 500 mmol, which reduces to an average of 2 mmol across all columns after treatment one. The calcium ion depletion in Figure 7-7 refers to this reduction in concentration, and has been represented as a cumulative value over time. The concentration of calcium ions in the column effluent shows that the efficiency of conversion of calcium ions to produce calcium carbonate precipitate declines over time for the control columns containing sand only and, to a lesser extent, the columns containing the pre-treated jute fibres, between treatments one and four. Where jute has been mixed with the sand the relationship between calcium ion conversion to produce calcium carbonate, i.e., depletion of the calcium ions, in respect of time is almost linear. This clearly demonstrates a beneficial effect of

the jute fibres on the MICP process. This effect is likely due to adsorption/absorption of bacteria by the jute fibres, which appears to have had a positive effect on bacterial cell growth/ viability. Cells adsorbed on surfaces replicate and grow into microcolonies (Renner and Weibel 2011).

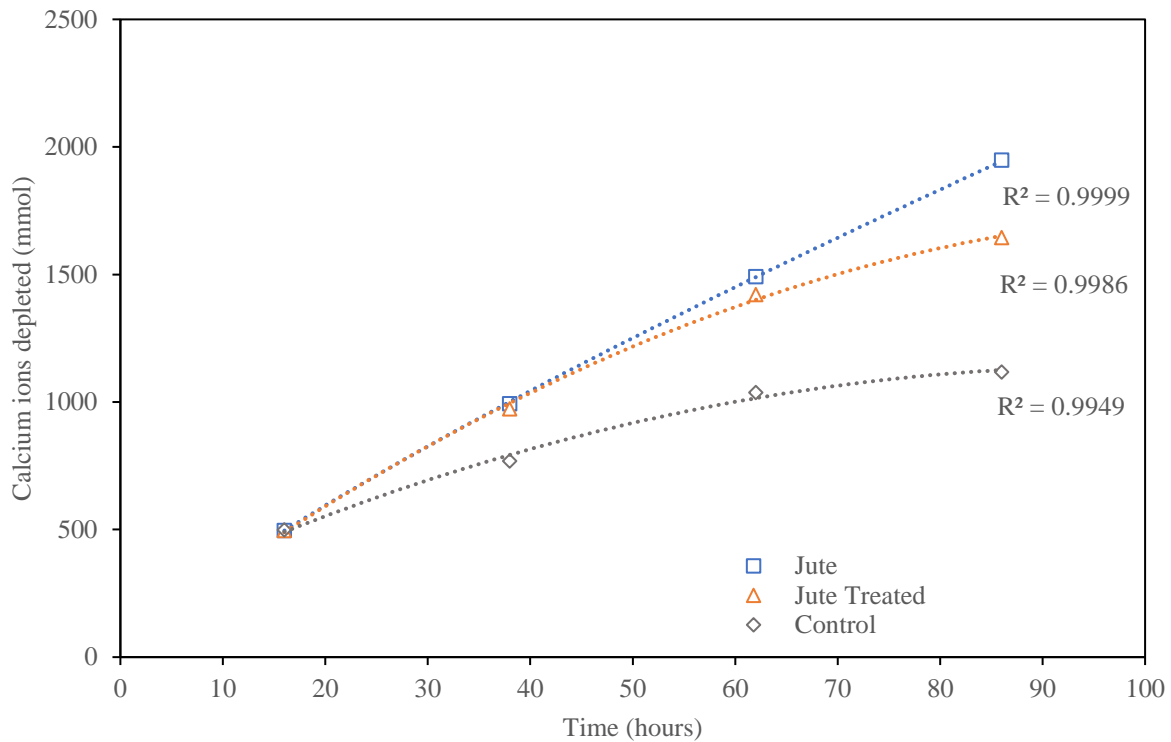


Figure 7-7. Cumulative reduction in concentration of calcium ions in Test P2 columns effluent following biocementation treatments one to four.

Figure 7-8 shows the chemical conversion efficiency following all five CM treatments, based on measurement of calcium ions in the effluent. Following treatment one the conversion efficiency is near 100% for all columns, despite the slightly reduced urease activity of the bacteria injected into columns compared to the batch study. There is a rise in efficiency following treatment five since columns had been left eight days before the first UCS test and subsequent flushing with tap water and collection of effluent. This increase at this stage is significant for the columns containing treated jute and is indicative of a slower but also sustained MICP process when compared to results for columns containing untreated jute. These results, along with those from Figure 7-6, are indicative of a lower urease activity in columns J4 to J6, suggesting that there are less viable bacteria in these columns at this stage compared to J1 to J3. Based on results in Table 7-7, bacteria had been fixed adequately following CM treatment one but the fibre pre-treatment may have rendered these fibres less able to absorb/adsorb bacteria and more bacteria may have instead adhered to the sand particles. The adhesion of bacteria to sand particles in columns J4 to J6 is likely somewhere between that of the sand only and sand and untreated jute columns. Adhesion of bacteria to a surface is affected by the physical properties of the surface and surface chemistry, with topography being the most influential factor on bacterial adhesion (Renner and Weibel

2011). The treatment of the fibres may have resulted in a smoothed outer surface, and will likely have also affected their ability to absorb bacteria.

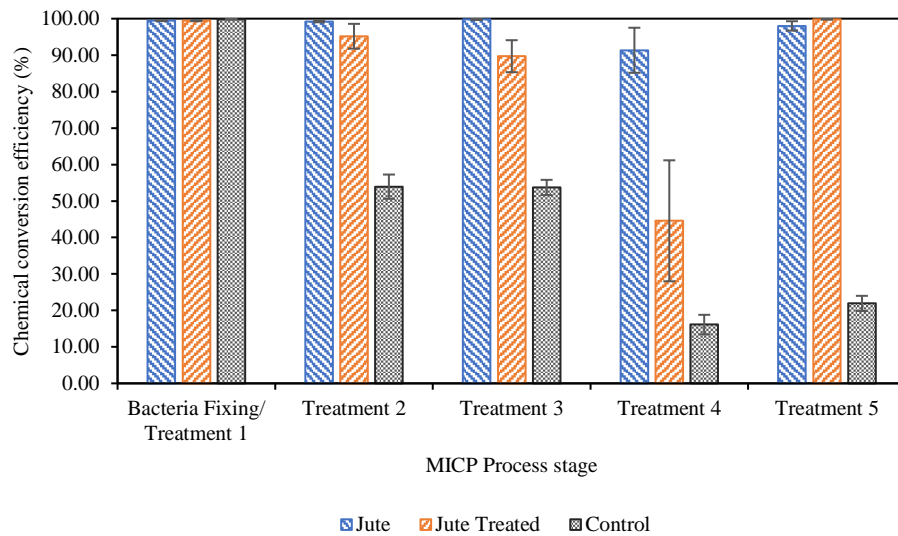


Figure 7-8. Chemical conversion efficiency, as determined from Ion Chromatography measurement of calcium ions within effluent from Test P2 columns following each biocementation treatment, with error bars showing standard error of means.

7.4.3.4 Unconfined Compressive Strength, and CaCO₃ Precipitated

Unconfined compression test results are shown in Figure 7-9. The average unconfined compressive strength of the three control columns containing sand only was 66 kPa. The average unconfined compressive strength of the columns containing untreated jute and treated jute fibres was 370 kPa, and 320 kPa, respectively. It is observed that on average the unconfined compressive strengths of columns containing untreated fibres are approximately 5.6 times higher than the columns containing sand only. Figure 7-9 (a) shows a relatively close relationship between the peak unconfined compressive strength results for columns J1 to J3, with the peak strengths all occurring close to 5 % strain. This is indicative of good repeatability for these columns. More variation between results is observed in Figure 7-9 (b), for columns J4 to J6 containing treated fibres, which appear to fail in a more brittle manner at varying strains between approximately 2.5 % and 5 % and have lower residual strengths. For this set of columns, the highest, and also the lowest, UCS is obtained out of the six columns containing fibres. The lower strength for column J5 is attributed to this splitting down the centre during the UCS test, as can be seen in Figure 7-10 (e). The highest strength obtained was 520 kPa for column J4 containing treated jute fibres. The variability between results for columns J4 to J6 may have been due to variable absorption or adsorption of bacteria by these fibres. The pre-treatment did not appear to hinder the mixing of fibres with sand.

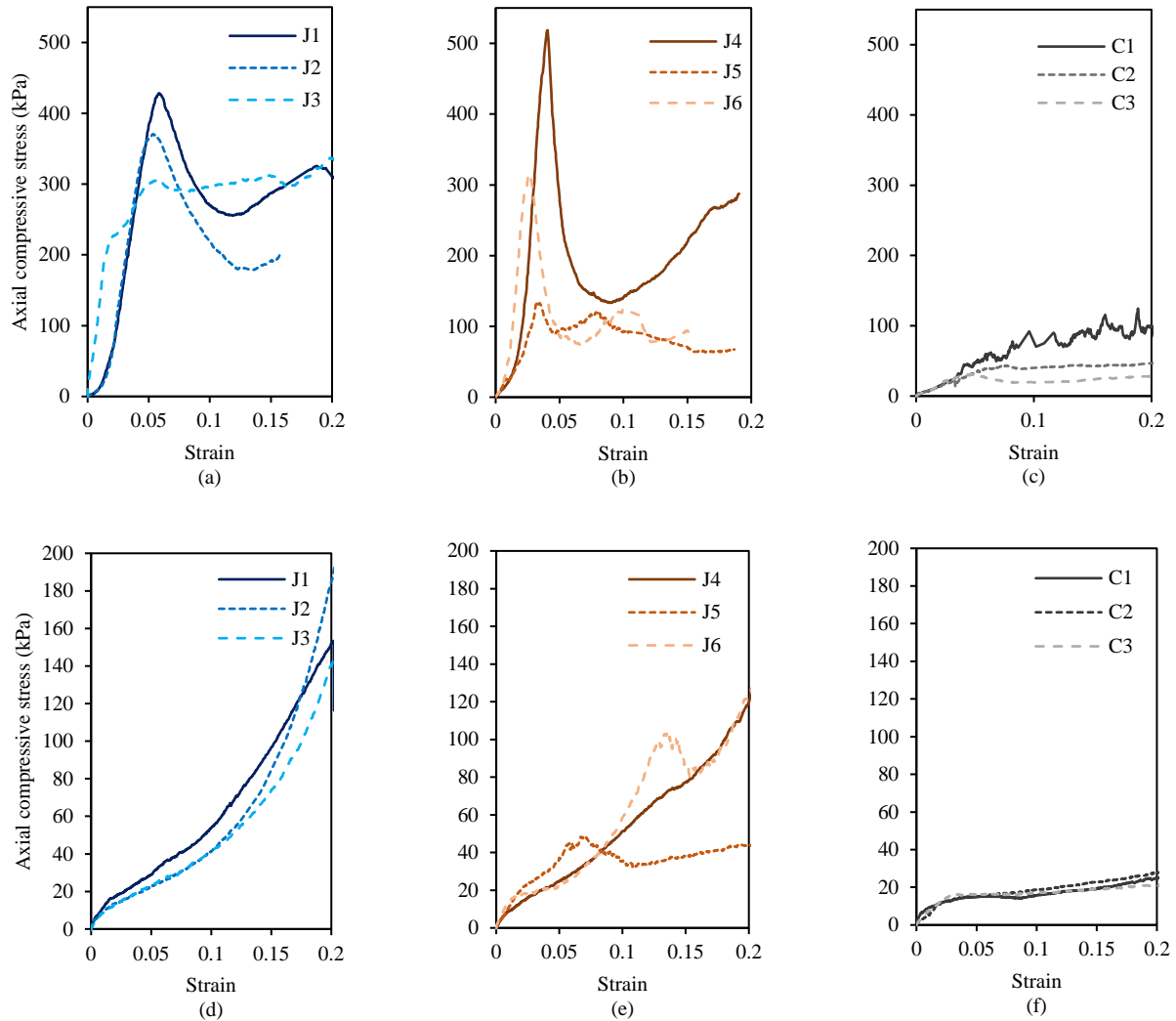


Figure 7-9. Unconfined compressive strength test results for UCS1 of Test P2 columns following biocementation treatment five (a–c), and UCS2 following column reconstitution, flushing, saturation with water and eight days of curing to test for self-healing (d–f).

These results demonstrated the significant contribution to strength of the jute fibres, when compared to controls, as a result of the mechanical properties of the fibres and greater precipitation of calcium carbonate within these columns. The confining effect of the latex membranes will have had a small contribution to strengths obtained, which is assumed to be consistent across all columns tested. Of interest in this study is the comparison between the results for columns tested.

Figure 7-9 (d–f) is indicative of longer-term strengths of the biocemented material following failure. Between the first set of unconfined compression test results (Figure 7-9 (a–c)) and second (Figure 7-9 (d–f)), the column contents contained within the latex membranes were reconstituted, this process itself will have had some effect on material properties and may contribute to some strength reduction. There is a noticeable difference in the trend of the UCS results for the reconstituted samples when comparing Figure 7-9 (d–f), with peaks only visible for columns containing treated jute fibres. When comparing

with the prior results with columns inoculated with jute, it can be observed that the failure of columns containing fibres, in particular, happens at smaller strains, at around 5 % strain. Thus, more brittle behaviour is evidenced when comparing to the earlier studies detailed in Chapter Six for which failure had been observed closer to 10 % strain for columns containing fibres.

Figure 7-10 shows images of the column samples following the onset of failure during the UCS1 test. The diagonal shear failure can be clearly seen in most samples. When comparing images, there is a greater inconsistency in observed failure mechanisms for the samples with treated fibres, J4 to J6. J5 was observed to break apart down the centre of the column during testing. The controls typically sheared across the middle third of the test specimen.

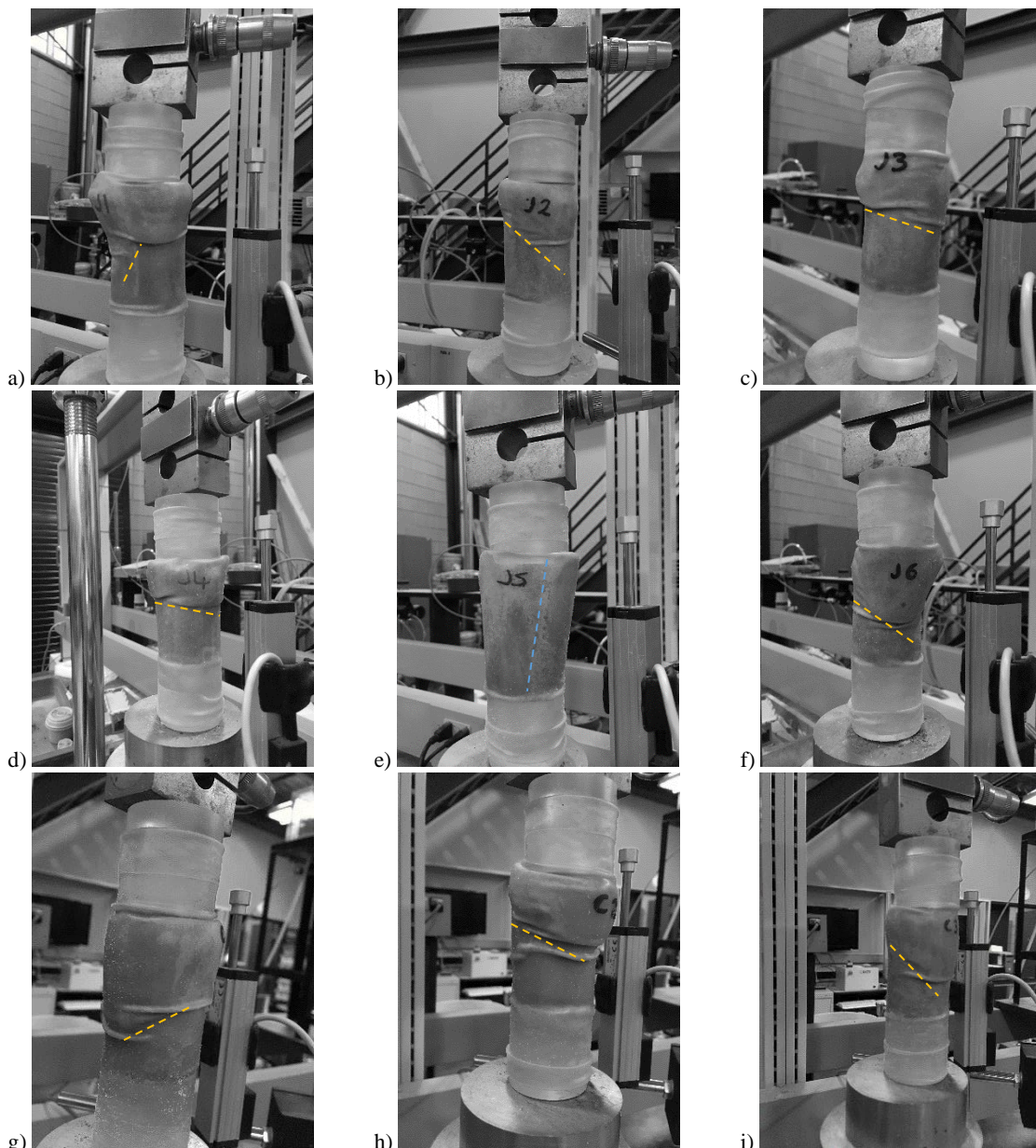


Figure 7-10. Photographic images of columns J1 to J3 (a–c), J4 to J6 (d–f) and C1 to C3 (g–i), following the onset of failure during UCS1 for Columns Test P2. Annotations indicate shear failure planes where observed and the vertical failure in column J5.

The columns containing jute had greater resistance to shear failure and the shear failure line appears higher up in the specimen, indicating strengths may have been greater towards the column inlet (base of column).

Figure 7-11 shows the sand columns during UCS2, shortly after failure. Some shearing was still visible in columns J1 to J3 and J6. Otherwise, there is a barrelling or crushing type failure, with the exception of column J5 which has again split down the centre vertically.

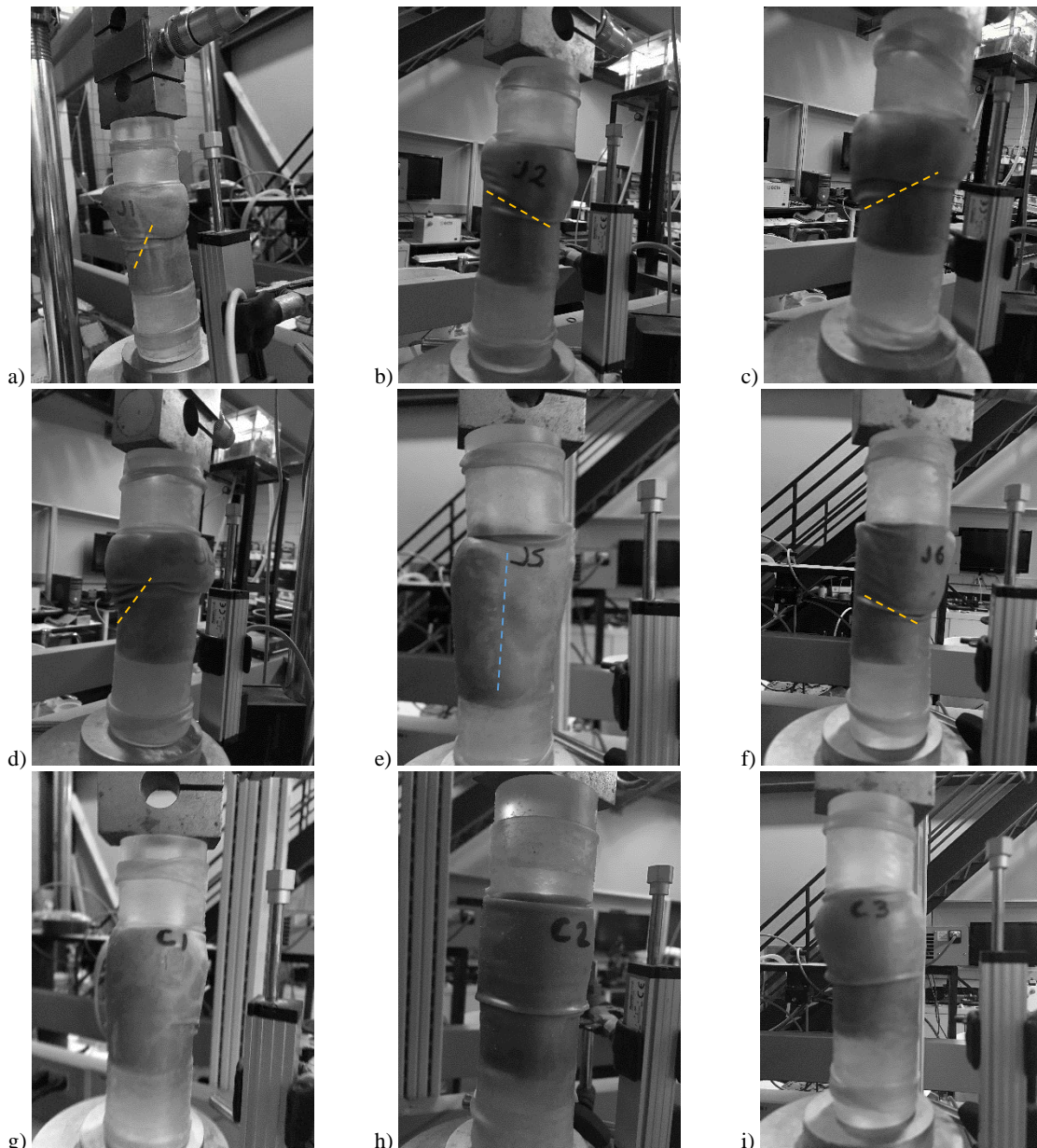


Figure 7-11. Photographic images of columns J1 to J3 (a–c), J4 to J6 (d–f) and C1 to C3 (g–i), following the onset of failure during unconfined compressive strength test 2 for Columns Test P2. Annotations indicate direction and location of shear failure planes where observed and the vertical failure in J5.

Figure 7-12 shows the unconfined compression tests results following the initial biocementation (peak 1 and residual 1) and after the reconstitution and self-healing test stage (peak 2). The self-healing stage consisted of saturation with sterile tap water and curing over eight days. When the ‘Peak 2’ strength is

compared with the residual strength from UCS1, the results for two columns (J2 and most notably J6) indicate some strength regain. In accordance with BS 1377-7:1990 the ‘Peak 2’ unconfined compressive strength has been determined from results at 20% axial strain for columns J1 to J3, J4 and J6 and C1 to C3.

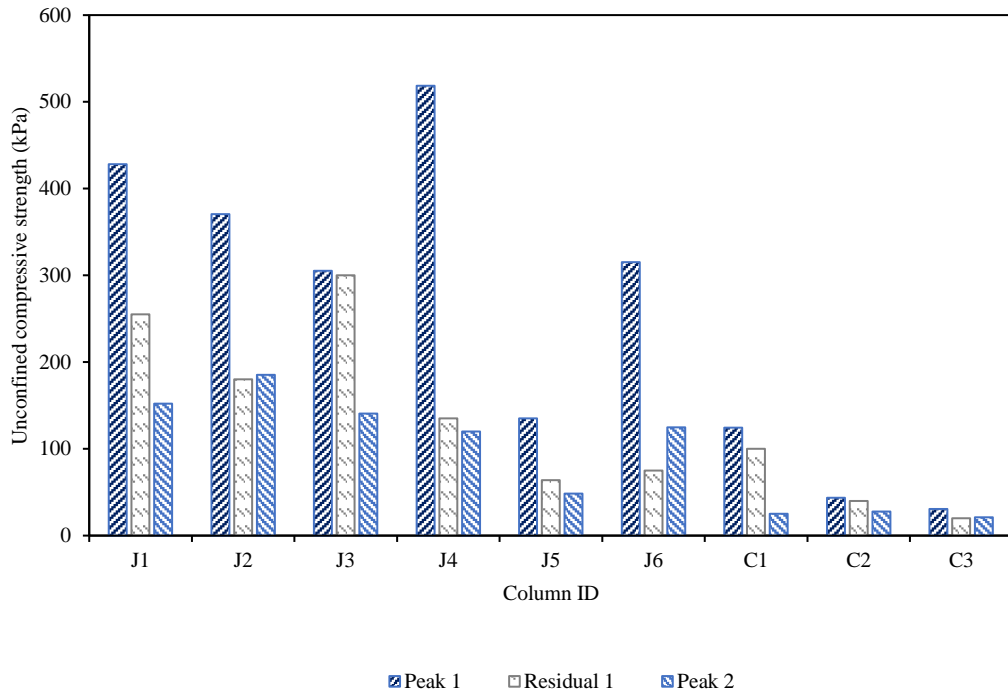


Figure 7-12. Results from UCS1 and UCS2 for Columns Test P2, showing peak and residual strengths from UCS1 and peak strengths from UCS2.

Following the second UCS test (UCS2), the columns were removed from the latex membranes and oven dried, to determine moisture contents, followed by measurement of calcium carbonate content, as given in Table 7-8.

Table 7-8. Moisture and CaCO₃ contents of biocemented columns from Columns Test P2 (averages from triplicates).

Columns	Moisture Content (%)	CaCO ₃ Content (%)
J1–J3	18.35 ± 0.34	3.98 ± 0.59
J4–J6	16.82 ± 1.33	4.63 ± 0.31
C1–C3	17.03 ± 0.39	1.08 ± 0.47

The results in Table 7-8 show that the inclusion of jute and treated jute in the columns has resulted in an increase in calcium carbonate content by 3.69 and 4.33 times, respectively, when compared to the

columns with no fibres. This increase is significant when compared to studies using synthetic fibres and in addition shows that jute outperforms natural basalt fibres. Choi et al. (2016) reported that MICP treated sand specimens containing 0.8% (by weight of sand) PVA fibres had just 1.06 times more calcium carbonate on average than those without fibres. Choi et al. (2016) report an average 28.18 % unconfined compressive strength increase resulting from PVA fibre additions, although it is noted that there is considerably more variability in the results they obtained. Li et al. (2016) found that the UCS of MICP-treated sand with 0.3 % (by weight of sand) polypropylene (Fibermesh 150) fibres was 2.4 times higher on average, which reduced to 1.5 times when the fibre percentage increased to 0.4 %. Improved results have been achieved using natural basalt fibres. Xiao et al. (2019) reported that inclusion of 0.4 % basalt fibres in biocemented sand results in a 4.9 times higher unconfined compressive strength on average, and 1.62 times greater calcium carbonate content when compared to specimens with no fibres. Similarly, Xiao et al. (2019) reported a UCS reduction to 1.7 times that of sand only specimens when the fibre percentage was doubled to 0.8 %. The greatest amount of calcium carbonate was precipitated within columns J4 to J6, despite the measured reduction in chemical conversion efficiency in these columns following MICP treatments 2 to 4. This is likely due to the leaching of the immobilised cementation medium.

The dried columns are shown in Figure 7-13. Columns containing jute will have had a higher void ratio prior to biocementation since columns containing fibres did not compact quite as well those containing sand only.



Figure 7-13. Photograph of columns from Test P2 following UCS2 and oven drying at 105°C.

The calcium carbonate contents of the nine individual columns, as determined using a calcimeter, are shown in Figure 7-14. This analysis relates the calcium carbonate contents to the tested unconfined compressive strengths of the columns. There had been a greater consistency between results for the controls and columns containing untreated jute.

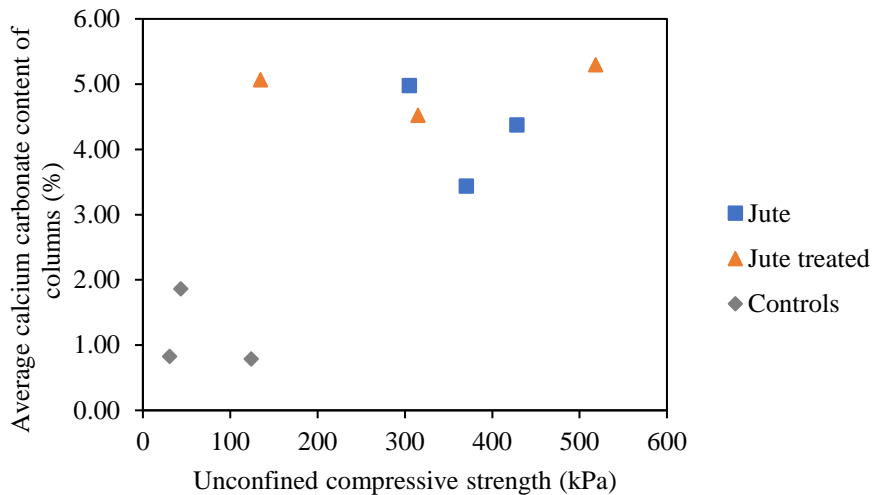


Figure 7-14. Average calcium carbonate content of Test P2 columns, as measured using a Calcimeter, showing relationship to UCS1.

The distribution of calcium carbonate precipitated along the column is shown in Figure 7-15. It has been reported in many studies that in these types of column experiments, calcium carbonate has been found to participate in greater concentration closer to the inlet end of the column into which the cementation medium is injected. The inlet had been located at the base of the columns. The absorption of bacteria by fibres as the bacterial suspension is pumped through the column will have contributed to the measured distribution of the calcium carbonate precipitate within columns. Figure 7-9 shows the shear failure plane occurs higher up in the columns where jute is present in comparison to controls, which is likely due to the greater percentage of precipitate towards the base of these columns. The pattern of precipitation differs for controls in that there is a greater concentration of precipitate towards the base and otherwise more uniform precipitation towards the centre and top of the column and hence the shear failure plane is further down in the column at an increased angle.

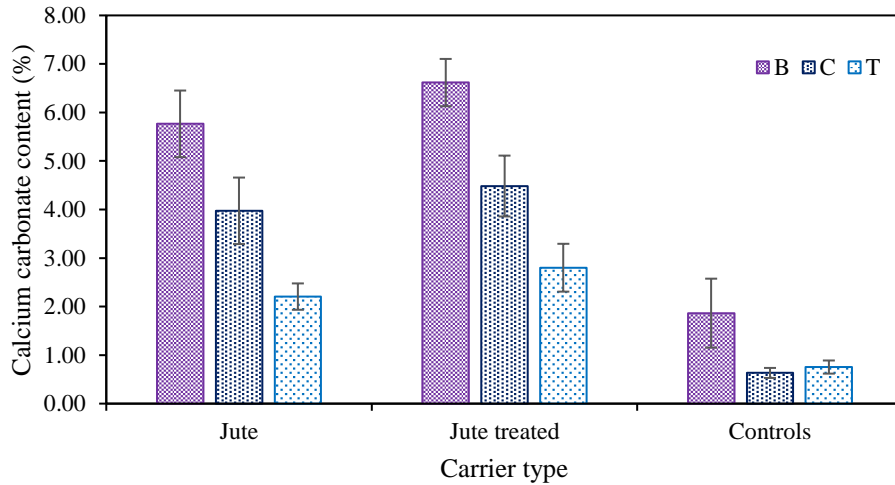


Figure 7-15. Distribution of calcium carbonate precipitated at the base (B), centre (C), and top (T) of Test P2 columns, with error bars showing standard errors of the means for the triplicates.

7.4.3.5 Morphology of CaCO_3 Precipitate and Jute Fibres

Samples used for this stage of analysis were J1, J4 and C1. Figure 7-16 shows the distribution of jute fibre diameters in samples taken from J1 ($n = 21$) and J4 ($n = 20$), with diameters measured using SEM. These results indicated that the treated fibres had swollen and were more variable in diameter. The average diameter of untreated fibres measured in J1 was $50.6 \mu\text{m}$, compared to $64.6 \mu\text{m}$ for treated fibres in J4.

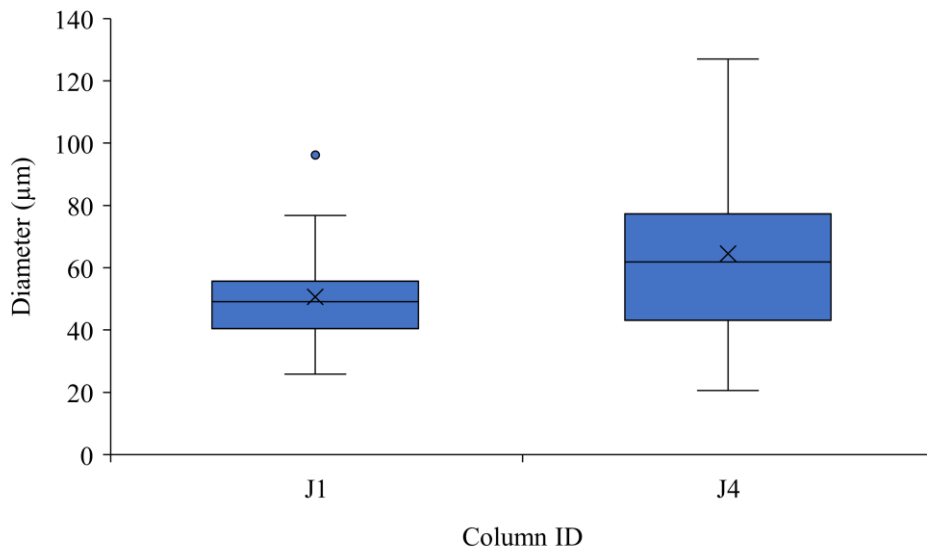
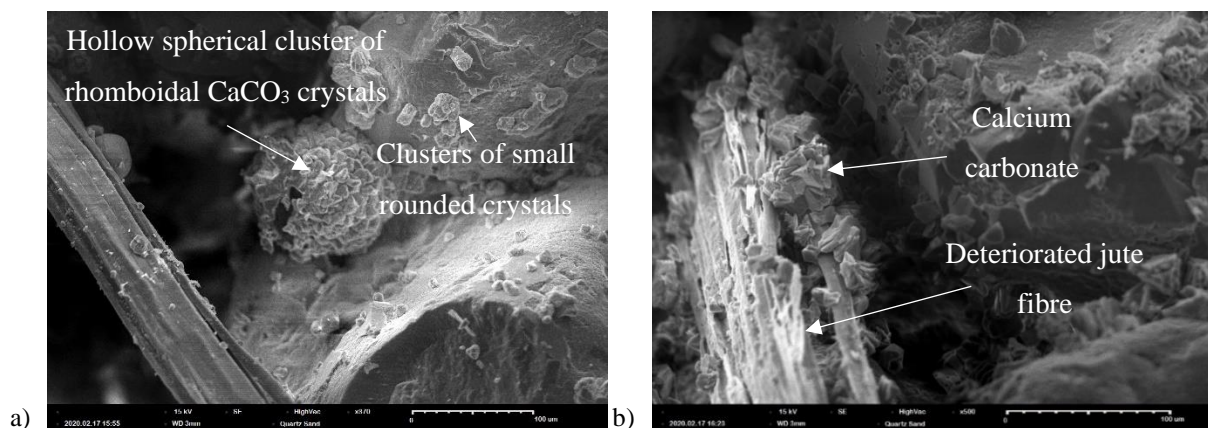


Figure 7-16. Box and whisker plot showing the distribution of measurements of jute fibre diameters in samples from columns J1 and J4 of Columns Test P2, observed and measured using a scanning electron microscope.

SEM images of the sample from J1 show that, where there is little to no fibre deterioration observed, as seen in Figure 7-17 (a), there is much less precipitate observed on the fibre surface when compared to the visibly deteriorated fibre in Figure 7-17 (b). The fibre shown in Figure 7-17 (b) has significant deterioration both on its surface and at depth, since it is breaking apart and has a much more roughened surface covered in CaCO_3 crystals. Rough fibres will be better at filtering and absorbing bacteria. The fractured fibres shown in 7-17 (f) suggest perhaps greater brittleness of fibres as a result of the pre-treatment process, although some fracturing was observed, albeit to a lesser extent, in the sample containing untreated jute as shown in Figure 7-17 (c). The samples containing fibres and untreated jute (Figure 7-17 (a–d)), show fibres and sand particles with a combination of rhombohedral, rounded and layered plates of calcium carbonate on the surface. In comparison, in samples containing treated jute, Figure 7-17 (e) and 7-17 (f), only single crystals of rhomboidal precipitate were observed. The images of samples containing biocemented sand only, 7-17 (g) and 7-17 (h), show rounded clusters of what appear to be more rhombohedral shaped calcium carbonate on the sand surface and bridging sand particles. It can be observed that the fibre and sand grain in Figure 7-17 (b) are bonded together by calcium carbonate crystals and that there were generally a greater number of crystals in samples from columns containing jute. The larger crystal forms consisting of layers of hexagonal plates, as can be seen in Figure 7-17 (d) were only observed in the samples containing untreated jute and generally more precipitate was observed in these samples. This supports the findings of chemical analyses that show the increased efficiency of substrate conversion to form calcium carbonate in the columns containing jute.

The agglomerated crystal structures observed on the grain surface, and at particle boundaries in Figure 7-17 (g-h) , are similar to those observed by Cheng et al. (2016) at low urease activity and which coincided with higher UCS values.



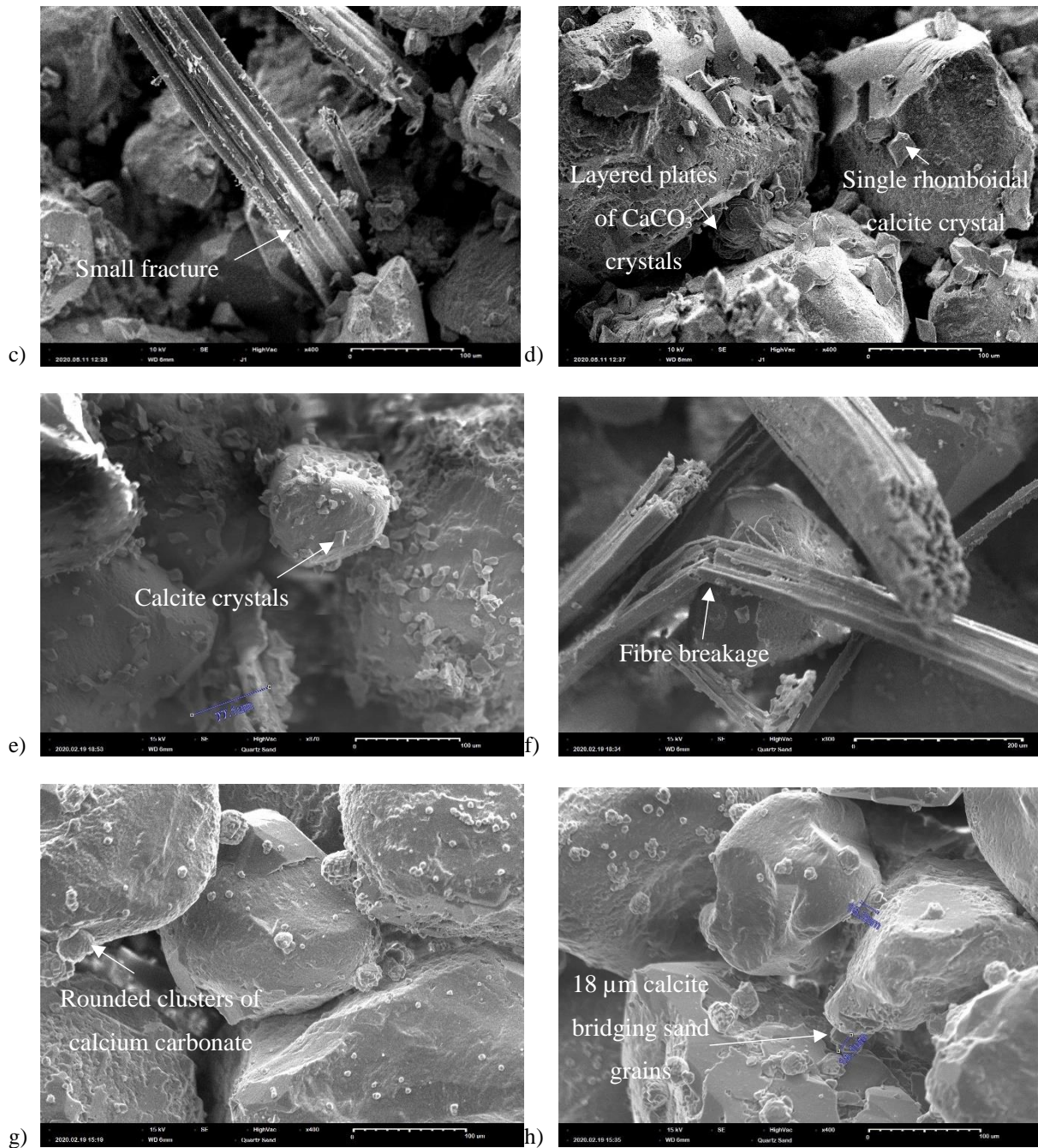


Figure 7-17. SEM images of samples from Test P2 biocemented sand column J1 containing jute (a to d), column J4 containing treated jute (e, f), and sand only control column C1 (g, h).

This spherical shape of some of the crystals observed has been associated with crystals of vaterite (Kawano et al. 2002; van Paassen 2009; Al Qabany and Soga 2013), with calcite reported to precipitate in a more rhombic form (Kawano et al. 2002). Vaterite has also been observed as a formation of large (10–20 μm) flakes (Hu et al. 2012), as shown in Figure 7-18 (a). These flakes were observed by Hu et al. (2012) to have grown out from smaller spheres of vaterite that were produced initially. A similar structure of vaterite was also reported by Fricke et al. (2006), as shown in Figure 7-18 (b). Figure 7-18 (a - b) bear a close resemblance to the layered precipitate observed in Figure 7-17 (d) which consists of plates measuring approximately 10 to 20 μm binding together the sand grains, thus identifying this

crystalline form as vaterite. Crystallisation of the vaterite polymorph is strongly associated with biogenic activities (Hu et al. 2012). Hu et al. (2012) found that vaterite formation was more prevalent than calcite when NH_3 diffusion rates increased and the concentration rose above 0.02 mol/L, when producing calcium carbonate via the NH_3 diffusion method. The three main polymorphs of anhydrous calcium carbonate are; vaterite, aragonite and calcite. Calcite is a more thermodynamically stable form of calcium carbonate than vaterite (Ni and Ratner 2008). Experimental evidence has demonstrated that vaterite can transform to aragonite in 60 min at 60 °C and to calcite in 24 h at room temperature (Grasby 2003).

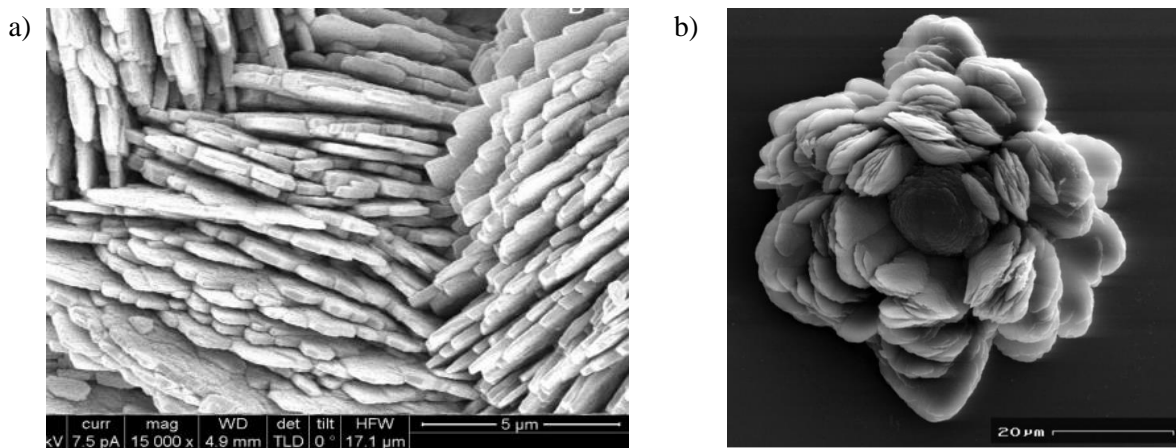


Figure 7-18. Vaterite grains composed of flakes of approximately 10 to 20 μm , as observed by a) Hu et al. (2012) and b) Fricke et al. (2006).

XRD analysis was performed to verify the crystal morphology of the observed precipitate. The XRD data was analysed using HighScore Plus, with results shown in Figure 7-19 to Figure 7-21. XRD data have been compared with reference patterns to determine crystalline phases present, with phases identified based upon the closest match between intensity and position of reference patterns and the diffraction peaks. These analyses verify the presence of calcite and vaterite polymorphs of calcium carbonate in all samples tested. Significant peaks for each crystalline phase are shown circled in Figure 7-19 to Figure 7-21. These results indicate that vaterite may be the more dominant of the calcium carbonate polymorphs present within all column samples, in particular those with untreated fibres (J1–J3), based upon height of peaks and intensity of the reference pattern. Nawarathna et al. (2019) reported that addition of chitosan as an organic additive to enhance MICP promoted the production of vaterite. This suggests that jute as an organic material may be influencing the crystal morphology in a similar manner, leading to the observed dominance of vaterite, due to the physicochemical properties of these fibres.

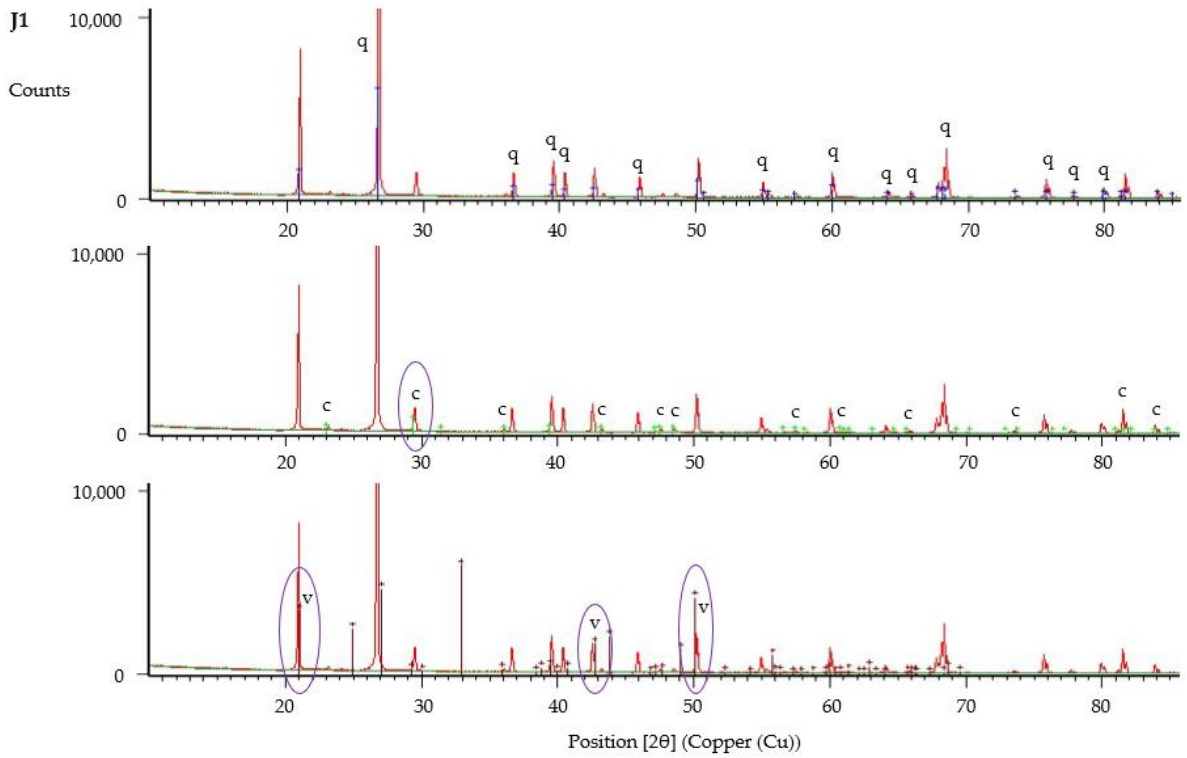


Figure 7-19. X-ray powder diffraction (XRD) analysis of sample from column J1, Test P2, showing identified peaks of quartz (q), calcite (c) and vaterite (v).

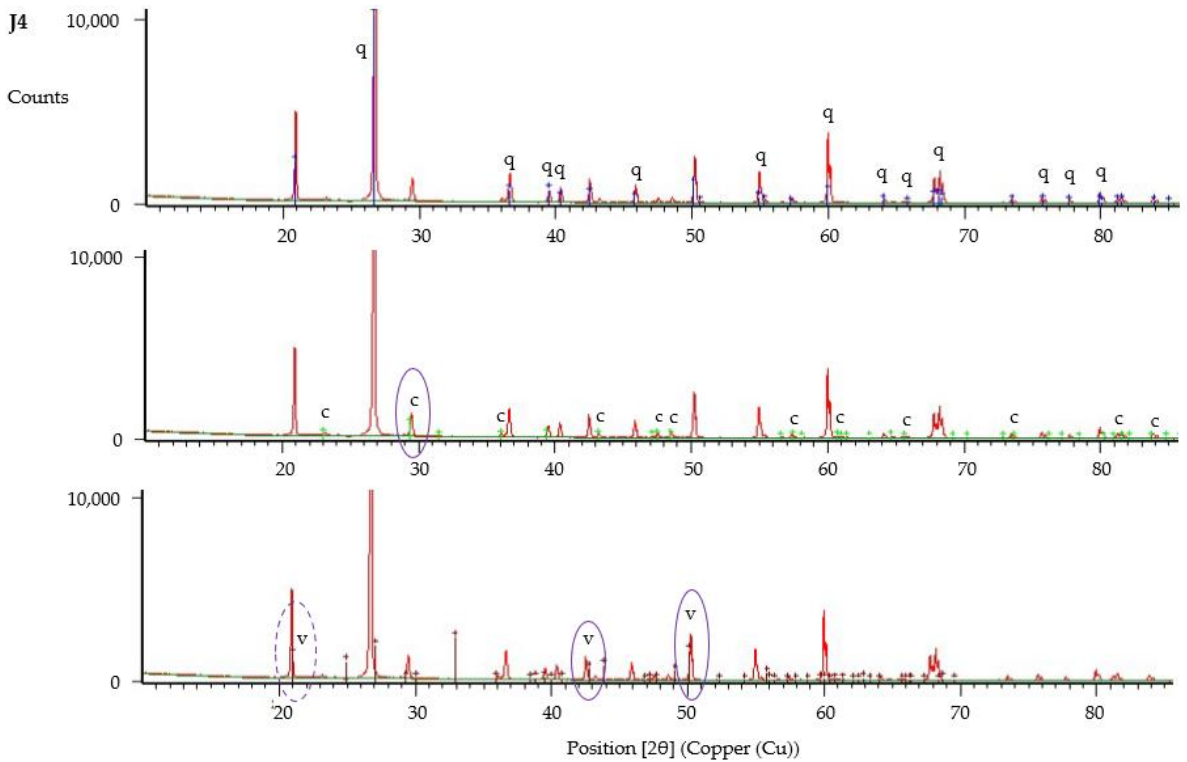


Figure 7-20. XRD analysis of sample from column J4, Test P2, showing identified peaks of quartz (q), calcite (c) and vaterite (v). The peak at 21 [°2θ] is identified as vaterite based on results for J1 and C1, however results for J4 alone suggest this could be also be quartz.

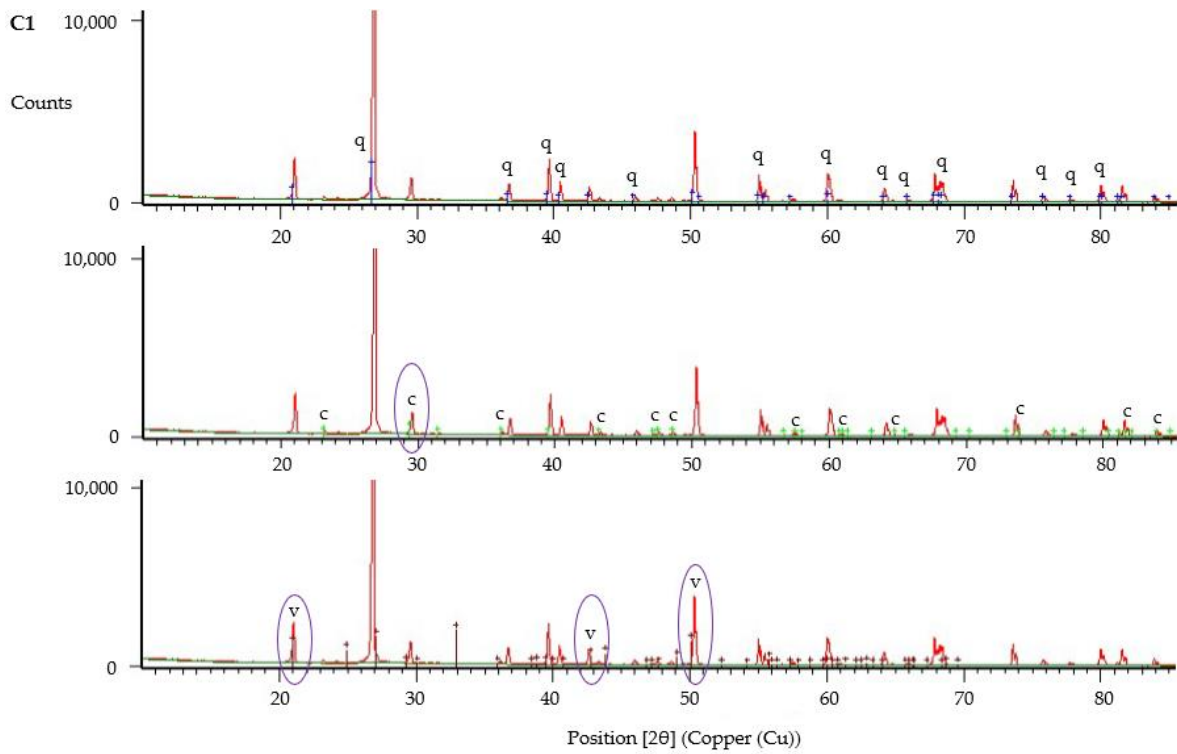


Figure 7-21. XRD analysis of sample from column C1, Test P2, showing identified peaks of quartz (q), calcite (c) and vaterite (v).

7.4.4 Columns Test P3 (3 g/L Oxoid CM0001)

This study was undertaken to test the effect of nutrient (Oxoid CM0001) concentration within the cementation medium. The cementation medium (CM3p) prepared for this test, for treatments 2 to 5, contained 3 g/L Oxoid CM0001. Table 7-9 summarises contents of the sand columns prepared for this test.

Table 7-9. Contents of sand columns prepared for Columns Test P3.

Column ID	Sand (g)	Jute (g)	Immobilised CM4 (g)
P2 - J1	133	1	0
P2 - J2	133	1	0
P2 - J3	133	1	0
P2 - J4	133	1	2.041
P2 - J5	133	1	1.763
P2 - J6	133	1	1.629
P2 - C1	143	0	0
P2 - C2	143	0	0
P2 - C3	143	0	0

7.4.4.1 Bacterial Fixation and Initial Activity

The liquid broth culture of *S. pasteurii* for test Column Test P3 was grown for the same amount of time as for test Column Test P2. The spectrophotometer measured optical density (OD₆₀₀) was 1.073, this being very close to that for Test P2 prior to centrifugation and resuspension. Taking into account losses in the supernatant, the resulting optical density following pelletisation of the bacteria and suspension in PBS was 1.05. The negligible losses of bacteria in the supernatant resulted in a slightly higher concentration of bacteria cells in this test since the same methodology is followed in respect of total quantity of bacterial suspension injected into columns. Urease activity had been measured as 4.56 mM/min (urea hydrolysed). Results in table Table 7-10 indicate that the bacterial retention in columns is slightly lower on average for columns containing jute, when compared to the prior test, whereas bacteria fixing in the controls would appear to be slightly improved. However, these results are deemed to have had a negligible effect when comparing results otherwise for the two tests given the low optical density of the effluent measured at this stage for both tests.

Table 7-10. Optical density of effluent discharged from 5 - 10 mm depth from Test P3 columns, during biocementation treatment two, following fixing of bacteria by treatment one.

Column ID	J1	J2	J3	J4	J5	J6	C1	C2	C3
Effluent OD₆₀₀ (5–10 mL)	0.038	0.038	0.015	0.035	0.060	0.014	0.036	0.06	0.006

7.4.4.2 Distribution of Bacterial Activity

Breakthrough curves for the pH and electrical conductivity of effluent displaced from columns during biocementation treatments are as shown in Figure 7-22 (a to j). The slightly higher measured electrical conductivities following treatment one (Figure 7-22 (a)), when comparing to Figure 7-6 (a), were likely due to the slightly increases bacteria inoculant cell concentration. Following treatment two, as shown in Figure 7-22 (d) and Figure 7-6 (d), the pH of effluent from controls in Test P3 had not reduced to the extent of that from Test P2. However, following treatment three, the pH of effluent from control columns in Test P3 was lower than that for Test P2. At this stage the influence of the higher nutrient content of CM2p used in Test P2 had been demonstrated. The pH results for the effluent for test two following treatment four are only slightly above 6.5 for all columns, indicating a reduction in MICP activity due to the lower quantity of nutrients in CM3p. The electrical conductivities of the effluent displaced from columns in Test P3 are similar across all columns following CM treatments one to five.

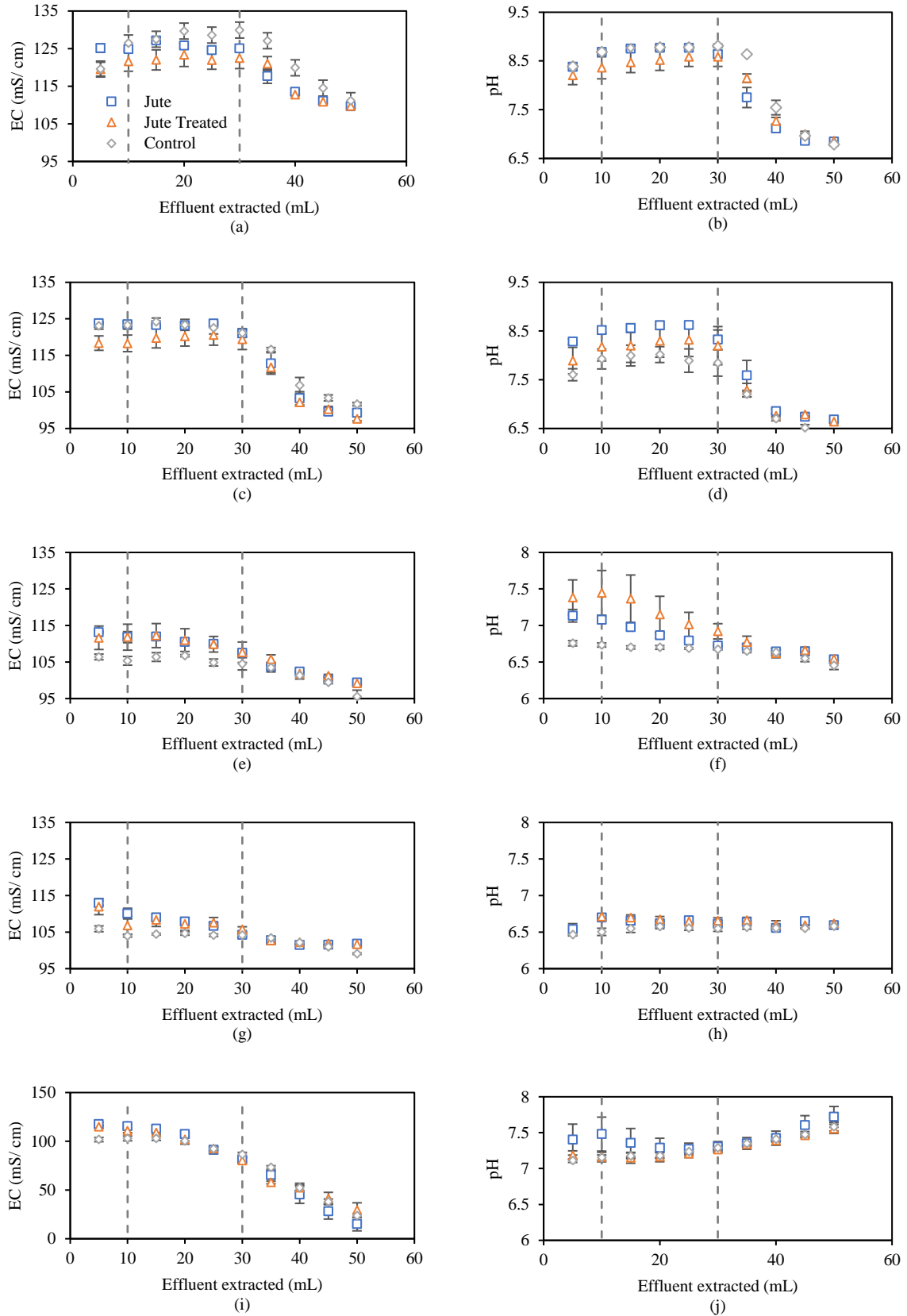


Figure 7-22: Electrical conductivity and pH of effluent from Test P3 columns following biocementation treatments 1 (a,b), 2 (c,d), 3 (e,f), 4 (g,h) and 5 (i,j), with error bars showing standard errors of the means for the triplicates.

7.4.4.3 Efficiency of Chemical Conversion

The chemical conversion efficiency results, as shown in Figure 7-23, for the treated jute columns are lowered by an inconsistent low result for column J6. This effect is also shown in Figure 7-24 up to treatment three. In comparison to the results shown in Figure 7-7 for Test P2 with 6 g/L nutrients in the CM, those in Figure 7-23 for Test P3 do not show a linear trend for columns containing untreated jute. This is a clear demonstration of the effect of varying the concentration of nutrients in the CM and shows that despite the slightly increased bacterial cell concentration of the column inoculant, and increased urease activity of the inoculant measured for Test P3, unless there are sufficient nutrients for the bacteria the calcium ion depletion starts to become noticeably inhibited beyond the second biocementation treatment. The difference between the three sets of results is less significant for Test P3.

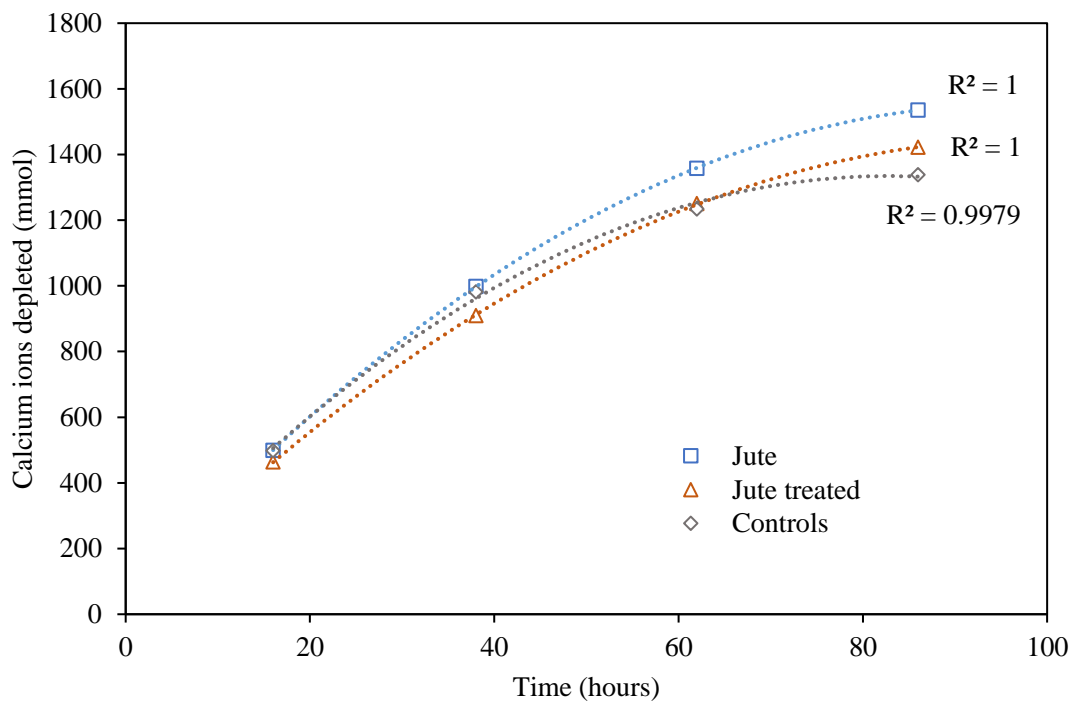


Figure 7-23. Cumulative reduction in concentration of calcium ions in Test P3 columns effluent following biocementation treatments one to four.

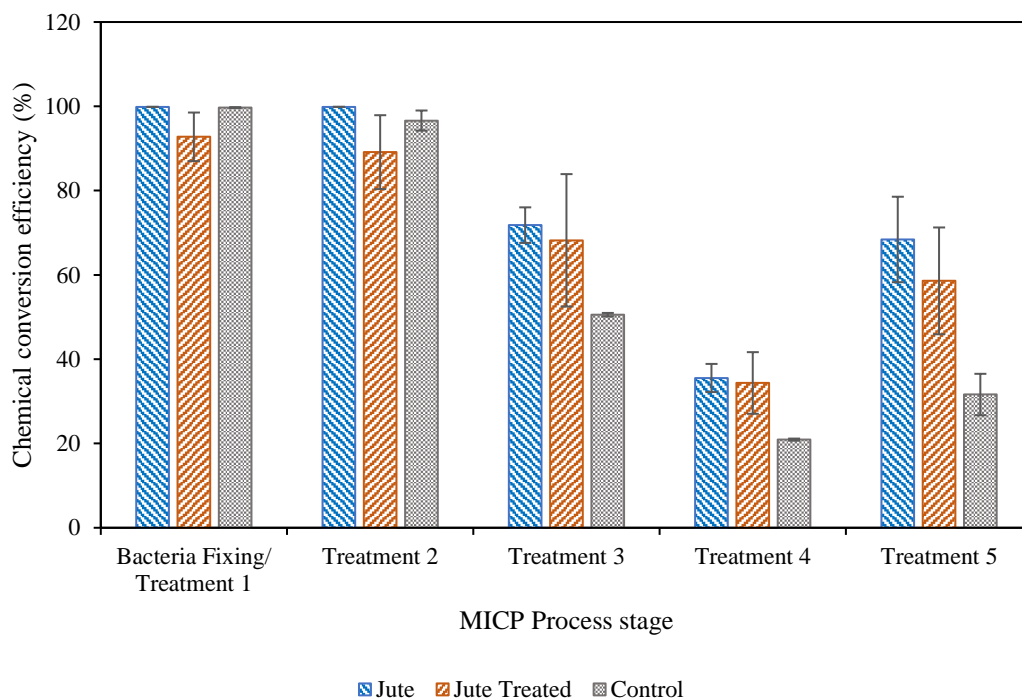


Figure 7-24. Chemical conversion efficiency, as determined from Ion Chromatography measurement of calcium ions within effluent from Test P3 columns following each biocementation treatment, with error bars showing standard errors of means for the triplicate sets of columns.

The results for chemical conversion efficiency for Columns Tests P2 and P3 are combined in Figure 7-25. These results give insight into the optimum concentration of the bacterial cells in the inoculant, this being close to an optical density OD_{600} of 1.0 for Test P3. Although the efficiency of chemical conversion reduces in the control columns for Test P3 following treatments three and four, when the retention time is increased to eight days for treatment five the chemical conversion is close to 100 % for the control columns and across all columns. Furthermore, regardless of the nutrient concentration in the CM injection, if the retention time is sufficient these results demonstrate that close to 100 % chemical conversion efficiency can be achieved for all columns. The study detailed in Chapter Nine gives further insight into this.

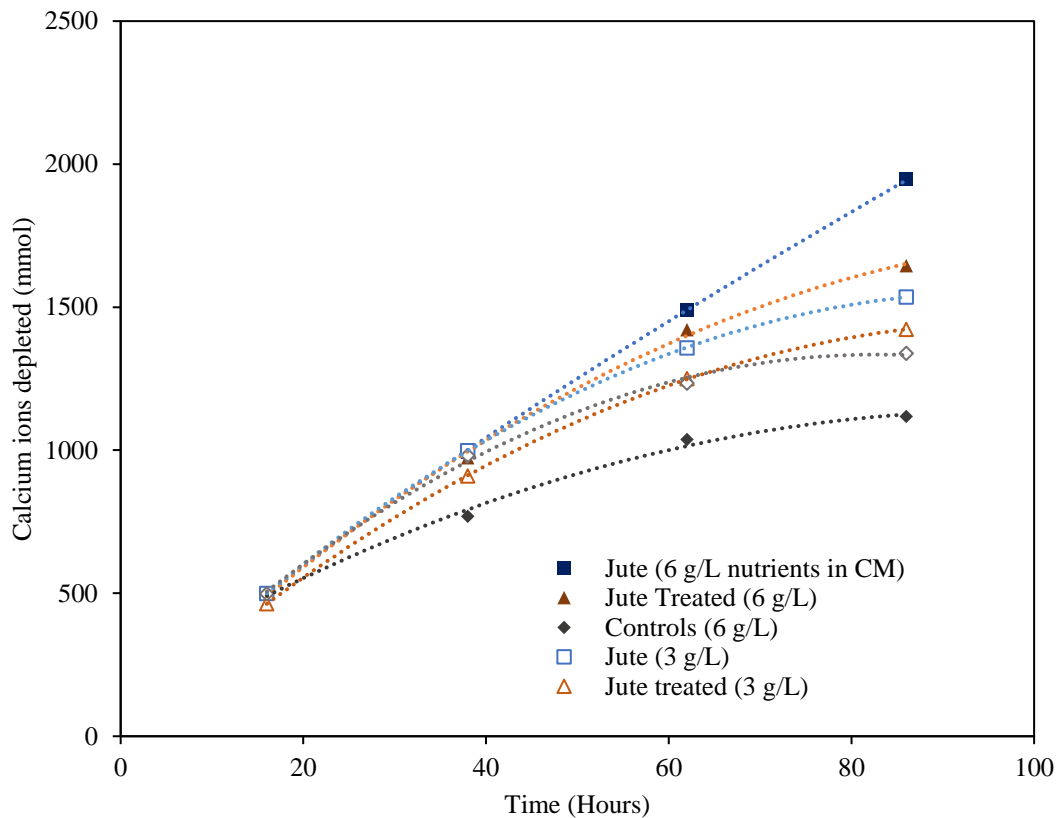


Figure 7-25. Combined results from Column Tests P2 (6 g/L nutrients in CM) and P3 (3 g/L nutrients in CM) showing cumulative depletion of calcium ions over time following biocementation treatments one to four. 500 mmol calcium ions are supplied with each treatment.

7.4.4.4 Unconfined Compressive Strength, and CaCO_3 Precipitated

The results shown in Figure 7-26 show much lower unconfined compressive strength values for the treated jute fibres when compared to columns containing untreated jute, and also when compared the results for test one. The treated fibres for both tests one and two were prepared at the same time, these were used in the columns with a few days of preparation for study one and stored for almost one month prior to use in test two. These lower unconfined compressive strengths when using treated fibres in test two show that these appear to have deteriorated and are therefore have little to no contribution to the biocemented columns compressive strength. It is possible that the concentrated chemicals used will degrade the fibres if treated too far in advance of the fibres being incorporated into the biocemented column system. There are greater variations between unconfined compressive strength values obtained for the biocemented columns containing untreated jute fibres in Test P3.

The average unconfined compressive strengths of triplicate columns containing jute, treated jute and control columns were 545 kPa, 160 kPa and 107 kPa respectively. The strength increase ratio between the controls and columns containing untreated jute is 5.09, a reduction when compared to test one of

this study. The overall higher strengths in comparison are otherwise likely due to the higher bacterial cell concentration of the inoculant. There is no indication of self-healing in results for Test P3.

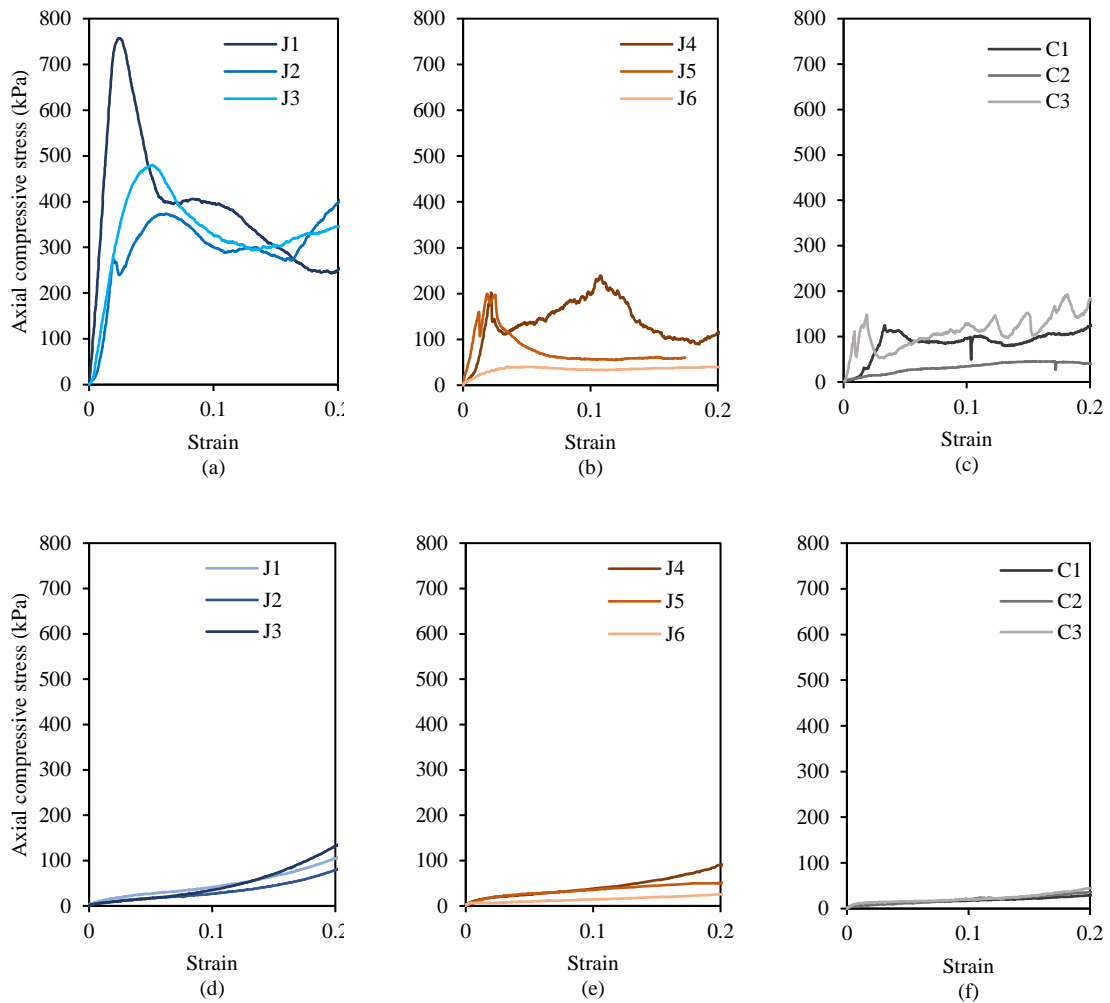


Figure 7-26. Unconfined compressive strength test results for UCS1 of Test P3 columns following biocementation treatment five (a–c), and UCS2 following column reconstitution, flushing, saturation with water and eight days of curing to test for self-healing (d–f).

Images of columns during the first unconfined compression test (UCS1) are shown in Figure 7-27. All samples show a clear shear failure line.

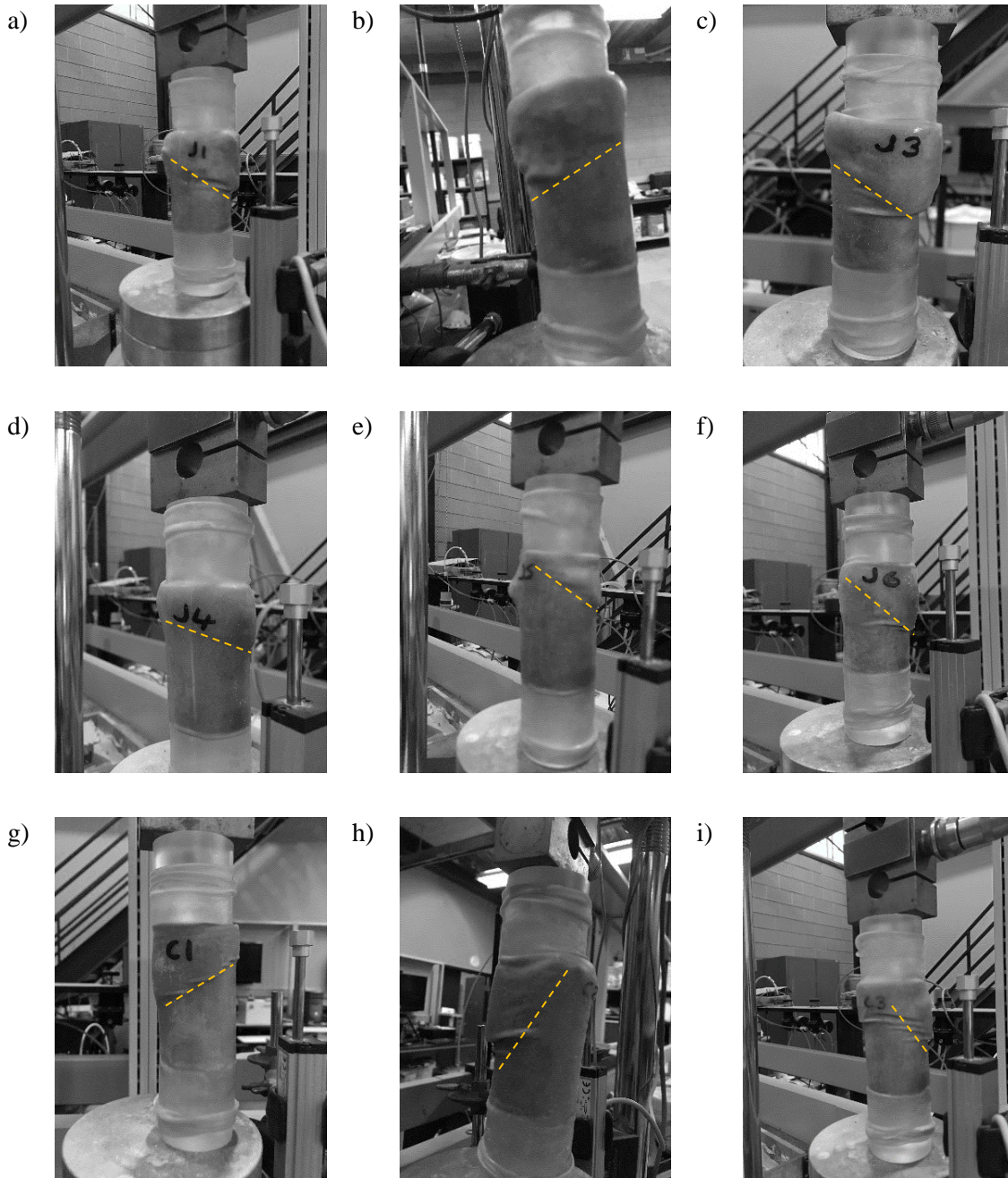


Figure 7-27. Images of columns J1 to J3 (a–c), J4 to J6 (d–f) and C1 to C3 (g–i), following the onset of failure during unconfined compressive strength test 1, for Columns Test P3. Annotations indicate direction and location of shearing plane.

Figure 7-28 shows images of the columns during UCS2 test two following the onset of failure. Other than those annotated, there were no clearly visible shear failure lines within the columns. The failures appear to be mostly a barrelling or crushing type of failure.

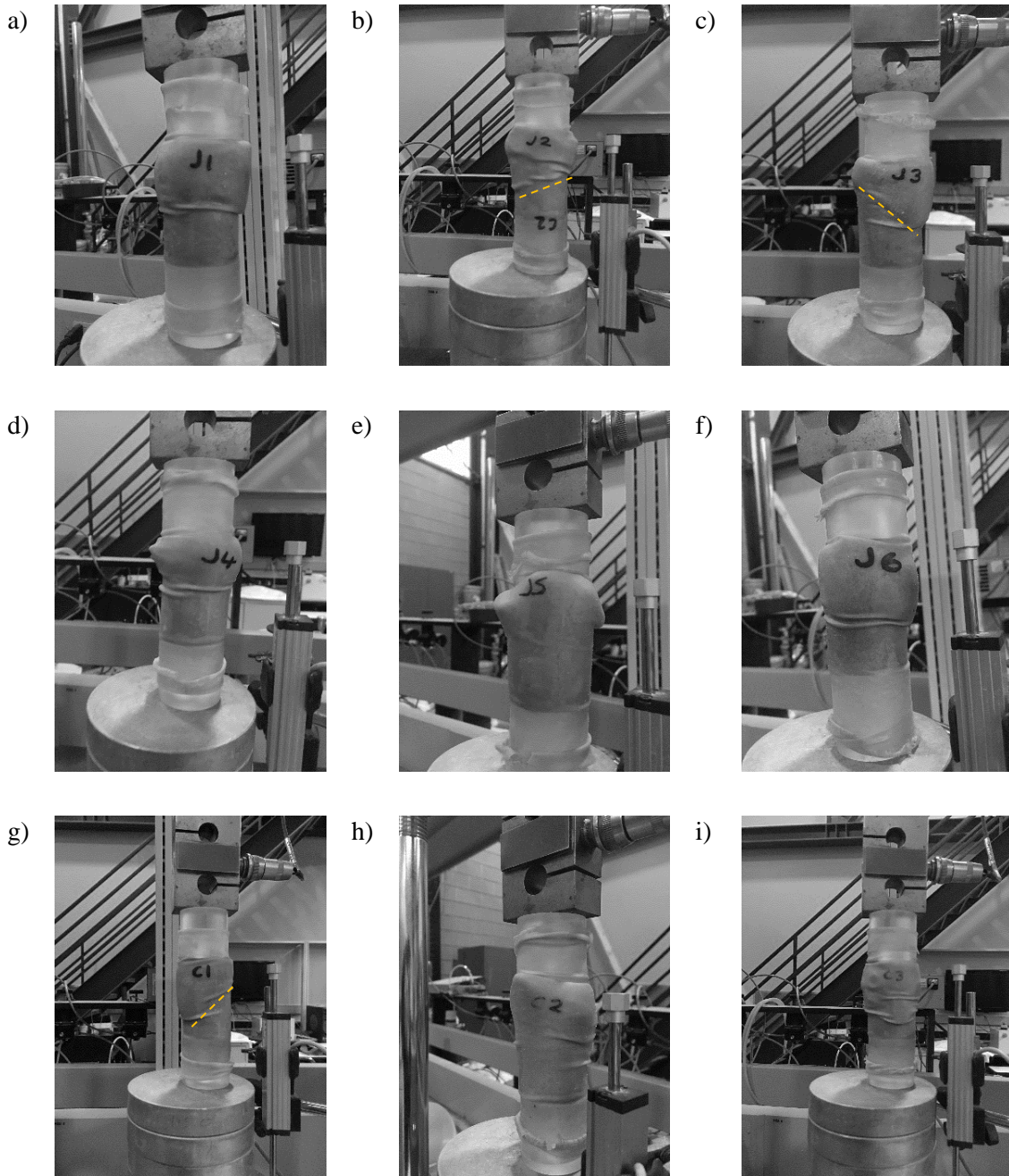


Figure 7-28. Images of columns J1 to J3 (a–c), J4 to J6 (d–f) and C1 to C3 (g–i), following the onset of failure during unconfined compressive strength test 2 (healing stage) of Columns Test P3.

Results shown in Figure 7-29 further show the effect of jute fibres on the MICP process and possible disadvantages of pre-treatment in advance of fibre use of fibres given unconfined compressive strengths of columns J4 to J5 are little higher than the controls. When compared to Test P2 and Figure 7-12 there is no evidence of self-healing.

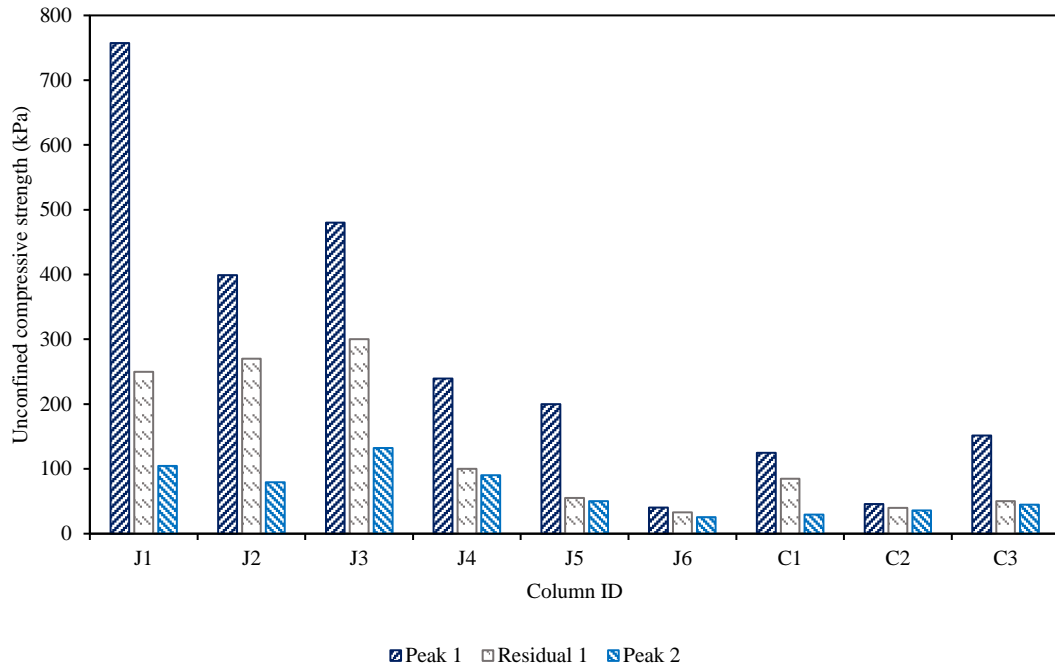


Figure 7-29. Results from UCS1 and UCS2 for Columns Test P3, showing peak and residual strengths from UCS1 and peak strengths from UCS2.

Results in Table 7-11 show that addition of untreated jute fibres resulted in an increase in calcium carbonate precipitation by 1.52 times on average, these being much less than found in test one of this study, however the increased bacterial cell concentration of the inoculant will have had some effect.

Table 7-11. Moisture and CaCO₃ contents of biocemented sand columns – Columns Test P3.

Column ID	Moisture content %	CaCO ₃ Content %
J1-J3	16.26 ± 1.13	3.20 ± 0.79
J4-J6	15.96 ± 1.00	3.17 ± 0.83
C1-C3	15.42 ± 0.28	2.10 ± 0.47

Figure 7-30 compares the UCS1 test results and average calcium carbonate contents of the biocemented sand columns, when comparing columns containing untreated jute and controls the pattern reflects that of test one. Results for columns containing treated jute are lower than had been expected following Test P2.

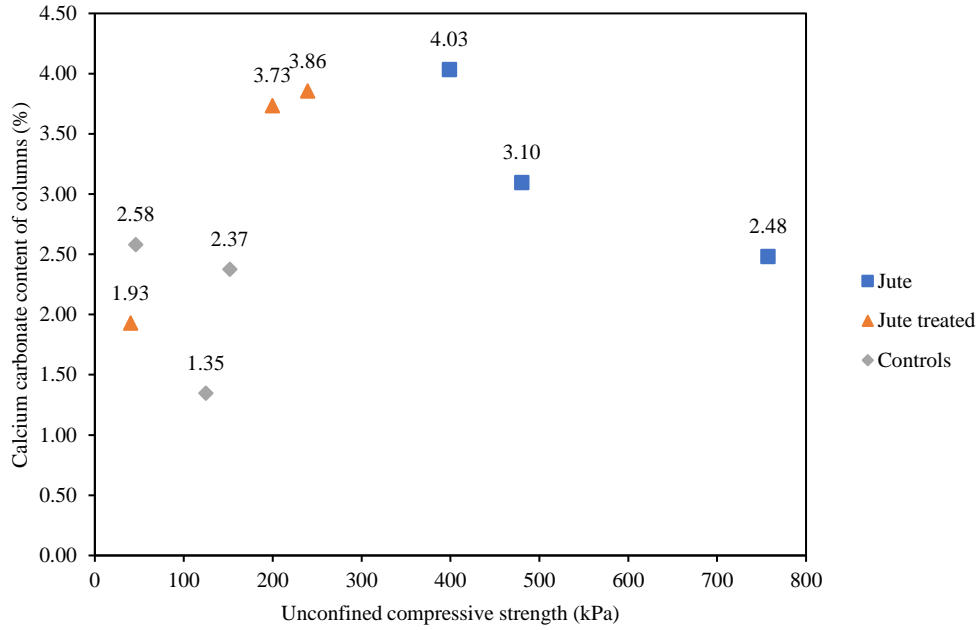


Figure 7-30. Average calcium carbonate content of Test P3 columns, as measured using a Calcimeter, showing relationship to UCS1.

The distribution of calcium carbonate precipitate within the biocemented sand columns, shown as an average for each set of triplicates, is shown in Figure 7-31. In comparison to test one the distribution is improved in columns J1 to J3. There is however much more variation across the central section of the columns as shown by the longer error bars in Figure 7-31.

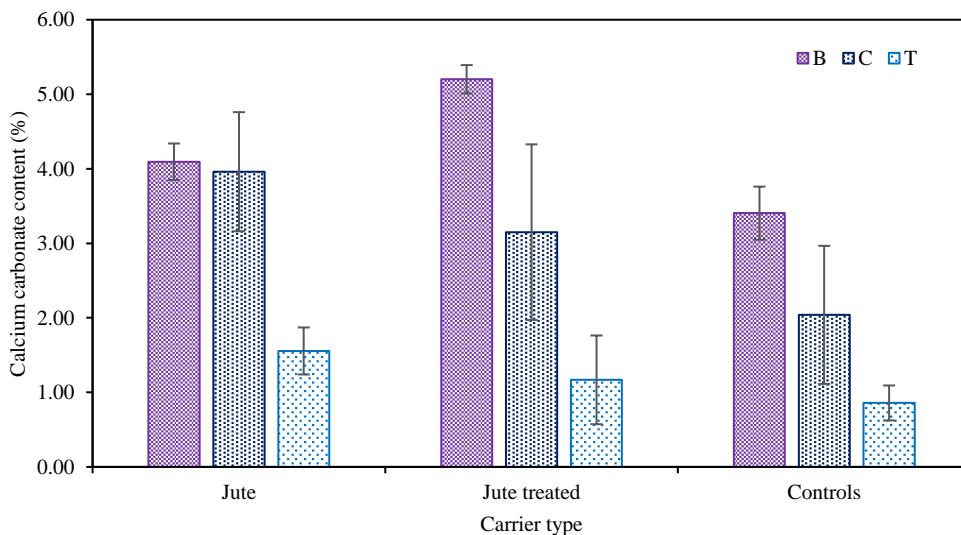


Figure 7-31. Distribution of calcium carbonate precipitated at the base (B), centre (C), and top (T) of Test P3 columns, with error bars showing standard errors of the means for the triplicates.

7.4.4.5 Morphology of CaCO_3 Precipitate

Prior to UCS2, the columns had been left hydrated for one month. This gives further insight into the identification of the polymorphs based on the shape observed under SEM. In Figure 7-32 (a to d) below there are clearly two distinct types of crystal structure. There were observed bundles of plate like crystals, as observed for samples from columns J1 and C1, and in contrast to these solid angular crystals observed in the sample from J4 (Figure 7-32 (b)). The latter are characteristic of calcite. The former are more likely to be vaterite, however the structural form of vaterite is less well observed in the literature and there is some inconsistency in respect of the descriptions of the structure form by other researchers.

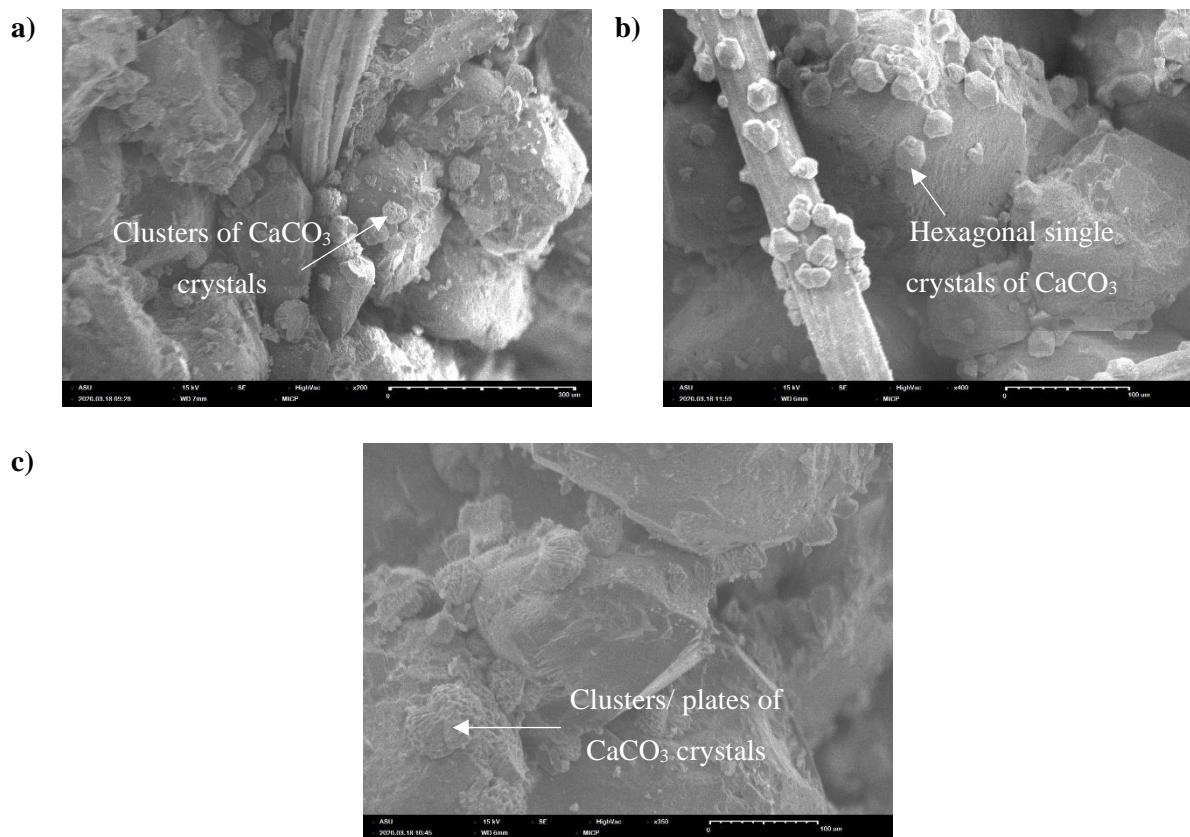


Figure 7-32. SEM images of samples from Test P3 biocemented sand columns containing jute (a), treated jute (b), and sand only controls (c).

Additional SEM images were not collected due to a subsequent fault with this equipment. The Scanning Electron Microscope (SEM) was also used for Energy Dispersive X-Ray analysis (EDX) of samples from columns J1, J4 and C1 Test P3 columns. The Energy Dispersive X-Ray Analyser was set to an accelerating voltage of 15 kV and samples analysed at a 100x magnification. EDX spectra and elemental analysis outputs are shown in Figures 7-33, 7-34 and 7-35. Whilst these give no further insight into crystal morphology, they verify the presence of calcium carbonate within these biocemented column samples. Percentages of elements present (by mass) are not indicative of the whole columns given the small size of the samples tested from the selected columns.

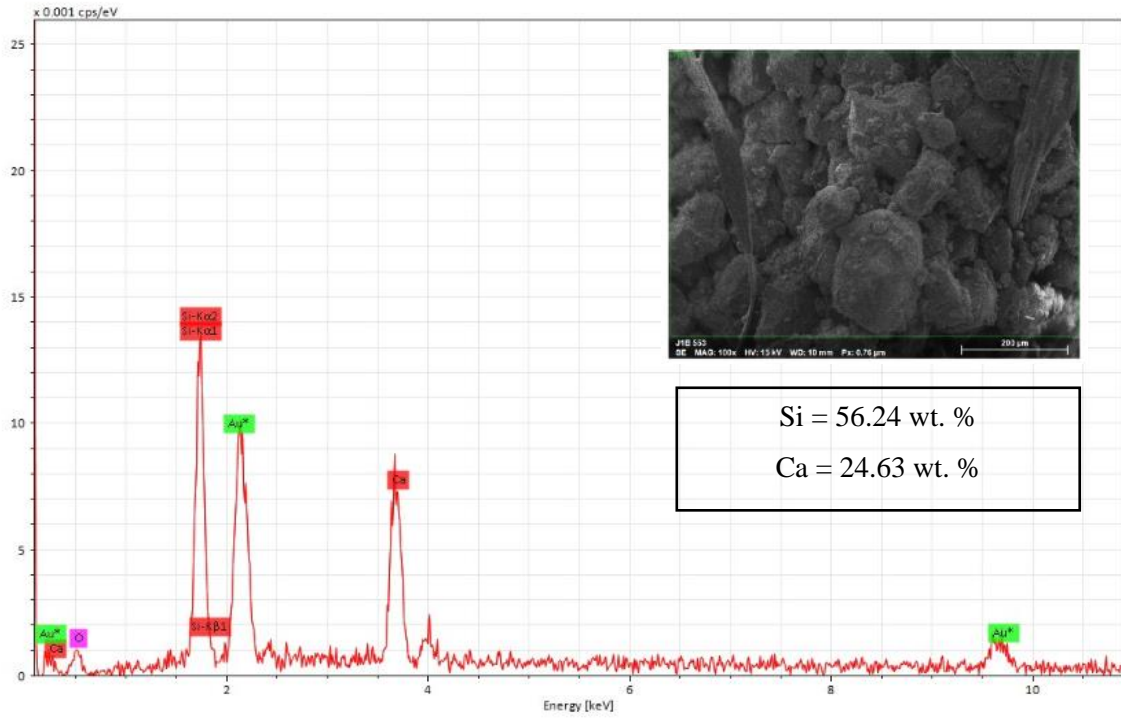


Figure 7-33. EDX spectrum and elemental analysis of sample from Test P3 column J1.

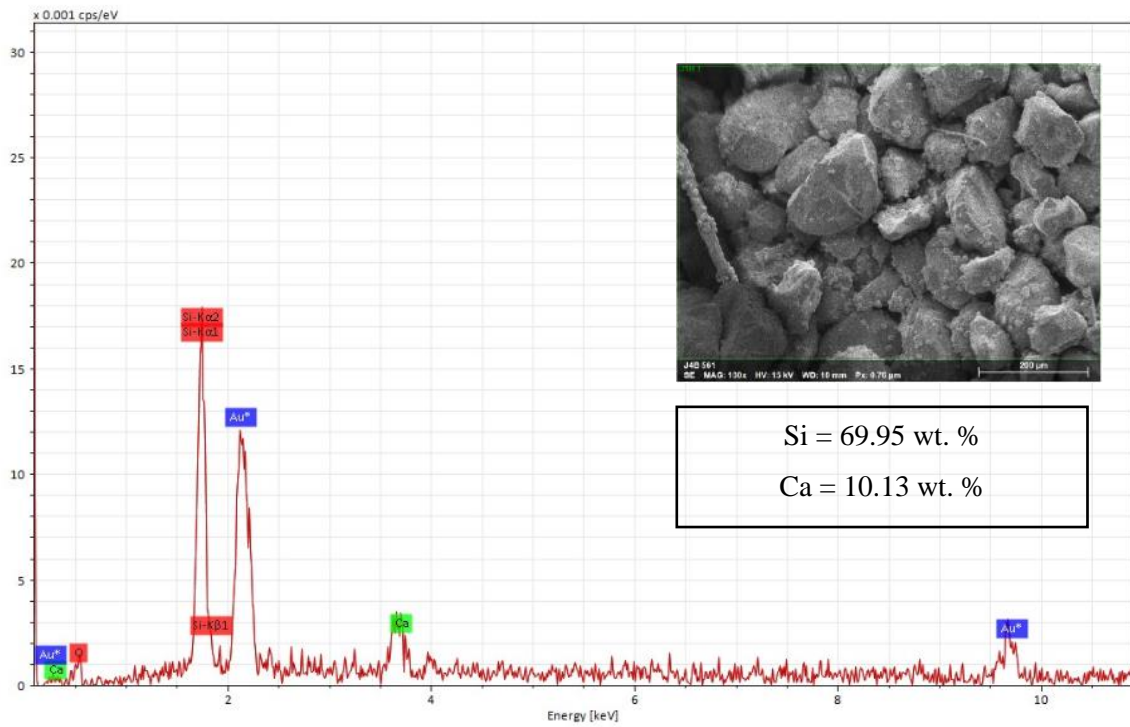


Figure 7-34. EDX spectrum and elemental analysis of sample from Test P3, column J4.

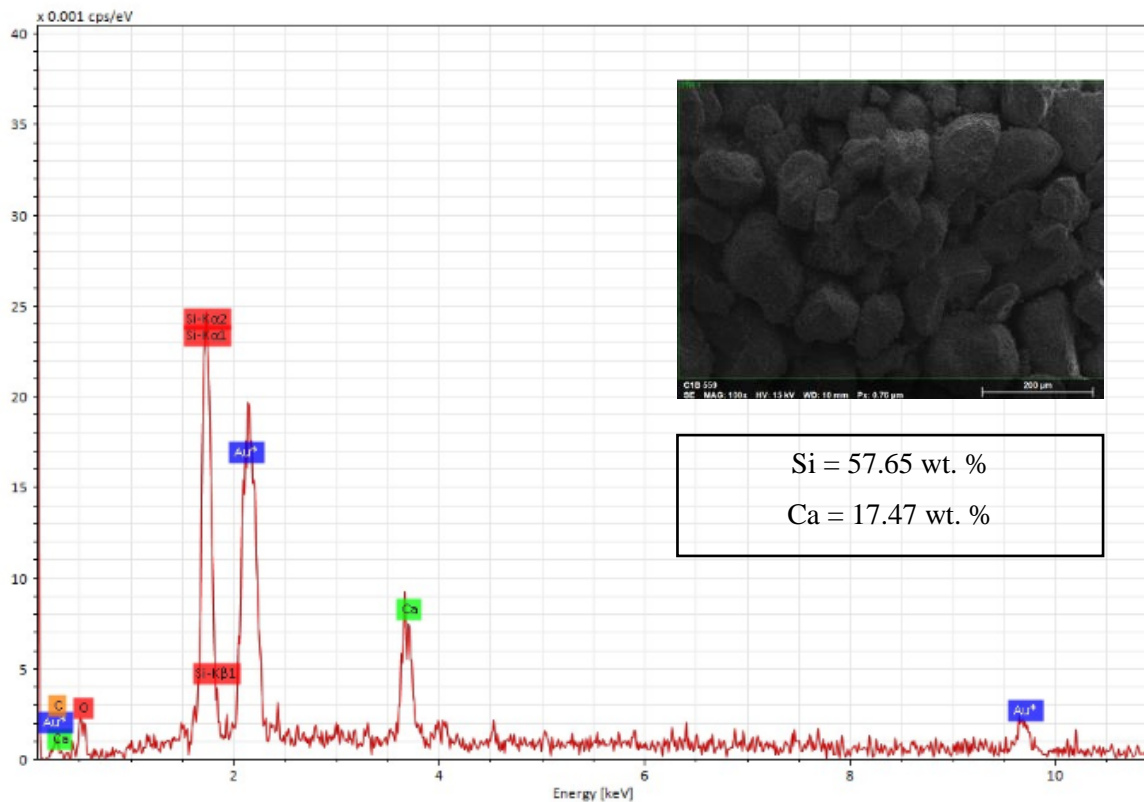


Figure 7-35. EDX spectrum and elemental analysis of sample from Test P3 column C1.

7.5 Conclusions

Column studies were undertaken to investigate the effect of jute fibres on both the process of MICP and on properties of biocemented sand including self-healing capability. Natural fibres, which are known for their ability to reinforce, had been incorporated within a biocement to improve strength characteristics. Biocemented sand columns were produced in triplicates, containing sand and untreated jute fibres, sand and treated jute fibres and sand only as controls. The treated fibres immobilised a concentrated cementation medium, with the aim of enabling self-healing via MICP.

Results showed that columns containing 0.75 % (by weight of sand) untreated jute fibres had unconfined compressive strengths approximately six times greater on average compared to biocemented sand columns without jute fibres when the nutrient content of the cementation medium had been 6 g/L. In comparison, when the nutrient content of the CM was reduced to 3 g/L, this strength increase of biocemented columns containing untreated jute reduced to approximately five times that of the controls on average.

Furthermore, efficiency of chemical conversion was found to be higher in columns containing untreated jute fibres, as measured using ion chromatography. Columns containing jute had calcimeter measured

CaCO₃ contents on average four times higher than those containing sand only. This reduces an average of 1.5 times higher when the nutrient content of the cementation medium is reduced to 3 g/L. It is noted that for Columns Test P3 the average calcium carbonate content of controls had been higher than that for P2, these being 2.10 ± 0.54 % and 1.08 ± 0.47 % respectively. This likely being due to the slightly increased urease activity for test P2.

The results showed that the incorporation of jute fibres within a biocemented sand material significantly increased the unconfined compressive strength of this material when compared to biocemented sand without the jute fibres. This strength increase results from the contribution to strength properties of not just the fibres themselves, but also the increased amount of calcium carbonate precipitated in the columns containing jute fibres. On the basis of the results obtained, the contribution to unconfined compressive strength increase by the fibres alone cannot be ascertained. In addition to increasing strength, the inclusion of fibres had a beneficial effect on the MICP process, improving efficiency of substrate conversion, likely as a result of sustaining the bacterial growth and, hence, urease activity. It is likely that bacteria had also been immobilised by the jute within the columns, both on the surface and within the fibre structure, and that this contributed to the positive findings. More investigation would be required to fully understand this effect. Tuson et al. (2013) reported that bacterial systems used for sensing and responding to surfaces are still not well understood. Surface roughness of the fibres also appears to have added to this effect given the higher density of calcium carbonate crystals observed on the surface of roughened fibres. Renner et al. (2011) reported the significant influence of surface topography on bacterial adhesion. Bacteria will likely have been less able to be immobilised by the fibres which had been treated (immobilised the concentrated CM4p).

A consequence of the fibre inclusions within the biocemented sand sustaining longer term activity of *Sporosarcina pasteurii* bacteria is the enabling of the continuation of the MICP process without the need for multiple injections of bacteria. This could reduce the cost of production of a biocemented sand material and would be beneficial where several treatments of cementation medium are required to achieve a low permeability and/or high strength.

The evaluation of self-healing effects and quantification of this has proved challenging, with only one column containing treated fibres showing any significant potential self-healing capacity. To achieve self-healing via MICP, the cementation medium would need to be stored within the biocemented material matrix for later release. Immobilisation may only be effective if a material embedded within the biocemented material can retain sufficient cementation medium during the initial MICP treatment process. Therefore, a material which enables a sufficiently slow release of immobilised chemicals would be required, or otherwise a more efficient MICP process involving fewer treatments. More testing is required on this aspect and alternatives such as encapsulation of CM, possibly by impermeable materials, explored.

The results from the set of columns containing the treated fibres may give some insight into effects of pre-treating fibres prior to use in MICP applications. These fibres were subject to chemical treatment with the concentrated cementation medium, and also some additional heat treatment while these fibres were dried at 50 °C following spraying on of the CM4p. This is an area which could be explored further and had not been a focus of this study. This study could be further extended using recycled jute fibres. It is expected that surface roughness of recycled fibres may further promote fixing of bacteria to fibres, however, any processing treatment fibres have undergone, contamination of fibres and potential deterioration should be taken into consideration.

Having exactly the same bacterial concentration and activity in the inoculant for both column tests P2 and P3 presented in this chapter was desired, however the difference between these for the two studies has yielded further insights into factors affecting MICP and ideal conditions for this treatment process. Despite the reduction in bacterial cell concentration, the urease activity across the two studies was similar, this having been measured as 4.37 mM urea hydrolysed/ min for Column Test P2 and 4.56 mM urea hydrolysed/ min for Column Test P3. Due to urease activity of the P3 inoculant being higher this will have had some effect and likely led to the increased values of chemical conversion efficiency for the Test P3 control samples, when compared to Test P2, despite the lower quantity of nutrients supplied. Nonetheless, the Test P2 results for calcium ion depletion are otherwise greater when compared to Test P3 for columns containing the jute fibres. There was much less differentiation between results for calcium ion depletion for the three sets of columns when the nutrient supply was reduced for Test 3P. The effect on MICP thereby appears to be more pronounced in conditions where the bacterial inoculant concentration is lowered, provided that there are sufficient nutrients for bacterial growth, i.e. 6 g/L of the Oxoid CM0001. These results show that doubling the nutrient supply in the cementation medium has a beneficial effect.

The urease activity of the liquid broth inoculant produced for the columns studies in chapter Seven is lower than that measured in subsequent chapters. This was likely due to the reduction in surface area to volume ratio within the larger 500 mL flasks used for production of liquid broth cultures at this stage, since each flask contained 150 mL of culture. For studies using 250 mL flasks to produce 50 mL of liquid broth culture in each the measured urease activity of the culture was higher in comparison. The results however showed that the addition of jute could boost the chemical conversion efficiency to close to 100% even when urease activity was reduced.

Following completion of this study, a study published by Al Imran et al. (2020) also considered effects of jute fibres on MICP, however the biogeochemical processes were not considered, only mechanical effects, not the effects on MICP itself. In comparison, the fibres used had been processed into twine of 2 mm thickness compared to being the raw loose fibres used in this study and *Micrococcus yunnanensis* was used to induce MICP. This study by Al Imran et al. (2020) had found the optimum fibre content to

be 3 % by weight of sand and they suggest that the fibres provide a source of nutrients for the bacteria, this is disputed however. Over time lignocellulosic natural fibres such as jute within a soil environment will be broken down by enzymes produced by bacteria within the soil. Examples of enzymes which break down/ degrade fibres include xylanase, cellulase and pectinase. Xylanases are hemicellulolytic (Bajpai 2014) and are typically using for pre-bleaching of fibres. The degree of fibre degradation is dependent upon enzyme concentration (Vigneswaran and Jayapriya 2010). High activity cellulase is required to extensively degrade insoluble cellulose to sugars. Pei et al. (2021) reported that it has been shown that *S. pasteurii* is unable to utilize glucose, from Norris (1981), and therefore yeast extracts are commonly used in laboratories as its carbon source.

8 COLUMN STUDY THREE: Encapsulation of Cementation Medium in Alginate-Based Hydrogel Beads

8.1 Materials and Methods

8.1.1 Sand

F60 sand, with properties as given in Chapter Seven, was used for this study. The sand was autoclave sterilised prior to use and oven dried at 105 °C.

8.1.2 Sodium Alginate and Cementation Medium Bead Production

The use of hydrogel beads produced using sodium alginate was explored as a means of encapsulating cementation medium. Beads were produced which contained a mixture of sodium alginate (Alginic acid, sodium salt, Acros Organics), urea, Oxoid CM0001 nutrient broth and calcium chloride (Alfa Aesar). Alginate-based hydrogel bead production, for use in columns inoculated with *S. pasteurii*, was based on the method developed by Palin et al. (2016), which uses a peristaltic pump to extrude beads through a syringe needle. The aim was to produce beads containing a x10 concentration of cementation medium in respect of urea and Oxoid CM0001. The calcium source is provided by a gelling agent used to form the beads.

To make the hydrogel beads, following the modified Palin (2016) method, firstly 100 mL of a 1.5 % (w/v) sodium alginate gel solution in autoclaved deionised water was prepared in a sterilised 250 mL beaker. To aid mixing, a magnetic stirrer was used. A higher sodium alginate content was found to not fully dissolve. The urea (60 g) and Oxoid CM0001 (6 g) were then added in powder form to this solution and using the magnetic stirrer this solution was mixed until these powders were fully dissolved. The resulting mixture was approximately 150 mL. This mixture was then covered and refrigerated until the air bubbles in the mixture had risen to the surface and dissipated. A 250 mL solution of 0.2 M calcium chloride, prepared using calcium chloride anhydrous, in deionised water, was prepared and autoclaved. The apparatus used to prepare the beads is as shown in Figure 8-1. Aseptic technique was followed as much as possible during the production of the beads, with the apparatus situated close to a Bunsen burner. The powdered chemicals used were not sterilised. Autoclaving of an alginate gel solution was found to result in some loss of viscosity.

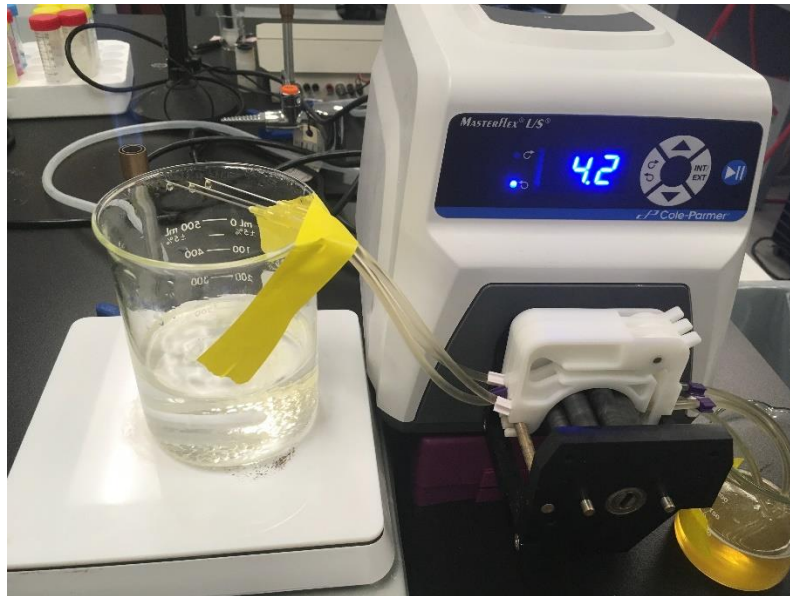


Figure 8-1. Photograph showing the production of alginate-based hydrogel beads encapsulating cementation medium and the apparatus used for bead extrusion.

Three lines of micropore Tygon 2.79 mm ID tubing were connected to a peristaltic pump using a multi-channel pump head. At one end of each tube a sterile disposable syringe needle (Air-Tite 20G 1/2") was attached and this end of the tubing was then secured with tape to a beaker containing the calcium chloride gelling agent solution. The syringe needle was positioned approximately 5 cm above the top of calcium chloride solution. The pump was set to a 1.5 mL/min pumping rate (Approx. 4.2 RPM). The highly viscous sodium alginate, urea, and Oxoid CM0001 solution was pumped through the syringe needles to form droplets which then fell into the calcium chloride gelling agent. The calcium chloride gelling agent was slowly stirred using a magnetic stirrer during this process to prevent clumping of beads. The solution containing the beads was then filtered and the beads transferred to a sterile flask, as shown in Figure 8-2 and covered with a permeable lid, which allowed for evaporation of excess liquid over 48 h at room temperature.

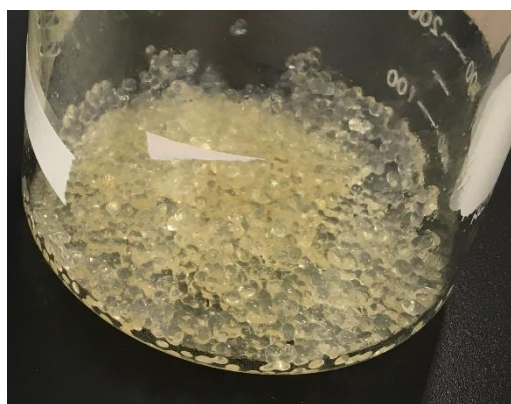


Figure 8-2. Beaker containing alginate-based beads encapsulating cementation medium.

To complete the drying process, to avoid beads sticking together, the beads were then transferred to a paper towel, with another paper towel placed over the top which was gently moved over the beads to

separate them before being replaced with a dry paper towel. The beads were then left to dry fully. Oven drying at 36 °C for 24 h, as reported by Palin et al. (2016), was not found to be an effective drying technique, this was found to potentially draw out chemicals from the beads since they were left reduced in size and surrounded by fluid, even if the temperature was lowered to 30°C. The dry beads were approximately 2 mm in diameter, as shown in Figure 8-3.



Figure 8-3. Dried alginate- based hydrogel beads encapsulating cementation medium.

8.1.3 Bacteria Culture

Sporosarcina pasteurii (ATCC 11859) was used for this study. Five 50 mL liquid broth cultures were prepared in 250 mL Erlenmeyer flasks, using an autoclave sterilised growth medium consisting of 13 g/L Oxoid CM0001 with 20 g/L urea added using a syringe filter and inoculated with 100 µL of an overnight liquid broth culture of *S. pasteurii*. These cultures were incubated at 23°C, 150 rpm, until late exponential growth was achieved. Urease activity of the culture was tested prior to use.

8.1.4 Cementation Medium and Treatments

Two cementation media CM1p and CM3p were prepared for this study, as per Table 8-1, and as used in the prior study. CM1p was used for treatment one, followed by CM2p for treatments two to four.

Table 8-1. Cementation media prepared for Columns Test P4.

Precursor Chemicals and Nutrients	CM1p (g/L)	CM3p (g/L)	Sterilisation Method
Calcium chloride dihydrate (CaCl ₂ ·2H ₂ O)	73.51	73.51	Autoclaved
Urea (NH ₂ (CO)NH ₂)	40	40	Syringe filtered
Ammonium chloride (NH ₄ Cl)	0	20	Autoclaved
Sodium bicarbonate (NaHCO ₃)	0	2.12	Syringe filtered
Oxoid CM0001	3	3	Autoclaved

The treatments schedule was as per Table 8-2. Retention times following each cementation medium (CM) injection were 16 h, 22 h, 24 h, 24 h and 192 h for the five treatments, with all treatments containing 3 g/L Oxoid CM0001.

Table 8-2. Schedule of biocementation treatments for Columns Test P4.

Treatment	Retention Time (h)	Column Injection
1	16	CM1p
2	22	CM2p
3	24	CM2p
4	24	CM2p
5	192	CM2p
N.A.	0	Tap Water

8.1.5 Leaching test

Prior to assembling columns, a leaching test was performed over 48 h. 1 g batches of beads were prepared in triplicate and placed into 50 mL centrifuge tubes, to which 35 mL of deionised water was added, this being the quantity of liquid used to prepare each column. The tubes were left at room temperature for 24 h and the liquid from these was then drained. Samples were taken from these and diluted and subjected to cations analysis using an ion chromatograph. After draining the fluid this was then replaced with an equal quantity of deionised water and drained again and tested after a further 24 h.

8.1.6 Column Preparation

Columns were prepared as per the methodology detailed in Chapter Four and Chapter Seven. Six columns were prepared with contents as per Table 8-3, consisting of three sets of duplicates, with two control columns containing no beads and otherwise two sets of columns with variations of bead content, with columns prepared with 1 g and 10 g beads per column, which amounted to 0.7% and 7% of the total mass of columns respectively. The effect of varying bead content was explored. Columns were compacted to an average density of 1.65 g/cm³ and 97% of the target density based on proctor compaction tests using the F60 sand alone.

Table 8-3. Contents of columns prepared for Columns Test P4.

Column	Beads (g)	Sand (g)	Total Mass (g)	% by mass of beads
B1	1	141	142	0.70
B2	1	141	142	0.70
B3	10	136	146	6.85
B4	10	136	146	6.85
C2	0	143	143	0
C3	0	143	143	0

The beads were added to the sand and mixed with the sand by hand before wet pluviation of the sand and bead mix into cementation medium CM1p within the columns.

8.1.7 Testing procedures

Testing was undertaken as per the methods detailed in Chapter Seven, Sections 7.3.7 to 7.3.10. During the treatment process, effluent discharged from the top of each column into the outlet tubing was collected in a series of 5 mL quantities in 15 mL polypropylene tubes. The pH and electrical conductivity of the effluent in each tube was measured within one hour of collection. The first 5 mL of effluent from each tube was then discarded and the next three tubes for each column (5 mL – 20 mL) mixed. 100 µl was taken from this mixture, for each column, to make a 1:500 dilution using a volumetric flask, from which 1 mL samples were taken and transferred to Dionex ion chromatography vials using a pipette. The calcium ion concentrations of these samples were measured using an ion chromatograph. Dionex ICS 5000+ Cation analysis was conducted using 20 mM methanesulfonic acid eluent starting concentration, on a Dionex CS12A column, using 112 mA suppressor output.

A Calcimeter was used to measure the calcium carbonate content of samples taken from each column. Samples of approximately 5 g were taken from the top centre and base of each column following oven drying at 105 °C.

8.2 Results and Discussion

8.2.1 Leaching Test

Results of the leaching test are shown in Figure 8-4. These show that most of the calcium had leached out of the beads after 24 h, under static conditions. The ammonium appears to leach out more slowly than calcium. The measurement of ammonium ions by ion chromatography was found to be higher than measurements obtained using nesslerisation, and therefore these values given are likely higher than the actual concentrations. Based on these values, 10 g of the alginate beads with immobilised CM would provide sufficient cementation medium for one MICP treatment for the whole column as just over 300 mmol/L of calcium ions would be provided.

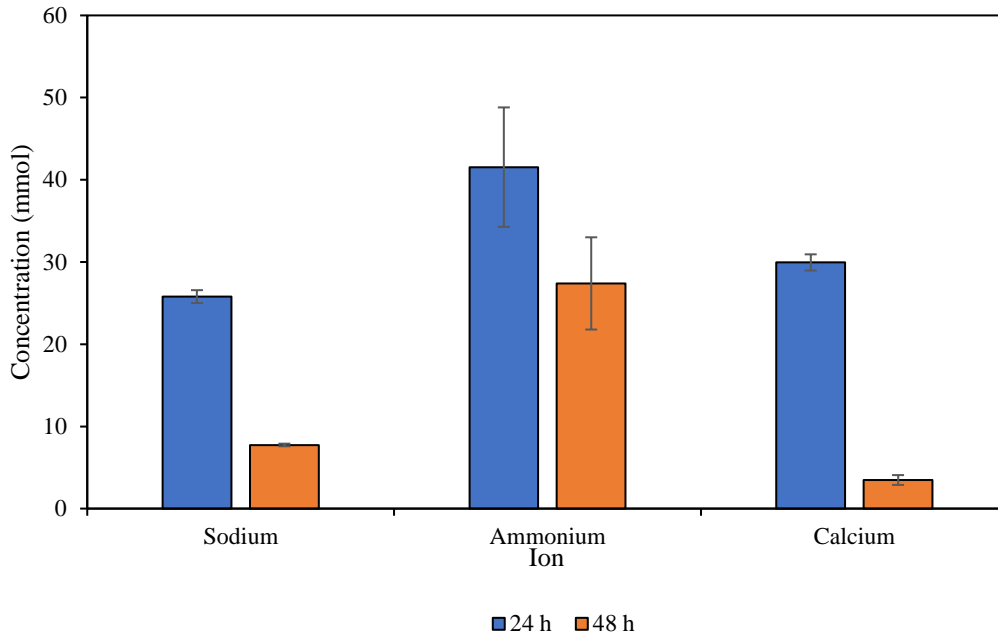


Figure 8-4. Concentrations of sodium, ammonium and calcium ions in solutions containing cementation medium constituents leached from alginate-based hydrogel beads after 24-h and 48-h periods of soaking samples of beads in deionised water, with liquid drained and fresh water added after the first 24-h soaking period. Error bars show standard errors of the means for the triplicates.

8.2.2 Columns Test P4

8.2.2.1 Distribution of Bacterial Activity

The bacterial culture had been grown to an optical density OD_{600} of 0.994, with minimal loss of bacteria in supernatant, this having had an optical density of 0.029. Figure 8-5 (a-j) shows the pH and electrical conductivity measurements of effluent displaced from columns during each treatment process. Initially there appears to be some inhibition of activity in columns B1-2, as can be seen in Figure 8-5 (a), otherwise following treatment one, the activity is similar for columns B3-4 and C1-2 (controls). This inhibition of activity for columns containing beads starts to reverse from treatment two onwards, following a similar pattern to that observed in the studies using jute. As the study progresses the activity within columns B1-B2 becomes greater than the other columns following treatment three onwards. Overall, the activity is greater in columns containing the beads following treatment two onwards.

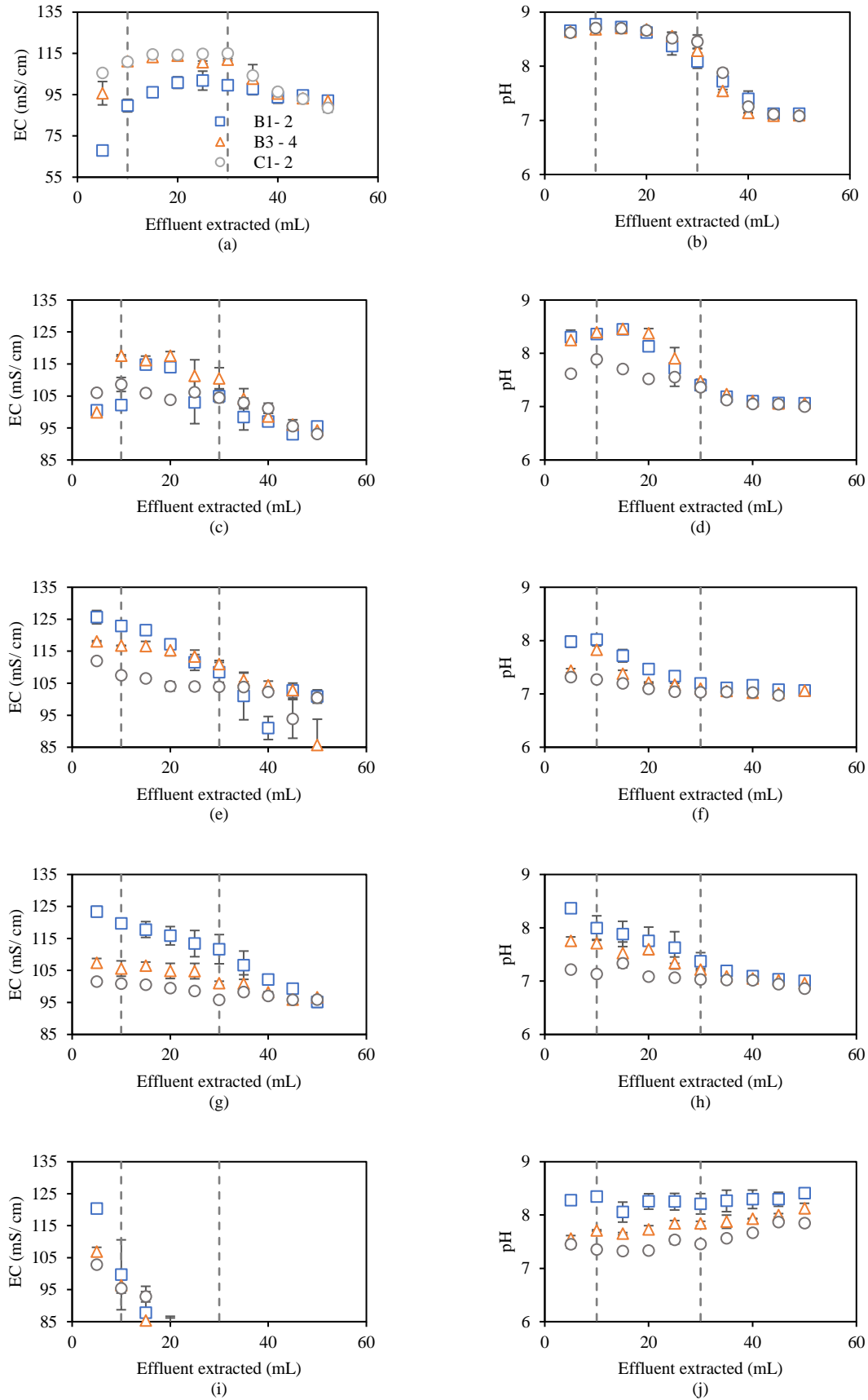


Figure 8-5. Electrical conductivity and pH of effluent from Test P4 columns following biocementation treatments 1 (a,b), 2 (c,d), 3 (e,f), 4 (g,h) and 5 (i,j), with error bars showing standard errors of the means for the duplicates.

8.2.2.2 Efficiency of Chemical Conversion

The efficiency of chemical conversion is shown in Figure 8-6. This shows that the alginate gel beads have had the effect of increasing the chemical conversion efficiency. The efficiency is however not as high for the columns containing 10 g of beads compared to those containing 1 g of beads. This suggests that for larger quantities of beads there is an inhibitory effect.

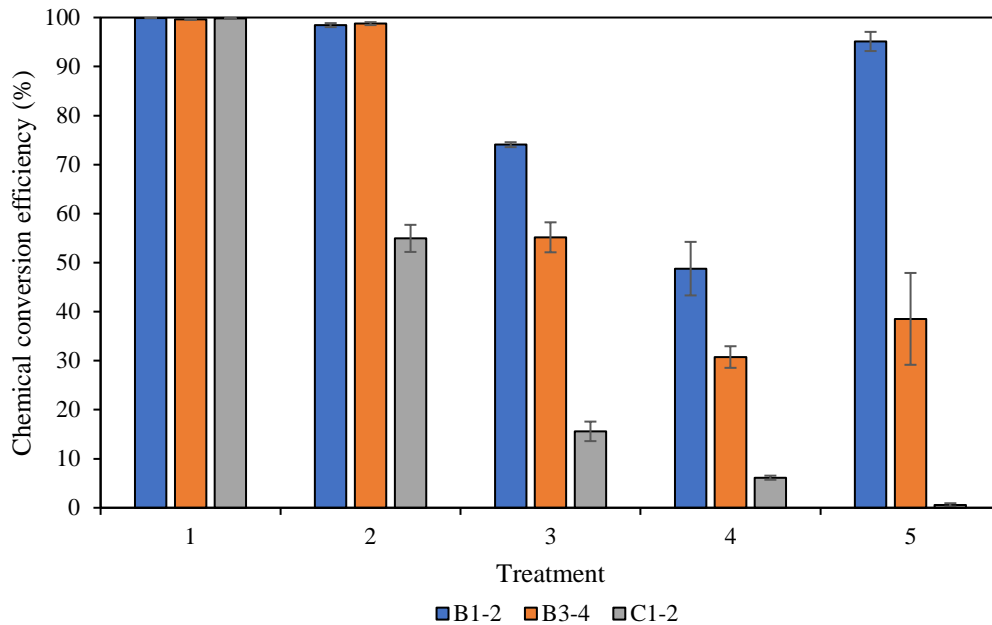


Figure 8-6. Chemical conversion efficiency, as determined from Ion Chromatography measurement of calcium ions within effluent from Test P4 columns following each biocementation treatment, with error bars showing standard errors of means for the duplicate sets of columns.

8.2.2.3 Unconfined Compressive Strength

Figure 8-7 (a to f) shows images of the columns during UCS testing shortly after failure. Apart from column B1, where shear failure is shown across the middle third of the column in Figure 8-7 (a), the columns with beads display a crushing type of failure in the top third of the column. Column B1 had the highest measured unconfined compressive strength of the six columns tested.

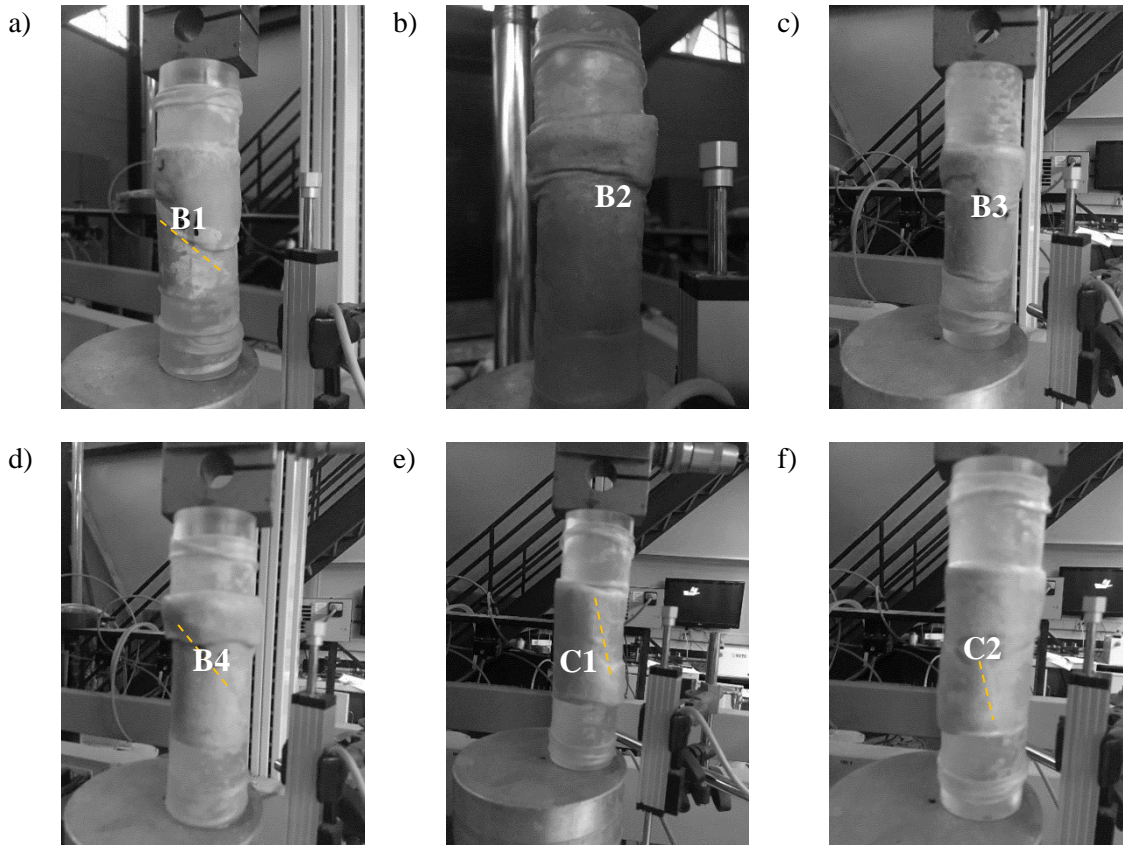


Figure 8-7. Photographic images of columns B1 to B2 (a–b), B3 to B4 (c–d) and C1 to C2 (e–f), following the onset of failure during unconfined compressive strength test 1 for Columns Test P4. Annotations indicate direction and location of shearing plane.

Figure 8-8 (a-f) shows images of the columns after failure during the second UCS test (UCS2). This was undertaken to test for self-healing effects. In contrast shear failure lines are observed in samples B1-B3 and appear clearer than those observed during UCS1. For columns B2 to B4 there had been observed a brittle/ crushing failure in the top third of the column during UCS1, whereas there is a shear plane diagonally through all of the columns containing the alginate gel beads following UCS2. This contrasts against earlier results whereby observations of failure were similar when comparing UCS1 and UCS2. The remaining columns show a barrelling type of failure.

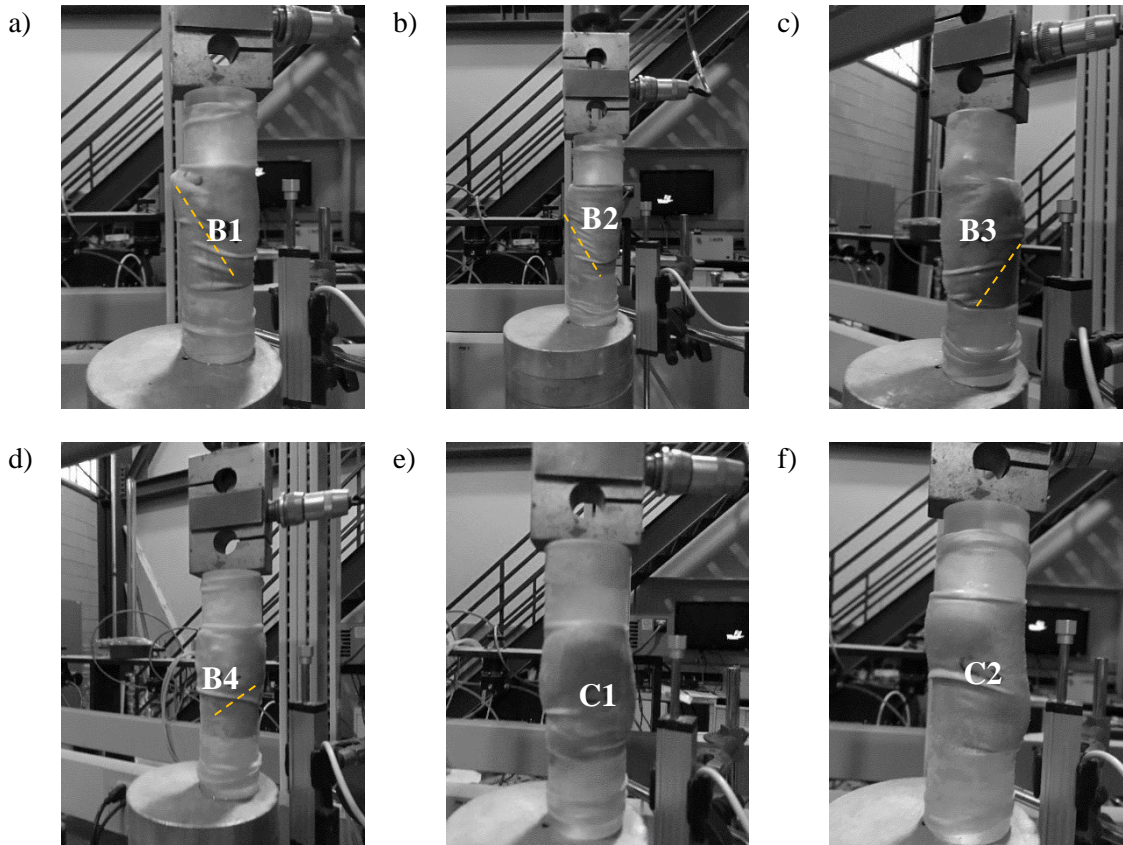


Figure 8-8. Photographic images of columns B1 to B2 (a–b), B3 to B4 (c–d) and C1 to C2 (e–f), following the onset of failure during unconfined compressive strength test 2, for columns Test P4. Annotations indicate direction and location of shearing plane.

Unconfined compressive strength results for UCS1 and UCS2 are shown in Figure 8-9 and are summarised below in Table 8-4. There are no indications of self-healing activity based on these results. The average peak strengths for the columns with 10 g beads (B3-4), 1 g beads (B1-2) and no beads (C1-2) are 85 kPa, 136 kPa and 70 kPa respectively. Larger quantities of beads are likely to have an adverse effect on compressive strength, as shown by the UCS results. The peak strengths for the columns B2 to B4 are at or near 20 % strain, as shown in the stress-strain graphs. This coincides with there not being a clear shear failure visible in these columns. This behaviour has not been seen in prior tests.

Table 8-4. UCS test results for Columns Test P4, reported to 2 significant figures.

Column	Peak 1 (kPa)	Residual 1 (kPa)	UCS2 (kPa)
B1	170	56	34
B2	105	52	36
B3	70	47	25
B4	100	51	22
C1	103	18	17
C2	38	20	22

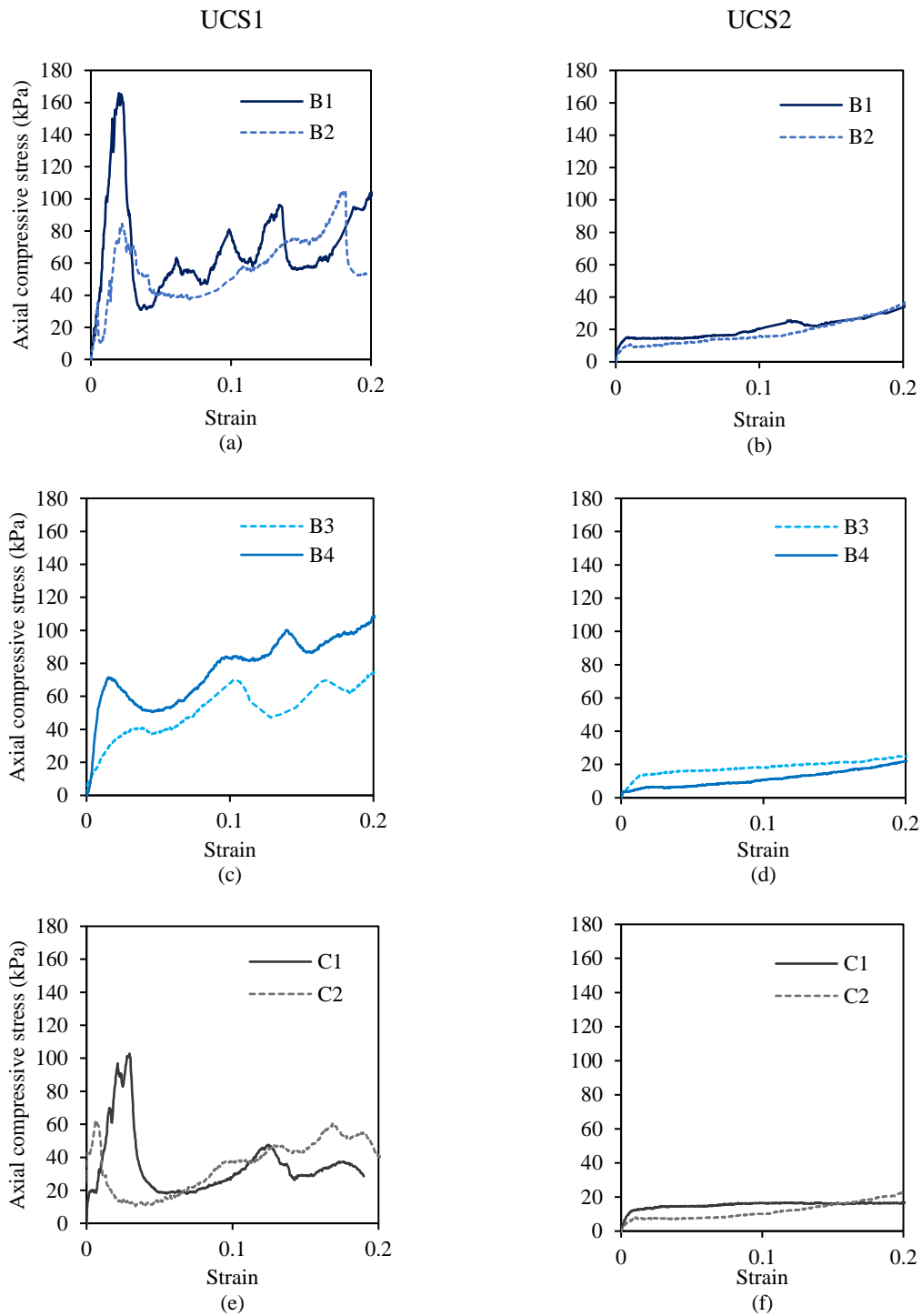


Figure 8-9. Unconfined compressive strength test results for UCS1 of Test P4 columns following biocementation treatment four (a, c, e), and UCS2 following column reconstitution, flushing, saturation with water and eight days of curing to test for self-healing (b, d, f).

8.2.2.4 Calcium Carbonate Precipitated

Figure 8-10 displays the calcium carbonate content of the columns. For this study, the increase in calcium carbonate content does not align with significantly increased strengths. This is likely due to the beads themselves having an adverse effect on strength. It is observed that in columns B1 to B2 the columns have an improved distribution of calcium carbonate in comparison to prior studies. The beads will likely have absorbed some of the bacteria. It is likely that where there was a greater quantity of beads these had absorbed bacteria. Where there had been a larger quantity of beads it is possible that while vibrating the columns these beads had clumped and collected more towards the base.

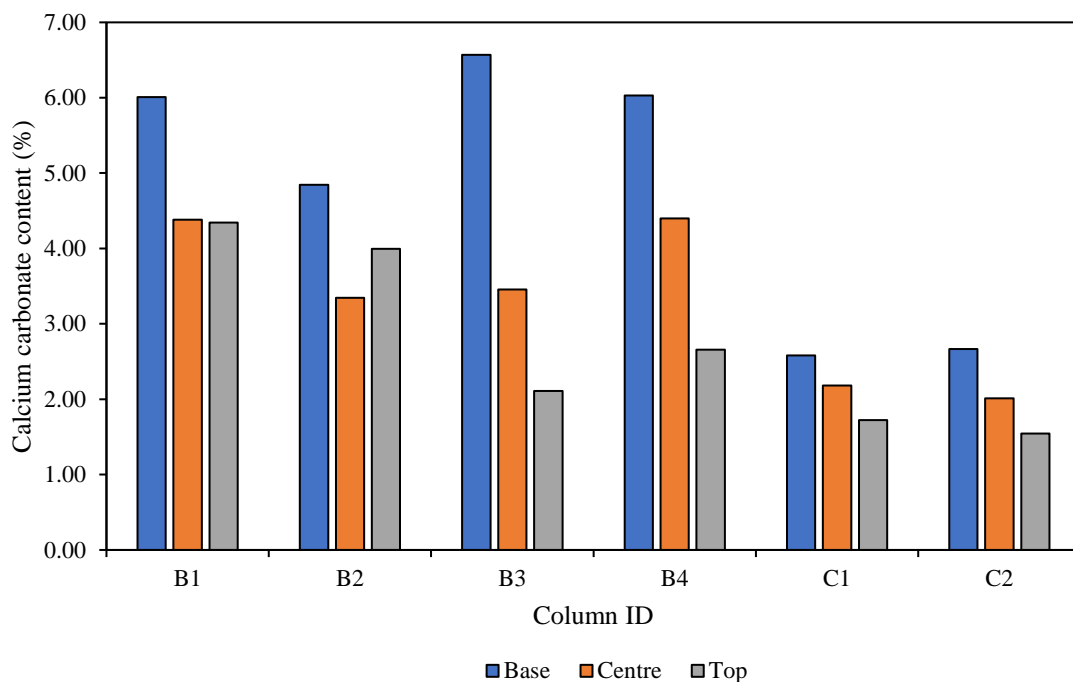


Figure 8-10. Distribution of calcium carbonate precipitated at the base (B), centre (C), and top (T) of Test P4 columns, with error bars showing standard errors of the means for the duplicates.

The relationship between the amount of calcium carbonate precipitated within the columns and the unconfined compressive strength is shown in Figure 8-11. This analysis shows that unlike previous studies increase in calcium carbonate precipitate does not always result in increased strength when using alginate gels beads as the immobilising material. For three out of four columns containing the beads

increased calcium carbonate precipitate did not result in any significant strength increase when compared to the controls.

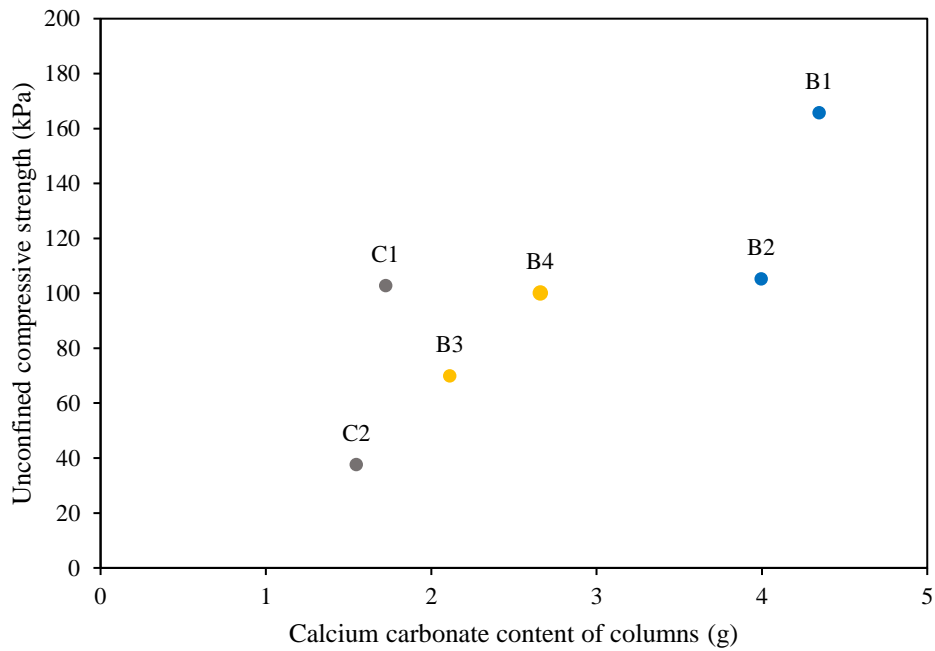


Figure 8-11. Relationship between UCS1 and CaCO_3 content of Test P4 columns.

Images in Figure 8-12 (a-b) show sections of columns containing 10 g of the alginate gel beads, towards the base (Figure 8-12 (a)) and near the centre (Figure 8-12 (b)). These show clumping of the beads, particularly near the base, and also some shrinkage of the beads following the biocementation treatments and subsequent flushing and drying, drying since these are surrounded by voids. These voids will have weakened the biocemented sand structure.

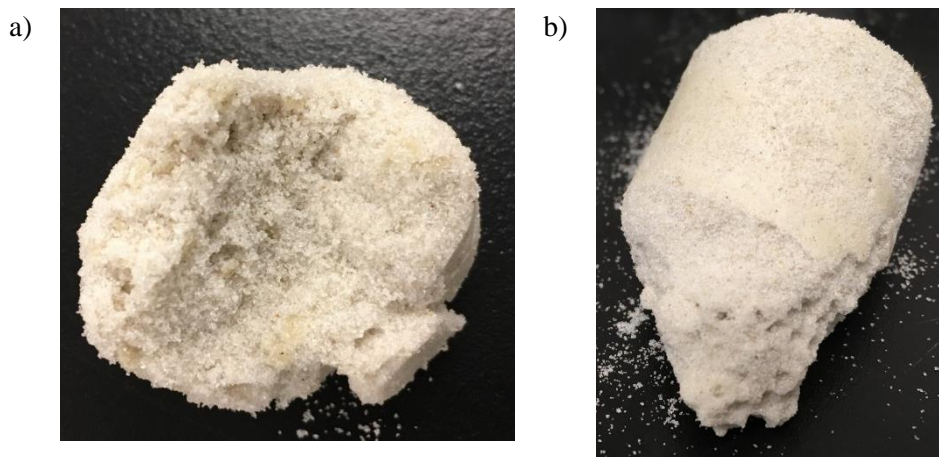


Figure 8-12. Biocemented column sections showing beads at locations of failure within biocemented Test P4 columns containing alginate-based hydrogel beads.

8.3 Conclusions

Columns were prepared in duplicates, containing 10 g and 1 g quantities of sodium alginate hydrogel beads and sand only controls. The columns containing sand only were prepared first, followed by those containing 10 g beads and lastly those containing 1 g beads. As the sand was wet pluviated, the beads will have started to hydrate once the columns were prepared and therefore those with 10 g beads will have contained beads that may have been hydrated to a greater extent than those containing 1 g beads prior to injection of bacteria given the sequence of column assembly. Each column took 10 – 15 min to prepare, following which the apparatus needed to be set up and the inlet tubing filled with bacteria before then attaching the inlet tubing to each column. This may have given sufficient time for hydration of beads in the columns with the higher quantity of beads and therefore for these to have immobilised some of the bacteria as this was being injected. To overcome this the experiment could be modified to dry pluviated the sand and bead mixture. It is unknown however how this may affect the bacteria dispersion within the columns.

The beads appeared to leach out the immobilised CM relatively quickly. This will have boosted production of precipitate during the first treatment of the columns with cementation medium. The alginate gel bead additions were found to have an adverse effect on the compressive strength of the biocemented columns. Wang et al. (2014c) reported compressive strength decrease of 15 % to 34 % of concrete comprising of 1 % to 5 % melamine-based microcapsules respectively. Wang et al. (2015) used sodium alginate hydrogel to encapsulate bacteria and the calcium source for self-healing MICP and reported that the addition of 0.5 % and 1 % by mass of cement of sodium alginate hydrogel resulted in a compressive strength decrease of 16.2 % and 23.4 % respectively.

When compared to the prior studies the effect of absorption/ adsorption of bacteria by carrier materials is evident. For those columns containing a relatively small amount of capsules the distribution of calcium carbonate within the column is less concentrated at the base than for columns which contained fibres. Where a greater amount of capsules are used the absorption/ adsorption of the bacteria will be greater and hence for these columns the concentration of the calcium carbonate near the column inlet is more significant, since as the bacteria is being pushed up the column the bacteria is fixing to the beads. This also shows that there is a limit to the amount of carrier material the columns may contain to mitigate against this concentration of calcium carbonate at the inlet.

9 COLUMN STUDY FOUR: Cementation Medium Optimisation – Effect of Augmentation with Ammonium Chloride.

9.1 Introduction

The cementation medium used throughout this doctoral research was augmented with ammonium chloride, with the exception of treatment one applied for the column tests in Chapters Seven and Eight. A small amount of sodium bicarbonate was also added to the medium, to act as a buffer.

Varying approaches to biocementation via microbially induced calcium carbonate precipitation (MICP) have been studied in recent years. The process of MICP requires a suitable bacterium along with nutrients and precursor chemicals for the MICP process, referred to as the cementation medium (CM). Biocementation as a result of ureolysis requires urea and a calcium source as the basic constituents of the cementation medium.

While a basic urea-calcium source medium is commonly used for MICP experiments (van Paassen et al. 2010), to achieve biocementation, a small number of studies have also included ammonium chloride in the cementation medium (Stocks-Fischer et al. 1999; Al Qabany and Soga 2013; Montoya and Dejong 2013). One of the first studies in this field by Stocks-Fischer et al. (1999) and research by Al Qabany and Soga (2013) and Montoya and Dejong (2015) also included 2.12 g/L sodium bicarbonate in the cementation medium, which is reported to stabilise the pH of the solution prior to injections (Al Qabany and Soga 2013). It is also likely that adding 0.025 M sodium bicarbonate will cause precipitation to occur earlier, as the cementation medium solution will be supersaturated from the start. It is not clear however the effect which the addition of ammonium chloride to the cementation medium has since this has not specifically been reported.

This chapter details the outcomes of a study which investigated the effect on the multiple-treatment MICP process of augmentation of the urea – calcium cementation medium with ammonium chloride and sodium bicarbonate. This study gives further insight into the optimum cementation medium for the multiple treatment MICP process. Reagents used in the cementation media for a selection of published studies are given in Chapter Two, Table 2-2.

9.2 Materials and Methods

9.2.1 MICP Batch Test

A batch study was set up to test the effect of the added substrates on MICP, following a process similar to that used by Stocks-Fischer et al. (1999).

An aqueous MICP study was initially carried out, over a 24 h period at an ambient room temperature of 23 °C, to test effects of adding ammonium chloride and sodium bicarbonate to the urea – calcium cementation medium. This test also explored the effect of varying the concentration of the calcium source. The calcium source used in the CM was calcium chloride dihydrate.

Liquid broth cultures of *S. pasteurii* were grown for this test, as per the procedure outlined in Chapter Four. The liquid broth culture was transferred to 16 x 50 mL sterile polypropylene centrifuge tubes, in 10 mL quantities, and centrifuged at 5000 rpm for 20 min to pelletise the bacteria, after which the supernatant was drained. The polypropylene tubes had been weighed and labelled prior to use. A small amount of autoclave-sterilised phosphate buffered saline (PBS) was added using a sterile pipette tip to each tube to make the quantities of bacterial suspension up to 5 mL and to enable the bacteria cells to be dispersed using a pipette prior to addition of the cementation medium. Two sets of eight polypropylene tubes containing varying concentrations of cementation medium components were prepared, as per Table 9-1. This duplication would test the repeatability of the procedures developed and improve accuracy of results.

Individual flasks of cementation medium were prepared for each pair of tubes. The concentration of these media had been prepared as double that given in Table 9-1, to achieve the concentrations given in this table, since this CM would be diluted by the PBS solution. 5 mL of cementation medium was added to each set of tubes, with the resulting concentrations of medium components given in Table 9-1. Tubes were then mixed gently using a vortex mixer, transferred to large beakers to keep these upright, and incubated at 23 °C, 150 rpm for 24 h. The cementation medium for tubes 9a to 10b was added to empty sterile centrifuge tubes, which did not contain the inoculant, and otherwise subjected to the same treatment as per the inoculated tubes.

Following 24 h of incubation, the tubes were centrifuged at 5000 rpm to separate out the precipitate and supernatant. The pH and electrical conductivity of the drained supernatant was measured. The tubes were then transferred to an oven to dry contents at 105 °C for 24 h. After cooling, the tubes were weighed to determine mass of precipitate, the mass of bacteria is assumed negligible at this stage.

Table 9-1. Contents of tubes prepared for batch test to test effect of augmentation of cementation medium with ammonium chloride and sodium bicarbonate.

Tube set	Calcium chloride dihydrate (M)	Urea (M)	Ammonium Chloride (M)	Sodium Bicarbonate (M)	Inoculated (Y/N)
1a-b	0.25	0.333	0.094	0.013	Y
2a-b	0.50	0.666	0.187	0.025	Y
3a-b	0.75	0.999	0.281	0.038	Y
4a-b	1.00	1.332	0.374	0.050	Y
5a-b	0.25	0.333	0	0	Y
6a-b	0.50	0.666	0	0	Y
7a-b	0.75	0.999	0	0	Y
8a-b	1.00	1.332	0	0	Y
9a-b	0.50	0.666	0.187	0.025	N
10a-b	1.00	1.332	0.374	0.050	N

9.2.2 Preparation of Cementation Medium

Two variations of the cementation medium (CM) were produced, as per Table 9-2, these being as per CM1p and CM3p for the prior studies detailed in Chapter Seven and Eight. For consistency, a sufficient quantity of each medium used was prepared in one batch at the start of the test. The basic constituents of the CM as required for the process of MICP are urea and a calcium source. Calcium chloride dihydrate was selected for the calcium source. A slightly higher molarity of urea was used in comparison to calcium chloride dihydrate, since this helps ensure all calcium can be utilised. In addition, a source of nutrients, Oxoid CM0001, was added to the CM to promote ongoing bacterial growth during treatment. CM1p consisted of 0.67 M urea and 0.50 M calcium chloride dihydrate in addition to 3 g/L Oxoid CM0001 and was used as a fixation medium to fix the bacteria to the sand within the columns. CM3p contained the same concentration of urea, calcium chloride dihydrate and quantity of Oxoid CM0001 as CM1p with the addition of 0.187 M Ammonium chloride and 0.0252 M sodium bicarbonate.

The cementation media were prepared using tap water, to further promote bacterial growth. CM1p was produced by first autoclaving a solution containing calcium chloride dihydrate and Oxoid CM0001, into which a solution containing urea was syringe filtered. To prepare 2.0 L of CM2, firstly the ammonium chloride and Oxoid CM0001 were dissolved in 1.6 L tap water. This solution was adjusted to pH 6.0 using 2.0 M HCl prior to then adding the powdered calcium chloride dihydrate. The pH adjustment prevented the calcium precipitating out into the solution. This solution was autoclaved then made up

to 2.0 L by adding a solution containing the urea and sodium bicarbonate using a 0.2 µm syringe filter in close proximity to a Bunsen burner.

Table 9-2. Cementation medium components and sterilisation methods used for Columns Test P5.

Precursor Chemicals and Nutrients	CM1p (g/L)	CM3p (g/L)	Sterilisation Method
Calcium chloride dihydrate (CaCl ₂ .2H ₂ O)	73.51	73.51	Autoclaved
Urea (NH ₂ (CO)NH ₂)	40	40	Syringe filtered
Ammonium chloride (NH ₄ Cl)		20	Autoclaved
Sodium bicarbonate (NaHCO ₃)		2.12	Syringe filtered
Oxoid CM0001 nutrient broth	3	3	Autoclaved

9.2.3 Bacteria Culture

Liquid broth cultures of *Sporosarcina pasteurii* (ATCC 11859, ACDP Group 1) were produced for Columns Test P5, as per methodology detailed in Chapter Four, in multiples of 50 mL using 250 mL Erlenmeyer flasks.

9.2.4 Columns Preparation, Treatment and Testing

Columns were assembled as described in Chapter Four. All columns were prepared with 143 g of F65 sand, with an approximately 1:2 diameter to depth ratio, as required for samples to be subjected to the UCS test in accordance with BS 1377-7:1990 (British Standards Institution 1999). Columns were prepared in two sets of triplicates. Columns were prepared by wet pluviation of the sand into PBS. The prepared columns had an average length of 75.3 ± 0.6 cm and average diameter of 38.7 ± 0.7 mm. The schedule of biocementation treatments applied was as per Table 9-3.

Table 9-3. Column treatment schedule for Columns Test P5.

Treatment	Retention Time (h)	Columns 1-3 Injection	Columns 4-6 Injection
1	16	CM1p	CM1p
2	22	CM1p	CM3p
3	24	CM1p	CM3p
4	120	CM1p	CM3p
N.A.	0	Tap water	Tap water

Testing of column effluent and biocemented columns was otherwise undertaken as detailed in Chapter Seven, Sections 7.3.7 to 7.3.10.

9.3 Results and Discussion

9.3.1 Batch Test Results

Bacteria for this test were grown to late exponential-stage optical density of 0.833, with minimal loss of bacteria in supernatant, this having been measured as having an optical density (OD_{600}) of 0.004 and therefore negligible. The measured electrical conductivities shown in Figure 9-1 show a rise as a result of the augmentation of the cementation medium with ammonium chloride and sodium bicarbonate additions. In contrast the pH in Figure 9-2 is slightly lower for the samples containing ammonium chloride and sodium bicarbonate. The mass of precipitate (assumed at this stage to be calcium carbonate) within the centrifuge tubes shows that without the addition of the ammonium chloride and sodium bicarbonate, the calcium concentration of the medium has an inhibiting effect on precipitation at higher concentrations. The ammonium chloride addition appears to have counteracted this effect. The results from this batch test show a positive effect of adding ammonium chloride when the cementation medium has a high calcium content close to 1 M, or a low concentration below 0.5 M. When the calcium chloride dihydrate concentration is between 0.5 M and 0.75 M, the addition of ammonium chloride and sodium bicarbonate to the cementation medium appears to have a negligible affect over the initial 24 h period tested and results in a slight drop in pH over this range.

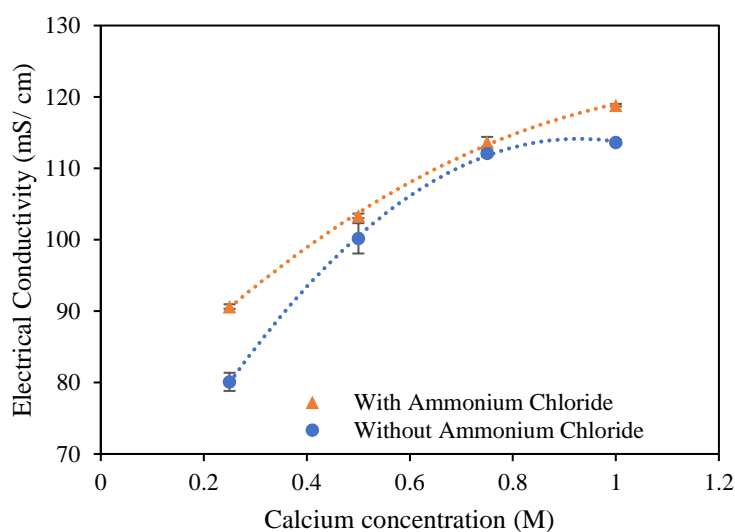


Figure 9-1. Electrical conductivity following 24 h incubation at 23 °C of *S. pasteurii* inoculated tubes containing urea-calcium cementation media and urea-calcium cementation media augmented with ammonium chloride. For each media variation four sets of triplicates were prepared with varying calcium chloride dihydrate content. Error bars show standard errors of the means for the triplicates.

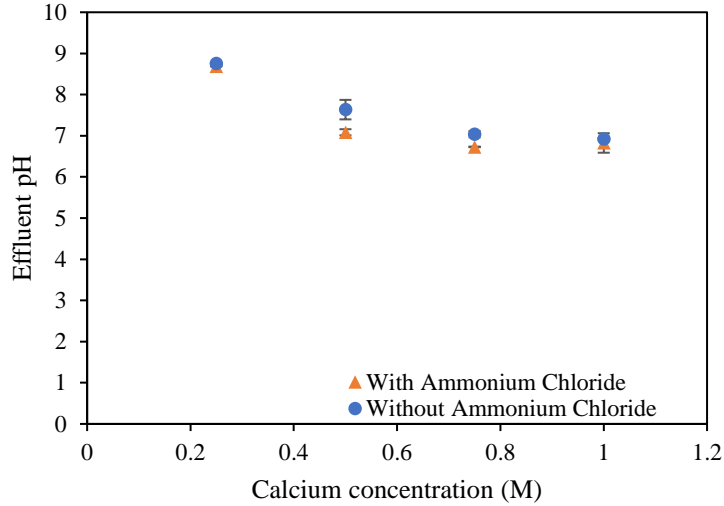


Figure 9-2. pH of effluent following 24 h incubation at 23 °C of *S. pasteurii* inoculated tubes containing urea-calcium cementation media and urea-calcium cementation media augmented with ammonium chloride. For each media variation four sets of triplicates were prepared with varying calcium chloride dihydrate content. Error bars show standard errors of the means for the triplicates.

For this 24 h batch test, the use of the augmented cementation medium appears to have had an inhibitory effect on precipitation of CaCO_3 when the calcium chloride dihydrate concentration is between 0.25 M and 0.75 M. The results with the augmented medium have a linear correlation, compared to the curve obtained with the urea-calcium medium. This again evidences that the augmentation of the medium has counteracted the inhibitory effect of the high levels of calcium chloride dihydrate content in the medium. For the results obtained in this set of batch tests, as shown in Figure 9-1 to Figure 9-3, the error bars are relatively small, which is indicative of good reliability and repeatability for these tests.

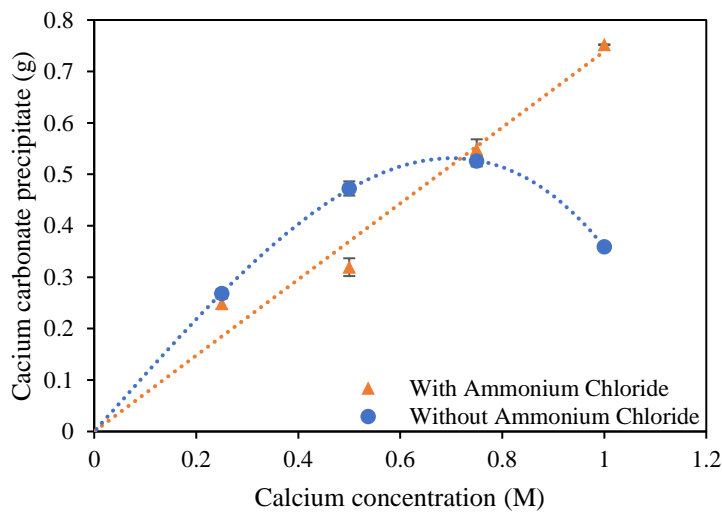


Figure 9-3. CaCO_3 precipitated after 24 h incubation at 23 °C of *S. pasteurii* inoculated tubes containing urea-calcium cementation media and urea-calcium cementation media augmented with ammonium chloride. For each media variation four sets of triplicates were prepared with varying calcium chloride dihydrate content. Error bars show standard errors of the means for the triplicates.

9.3.2 Material Properties

Figure 9-4 gives the optimum dry density of the F65 sand for compaction, this being 1.710 g/cm³. This is the target density for compacting of sand within the columns.

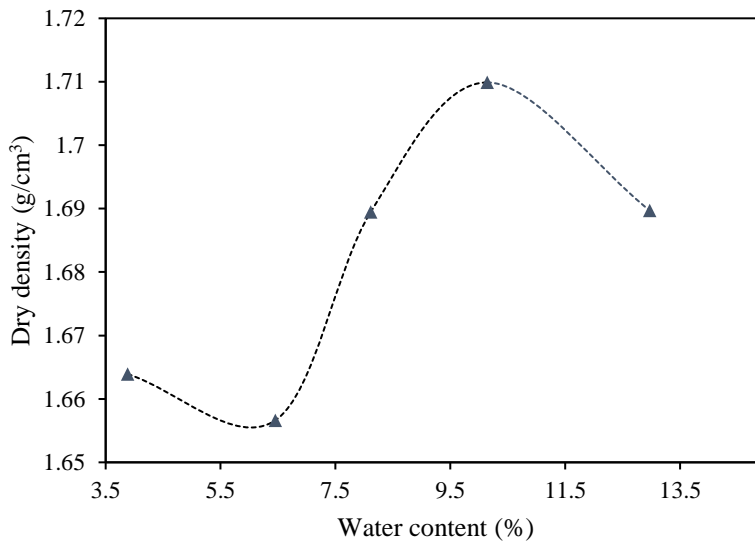


Figure 9-4. Proctor compaction test results for Ottawa F65 sand.

Results obtained for particle size distribution, as shown in Figure 9-5, are in close alignment with those reported by U.S. Silica. The parameters determined from the gradation curve for the F65 sand are given in Table 9-4. The coefficient of curvature (C_z) value of 1.280 indicates, along with the low coefficient of uniformity (C_u) value of 2.038, that the F65 sand is poorly graded, albeit with slightly better grading than F60.

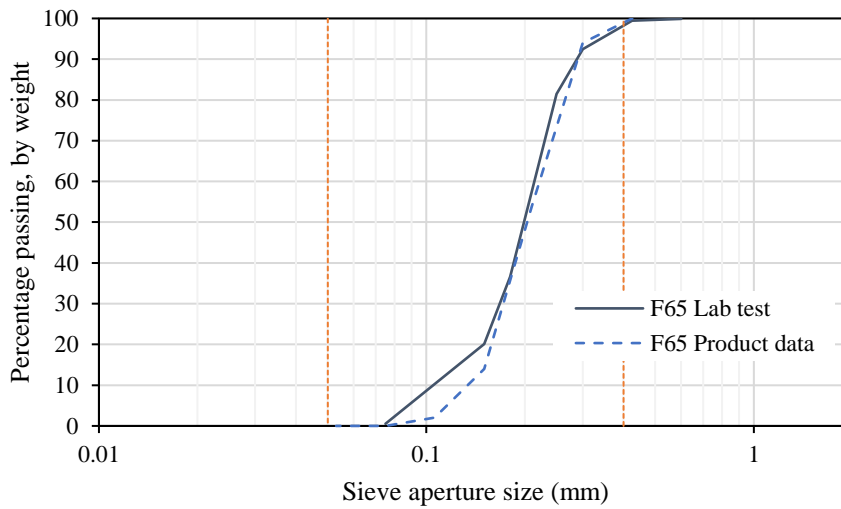


Figure 9-5. Particle size distribution of F65 sand, as measured in the lab and as per product data provided by US Silica.

Table 9-4. F65 sand parameters, as derived from lab test data for particle size distribution.

D₁₀	D₅₀	D₆₀	D₃₀	C_u	C_z
0.104	0.199	0.212	0.168	2.038	1.280

9.3.3 Columns Test P5

9.3.3.1 Bacterial Fixation and Initial Activity

The following column study further explored the effect of use of the cementation medium augmented with ammonium chloride and sodium bicarbonate, when biocementing fine sand using multiple treatments consisting of injection of cementation medium.

The optical density (OD₆₀₀) of the liquid broth culture of *S. pasteurii* grown for this study was measured as 1.086 using a spectrophotometer. The supernatant had a low optical density of 0.010, with the resulting optical density being 1.076. Urease activity was measured as 5.67 mM/min, taken as an average of three tests in accordance with the procedure outlined by Harkes et al. (2010). The bacteria had been successfully fixed using CM1p, as shown by the low optical densities of column effluent in Table 9-5, as measured during treatment two. Some bacterial losses were observed in effluent just after one pore volume of CM had been pumped into the column. The cloudiness (precipitation) within the effluent displaced from columns at this point was indicative of *S. pasteurii* bacteria having leached from the columns.

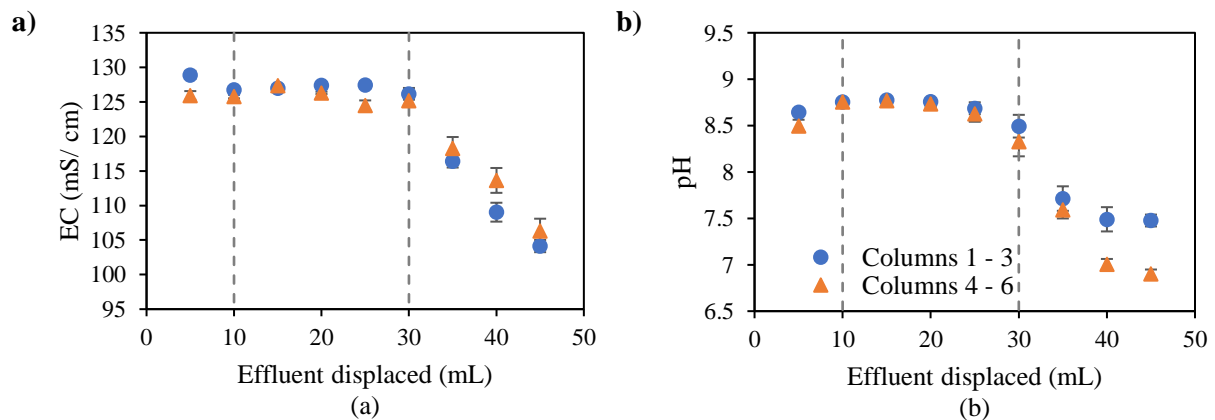
Table 9-5. Optical density of effluent discharged from 5 - 10 mm depth from Test P5 columns, during biocementation treatment two, following fixing of bacteria by treatment one.

Column	1	2	3	4	5	6
Effluent OD ₆₀₀ (5 - 10ml)	0.004	0.007	0.022	0.057	0.068	0.582

9.3.3.2 Distribution of Bacterial Activity

The measured conductivities in Figure 9-6 (a-h) are indicative of the distribution of the bacteria within the columns and indicate that the distribution is fairly even for the control columns one to three, with slightly more variation in the columns injected with the augmented medium C2 from treatment two onwards, as shown by the error bars. The dashed lines in these figures represent the approximate locations of the column boundaries at the outlet and inlet. The pH of the standard urea-calcium medium and medium containing ammonium chloride and sodium, bicarbonate was 7.66 and 6.89 respectively. The tap water in the Tempe area of Arizona in the US had a slightly alkaline pH, resulting in the pH of CM1p being slightly alkaline.

Treatment one was the same for all columns. Following results of the batch test, the standard urea-calcium medium (CM1p) was used for all columns for the first treatment and for all treatments for control columns one to three, with the augmented medium (CM3p) then being injected into columns four to six from treatment two onwards. There is little difference between the pH and electrical conductivity measurements for each set of columns following treatment two, the different is more pronounced after treatment three, which suggests that the augmented medium has a beneficial effect on the MICP process when multiple treatments are applied, as can be seen by the significant differences in pH and electrical conductivity measurements. Following biocementation treatment four columns were flushed with sterile tap water and therefore the electrical conductivity reduces to almost zero, the pH remains at around 8 given the alkalinity of the water in the Tempe area of the US.



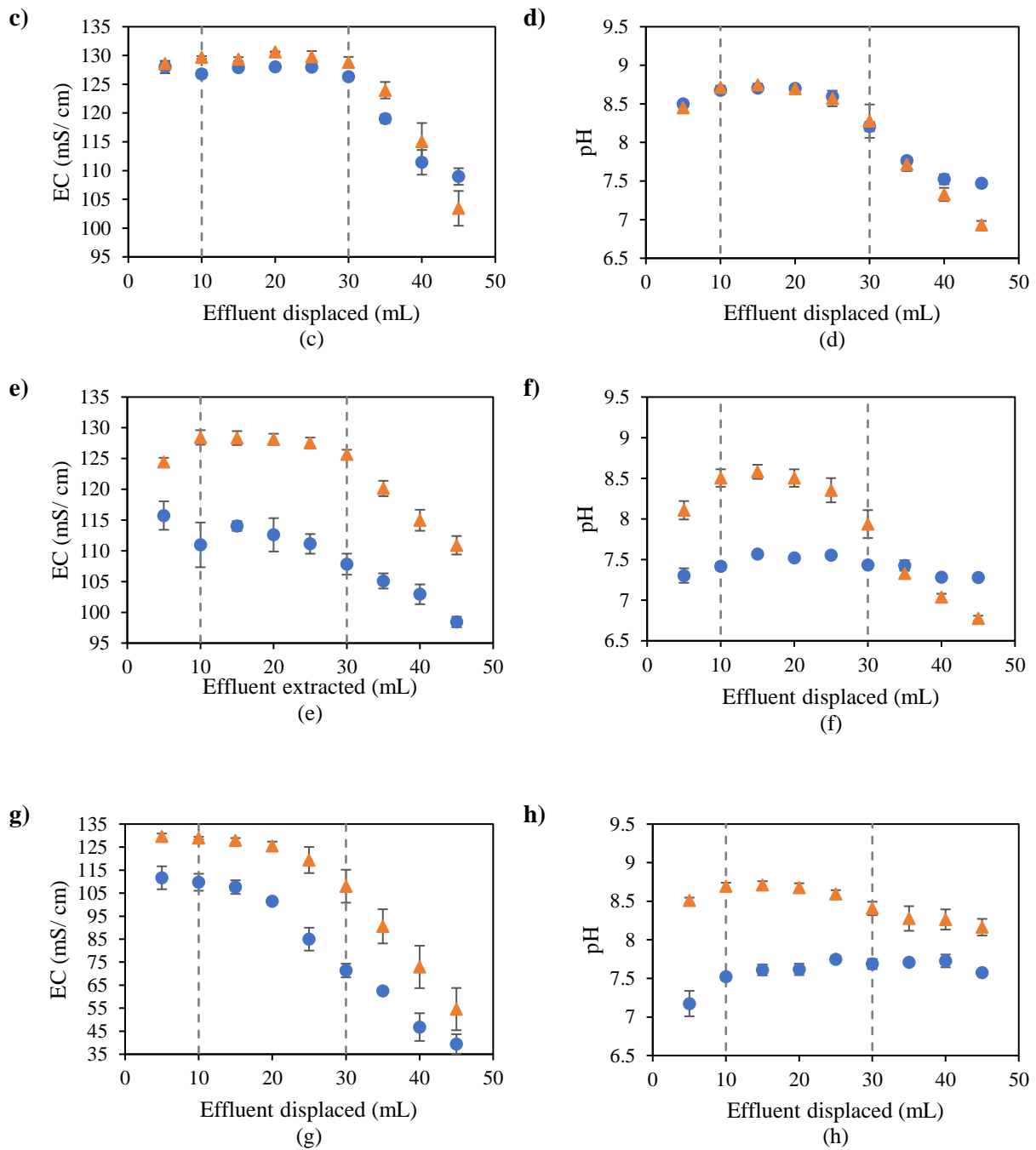


Figure 9-6. Electrical conductivity and pH of effluent from Test P5 columns following biocementation treatments 1 (a,b), 2 (c,d), 3 (e,f) and 4 (g,h), with error bars showing standard errors of the means for the triplicates.

9.3.3.3 Efficiency of Chemical Conversion

Figure 9-7 shows the chemical conversion efficiency following all four treatments. There is close to 100 % efficiency of chemical conversion, based on calcium ion measurements, in columns injected with the augmented medium. In contrast there is a significant reduction in chemical conversion efficiency following treatments three and four when only the standard urea – calcium medium (CM1p) is used for all treatments.

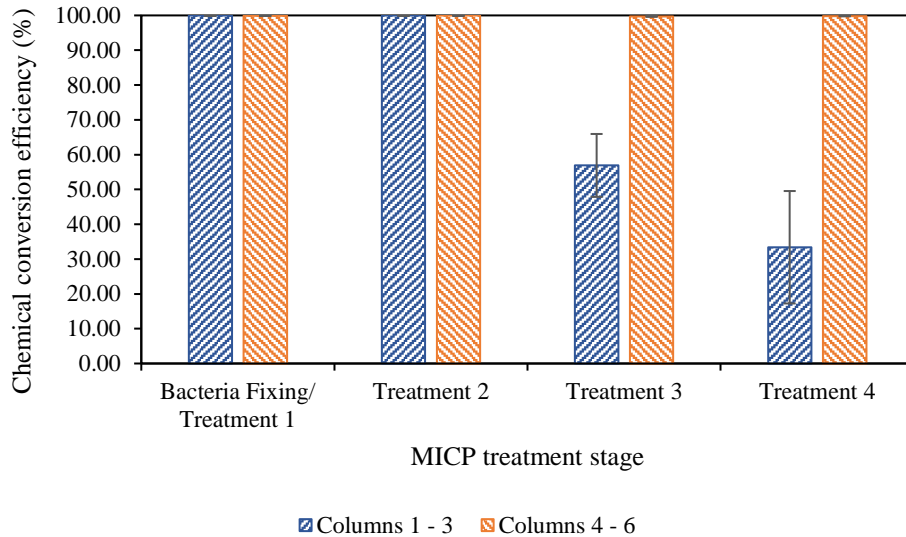


Figure 9-7. Chemical conversion efficiency over the eight-day treatment process for Columns Test P5, based on measurement of calcium ions in column effluent, with retention times of 16 h, 22 h, 24 h and 120 h for treatments one to four respectively. Error bars represent the standard errors of the means for each triplicate set of columns.

The concentration of calcium ions in the column effluent shows that the efficiency of conversion of calcium ions to produce calcium carbonate declines over time for the columns which were not treated with the medium containing ammonium chloride. There is near 100 % efficiency of conversion for columns injected with the augmented medium containing ammonium chloride. Results in Figure 9-7 also show the effect of the concentration of bacteria injected and possibly also urease activity. The retention for treatment four has been increased following findings of prior studies. This provides some further insight into the prior study suggesting Jute had been particularly beneficial when the bacterial concentration was lower.

The Nessler method was used to measure the conversion of urea into ammonium ions. The ammonium chloride is added to the cementation medium following treatment one and therefore the effects can be seen in results from treatment two onwards. For this set of columns there had been lower activity in one of the controls, however despite this efficiency increases and the individual results for this particular column improve. At this stage the IC results for ammonium ions were not deemed accurate. The analysis takes into account the added 0.187 M ammonium chloride added to the cementation from treatment two onwards and deducts this from the measured result before calculation of the conversion efficiency. Excess urea is included within the cementation medium so as not to inhibit calcium ion conversion. Results show that it may be possible to include less ammonium chloride.

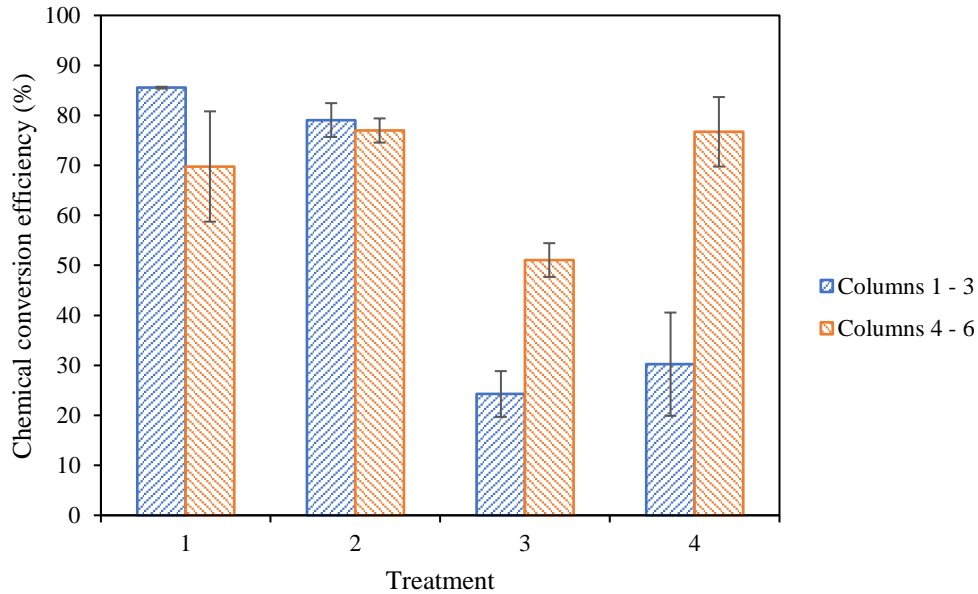


Figure 9-8. Efficiency of substrate conversion to form ammonium ions based on urea concentration of medium and concentration of ammonium ions in Test P5 columns effluent as determined by Nesslerisation, and taking into account added ammonium chloride, with error bars showing standard errors of means.

9.3.3.4 Unconfined Compressive Strength

Unconfined compression test results are shown in Figure 9-9. The average unconfined compressive strength (UCS) of columns one to three was 149.91 kPa. This increases to 271.28 kPa for columns four to six which were treated with the augmented cementation medium. There is more deviation between results for columns injected with the medium containing ammonium chloride, however all UCS results for this set of three columns are higher than those for columns one to three. The point of failure has been taken as the highest point before 20 % strain is reached, since columns had been visually observed to fail within this period. The UCS test is intended for use on saturated cohesive soils. This has however been used to test the strength of biocemented sand in many prior studies, in the absence of an otherwise recommended test for this material. Although samples had been in a saturated state, the material tested is granular and this may therefore give rise to some inaccuracies and inconsistencies in results when using the UCS test. Therefore, this test alone is not used to assess the effect of changes to the cementation medium.

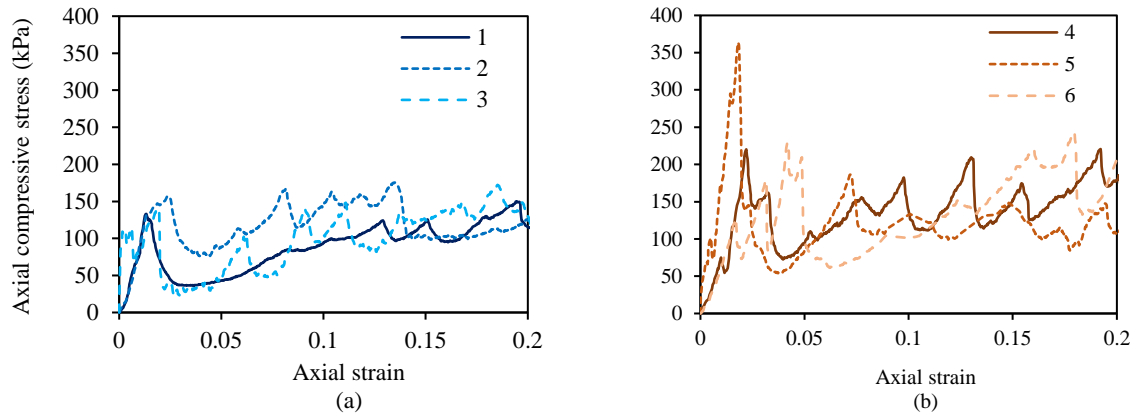


Figure 9-9. Unconfined compressive strength (UCS) test results for Test P5 columns 1 to 3 (a) and 4 to 6 (b).

Images of the columns shortly after the onset of failure show clear shear failure planes as shown in Figure 9-10 photographs.

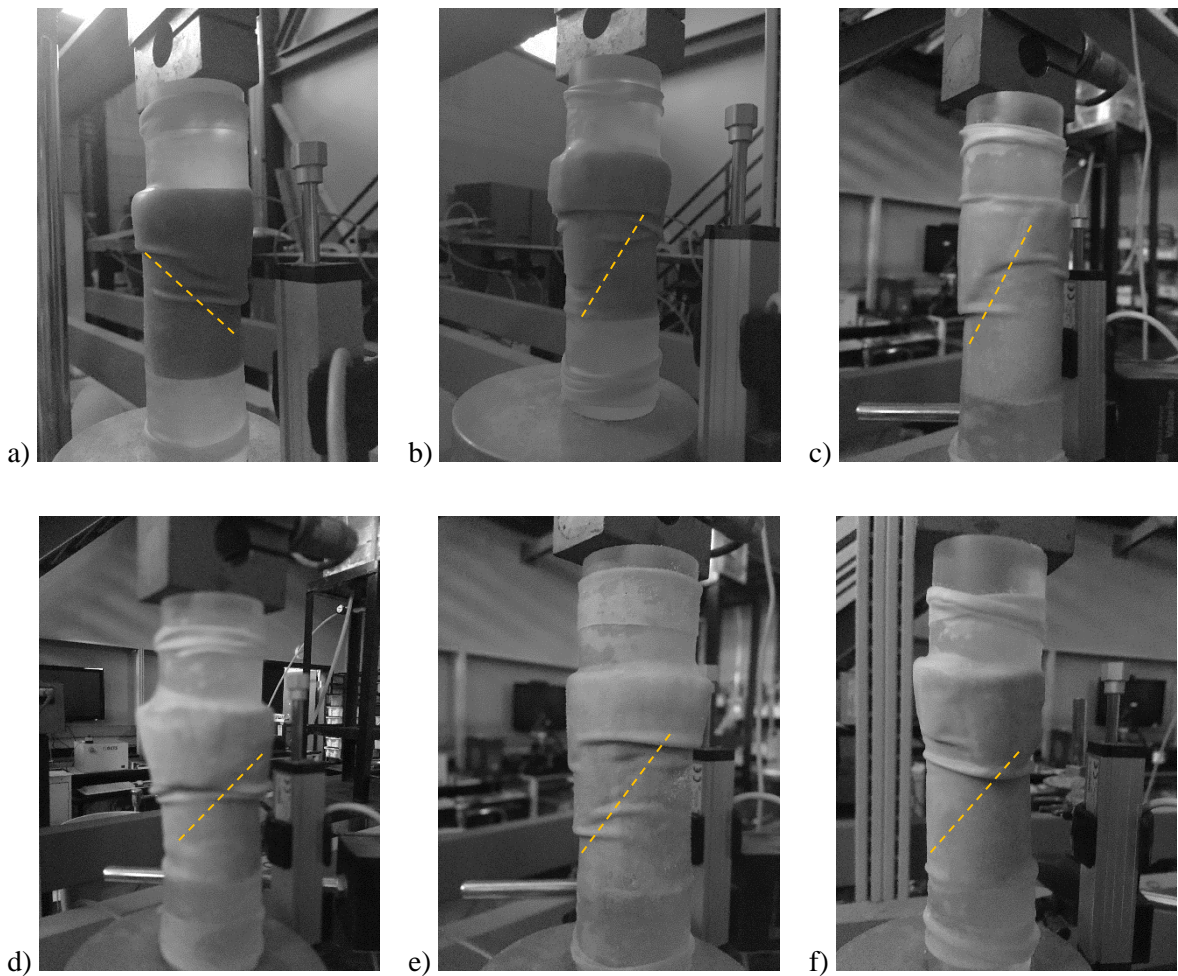


Figure 9-10. Photographic images of Test P5 columns 1 to 6 during UCS testing, shortly after failure, with annotation showing the approximate path of the shear failure.

Table 9-6. UCS Test Parameters for Columns Test P5.

Column	UCS (kPa)	Strain at failure (%)	moisture content (%)	Dry density (g/ cm ³)	(%) Target density
1	133.00	1.31	17.10	1.63	95.45
2	175.02	2.32	16.80	1.61	94.43
3	141.70	1.86	15.94	1.58	92.25
4	220.25	2.20	16.19	1.57	91.81
5	363.46	1.80	15.78	1.67	97.38
6	230.15	4.19	16.30	1.66	96.91

Although some variation in density is observed, there appears not to be a close correlation with UCS within this range of results. For example, among columns one to three the column with the lowest UCS value, column 1, has the highest density. The average % target density achieved for compaction across all columns was 95 %.

9.3.3.5 Calcium Carbonate Precipitated

The average calcium carbonate content of each of the columns, as determined using a Calcimeter, are shown in Figure 9-11. This analysis relates the calcium carbonate contents to the tested unconfined compressive strengths of the columns. It can be observed that the columns treated with a medium containing ammonium chloride all have higher calcium carbonate contents than those treated with the urea-calcium medium only. Although there is some variation in strength between columns four to six the calcium carbonate contents show much less deviation.

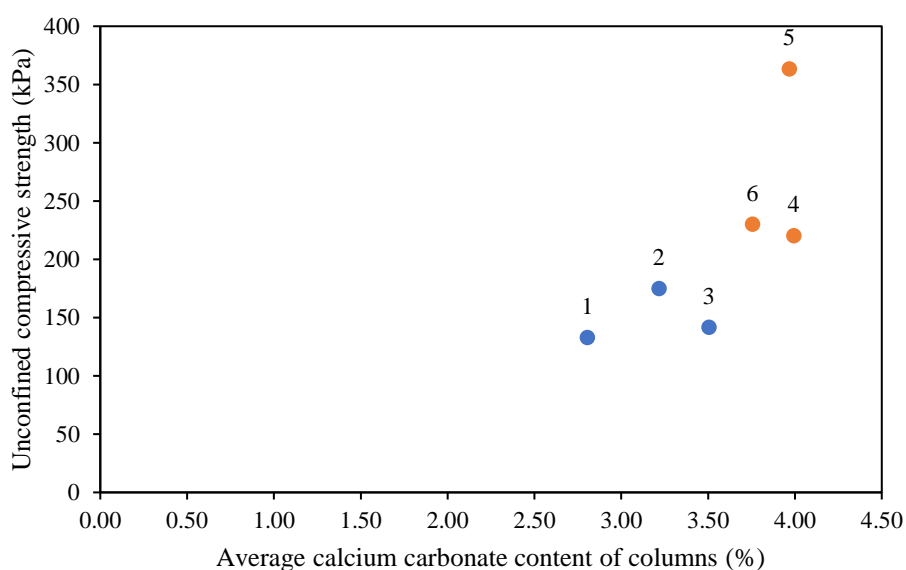


Figure 9-11. Average calcium carbonate content of Test P5 columns, as measured using a Calcimeter, showing relationship to UCS results.

The calcium carbonate distribution, as quantified via Calcimeter measurement, at the base, centre and top of the columns is shown in Figure 9-12. When comparing to previous column studies in Chapter Seven, it can be seen that wet pluviation of the sand into PBS within the column has not improved the distribution of bacterial/ urease activity when comparing to wet pluviation into a cementation medium and therefore preparation of the columns with cementation medium would not appear to have had an adverse effect. More investigation is required to improve this distribution.

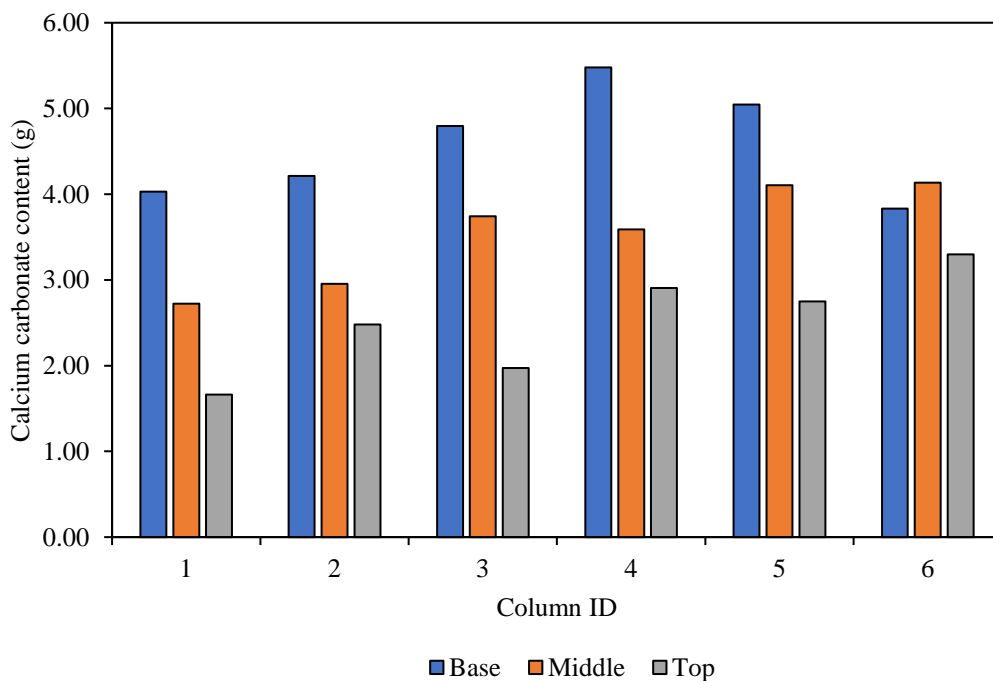


Figure 9-12. Distribution of calcium carbonate precipitated at the base (B), centre (C), and top (T) of Test P5 columns, with error bars showing standard errors of the means for the triplicates.

9.4 Conclusions

The effect of adding ammonium chloride and sodium bicarbonate to the cementation medium had been tested. It is likely that the beneficial effects observed were largely due to the ammonium chloride addition as opposed to the addition of sodium bicarbonate. The latter is reported to stabilise pH of the cementation medium prior to injection.

The initial batch test showed that it may not be beneficial to augment the medium for the first treatment of columns with cementation medium if the concentration of calcium chloride dihydrate used is below 0.75 M, it would appear to otherwise be beneficial to include ammonium chloride in the cementation medium at this early stage of treatment. The batch results suggest that augmentation of the cementation

medium with ammonium chloride could help improve chemical conversion efficiency and calcium carbonate precipitation when using a 1.0 M calcium source in the cementation medium. For the column studies completed using *S. pasteurii* for studies completed at Arizona State University the common urea-calcium medium was used for columns treatment one, which also fixed the bacteria within columns. Nutrient broth only was added to this first treatment. The augmented cementation medium was used for the following treatments.

It was found that the addition of 0.187 M ammonium chloride to the urea-calcium cementation medium had a particularly noticeable effect following the third injection of this medium into a set of sand columns, compared with columns treated with the urea – calcium medium only. Significant increases in electrical conductivity and pH and calcium ion depletion resulted from use of the augmented medium from this point onwards and consequently increased calcium carbonate precipitation. Nesslerisation was used to measure the ammonium ion content of columns effluent and also indicated greater efficiency of chemical conversion from the third treatment onwards when using the augmented cementation medium.

Results also showed the influence of the initial concentration of the bacterial inoculant, and urease activity, when compared to prior studies.

Despite the lack of carrier material in this study, and the wet pluviation of column contents into PBS instead of cementation medium, there was still an observed greater concentration of calcium carbonate towards the inlet end of the columns, less so when the augmented medium was used. Therefore, potentially it could be beneficial to include ammonium chloride in treatment one. Also, these results show that the wet pluviation of the column contents into cementation medium, and travel of the bacteria through this medium during treatment one, does not appear to have caused bacteria to be fixed any more towards the inlet of the column. It is possible that use of F65 instead of F60 may have had some effect, the sand had been changed at this stage as it had not been possible to source more F60 when the supplies had been depleted.

10 CONCLUSIONS AND RECOMMENDATIONS

10.1 Summary

The initial aim of this doctoral research project had been to embed self-healing capability within a biocemented sand. Prior studies had demonstrated that in principle self-healing of biocemented sand (and consequently suitable soils) via MICP can be achieved, however for this process to be implemented in construction practice, and for in-situ applications, a long-term supply of the cementation medium will be required, to enable self-healing to take place autonomously where this is needed. Incorporating self-healing ability into biocemented sand or soil structures will improve sustainability of these structures and help to mitigate against significant damage and failure of geotechnical structures.

To refine the scope, the process of MICP via ureolysis was adopted for biocementation and for the mechanism by which self-healing capability would be engineered into the biocemented sand. It had been established that in order to achieve this aim the key requirements would be a supply of the nutrients and precursor chemicals required for the self-healing MICP process within the biocemented sand material and bacteria capable of long-term survival within the biocemented material as spores. A study of the literature on self-healing developments in cementitious materials gave insight into possibilities for storage of cementation medium within biocemented soil. This project focussed on immobilisation as a means of storage and potentially suitable carrier materials were selected following a desk study.

Sporosarcina ureae and *Sporosarcina pasteurii* were selected as ureolytic bacteria known to form spores. The ability of both *S. ureae* and *S. pasteurii* to sporulate was demonstrated, by use of a suitable sporulation medium, and in low nutrient conditions in aqueous studies.

Of the selected carrier materials subjected to investigation, results obtained demonstrated that diatomaceous earth, expanded perlite and jute and hemp fibres have the potential to be utilised for the immobilisation and supply of the required nutrients and precursor chemicals to enable self-healing via MICP. The preliminary studies indicated that diatomaceous earth may have a beneficial effect on the MICP process as shown by increasing calcium carbonate precipitation. Coir was deemed unsuitable at the preliminary stage of testing due to the low capacity for immobilisation of cementation medium when compared to other carriers tested.

A series of column studies was undertaken, firstly using *S. ureae*, followed by use of *S. pasteurii* to promote MICP. When using *S. ureae*, combined with daily injections, the columns were only partially

cemented due to the MICP process being significantly slower when using *S. ureae* compared to use of *S. pasteurii*. However, past studies undertaken by Botusharova (2017) in which several cementation medium injections were supplied five to seven days apart achieved similarly low levels of biocementation based on measured unconfined compressive strengths of the columns. The slow rate of chemical conversion when using *S. ureae* for MICP enabled the leaching of the immobilised cementation medium from carriers to be observed, through testing of calcium ion concentrations of columns effluent. This evidenced that cementation medium could remain immobilised by the tested carrier materials following multiple cementation medium injections into the columns.

Hemp and jute fibres and expanded perlite were initially utilised as carrier materials within the sand columns biocemented using *S. ureae*. Results obtained had shown some indication of self-healing response. Self-healing response of columns was tested by means of strength regain following mechanical damage. Following biocementation and a period of drying, the unconfined compressive strength of columns was tested, this test resulted in mechanical damage to the columns. Columns were then flushed with water to rehydrate and after allowing time for release of immobilised cementation medium from carriers, bacterial spore regeneration, and self-healing via MICP columns were again dried and the UCS test repeated. Self-healing was defined as strength increase above the residual, when comparing the peak strength obtained during the second UCS test and the residual strength from the first UCS test.

Subsequent column tests undertaken at Arizona State University, and using *S. pasteurii*, applied similar methodology for strength testing, however columns were not dried at this stage before the UCS test and hence any self-healing responses observed would likely be due to vegetative bacteria. Had this yielded positive results in respect of self-healing then the process would have been developed further to test for self-healing responses due to spores of bacteria. At this stage self-healing responses were not as evident. There were however significant findings made in respect of the effects of jute fibres on the MICP process, in addition to effects of jute fibres on the strength of biocemented sand. The carrier materials themselves were expected to have effects on material properties when incorporated into biocemented sand structures and this was therefore also explored as part of the research undertaken. The evidenced effects on the MICP process itself as a result of use of the carrier materials added to findings obtained and prompted further exploration.

Findings from column studies also highlighted the importance of urease activity. It was shown that bacterial cell density (as estimated from spectrophotometer measurements) was not necessarily a good indicator of bacterial activity. Oxygen availability during bacteria culturing appeared to have a significant effect on urease activity. Hence this likely also impacts on urease activity within the sand columns.

Encapsulation using alginate-based hydrogel beads was also tested as a means of storage and release of cementation medium for SH-MICP. This study similarly gave results which showed a beneficial effect on MICP of this additive. There were however observed some negative effects of use of these beads in respect of strength properties of the biocemented sand. Hence no further investigation was deemed necessary with this carrier material.

As part of the studies undertaken, optimisation of the cementation medium used for biocementation of sand was investigated. Although some researchers have augmented the standard urea-calcium cementation used for MICP with ammonium chloride and sodium bicarbonate, the benefits of adding ammonium chloride in the cementation medium had not been explained or evidenced. Results obtained clearly showed a beneficial impact on the MICP process efficiency and calcium carbonate precipitation of using this augmented medium when applying repeated treatments of cementation medium to biocement the sand columns over several days.

10.2 Key Findings and Significance

The use of natural fibres, as an immobilising carrier material to enable self-healing of biocemented sand, is a novel approach. Natural fibres had not previously been combined with sand or soil biocementation systems, therefore the effect of the fibres on the biocemented material properties and MICP process was unknown. Key findings are summarised as follows.

Effects of jute fibre additions:

- Jute additions result in a significant increase in strength of biocemented fine sand.
- Inclusion of jute fibres in a sandy soil subjected to biocementation treatments increases the MICP process efficiency, resulting in an increase in calcium carbonate precipitate.
- Jute additions enhance/ boost MICP efficiency up to 100%, even when the bacterial concentration of the columns inoculant is low/ reduced and urease activity is relatively low, provided that there are sufficient nutrients available. A concentration of 6 g/L Oxoid CM0001 was found to be the optimum nutrient content within cementation medium for biocementation mediated by *S. pasteurii*.

Use of pre-treated jute fibres (jute fibres immobilising cementation medium):

- The processes utilised to immobilise cementation medium within natural fibres such as jute and hemp may increase reabsorption capacity, as a result of the additional heat treatment fibres are subjected to during drying following immobilisation of cementation medium.
- Fibres immobilising cementation medium (CM) will likely absorb less of the bacteria introduced into the column since the void spaces within the fibre will be filled with CM at the

time of column assembly. While some CM may leach out at this initial stage, the studies undertaken have shown that leaching of immobilised CM occurs over a number of biocementation treatments. In addition, the fibre pre-treatment process will affect surface properties of the fibres and hence adsorption capability.

- Very little to no self-healing activity was observed when using untreated fibres (with no CM immobilised), with self-healing activity only observed using treated fibres, for both bacteria used.
- Columns appear to compact a little better when treated fibres are used as opposed to untreated.
- Fibres may also be immobilising the urease enzyme, and this immobilisation capacity will be adversely affected when the fibres have been utilised for immobilisation of cementation medium.

These studies provide insight into the optimum bacterial cell concentration when using *S. pasteurii* for multiple treatment MICP processes. The studies undertaken suggest that an optical density of approximately 1.0 is required for more sustained 100% conversion efficiency, provided the CM is also augmented with ammonium chloride and sodium bicarbonate. Prior studies suggest a range between 0.8 and 1.2 for high reaction efficiency (Al Qabany and Soga 2013). The study by Al Qabany and Soga (2013) only gives results for efficiency following one injection of CM however.

10.3 Contributions to Knowledge

The development of a biocemented sand material with embedded self-healing capability has not previously been studied. Results in Chapter Six in particular showed some promise in respect of achieving this aim given the evidence of self-healing capability observed.

The use of the selected additives to improve properties of biocemented sand and efficiency of the MICP process is novel. This is the first study to have enhanced biocemented sand with jute fibre additions and remains currently the only study which has investigated the effect of jute fibres on the MICP process itself in addition to demonstrating strength enhancement. The addition of hemp, expanded perlite, diatomaceous earth and sodium alginate hydrogel to biocemented sand systems has not previously been reported. The results reported in Chapter Nine clearly demonstrated the beneficial effect of adding ammonium chloride to the cementation medium when applying multiple injections of cementation medium to biocement sand, which had not been clearly demonstrated or explained in the literature in this area. Hence all studies undertaken and reported in this thesis have added to the knowledge in this area of research.

The beneficial effect of jute fibre additions on the MICP process efficiency has been demonstrated, as reported in Chapter Seven. In addition, results obtained have given insight into the effect of varying nutrient content of the cementation medium on the MICP process when using jute fibre additions.

The testing procedures used to assess the capacity of the selected carrier materials for the i) immobilisation of cementation medium and ii) rate of release of cementation medium and iii) effect on MICP in aqueous solutions, were designed and developed for this research project. These were shown to have good repeatability and hence reliability.

10.4 Suggested Improvements

The efficiency of immobilisation could be improved by the use of a vacuum (Alghamri et al. 2016). A vacuum was also utilised by Wiktor and Jonkers (2011) and Zhang et al. (2017b) for immobilisation purposes when using expanded clay and perlite respectively as immobilising materials.

A slower release of cementation medium from the immobilising carrier materials is desirable to improve self-healing responses of the biocemented sand. To ensure longevity of cementation medium supply for self-healing, the retention of cementation medium components during the biocementation process requires improvement. For a single treatment process the materials tested would likely retain sufficient cementation medium for a self-healing treatment. However, to sufficiently reduce permeability of the biocement, and increase strength, a number of biocementation treatments would usually be required.

Culture of *S. ureae* at a lower temperature than 30 °C may have helped to improve urease activity, this requires further investigation. Since less research has been undertaken using *S. ureae* for MICP, the optimal conditions for this bacterium within biocementation systems are less well known when compared to *S. pasteurii*.

10.5 Industrial Application

This research had not progressed to the stage of scaling-up given constraints. Natural fibres and other carrier materials would need to be incorporated into a geotechnical structure as admixtures. Barriers to industrial application include economics and environmental impact when considering ammonia and excess ammonium ion production. Ammonia/ ammonium removal processes may need to be taken into consideration.

Research into MICP and its uses is still in its infancy and the methodology has yet to be adopted by industry. When compared to cementitious materials, biocement is not dependent on aging/ hydration, the process is rapid.

For field application, it would be possible to inject a solution of *S. ureae* and cementation medium directly into soil by preparing a solution equal to the estimated pore volume for the area to be treated. The two-stage biocementation treatment process involving injection of a bacterial suspension, followed by injection of cementation medium, can also be replicated in-situ.

A self-healing MICP system may be of particular interest and suitability for seepage control, such as within a dam core or within grouting systems. Addition of jute fibres would help to facilitate multiple biocementation treatments to achieve sufficiently low permeability of core/ grout material. It is then assumed the self-healing MICP process would be activated upon water ingress into this material should micro-cracking occur, to help prevent piping within dams for example.

10.6 Challenges to Overcome

Spatial inhomogeneity had been observed within the columns (where calcium carbonate content was measured) during this research. More uniform distribution of calcium carbonate has been reported to occur at lower levels of concentration of treatment (0.25 M Ca-urea) (Al Qabany and Soga 2013). Use of a higher concentration of cementation medium had however been preferable to reduce leaching of the immobilised cementation medium from the carrier materials. Further research would be required to improve the homogeneity of calcium carbonate content within the biocemented sand columns when incorporating the carrier material additions.

The unconfined compression test, in accordance with British Standards, is designed for the testing of the undrained shear strength of saturated cohesive soils. It has not been designed for the testing of a material such as biocemented sand. This therefore raises the question of whether such a test is suitable for testing the strength of biocemented sand specimens, and what other possible testing alternatives may yield potentially more reliable results. As an alternative to unconfined compression, the testing of hydraulic conductivity for example using the falling head test was not considered suitable for this research since this would result in further leaching of immobilised cementation medium following each biocementation treatment.

During the earlier stage of columns testing with *S. ureae*, columns had been dried prior to UCS testing, this being a departure from the British Standards for this test. This was done with the aim of ensuring only spores of bacteria remained in the biocement. As an alternative to drying columns, use of a bactericide such as hydrogen peroxide was considered, however there are a lack of studies showing the effectiveness of hydrogen peroxide as a bactericide. The sporicidal action of hydrogen peroxide is reported to occur at a concentration of 3% (0.88 mol/L), and bactericidal action above 0.5% (0.15 mol/L). The latter is reported to be poor in comparison to the use of hydrogen peroxide as a sporicide (Baldry 1983). In addition, this additional treatment stage with a bactericide would have resulted in

further washing out of immobilised cementation medium. More evidence is required to prove self-healing is being facilitated by bacterial spores.

10.7 Future Work and Recommendations

The use of sodium alginate to encapsulate cementation medium could be further explored. It is possible that for any capsule-based systems the capsules/ beads may need to be manufactured in an external industrial lab whereby capsules/ beads could be produced in large quantities that contained a concentrated sterile source of cementation medium. Effective self-healing systems may also require spores of bacteria to be encapsulated/ immobilised, this would require further investigation.

The immobilisation methodology developed in this research could also be applied to cementitious materials.

Removal of and uses of any excess ammonium ions during biocementation should be considered, to ensure that there are no adverse environmental impacts, in order to promote an eco-friendly process. Ammonium is a by-product of the MICP process, which could be harvested for other uses. The ability for *S. ureae* or *S. pasteurii* to convert urea to ammonia has important potential applications in the production of biofuels and fertilizers. Ammonia has the potential to be used for a carbon-alternative fuel source. Traditionally ammonia for fertiliser is generated using natural gas. A life cycle analysis could be undertaken to evaluate the environmental impact of the self-healing MICP process, to include potential for recycling of the sand and carrier mixtures.

Further exploration could be undertaken using diatomaceous earth, results obtained in aqueous MICP experiments suggested that this material may have a beneficial effect on MICP. It had not been selected as a powdered carrier material for use in the column studies in since it has a mass loss on ignition of 3.2-10.0 %. Hence for studies undertaken at Cardiff University it would not have been possible to quantify mass of calcium carbonate precipitated given equipment and facilities available. More detailed analysis of calcium carbonate content of columns at Cardiff University would have involved quantifying calcium carbonate content via mass loss on ignition. This methodology could not have been applied to columns containing diatomaceous earth given the mass loss on ignition of this material.

It is not yet fully understood why the additions of natural fibres such as jute result in significant improvement to MICP efficiency. It is hypothesised that this is due to the physicochemical properties of the jute fibres and their potential ability to immobilise urease enzyme and/ or bacteria. More research is required to better understand this outcome and prove this hypothesis. This would require study of the adhesion of bacteria to fibres and sand particles at a microscopic level.

There has been little reported observation of the vaterite polymorph of calcium carbonate precipitate when assessing the morphology of calcium carbonate precipitated within a biocemented sand or soil matrix. More research is required to understand why the organic fibre additions have led to formation of vaterite. The structure of vaterite is also not well defined in the literature, with further fundamental work required in this area.

Self-healing following chemical damage was not considered as part of this doctoral study. Chemical damage may occur due to CO₂ rich water. The biocemented material may be subject to acid attack, from acid rain or landfill leachates such as sulphuric acid. Sulphate acid corrosion has been found to result in the production of calcium sulphate crystals, which although have lower strength compared to calcium carbonate result in some mitigation against the strength reduction (Li et al. 2019). It is possible that self-healing may occur via a dissolution and recrystallisation process.

BIBLIOGRAPHY

- Abbas, A.A., Planchon, S., Jobin, M. and Schmitt, P. 2014. Absence of oxygen affects the capacity to sporulate and the spore properties of *Bacillus cereus*. *Food Microbiology* 42, pp. 122–131. doi: 10.1016/j.fm.2014.03.004.
- Achal, V., Mukherjee, A., Basu, P.C. and Reddy, M.S. 2009. Strain improvement of *Sporosarcina pasteurii* for enhanced urease and calcite production. *Journal of Industrial Microbiology & Biotechnology* 36(7), pp. 981–988. doi: 10.1007/s10295-009-0578-z.
- Aggregate Industries UK Ltd. 2013. Garside Sands Washed Fine Silica Sand (WFSS).
- Al Imran, M., Gowthaman, S., Nakashima, K. and Kawasaki, S. 2020. The influence of the addition of plant-based natural fibers (Jute) on biocemented sand using MICP method. *Materials* 13(18).
- Al Qabany, A. and Soga, K. 2013. Effect of chemical treatment used in MICP on engineering properties of cemented soils. *Geotechnique* 63(4), pp. 331–339. doi: 10.1680/geot.SIP13.P.022.
- Al Qabany, A., Soga, K. and Santamarina, C. 2012. Factors Affecting Efficiency of Microbially Induced Calcite Precipitation. *Journal of Geotechnical and Geoenvironmental Engineering* 138(8), pp. 992–1001. doi: 10.1061/(ASCE)GT.1943-5606.0000666.
- Aldaef, A.A. and Rayhani, M.T. 2015. Hydraulic performance of compacted clay liners under simulated daily thermal cycles. *Journal of Environmental Management* 162, pp. 171–178. doi: 10.1016/j.jenvman.2015.07.036.
- Alghamri, R., Kanellopoulos, A. and A-Tabbaa, A. 2016. Impregnation and encapsulation of lightweight aggregates for self-healing concrete. *Construction and Building Materials* 124, pp. 910–921. doi: 10.1016/j.conbuildmat.2016.07.143.
- Al-Tabbaa, A. and Harbottle, M.J. 2015. Self-healing materials and structures for geotechnical and geo-environmental applications. In: *Geotechnical Engineering for Infrastructure and Development*. Conference Proceedings. ICE Publishing, pp. 589–594.
- ASTM International 2012. *ASTM D1557-12e1 Standard Test Methods for Laboratory Compaction Characteristics of Soil Using Modified Effort (56,000 ft-lbf/ft³ (2,700 kN-m/m³))*. West Conshohocken, PA.
- ASTM International 2017. *ASTM D6913/D6913M-17. Standard Test Methods for Particle-Size Distribution (Gradation) of Soils Using Sieve Analysis*. West Conshohocken, PA.
- Badiee, H., Sabermahani, M., Tabandeh, F. and Saeedi Javadi, A. 2019. Application of an indigenous bacterium in comparison with *Sporosarcina pasteurii* for improvement of fine granular soil. *International Journal of Environmental Science and Technology* 16(12), pp. 8389–8400. doi: 10.1007/s13762-019-02292-9.
- Bajpai, P. 2014. Chapter 8 - Industrial Applications of Xylanases. In: Bajpai, P. ed. *Xylanolytic Enzymes*. Amsterdam: Academic Press, pp. 69–104. Available at: <http://www.sciencedirect.com/science/article/pii/B9780128010204000081> [Accessed: 8 February 2020].

- Balam, N.H., Mostofinejad, D. and Eftekhari, M. 2017. Use of carbonate precipitating bacteria to reduce water absorption of aggregates. *Construction and Building Materials* 141, pp. 565–577. doi: 10.1016/j.conbuildmat.2017.03.042.
- Baldry, M.G.C. 1983. The bactericidal, fungicidal and sporicidal properties of hydrogen peroxide and peracetic acid. *Journal of Applied Bacteriology* 54(3), pp. 417–423. doi: 10.1111/j.1365-2672.1983.tb02637.x.
- Banerjee, P.K. 2012. Environmental textiles from jute and coir. In: *Handbook of Natural Fibres*. Woodhead Publishing. Available at: [https://www.sciencedirect-com.abc.cardiff.ac.uk/book/9781845696986/handbook-of-natural-fibres](https://www.sciencedirect.com/abc.cardiff.ac.uk/book/9781845696986/handbook-of-natural-fibres) [Accessed: 12 October 2018].
- Basha, S. et al. 2018. Subsurface Endospore-Forming Bacteria Possess Bio-Sealant Properties. *Scientific Reports* 8(1), p. 6448. doi: 10.1038/s41598-018-24730-3.
- Baskar, S., Baskar, R., Mauclair, L. and McKenzie, J.A. 2006. Microbially induced calcite precipitation in culture experiments: possible origin for stalactites in Sahastradhara caves, Dehradun, India. *Current science*, pp. 58–64.
- Beltran, M.G.S. and Jonkers, H.M. 2015. Crack self-healing technology based on bacteria. *Journal of Ceramic Processing Research* 16, pp. 33–39.
- Berg, R.W. and Sandine, W.E. 1970. Activation of bacterial spores. A Review. *Journal of Milk and Food Technology* 33, pp. 435–441.
- Bhaskar, S., Hossain, K.M.A., Lachemi, M., Wolfaardt, G. and Kroukamp, M.O. 2017. Effect of self-healing on strength and durability of zeolite-immobilized bacterial cementitious mortar composites. *Cement & Concrete Composites* 82, pp. 23–33. doi: 10.1016/j.cemconcomp.2017.05.013.
- Botusharova, S. 2017. *Self-healing Geotechnical Structures Via Microbial Action*. Ph.D. Thesis, Cardiff, UK: Cardiff University.
- British Standards Institution 1990. *BS 1377-1:1990 Methods of test for Soils for civil engineering purposes - Part 1: General requirements and sample preparation*. London, UK.
- British Standards Institution 1996. *BS 1377-2:1990 Methods of test for Soils for civil engineering purposes. Part 2: Classification tests*. London, UK.
- British Standards Institution 1999. *BS 1377-7:1990 Methods of test for soils for civil engineering purposes. Part 7: Shear strength tests (total stress)*. London, UK.
- Bundur, Z.B., Kirisits, M.J. and Ferron, R.D. 2017. Use of pre-wetted lightweight fine expanded shale aggregates as internal nutrient reservoirs for microorganisms in bio-mineralized mortar. *Cement and Concrete Composites* 84(Supplement C), pp. 167–174. doi: 10.1016/j.cemconcomp.2017.09.003.
- Burbank, M.B., Weaver, T.J., Green, T.L., Williams, B.C. and Crawford, R.L. 2011. Precipitation of Calcite by Indigenous Microorganisms to Strengthen Liquefiable Soils. *Geomicrobiology Journal* 28(4), pp. 301–312. doi: 10.1080/01490451.2010.499929.
- Chen, F. et al. 2016. Biostabilization of Desert Sands Using Bacterially Induced Calcite Precipitation. *Geomicrobiology Journal* 33(3–4), pp. 243–249. doi: 10.1080/01490451.2015.1053584.

- Chen, H. and Qian, C. 2016. Self-healing cementitious materials based on bacteria and nutrients immobilized respectively. *Construction and Building Materials* 126, pp. 297–303. doi: 10.1016/j.conbuildmat.2016.09.023.
- Cheng, L. and Cord-Ruwisch, R. 2012. In situ soil cementation with ureolytic bacteria by surface percolation. *Ecological Engineering* 42, pp. 64–72. doi: 10.1016/j.ecoleng.2012.01.013.
- Cheng, L. and Cord-Ruwisch, R. 2014. Upscaling effects of soil improvement by microbially induced calcite precipitation by surface percolation. *Geomicrobiology Journal* 31(5), pp. 396–406.
- Cheng, L., Cord-Ruwisch, R. and Shahin, M.A. 2013. Cementation of sand soil by microbially induced calcite precipitation at various degrees of saturation. *Canadian Geotechnical Journal* 50(1), pp. 81–90. doi: 10.1139/cgj-2012-0023.
- Cheng, L., Shahin, M.A. and Mujah, D. 2016. Influence of Key Environmental Conditions on Microbially Induced Cementation for Soil Stabilization. *Journal of Geotechnical and Geoenvironmental Engineering* 143(1), pp. 04016083-1–11. doi: 10.1061/(SCE)GT.1943-5606.0001586.
- Cheshomi, A., Mansouri, S. and Amoozegar, M.A. 2018. Improving the Shear Strength of Quartz Sand using the Microbial Method. *Geomicrobiology Journal* 35(9), pp. 749–756. doi: 10.1080/01490451.2018.1462868.
- Choi, S.-G., Wang, K. and Chu, J. 2016. Properties of biocemented, fiber reinforced sand. *Construction and Building Materials* 120, pp. 623–629. doi: 10.1016/j.conbuildmat.2016.05.124.
- Clarà Saracho, A. and Haigh, S.K. 2019. Experimental optimization of microbially induced calcite precipitation (Micp) for contact erosion control in earth dams. In: Keh-Chia Y. ed. *Scour and Erosion IX - Proceedings of the 9th International Conference on Scour and Erosion, ICSE 2018*. CRC Press/Balkema, pp. 43–50.
- Craig, R.F. 2004. *Craig's Soil Mechanics: Seventh Edition*. Abingdon, UK: E & FN Spon.
- Cui, M.-J., Zheng, J.-J., Zhang, R.-J., Lai, H.-J. and Zhang, J. 2017. Influence of cementation level on the strength behaviour of bio-cemented sand. *Acta Geotechnica* 12(5), pp. 971–986. doi: 10.1007/s11440-017-0574-9.
- De Belie, N. 2010. Microorganisms versus stony materials: a love-hate relationship. *Materials and Structures* 43(9), pp. 1191–1202. doi: 10.1617/s11527-010-9654-0.
- De Muynck, W., De Belie, N. and Verstraete, W. 2010. Microbial carbonate precipitation in construction materials: A review. *Ecological Engineering* 36(2), pp. 118–136. doi: 10.1016/j.ecoleng.2009.02.006.
- DeJong, J.T., Mortensen, B.M., Martinez, B.C. and Nelson, D.C. 2010. Bio-mediated soil improvement. *Ecological Engineering* 36(2), pp. 197–210. doi: 10.1016/j.ecoleng.2008.12.029.
- Deng, W. and Wang, Y. 2018. Investigating the factors affecting the properties of coral sand treated with microbially induced calcite precipitation. *Advances in Civil Engineering* 2018.
- Dhami, N., Reddy, M. and Mukherjee, A. 2014. Application of calcifying bacteria for remediation of stones and cultural heritages. *Frontiers In Microbiology* 5(304), pp. 1–12. doi: 10.3389/fmicb.2014.00304.

- Dhami, N.K., Alsubhi, W.R., Watkin, E. and Mukherjee, A. 2017. Bacterial Community Dynamics and Biocement Formation during Stimulation and Augmentation: Implications for Soil Consolidation. *Frontiers in Microbiology* 8, p. 1267. doi: 10.3389/fmicb.2017.01267.
- Doran, P.M. 2013. Chapter 10 - Mass Transfer. In: Doran, P. M. ed. *Bioprocess Engineering Principles (Second Edition)*. London, UK: Academic Press, pp. 379–444. Available at: <http://www.sciencedirect.com/science/article/pii/B9780122208515000101> [Accessed: 31 October 2020].
- Dupre Minerals 2018. Perlite. Available at: <https://www.dupreminerals.com/perlite/> [Accessed: 24 September 2018].
- Eigenbrod, K.D. 2003. Self-healing in fractured fine-grained soils. *Canadian Geotechnical Journal* 40(2), pp. 435–449. doi: 10.1139/t02-110.
- Eijkelkamp Soil & Water 2018. *Calcimeter: Manual*. Netherlands: Eijkelkamp Soil & Water., p. 8. Available at: https://www.eijkelkamp.com/download.php?file=M0853e_Calcimeter_b21b.pdf [Accessed: 1 November 2019].
- Erez, J. 2003. The Source of Ions for Biomineralization in Foraminifera and Their Implications for Paleoceanographic Proxies. *Reviews in Mineralogy and Geochemistry* 54, pp. 115–149. doi: 10.2113/0540115.
- Ersan, Y.C., de Belie, N. and Boon, N. 2015. Microbially induced CaCO₃ precipitation through denitrification: An optimization study in minimal nutrient environment. *Biochemical Engineering Journal* 101, pp. 108–118. doi: 10.1016/j.bej.2015.05.006.
- Ersan, Y.C., Wang, J.Y., Boon, N. and De Belie, N. 2014. *Ureolysis and denitrification based microbial strategies for self-healing concrete*. Grantham, M., Basheer, P. a. M., Magee, B., and Soutsos, M. eds. Boca Raton: Crc Press-Taylor & Francis Group.
- Esteban, R., Ariz, I., Cruz, C. and Moran, J.F. 2016. Review: Mechanisms of ammonium toxicity and the quest for tolerance. *Plant Science* 248, pp. 92–101. doi: 10.1016/j.plantsci.2016.04.008.
- Ezekiel, N., Ndazi, B., Nyahumwa, C. and Karlsson, S. 2011. Effect of temperature and durations of heating on coir fibers. *Industrial Crops and Products* 33(3), pp. 638–643. doi: 10.1016/j.indcrop.2010.12.030.
- Fan, L., Lehmann, P. and Or, D. 2015. Effects of hydromechanical loading history and antecedent soil mechanical damage on shallow landslide triggering. *Journal of Geophysical Research-Earth Surface* 120(10), pp. 1990–2015. doi: 10.1002/2015JF003615.
- Fidelis, M., Pereira, T., Gomes, O., Silva, F. and Toledo Filho, R. 2013. The effect of fiber morphology on the tensile strength of natural fibers. *Journal of Materials Research and Technology* 2, pp. 149–157. doi: 10.1016/j.jmrt.2013.02.003.
- Flexicon Corporation 2018. Diatomaceous Earth - Materials Handled - Flexicon Corporation. Available at: <https://www.flexicon.com/Materials-Handled/Diatomaceous-Earth.html> [Accessed: 18 November 2018].
- Fricke, M., Volkmer, D., Krill, C.E., Kellermann, M. and Hirsch, A. 2006. Vaterite Polymorph Switching Controlled by Surface Charge Density of an Amphiphilic Dendron-calix[4]arene. *Crystal Growth & Design* 6(5), pp. 1120–1123. doi: 10.1021/cg050534h.

- Fujita, Y. et al. 2008. Stimulation of microbial urea hydrolysis in groundwater to enhance calcite precipitation. *Environmental science & technology* 42(8), pp. 3025–3032.
- Gao, Y., Tang, X., Chu, J. and He, J. 2019. Microbially Induced Calcite Precipitation for Seepage Control in Sandy Soil. *Geomicrobiology Journal* 36(4), pp. 366–375. doi: 10.1080/01490451.2018.1556750.
- Gassan, J. and Bledzki, A.K. 2001. Thermal degradation of flax and jute fibers. *Journal of Applied Polymer Science* 82(6), pp. 1417–1422. doi: 10.1002/app.1979.
- Gat, D., Ronen, Z. and Tsesarsky, M. 2016. Soil Bacteria Population Dynamics Following Stimulation for Ureolytic Microbial-Induced CaCO₃ Precipitation. *Environmental Science & Technology* 50(2), pp. 616–624. doi: 10.1021/acs.est.5b04033.
- Gomez, M.G., Graddy, C.M.R., DeJong, J.T., Nelson, D.C. and Tsesarsky, M. 2018. Stimulation of native microorganisms for biocementation in samples recovered from field scale treatment depths. *Journal of Geotechnical and Geoenvironmental Engineering* 144(1), p. 1804. doi: 10.1061/(ASCE)GT.1943-5606.0001804.
- Gomez, M.G., Martinez, B.C., DeJong, J.T., Hunt, C.E., deVlaming, L.A., Major, D.W. and Dworatzek, S.M. 2015. Field-scale bio-cementation tests to improve sands. *Proceedings of the Institution of Civil Engineers-Ground Improvement* 168(3), pp. 206–216. doi: 10.1680/grim.13.00052.
- Gowthaman, S., Iki, T., Nakashima, K., Ebina, K. and Kawasaki, S. 2019a. Feasibility study for slope soil stabilization by microbial induced carbonate precipitation (MICP) using indigenous bacteria isolated from cold subarctic region. *SN Applied Sciences* 1(11), p. 1480. doi: 10.1007/s42452-019-1508-y.
- Gowthaman, S., Mitsuyama, S., Komatsu, M., Nakashima, K. and Kawasaki, S. 2019b. Microbial induced slope surface stabilization using industrial-grade chemicals: A preliminary laboratory study. *International Journal of GEOMATE* 17, pp. 110–116. doi: 10.21660/2019.60.8150.
- Grasby, S.E. 2003. Naturally precipitating vaterite (μ -CaCO₃) spheres: unusual carbonates formed in an extreme environment. *Geochimica et Cosmochimica Acta* 67(9), pp. 1659–1666. doi: 10.1016/S0016-7037(02)01304-2.
- Greenburg, A.E., Clesceri, L.S. and Eaton, A.D. 1992. *Standard methods: for the examination of water and wastewater*. 18th ed. Washington, DC: American Public Health Association.
- Guida, S., Potter, C., Jefferson, B. and Soares, A. 2020. Preparation and evaluation of zeolites for ammonium removal from municipal wastewater through ion exchange process. *Scientific Reports* 10(1), p. 12426. doi: 10.1038/s41598-020-69348-6.
- Guo, Y., Loria, M., Rhoades, K. and Yu, X.B. 2018. Effects of Microbial Induced Calcite Precipitation on Bentonite Cracking Remediation. In: Stuedlein A.W., Lemnitzer A., and Suleiman M.T. eds. *Geotechnical Special Publication*. American Society of Civil Engineers (ASCE), pp. 135–144.
- Gussone, N., Nehrke, G. and Teichert, B.M.A. 2011. Calcium isotope fractionation in ikaite and vaterite. *Chemical Geology* 285(1), pp. 194–202. doi: 10.1016/j.chemgeo.2011.04.002.
- Hamad, S.F., Stehling, N., Holland, C., Foreman, J.P. and Rodenburg, C. 2017. Low-Voltage SEM of Natural Plant Fibers: Microstructure Properties (Surface and Cross-Section) and their Link to

- the Tensile Properties. *Procedia Engineering* 200, pp. 295–302. doi: 10.1016/j.proeng.2017.07.042.
- Hamdan, N. 2015. *Applications of Enzyme Induced Carbonate Precipitation (EICP) for Soil*. Ph.D. Thesis, Arizona State University, US.
- Harborlite Corporation 2008. Perlite Products for Industrial Filtration. Available at: <https://www.whitchem.co.uk/wp-content/uploads/2019/12/Imerys-Filtration-Harborlite-Perlite-Filter-Aids.pdf> [Accessed: 18 November 2018]
- Harbottle, M.J., Lam, M.-T., Botusharova, S. and Gardner, D.R. 2014. Self-healing soil: Biomimetic engineering of geotechnical structures to respond to damage. In: *7th International Congress on Environmental Geotechnics*. Melbourne
- Harbottle, M.J., Zhang, J. and Gardner, D.R. 2013. Combined physical and biological gel-based healing of cementitious materials. In: *Proceedings of the Fourth International Conference on Self-Healing Materials*. Ghent, pp. 207–210.
- Harkes, M.P., van Paassen, L.A., Booster, J.L., Whiffin, V.S. and van Loosdrecht, M.C.M. 2010. Fixation and distribution of bacterial activity in sand to induce carbonate precipitation for ground reinforcement. *Ecological Engineering* 36(2), pp. 112–117. doi: 10.1016/j.ecoleng.2009.01.004.
- Hasriana, Samang, L., Djide, M.N. and Harianto, T. 2018. A study on clay soil improvement with *Bacillus subtilis* bacteria as the road subbase layer. *International Journal of GEOMATE* 15(52), pp. 114–120. doi: 10.21660/2018.52.97143.
- He, J., Wang, Y., Li, Y. and Ruan, X. 2015. Effects of leachate infiltration and desiccation cracks on hydraulic conductivity of compacted clay. *Water Science and Engineering* 8(2), pp. 151–157. doi: 10.1016/j.wse.2015.04.004.
- Hejazi, S.M., Sheikhzadeh, M., Abtahi, S.M. and Zadhoush, A. 2012. A simple review of soil reinforcement by using natural and synthetic fibers. *Construction and Building Materials* 30, pp. 100–116. doi: 10.1016/j.conbuildmat.2011.11.045.
- Hoben International 2018. Ultrafine - Hoben International. Available at: <https://www.hobeninternational.com/perlite/grades/ultrafine> [Accessed: 18 November 2018].
- Hu, Q., Zhang, J., Teng, H. and Becker, U. 2012. Growth process and crystallographic properties of ammonia-induced vaterite. *American Mineralogist* 97. doi: 10.2138/am.2012.3983.
- Ibraim, E., Diambra, A., Russell, A.R. and Muir Wood, D. 2012. Assessment of laboratory sample preparation for fibre reinforced sands. *Geotextiles and Geomembranes* 34, pp. 69–79. doi: 10.1016/j.geotextmem.2012.03.002.
- Imerys Performance Minerals 2018. Harborlite 800. Available at: https://www.imerys-performance-minerals.com/system/files/2021-02/DATP_Harborlite_800_RUB_2018-02.pdf [Accessed: 26 May 2021].
- Institute of Medicine (US) Committee on Standards for Systematic Reviews of Comparative Effectiveness Research 2011. *Standards for Reporting Systematic Reviews*. Eden, J., Levit, L., Berg, A., and Morton, S. eds. National Academies Press (US). Available at: <https://www.ncbi.nlm.nih.gov/books/NBK209507/> [Accessed: 8 May 2021].

- Jacob, D.E., Wirth, R., Agbaje, O.B.A., Branson, O. and Eggins, S.M. 2017. Planktic foraminifera form their shells via metastable carbonate phases. *Nature Communications* 8(1), p. 1265. doi: 10.1038/s41467-017-00955-0.
- Jiang, N.-J. and Soga, K. 2017. The applicability of microbially induced calcite precipitation (MICP) for internal erosion control in gravel-sand mixtures. *Geotechnique* 67(1), pp. 42–55. doi: 10.1680/jgeot.15.P.182.
- Jiang, N.-J., Soga, K. and Kuo, M. 2017. Microbially Induced Carbonate Precipitation for Seepage-Induced Internal Erosion Control in Sand-Clay Mixtures. *Journal of Geotechnical and Geoenvironmental Engineering* 143(3), pp. 04016100-1–14. doi: 10.1061/(ASCE)GT.1943-5606.0001559.
- Jiang, N.-J., Tang, C.-S., Yin, L.-Y., Xie, Y.-H. and Shi, B. 2019. Applicability of Microbial Calcification Method for Sandy-Slope Surface Erosion Control. *Journal of Materials in Civil Engineering* 31(11).
- Jonkers, H.M. 2011. Bacteria-based self-healing concrete. *Heron* 56(1–2), pp. 5–16.
- Jonkers, H.M. and Schlangen, E. 2007. *Self-healing of cracked concrete: A bacterial approach*. Carpinteri, A., Gambarova, P. G., Ferro, G., and Plizzari, G. A. eds. London: Taylor & Francis Ltd.
- Jonkers, H.M. and Schlangen, E. 2008. *Development of a bacteria-based self healing concrete*. Walraven, J. C. and Stoelhorst, D. eds. Boca Raton: Crc Press-Taylor & Francis Group.
- Jonkers, H.M., Thijssen, A., Muyzer, G., Copuroglu, O. and Schlangen, E. 2008. Application of bacteria as self-healing agent for the development of sustainable concrete. *Ecological Engineering* 36(2), pp. 230–235. doi: 10.1016/j.ecoleng.2008.12.036.
- Kakuturu, S. and Reddi, L.N. 2006. Evaluation of the parameters influencing self-healing in earth dams. *Journal of Geotechnical and Geoenvironmental Engineering* 132(7), pp. 879–889. doi: 10.1061/(ASCE)1090-0241(2006)132:7(879).
- Kalantary, F., Abbasi Govanjik, D. and Safdari Seh Gonbad, M. 2019. Stimulation of Native Microorganisms for Improving Loose Salty Sand. *Geomicrobiology Journal* 36(6), pp. 533–542. doi: 10.1080/01490451.2019.1579876.
- Karnati, V.R., Munaga, T., Gonavaram, K.K. and Amitava, B. 2020. Study on Strength and Leaching Behavior of Biogeochemical Cemented Sand. *Geomicrobiology Journal* 37(7), pp. 670–681. doi: 10.1080/01490451.2020.1761912.
- Kawano, J., Shimobayashi, N., Kitamura, M., Shinoda, K. and Aikawa, N. 2002. Formation process of calcium carbonate from highly supersaturated solution. *Journal of Crystal Growth* 237–239, pp. 419–423. doi: 10.1016/S0022-0248(01)01866-8.
- Kennedy, H., Kennedy, H. and Papadimitriou, S. 2005. The effect of acidification on the determination of organic carbon, total nitrogen and their stable isotopic composition in algae and marine sediment. *Rapid communications in mass spectrometry* 19(8), pp. 1063–1068.
- Keykha, H.A., Asadi, A., Huat, B.B.K. and Kawasaki, S. 2018. Microbial induced calcite precipitation by *Sporosarcina pasteurii* and *Sporosarcina aquimarina*. *Environmental Geotechnics* 6(8), pp. 562–566. doi: 10.1680/jenge.16.00009.

- Khaliq, W. and Ehsan, M.B. 2015. Crack healing in concrete using various bio influenced self-healing techniques. *Construction and Building Materials* 102, pp. 349–357. doi: 10.1016/j.conbuildmat.2015.11.006.
- Khodadadi, T.H., Kavazanjian, E., Paassen, L.V. and Dejong, J. 2017. Bio-Grout Materials: A Review. *Geotechnical Special Publication* (288 GSP), pp. 1–12. doi: 10.1061/9780784480793.001.
- Kim, G., Kim, J. and Youn, H. 2018. Effect of Temperature, pH, and Reaction Duration on Microbially Induced Calcite Precipitation. *Applied Sciences* 8, p. 1277. doi: 10.3390/app8081277.
- Kim, G. and Youn, H. 2016. Microbially Induced Calcite Precipitation Employing Environmental Isolates. *Materials* 9(6), p. 468. doi: 10.3390/ma9060468.
- Kitchenham, B. 2004. Procedures for Performing Systematic Reviews. *Keele, UK, Keele Univ.* 33
- Koh, C.M. 2013. Chapter Two - Storage of Bacteria and Yeast. In: Lorsch, J. ed. *Methods in Enzymology*. Laboratory Methods in Enzymology: Cell, Lipid and Carbohydrate. Academic Press, pp. 15–21. Available at: <https://www.sciencedirect.com/science/article/pii/B9780124200678000027> [Accessed: 26 November 2021].
- Komada, T., Anderson, M.R. and Dorfmeier, C.L. 2008. Carbonate removal from coastal sediments for the determination of organic carbon and its isotopic signatures, $\delta^{13}\text{C}$ and $\Delta^{14}\text{C}$: comparison of fumigation and direct acidification by hydrochloric acid. *Limnology and Oceanography: Method* 6, pp. 254–262.
- Kua, H.W., Gupta, S., Aday, A.N. and Srubar, W.V. 2019. Biochar-immobilized bacteria and superabsorbent polymers enable self-healing of fiber-reinforced concrete after multiple damage cycles. *Cement and Concrete Composites* 100, pp. 35–52. doi: 10.1016/j.cemconcomp.2019.03.017.
- Kutanaei, S.S. and Choobbasti, A.J. 2015. Triaxial behavior of fiber-reinforced cemented sand. *Journal of Adhesion Science and Technology* 30, pp. 579–593. doi: 10.1080/01694243.2015.1110073.
- Le Metayer-Levrel, G., Castanier, S., Oriol, G., Loubiere, J.-F. and Perthuisot, J.-P. 1999. Applications of bacterial carbonatogenesis to the protection and regeneration of limestones in buildings and historic patrimony. *Sedimentary geology* 126(1), pp. 25–34.
- Lee, M.L., Ng, W.S. and Tanaka, Y. 2013. Stress-deformation and compressibility responses of bio-mediated residual soils. *Ecological Engineering* 60, pp. 142–149. doi: 10.1016/j.ecoleng.2013.07.034.
- Li, C., Wang, Y., Zhou, T., Bai, S., Gao, Y., Yao, D. and Li, L. 2019. Sulfate Acid Corrosion Mechanism of Biogeomaterial Based on MICP Technology. *Journal of Materials in Civil Engineering* 31(7). doi: 10.1061/(ASCE)MT.1943-5533.0002695.
- Li, M., Li, L., Ogbonnaya, U., Wen, K., Tian, A. and Amini, F. 2016. Influence of Fiber Addition on Mechanical Properties of MICP-Treated Sand. *Journal of Materials in Civil Engineering* 28(4), p. 04015166. doi: 10.1061/(ASCE)MT.1943-5533.0001442.

- Li, M., Wen, K., Li, Y. and Zhu, L. 2018. Impact of Oxygen Availability on Microbially Induced Calcite Precipitation (MICP) Treatment. *Geomicrobiology Journal* 35(1), pp. 15–22. doi: 10.1080/01490451.2017.1303553.
- Liberati, A. et al. 2009. The PRISMA statement for reporting systematic reviews and meta-analyses of studies that evaluate healthcare interventions: explanation and elaboration. *BMJ* 339, p. b2700. doi: 10.1136/bmj.b2700.
- Lin, H., Suleiman, M.T. and Brown, D.G. 2020. Investigation of pore-scale CaCO₃ distributions and their effects on stiffness and permeability of sands treated by microbially induced carbonate precipitation (MICP). *Soils and Foundations* 60(4), pp. 944–961. doi: 10.1016/j.sandf.2020.07.003.
- Lin, H., Suleiman, M.T., Jabbour, H.M., Brown, D.G. and Kavazanjian, E. 2016. Enhancing the Axial Compression Response of Pervious Concrete Ground Improvement Piles Using Biogrouting. *Journal of Geotechnical and Geoenvironmental Engineering* 142(10), pp. 04016045-1–12. doi: 10.1061/(ASCE)GT.1943-5606.0001515.
- Liu, J., Bai, Y., Feng, Q., Song, Z., Wei, J., Sun, S. and Kanungo, D.P. 2018a. Strength Properties of Sand Reinforced with a Mixture of Organic Polymer Stabilizer and Polypropylene Fiber. *Journal of Materials in Civil Engineering* 30(12), p. 04018330. doi: 10.1061/(ASCE)MT.1943-5533.0002541.
- Liu, L., Liu, H., Xiao, Y., Chu, J., Xiao, P. and Wang, Y. 2018b. Biocementation of calcareous sand using soluble calcium derived from calcareous sand. *Bulletin of Engineering Geology and the Environment* 77(4), pp. 1781–1791. doi: 10.1007/s10064-017-1106-4.
- Liu, M., Thygesen, A., Summerscales, J. and Meyer, A. 2017. Targeted pre-treatment of hemp bast fibres for optimal performance in biocomposite materials: A review. *Industrial Crops and Products* 108, pp. 660–683. doi: 10.1016/j.indcrop.2017.07.027.
- Liu, P., Shao, G.-H. and Huang, R.-P. 2019. Study of the interactions between *S. pasteurii* and indigenous bacteria and the effect of these interactions on the MICP. *Arabian Journal of Geosciences* 12(23).
- Luo, M. and Qian, C. 2016. Influences of bacteria-based self-healing agents on cementitious materials hydration kinetics and compressive strength. *Construction and Building Materials* 121, pp. 659–663. doi: 10.1016/j.conbuildmat.2016.06.075.
- Luu, S., Cruz-Mora, J., Setlow, B., Feeherry, F.E., Doona, C.J. and Setlow, P. 2015. The Effects of Heat Activation on Bacillus Spore Germination, with Nutrients or under High Pressure, with or without Various Germination Proteins. *Appl. Environ. Microbiol.* 81(8), pp. 2927–2938. doi: 10.1128/AEM.00193-15.
- Ma, L., Pang, A.-P., Luo, Y., Lu, X. and Lin, F. 2020. Beneficial factors for biomineralization by ureolytic bacterium *Sporosarcina pasteurii*. *Microbial Cell Factories* 19(1), p. 12. doi: 10.1186/s12934-020-1281-z.
- MacDonald, R.E. and MacDonald, S.W. 1962. The physiology and natural relationships of the spore forming sarcinae. *Canadian Journal of Microbiology* 8(5), pp. 795–808. doi: <https://doi.org/10.1139/m62-101>.
- Mahawish, A., Bouazza, A. and Gates, W.P. 2019a. Factors affecting the bio-cementing process of coarse sand. *Proceedings of the Institution of Civil Engineers: Ground Improvement* 172(1), pp. 25–36. doi: 10.1680/jgrim.17.00039.

- Mahawish, A., Bouazza, A. and Gates, W.P. 2019b. Unconfined Compressive Strength and Visualization of the Microstructure of Coarse Sand Subjected to Different Biocementation Levels. *Journal of Geotechnical and Geoenvironmental Engineering* 145(8).
- Marrot, L., Lefeuvre, A., Pontoire, B., Bourmaud, A. and Baley, C. 2013. Analysis of the hemp fiber mechanical properties and their scattering (Fedora 17). *Industrial Crops and Products* 51, pp. 317–327. doi: 10.1016/j.indcrop.2013.09.026.
- Martin, D., Dodds, K., Ngwenya, B.T., Butler, I.B. and Elphick, S.C. 2012. Inhibition of *Sporosarcina pasteurii* under Anoxic Conditions: Implications for Subsurface Carbonate Precipitation and Remediation via Ureolysis. *Environmental Science & Technology* 46(15), pp. 8351–8355. doi: 10.1021/es3015875.
- Masoodi, R. and Pillai, K.M. 2012. A study on moisture absorption and swelling in bio-based jute-epoxy composites. *Journal of Reinforced Plastics and Composites* 31(5), pp. 285–294. doi: 10.1177/0731684411434654.
- McCoy, D.D., Cetin, A. and Hausinger, R.P. 1992. Characterization of urease from *Sporosarcina ureae*. *Archives of Microbiology* 157(5), pp. 411–416. doi: 10.1007/BF00249097.
- Michael Whitaker, J., Vanapalli, S. and Fortin, D. 2018. Improving the strength of sandy soils via ureolytic CaCO₃ solidification by *Sporosarcina ureae*. *Biogeosciences* 15(14), pp. 4367–4380. doi: 10.5194/bg-15-4367-2018.
- Midgley, T.L., Fox, G.A., Wilson, G.V., Heeren, D.M., Langendoen, E.J. and Simon, A. 2013. Seepage-Induced Streambank Erosion and Instability: In Situ Constant-Head Experiments. *Journal of Hydrologic Engineering* 18(10), pp. 1200–1210. doi: 10.1061/(ASCE)HE.1943-5584.0000685.
- Montoya, B.M. and DeJong, J.T. 2013. Healing of biologically induced cemented sands. *Geotechnique Letters* 3, pp. 147–151. doi: 10.1680/geolett.13.00044.
- Montoya, B.M. and DeJong, J.T. 2015. Stress-Strain Behavior of Sands Cemented by Microbially Induced Calcite Precipitation. *Journal of Geotechnical and Geoenvironmental Engineering* 141(6), p. 04015019. doi: 10.1061/(ASCE)GT.1943-5606.0001302.
- Mortensen, B.M., Haber, M.J., DeJong, J.T., Caslake, L.F. and Nelson, D.C. 2011. Effects of environmental factors on microbial induced calcium carbonate precipitation. *Journal of Applied Microbiology* 111(2), pp. 338–349. doi: 10.1111/j.1365-2672.2011.05065.x.
- Mujah, D., Cheng, L. and Shahin, M.A. 2019. Microstructural and geomechanical study on biocemented sand for optimization of MICP process. *Journal of Materials in Civil Engineering* 31(4).
- Mukherjee, S., Sahu, R., Mukherjee, J. and Sadhu, S. 2019. Application of Microbial-Induced Carbonate Precipitation for Soil Improvement via Ureolysis. In: *Lecture Notes in Civil Engineering*., pp. 85–94. doi: 10.1007/978-981-13-0559-7_10.
- Mumpton, F.A. 1999. La roca magica: Uses of natural zeolites in agriculture and industry. *Proceedings of the National Academy of Sciences of the United States of America* 96(7), pp. 3463–3470. doi: 10.1073/pnas.96.7.3463.
- Nawarathna, T.H.K., Nakashima, K. and Kawasaki, S. 2019. Chitosan enhances calcium carbonate precipitation and solidification mediated by bacteria. *International Journal of Biological Macromolecules* 133, pp. 867–874. doi: 10.1016/j.ijbiomac.2019.04.172.

- Ng, W.-S., Lee, M.-L. and Hii, S.-L. 2012. An Overview of the Factors Affecting Microbial-Induced Calcite Precipitation and its Potential Application in Soil Improvement. *International Journal of Civil and Environmental Engineering* 6(2), pp. 188–194.
- Ni, M. and Ratner, B.D. 2008. Differentiation of Calcium Carbonate Polymorphs by Surface Analysis Techniques – An XPS and TOF-SIMS study. *Surface and interface analysis : SIA* 40(10), pp. 1356–1361. doi: 10.1002/sia.2904.
- Norris, J.R. 1981. *Sporosarcina and Sporolactobacillus. In the Aerobic, Endosporeforming Bacteria*. Berkeley, R. C. W. and Goodfellow, M. eds. Academic Press: London.
- OpenStax 2016. *Microbiology*. Rice University, Houston, TX: OpenStax. Available at: <https://openstax.org/details/books/microbiology> [Accessed: 9 May 2021].
- Otsubo, Y. and Yamaguchi, K. 1961. Thermochemical Properties and Reaction Processes of Alkali Carbonate-Ferric Oxide System as Investigated by Means of Differential Thermal Method .4. Comparison Between Ceramic and Single Crystal Forms. *Nippon Kagaku Zasshi* 82(6), pp. 683-. doi: 10.1246/nikkashi1948.82.6_683.
- van Paassen, L. 2009. *Biogrout, ground improvement by microbial induced carbonate precipitation*. Ph.D. Thesis, Delft, Netherlands: Delft University of Technology.
- van Paassen, L.A., Ghose, R., van der Linden, T.J.M., van der Star, W.R.L. and van Loosdrecht, M.C.M. 2010. Quantifying Biomediated Ground Improvement by Ureolysis: Large-Scale Biogrout Experiment. *Journal of Geotechnical and Geoenvironmental Engineering* 136(12), pp. 1721–1728. doi: 10.1061/(ASCE)GT.1943-5606.0000382.
- Pacton, M. et al. 2013. The role of microorganisms in the formation of a stalactite in Botovskaya Cave, Siberia paleoenvironmental implications. *Biogeosciences* 10(9), pp. 6115–6130.
- Pakpour, N. and Horgan, S. 2021. Standard Plate Count. Available at: <https://bio.libretexts.org/@go/page/24024> [Accessed: 26 November 2021].
- Palin, D., Wiktor, V. and Jonkers, H.M. 2016. A bacteria-based bead for possible self-healing marine concrete applications. *Smart Materials and Structures* 25(8), pp. 1–6. doi: 10.1088/0964-1726/25/8/084008.
- Pan, L. et al. 2019. Effects of different calcium sources on the mineralization and sand curing of CaCO₃ by carbonic anhydrase-producing bacteria. *RSC Advances* 9(70), pp. 40827–40834. doi: 10.1039/c9ra09025h.
- Parastar, F., Hejazi, S.M., Sheikhzadeh, M. and Alirezazadeh, A. 2017. A parametric study on hydraulic conductivity and self-healing properties of geotextile clay liners used in landfills. *Journal of Environmental Management* 202, pp. 29–37.
- Park Sung-Sik, Choi Sun-Gyu, and Nam In-Hyun 2014. Effect of Plant-Induced Calcite Precipitation on the Strength of Sand. *Journal of Materials in Civil Engineering* 26(8), p. 06014017. doi: 10.1061/(ASCE)MT.1943-5533.0001029.
- Pei, D., Liu, Z., Wu, W. and Hu, B. 2021. Transcriptome analyses reveal the utilization of nitrogen sources and related metabolic mechanisms of *Sporosarcina pasteurii*. *PLOS ONE* 16(2), p. e0246818. doi: 10.1371/journal.pone.0246818.

- Peng, J. and Liu, Z. 2019. Influence of temperature on microbially induced calcium carbonate precipitation for soil treatment. Achal, V. ed. *PLOS ONE* 14(6), p. e0218396. doi: 10.1371/journal.pone.0218396.
- Peruzzo, L., Schmutz, M., Franceschi, M., Wu, Y. and Hubbard, S.S. 2018. The Relative Importance of Saturated Silica Sand Interfacial and Pore Fluid Geochemistry on the Spectral Induced Polarization Response. *Journal of Geophysical Research. Biogeosciences* 123(5).
- Phillips, A.J., Gerlach, R., Lauchnor, E., Mitchell, A.C., Cunningham, A.B. and Spangler, L. 2013. Engineered applications of ureolytic biomineralization: a review. *Biofouling* 29(6), pp. 715–733. doi: 10.1080/08927014.2013.796550.
- Portland Cement Association 1995. *Soil-Cement Construction Handbook*.
- Prasanna, S. and Mendes, N.M. 2020. Application of Jute Fiber in Soil Stabilization. doi: 10.20944/preprints202008.0534.v1.
- Rahman, M.M., Mallik, A.K. and Khan, M.A. 2007. Influences of various surface pretreatments on the mechanical and degradable properties of photografted oil palm fibers. *Journal of Applied Polymer Science* 105(5), pp. 3077–3086. doi: 10.1002/app.26481.
- Ramachandran, S.K., Ramakrishnan, V. and Bang, S.S. 2001. Remediation of Concrete Using Microorganisms. *Materials Journal* 98(1), pp. 3–9. doi: 10.14359/10154.
- Rebata-Landa, V. 2007. *Microbial activity in sediments: effects on soil behaviour*. Ph.D. Thesis, Atlanta, GA, USA: Georgia Institute of Technology.
- Reddi, L.N. and Kakuturu, S.P. 2004. Self-healing of concentrated leaks at core-filter interfaces in earth dams. *Geotechnical Testing Journal* 27(1), pp. 89–98.
- Renner, L.D. and Weibel, D.B. 2011. Physicochemical regulation of biofilm formation. *MRS Bulletin* 36(5), pp. 347–355. doi: 10.1557/mrs.2011.65.
- Richardson, A., A. Coventry, K., M. Forster, A. and Jamison, C. 2014. Surface consolidation of natural stone materials using microbial induced calcite precipitation. *Structural Survey* 32(3), pp. 265–278. doi: 10.1108/SS-07-2013-0028.
- Rodriguez-Blanco, J.D., Shaw, S. and Benning, L.G. 2011. The kinetics and mechanisms of amorphous calcium carbonate (ACC) crystallization to calcite, viavaterite. *Nanoscale* 3(1), pp. 265–271. doi: 10.1039/C0NR00589D.
- Rowell, R.M. and Stout, H.P. 1998. Jute and Kenaf. In: *Handbook of Fiber Chemistry: 2nd edition*. New York: Marcel Dekker, Inc, pp. 466–488. Available at: <https://www.crcpress.com/Handbook-of-Fiber-Chemistry/Lewin/p/book/9780824725655> [Accessed: 12 October 2018].
- Schaeffer, A.B. and Fulton, M.D. 1993. A Simplified Method of Staining Endospores. *Science* 77(1990), pp. 194–194. doi: 10.1126/science.77.1990.194.
- Schafer, P. 2011. *The Chinese Medicinal Herb Farm: A Cultivator's Guide to Small-scale Organic Herb Production*. White River Junction, Vermont: Chelsea Green Publishing.
- Schlegel, H.G. 1993. *General microbiology*. 7th ed. Cambridge, UK: Cambridge University Press.

- Seifan, M. and Berenjian, A. 2019. Microbially induced calcium carbonate precipitation: a widespread phenomenon in the biological world. *Applied Microbiology and Biotechnology* 103(12), pp. 4693–4708. doi: 10.1007/s00253-019-09861-5.
- Seifan, M., Ebrahiminezhad, A., Ghasemi, Y., Samani, A.K. and Berenjian, A. 2018. Amine-modified magnetic iron oxide nanoparticle as a promising carrier for application in bio self-healing concrete. *Applied Microbiology and Biotechnology* 102(1), pp. 175–184. doi: 10.1007/s00253-017-8611-z.
- Seifan, M., Samani, A.K. and Berenjian, A. 2016. Induced calcium carbonate precipitation using *Bacillus* species. *Applied Microbiology and Biotechnology* 100(23), pp. 9895–9906. doi: 10.1007/s00253-016-7701-7.
- Senese, F. 2010. General Chemistry Online: FAQ: Introduction to inorganic chemistry: What happens when sodium bicarbonate is heated? Available at: <http://antoine.frostburg.edu/chem/senese/101/inorganic/faq/carbonate-decomposition.shtml> [Accessed: 12 December 2018].
- Setlow, P. 2013. Summer meeting 2013 – when the sleepers wake: the germination of spores of *Bacillus* species. *Journal of Applied Microbiology* 115(6), pp. 1251–1268. doi: 10.1111/jam.12343.
- Setlow, P. 2014. Germination of Spores of *Bacillus* Species: What We Know and Do Not Know. *Journal of Bacteriology* 196(7), pp. 1297–1305. doi: 10.1128/JB.01455-13.
- Shi, P., Zhang, Y., Hu, Z., Ma, K., Wang, H. and Chai, T. 2017. The response of soil bacterial communities to mining subsidence in the west China aeolian sand area. *Applied Soil Ecology* 121, pp. 1–10. doi: 10.1016/j.apsoil.2017.09.020.
- Shimadzu 2021. Important Points about Ion Chromatography. Available at: <https://www.shimadzu.com/an/service-support/technical-support/analysis-basics/ion/42lab.html> [Accessed: 20 April 2021].
- Shukla, S.K. 2017. *Fundamentals of Fibre-Reinforced Soil Engineering*. Singapore: Springer.
- Siakeng, R., Jawaid, M., Ariffin, H. and Sapuan, S.M. 2018. Thermal properties of coir and pineapple leaf fibre reinforced polylactic acid hybrid composites. *IOP Conference Series: Materials Science and Engineering* 368, p. 012019. doi: 10.1088/1757-899X/368/1/012019.
- Sierra-Beltran, M.G., Jonkers, H.M. and Schlangen, E. 2014. Characterization of sustainable bio-based mortar for concrete repair. *Construction and Building Materials* 67, pp. 344–352. doi: 10.1016/j.conbuildmat.2014.01.012.
- Sigma Aldrich 2013. Product information 04551 Schaeffer and Fulton Spore Stain Kit. Available at: <https://www.sigmaaldrich.com/content/dam/sigma-aldrich/docs/Sigma-Aldrich/Datasheet/1/04551dat.pdf> [Accessed: 25 July 2018].
- Sigma Aldrich 2017. Celite S. Available at: <https://www.sigmaaldrich.com/catalog/product/sigald/06858> [Accessed: 20 April 2021].
- Stewart, D.J. 1965. The Urease Activity of Fluorescent *Pseudomonads*. *Journal of General Microbiology* 41(2), pp. 169–174. doi: 10.1099/00221287-41-2-169.
- Stocks-Fischer, S., Galinat, J.K. and Bang, S.S. 1999. Microbiological precipitation of CaCO₃. *Soil Biology and Biochemistry* 31(11), pp. 1563–1571. doi: 10.1016/S0038-0717(99)00082-6.

- Sun, X., Miao, L. and Chen, R. 2019. Effects of Different Clay's Percentages on Improvement of Sand-Clay Mixtures with Microbially Induced Calcite Precipitation. *Geomicrobiology Journal* 36(9), pp. 810–818. doi: 10.1080/01490451.2019.1631912.
- Tabassum, T. and Bheemasetti, T.V. 2020. Self-Healing and Desiccation Crack Behavior of Kaolinite-Rich Clay Soil. In: Hambleton J.P., Makhnenko R., and Budge A.S. eds. *Geotechnical Special Publication*. American Society of Civil Engineers (ASCE), pp. 582–591.
- Thermo Fisher Scientific 2018. CM0001, Nutrient Broth | Oxoid - Product Detail. Available at: http://www.oxoid.com/UK/blue/prod_detail/prod_detail.asp?pr=CM0001&c=UK&lang=EN&org=&print=Y [Accessed: 17 November 2018].
- Tobler, D.J., Cuthbert, M.O., Greswell, R.B., Riley, M.S., Renshaw, J.C., Handley-Sidhu, S. and Phoenix, V.R. 2011. Comparison of rates of ureolysis between *Sporosarcina pasteurii* and an indigenous groundwater community under conditions required to precipitate large volumes of calcite. *Geochimica et Cosmochimica Acta* 75(11), pp. 3290–3301. doi: 10.1016/j.gca.2011.03.023.
- Torres-Aravena, Á.E., Duarte-Nass, C., Azócar, L., Mella-Herrera, R., Rivas, M. and Jeison, D. 2018. Can microbially induced calcite precipitation (MICP) through a ureolytic pathway be successfully applied for removing heavy metals from wastewaters? *Crystals* 8(11).
- Turchyn, A.V., Bradbury, H.J., Walker, K. and Sun, X. 2021. Controls on the Precipitation of Carbonate Minerals Within Marine Sediments. *Frontiers in Earth Science* 9, p. 57. doi: 10.3389/feart.2021.618311.
- Tuson, H.H. and Weibel, D.B. 2013. Bacteria-surface interactions. *Soft matter* 9(18), pp. 4368–4380. doi: 10.1039/C3SM27705D.
- Tziviloglou, E. et al. 2016. Bio-Based Self-Healing Concrete: From Research to Field Application. In: Hager, M. D., VanDerZwaag, S., and Schubert, U. S. eds. *Self-Healing Materials*. Berlin: Springer-Verlag Berlin, pp. 345–385.
- US EPA, O. 2019. EPA Method 350.1: Determination of Ammonia Nitrogen by Semi-Automated Colorimetry. Available at: <https://www.epa.gov/esam/epa-method-3501-determination-ammonia-nitrogen-semi-automated-colorimetry> [Accessed: 26 November 2021].
- Vail, M., Zhu, C., Tang, C.-S., Anderson, L., Moroski, M. and Montalbo-Lombay, M.T. 2019. Desiccation Cracking Behavior of MICP-Treated Bentonite. *Geosciences* 9(9). doi: 10.3390/geosciences9090385.
- Van de Velde, K. and Baetens, E. 2001. Thermal and Mechanical Properties of Flax Fibres as Potential Composite Reinforcement. *Macromolecular Materials and Engineering* 286(6), pp. 342–349. doi: 10.1002/1439-2054(20010601)286:6<342::AID-MAME342>3.0.CO;2-P.
- Varma, D.S., Varma, M. and Varma, I.K. 1986. Thermal behaviour of coir fibres. *Thermochimica Acta* 108, pp. 199–210. doi: 10.1016/0040-6031(86)85092-4.
- Vidal, H. 1969. The Principle of Reinforced Earth. *Highway Research Record* (282), p. 16.
- Vigneswaran, C. and Jayapriya, J. 2010. Effect on physical characteristics of jute fibres with cellulase and specific mixed enzyme systems. *The Journal of The Textile Institute* 101(6), pp. 506–513. doi: 10.1080/00405000802542333.

- Wang, J., Dewanckele, J., Cnudde, V., Van Vlierberghe, S., Verstraete, W. and De Belie, N. 2014a. X-ray computed tomography proof of bacterial-based self-healing in concrete. *Cement & Concrete Composites* 53, pp. 289–304. doi: 10.1016/j.cemconcomp.2014.07.014.
- Wang, J., Jonkers, H.M., Boon, N. and De Belie, N. 2017. *Bacillus sphaericus* LMG 22257 is physiologically suitable for self-healing concrete. *Applied Microbiology and Biotechnology* 101(12), pp. 5101–5114. doi: 10.1007/s00253-017-8260-2.
- Wang, J., Mignon, A., Snoeck, D., Wiktor, V., Van Vlierberghe, S., Boon, N. and De Belie, N. 2015. Application of modified-alginate encapsulated carbonate producing bacteria in concrete: a promising strategy for crack self-healing. *Frontiers in Microbiology* 6(Article 1088), pp. 1–14. doi: 10.3389/fmicb.2015.01088.
- Wang, J., Van Tittelboom, K., De Belie, N. and Verstraete, W. 2011. Use of silica gel or polyurethane immobilized bacteria for self-healing concrete. *Construction and Building Materials* 26(1), pp. 532–540. doi: 10.1016/j.conbuildmat.2011.06.054.
- Wang, J.Y., De Belie, N. and Verstraete, W. 2012. Diatomaceous earth as a protective vehicle for bacteria applied for self-healing concrete. *Journal of Industrial Microbiology & Biotechnology* 39(4), pp. 567–577. doi: 10.1007/s10295-011-1037-1.
- Wang, J.Y., Snoeck, D., Van Vlierberghe, S., Verstraete, W. and De Belie, N. 2014b. Application of hydrogel encapsulated carbonate precipitating bacteria for approaching a realistic self-healing in concrete. *Construction and Building Materials* 68, pp. 110–119.
- Wang, J.Y., Soens, H., Verstraete, W. and De Belie, N. 2014c. Self-healing concrete by use of microencapsulated bacterial spores. *Cement and Concrete Research* 56, pp. 139–152. doi: 10.1016/j.cemconres.2013.11.009.
- Warth, A.D. 1978. Relationship Between the Heat Resistance of Spores and the Optimum and Maximum Growth Temperatures of *Bacillus* Species. *Journal of Bacteriology* 134(3), pp. 699–705.
- Weiner, S., Sagi, I. and Addadi, L. 2005. Choosing the Crystallization Path Less Traveled. *Science* 309(5737), pp. 1027–1028.
- Whiffin, V.S., Murdoch University., and Division of Science and Engineering. 2004. *Microbial CaCO₃ precipitation for the production of biocement*. Ph.D. Thesis, Perth, Western Australia: Murdoch University.
- Wijaya, M., Leong, E.C. and Abuel-Naga, H. 2019. Shrinkage curves for powder and granular bentonites. In: Ibraim E. and Tarantino A. eds. *E3S Web of Conferences*. EDP Sciences.
- Wiktor, V. and Jonkers, H.M. 2011. Quantification of crack-healing in novel bacteria-based self-healing concrete. *Cement & Concrete Composites* 33(7), pp. 763–770. doi: 10.1016/j.cemconcomp.2011.03.012.
- Xiao, Y. et al. 2021. Homogeneity and mechanical behaviors of sands improved by a temperature-controlled one-phase MICP method. *Acta Geotechnica* 6(5), pp. 1417–1427. doi: 10.1007/s11440-020-01122-4.
- Xiao, Y., He, X., Evans, T.M., Stuedlein, A.W. and Liu, H. 2019. Unconfined Compressive and Splitting Tensile Strength of Basalt Fiber-Reinforced Biocemented Sand. *Journal of Geotechnical and Geoenvironmental Engineering* 145(9), p. 04019048. doi: 10.1061/(ASCE)GT.1943-5606.0002108.

- Xu, H., Zheng, H., Wang, J.-N., Ding, X.-Q. and Chen, P. 2019. Laboratory method of microbial induced solidification/stabilization for municipal solid waste incineration fly ash. *MethodsX* 6, pp. 1036–1043. doi: 10.1016/j.mex.2019.05.006.
- Xu, Z., Bai, T., Pang, Y., Zhou, F. and Huang, J. 2016. Experimental Study of the Filling Effect of MICP Microbial Grouting in Silt. In: Dong, L. C., Huang, P. H., and Ozbakkaloglu, T. eds. *Proceedings of the 2016 International Conference on Architectural Engineering and Civil Engineering*. Paris: Atlantis Press, pp. 480–484.
- Yang, H., Yan, R., Chen, H., Lee, D.H. and Zheng, C. 2007. Characteristics of hemicellulose, cellulose and lignin pyrolysis. *Fuel* 86(12), pp. 1781–1788. doi: 10.1016/j.fuel.2006.12.013.
- Yasuhara, H., Neupane, D., Hayashi, K. and Okamura, M. 2012. Experiments and predictions of physical properties of sand cemented by enzymatically-induced carbonate precipitation. *Soils and Foundations* 52(3), pp. 539–549. doi: 10.1016/j.sandf.2012.05.011.
- Zhang, J. et al. 2017a. Optimization of a Binary Concrete Crack Self-Healing System Containing Bacteria and Oxygen. *Materials* 10(116), pp. 1–11. doi: 10.3390/ma10020116.
- Zhang, J., Liu, Y., Feng, T., Zhou, M., Zhao, L., Zhou, A. and Li, Z. 2017b. Immobilizing bacteria in expanded perlite for the crack self-healing in concrete. *Construction and Building Materials* 148, pp. 610–617. doi: 10.1016/j.conbuildmat.2017.05.021.
- Zhang, L., Higgins, M.L. and Piggot, P.J. 1997. The division during bacterial sporulation is symmetrically located in *Sporosarcina ureae*. *Molecular Microbiology* 25(6), pp. 1091–1098. doi: 10.1046/j.1365-2958.1997.5341892.x.
- Zhao, Y., Fan, C., Ge, F., Cheng, X. and Liu, P. 2020. Enhancing Strength of MICP-Treated Sand with Scrap of Activated Carbon-Fiber Felt. *Journal of Materials in Civil Engineering* 32(4), p. 04020061. doi: 10.1061/(ASCE)MT.1943-5533.0003136.

APPENDICES

A1: Product Data Sheets

AGGREGATE INDUSTRIES

Specialist silica sands

Garside Sands Washed Fine Silica Sand (WFSS)



A free draining washed fine silica sand which is pale in colour.

Applications

- Equestrian
- Greyhound tracks
- Outdoor play areas
- Jumping pits
- Heritage lime mortars.

Sectors

- Sports and leisure
- Horticulture and agriculture
- Construction.

Available in

- Loose: tippers
- Bulk bags (tote).

Mechanical analysis

Sieve size (mm)	Average % passing	% cumulative passing
2.530	100	100
1.180	100	95 - 100
0.600	96	85 - 100
0.300	80	60 - 100
0.150	24	15 - 50
0.063	1	0 - 10

Colour	Pale yellow*
Texture	Fine
Properties	Clean and Free-draining
Specific gravity apparent	2.65
Uncompacted bulk density	1.4 mg/m ³

*Colour may vary slightly as is a naturally occurring material

Garside washed fine silica sand

Source:	Leighton Buzzard, Bedfordshire
Geology:	Lower Greensand of the Cretaceous period
Composition:	Quartz
Grain shape:	Sub angular to rounded





FOUNDRY SAND SERIES

WHOLE GRAIN SILICA

PLANT: OTTAWA, ILLINOIS

TYPICAL PARTICLE SIZE ANALYSIS <i>(These do not represent a specification)</i>					
U.S.A. STANDARD SIEVE SIZE	INDIVIDUAL % RETAINED ON SIEVE				
	F-35	F-50	F-55	F-60	F-65
20	0				
30	3	0			
40	57	2	0	0	0
50	34	42	32	21	6
70	5	39	41	40	40
100	1	13	21	29	40
140	0	3	5	8	12
200		1	1	2	2
270		0	0	0	0
AFS* GRAIN FINENESS	35	51	55	60	66

GENERAL PROPERTIES			
Color	White	Shape	Round
Bulk Density (lb/ft ³)	95	SiO ₂ (Silicon Dioxide)	>99%
Mineral	Quartz	Specific Gravity	2.65
pH	7		

*American Foundry Society

January 2018 (v.2)

U. S. Silica Company
 24275 Katy Freeway, Suite 600
 Katy, TX 77494
 (800) 243-7500 (toll-free)
ussilica.com

DISCLAIMER: The information set forth in this Product Data Sheet represents typical properties of the product described; the information and the typical values are not specifications. U.S. Silica Company makes no representation or warranty concerning the Products, expressed or implied, by this Product Data Sheet.

WARNING: The product contains crystalline silica - quartz, which can cause silicosis (an occupational lung disease) and lung cancer. For detailed information on the potential health effect of crystalline silica - quartz, see the U.S. Silica Company Safety Data Sheet.



A2: Schedule of Column Studies

Column Test	Bacterium	Sand	Cementation media
U1	<i>S. ureae</i>	Garside Sands WFSS	CM1u
U2	<i>S. ureae</i>	Garside Sands WFSS	CM1u
U3	<i>S. ureae</i>	Garside Sands WFSS	CM1u
U4	<i>S. ureae</i>	Garside Sands WFSS	CM1u
P1	<i>S. pasteurii</i>	Garside Sands WFSS	CM1u
P2	<i>S. pasteurii</i>	F60	CM1p, CM2p
P3	<i>S. pasteurii</i>	F60	CM1p, CM3p
P4	<i>S. pasteurii</i>	F60	CM1p, CM3p
P5	<i>S. pasteurii</i>	F65	CM1p, CM3p